# Phytochemical analysis and potential anti-cancer properties of some Libyan plants

Thesis submitted by

## Rajab Abdusalam Mohamed Atraiki

For the degree of Doctor of Philosophy

Strathclyde Institute of Pharmacy and Biomedical Sciences,
University of Strathclyde
161 Cathedral Street
Glasgow G4 0NR
UK

# By the name of Allah

*Dedicated to Libya and my family*

# Dedication

I would like to dedicate my thesis to my beloved late mother **Khadeejah Hamed Ahweedi.** Although she is no longer here with us to celebrate this achievement, she waited patiently for this day to come. She taught me great resilience when she fought against heart disease multiple times, I learnt not to give up and work hard until I achieve what I desired for and although her loss was a heart breaker, I am glad that I made her proud.

# Acknowledgements

# Abstract

This thesis examined the *in vitro* phytochemical and cytotoxicity/anticancer activities of four selected plants from the Libyan flora. Based on information on traditional medicinal uses and a literature survey, *Bougainvillea spectabilis* Willd. (Fam: Nyctaginaceae), *Alhagi graecorum* Boiss (Fam: Fabaceae) *Retama raetam* (Forssk.) Webb & Berthel. (Fam: Fabaceae), and *Psoralea plicata* (Fam: Fabaceae) were selected. The four plants were investigated phytochemically and a range of compounds were elucidated, including: pinitol, allantoin, trigonelline, narcissin, alpinumisoflavone, 8-$\beta$-D-glucopyranosylgenistein, ephedroidin, plicatin-A, psoralen, angelicin and daidzein.

The study concentrated on the evaluation of *n*-hexane, ethyl acetate (EtOAc), methanol (MeOH) and ethanol (EtOH) solvent plant extracts and some of the isolated compounds for cytotoxicity based on metabolic activity to evaluate the potential anticancer activity against six human tumour cell lines: human caucasian hepatocyte carcinoma (HepG2), human malignant melanoma (A375), human caucasian lung carcinoma (A549), human caucasian pancreas carcinoma (PANC-1), human caucasian breast adenocarcinoma (MCF7), human caucasian prostate carcinoma (LNCaP), and non-cancerous human normal prostate (PNT2) cells as the normal control. Cytotoxicity at different concentrations (1.95, 3.90, 7.81, 15.62, 31.25, 62.5, 125 and 250 µg/ml) of these extracts was evaluated using a resazurin assay.

*B. spectabilis* extracts and its isolated constituents pinitol (**Bs-1**), allantoin (**Bs-2**) and trigonelline (**Bs-3**) showed no cytotoxic activity on any of the cell lines. Similarly, *A. graecorum* extracts and its isolated constituent narcissin (**Ag-1**) showed no cytotoxic activity. The EtOAc extract of *R. raetam* was toxic to HepG2, A375, PANC-1 and PNT2 at 250 µg/ml with $IC_{50}$ values of 139.2 µg/ml, 143.9 µg/ml, 129.1 µg/ml, and 154.3 µg/ml, respectively, and was also toxic to LNCaP at 125 µg/ml with an $IC_{50}$ value of 67.6 µg/ml. However, this extract was not toxic to A549 and MCF7 cells.

In addition, alpinumisoflavone **(Rr-1)** was toxic against HepG2, A375, A549, PANC-1, MCF7 and PNT2 at 125 μg/ml with $IC_{50}$ values of 63.9 μg/ml, 64.2 μg/ml, 118.8 μg/ml, 64.1 μg/ml, 72.9 μg/ml, and 112.6 μg/ml respectively, while it was highly toxic to LNCaP at 62.5 μg/ml with an $IC_{50}$ value of 43.6 μg/ml. The *n*-hexane, MeOH, 8-*β*-D-glucopyranosylgenistein **(Rr-2)** and ephedroidin **(Rr-3)** exhibited no cytotoxic activity on the cell lines.

Fraction 2 of *P. plicata* EtOH extract (PpFr-2) which contains plicatin A **(Pp-1)**, daidzein **(Pp-3)**, and a mixture of psoralen **(Pp-2a)** and angelicin **(Pp-2b)** was toxic against all the cell lines. It was toxic to HepG2, PANC-1, and PNT2 at 250 μg/ml with $IC_{50}$ values of 161.5 μg/ml, 125.9 μg/ml, and 126.1 μg/ml respectively, and was toxic against A375 at 125 μg/ml with an $IC_{50}$ value of 118.0 μg/ml, while it was highly toxic against MCF7 and LNCaP at 62.5 μg/ml with $IC_{50}$ values of 51.2 μg/ml, 34.7 μg/ml, respectively. However, this extract was not toxic to A549, while the other fractions demonstrated no cytotoxic activity on the cell lines.

In further studies, **Rr-1** and **PpFr-2** showed selective activity on LNCaP and MCF7 cells. Both Rr-1 and PpFr-2 had an inhibitory effect on adhesion, migration on LNCaP and MCF7 cells. The effect of Rr-1 and PpFr-2 inhibited adhesion of LNCaP and MCF7 cells to fibronectin. The % of inhibition of adhesion on LNCaP and MCF7 was 60% - 75% and 50% - 80% respectively, while the % of inhibition of migration was 50% - 70% and 75% - 90% respectively.

Therefore, Rr-1 and PpFr-2 have the potential to treat prostate and breast cancer by inhibition of cell adhesion and migration as a result of reduced or inhibited attachment to fibronectin.

# Table of Contents

# List of Abbreviations

| | |
|---|---|
| δ | Chemical shift |
| 1D | One Dimension |
| 2D | Two Dimension |
| A375 | Human malignant melanoma cell line |
| A549 | Human caucasian lung carcinoma cell line |
| Ag | *Alhagi graecorum* |
| ANOVA | Analysis of Variance |
| BHT | Butylated hydroxytoluene |
| BM | Basement Membrane |
| BSA | Bovine Serum Albumin |
| Bs | *Bougainvillea spectabilis* |
| BuOH | Butanol |
| $^{13}$C | Carbon 13 |
| CC | Column chromatography |
| $CD_3COCD_3$ | Deuterated acetone |
| $CDCl_3$ | Deuterated chloroform |
| $CHCl_3$ | Chloroform |
| $CH_2Cl_2$ | Dichloromethane |
| $CH_3COCH_3$ | Acetone |
| COSY | $^1$H-$^1$H Correlation Spectroscopy |
| d | Doublet |
| dd | Doublet of a Doublet |
| DEPT | Distortionless Enhancement by Polarisation Transfer |
| DW | Deionized water |
| DMEM | Dulbecco's Modified Eagle Medium |
| DMSO | Dimethyl sulphoxide |

| | |
|---|---|
| DMSO-*d6* | Deuterated dimethyl sulphoxide |
| DPPH | 2,2-Diphenyl-1-picrylhyrazyl |
| ECACC | European Collection of Authenticated Cell Cultures |
| ECM | Extracellular Matrix |
| EtOH | Ethanol |
| EtOAc | Ethyl acetate |
| FBS | Foetal Bovine Serum |
| Fr | Fraction |
| GC | Gas Chromatography |
| GC-MS | Gas chromatography-Mass spectrum |
| $^{1}$H | Proton |
| $H_2SO_4$ | Sulphuric acid |
| HBSS | Hank's Balanced Salt Solution |
| HDI | Human Development Index |
| HDL | High-Density Lipoprotein |
| HepG2 | Human caucasian hepatocyte carcinoma cell line |
| HMBC | Heteronuclear Multiple Bond Coherence |
| HPLC | High-Pressure Liquid Chromatography |
| HRESI-MS | High-resolution Electrospray Ionization Mass Spectrometry |
| HSQC | Heteronuclear Single Quantum Coherence |
| Hz | Hertz |
| $IC_{50}$ | Inhibitory Concentration |
| *J* | Coupling constant |
| $Km^2$ | Square Kilometre |
| LC-MS | Liquid Chromatography-Mass Spectroscopy |
| LNCaP | Human caucasian prostate carcinoma cell line |
| m | Multiple |
| *m/z* | Mass of charge |

| MBC | Minimum Bacterial Concentrations |
| MCF7 | Human caucasian breast adenocarcinoma cell line |
| MeOH | Methanol |
| MHz | Megahertz |
| MIC | Minimum Inhibitory Concentration |
| MS | Mass Spectroscopy |
| MTT | 3-[4,5-Dimethylthiazol-2-yl]-2,5 diphenyl tetrazolium bromide |
| Mult | Multiplicity of the NMR signals |
| $[M]^+$ | Molecular ion |
| NADH | Nicotinamide Adenine Dinucleotide Dehydrogenase |
| NMR | Nuclear Magnetic Resonance |
| NOESY | Nuclear Overhauser Enhancement SpectroscopY |
| OD | Optical Denisty |
| P | Propability |
| PANC-1 | Human caucasian pancreas carcinoma cell line |
| PBS | Phosphate Buffered Saline |
| PNT2 | Human normal prostate cell line |
| Pp | *Psoralea plicata* |
| PTLC | Preparative Thin Layer Chromatography |
| REDOX | OXidation-REDuction |
| R*f* | Retardation factor |
| RPMI | Roswell Park Memorial Institute |
| Rr | *Retama raetam* |
| s | Singlet |
| SEC | Size-Exclusion Chromatography |
| SEM | Standard Error Mean |
| STZ | Streptozotecin |
| t | Triplet |

| | |
|---|---|
| TLC | Thin Layer Chromatography |
| UV | Ultraviolet |
| VLC | Vacuum Liquid Chromatography |
| WHO | World Health Organization |

# List of Figures

# List of Tables

# List of Schemes

# Chapter1

# *Introduction*

## 1.1 Herbal medicine

The relationship between humans and plants has been long-established, using plants for clothing, nutrition, shelter and for herbal medicines to treat various diseases. Egyptian papyrus and Mesopotamian clay tablets were the first written records which indicated that primitive people used medicinal plants with experimentation and differentiated between types of plants which have active effects and others that have adverse effects on human health (Ahmad *et al.*, 2006).

Recently, there has been a significant revival in the use of medicinal plants, especially in the last three decades in both developed and developing countries. The World Health Organization (WHO) reported that 80% of people worldwide used herbal medicines for their curative needs, and 25% of prescribed medication has originated from in medicinal plants (Haq, 2004). The WHO informed that 88% from 170 member states have acknowledged their use of traditional and complementary medicine. They have applied laws, regulations, programmes, formally developed policies and offices for traditional and complementary medicine (Organization, 2019).

There are around 250,000 species of higher plants on earth, and more than 80,000 species are registered to have active compounds and approximately 5000 species have definite medicinal effects and are classified based on many factors such as the habitat, habit, part used and their medicinal use (Pan *et al.*, 2013).

In most developing countries, there are no rules to regulate herbal medicine, nevertheless, it is the most popular method used to cure health problems due to poverty and the high cost of modern medicines. For instance, in Ghana the Practitioner: Patient ratio is 1:400 in herbal medicine compared to 1:12.000 in modern medicine (Haq, 2004). While in Ethiopia, according to the Hadiya Zone Study around 38% of herbs and 32% of roots are popular forms of herbal medicine used (Agisho *et al.*, 2014).

The herbal medicine market has increased significantly in the world since 1985 and numerous factors are helping the growth of this market as the interest of people in natural medications is because they believe that herbal drugs are safe and efficacious and are preferred the pharmaceuticals. Additionally, elderly patients choose herbal medicine as an alternative, with increasing trends in self-therapy, and due to the expense of modern medicines (Calixto, 2000).

## 1.2 Medicinal plants for disease treatment

Natural products continue to be a major source of pharmaceuticals. Various plant compounds including alkaloids, terpenes, sterols, flavonoids, lignans, saponins, quassinoids, macrolides, anthrapyrazoles, essential oils and other miscellaneous compounds. Natural products are a valuable source of inspiration as lead compounds for the design and development of new drug candidates (Patel *et al.*, 2011). For example, more than 100 new products, particularly anticancer agents and anti-invectives, are derived from natural products (Newman and Cragg, 2016b). Some examples of drugs, derived from plants, and their activities are shown in Table 1.1

**Table 1.1:** Some natural products: currently used, originally derived from plants and their clinical use.

| Drug | Trade name | Plant | Year introduced | Activity |
|------|-----------|-------|-----------------|----------|
| Morphine | Roxanol | *Papaver somniferum* | 1805 | Analgesic |
| Colchicine | Mitigare | *Colchicum autumnale* | 1820 | Antibacterial |
| Theophylline | Phyllocontin | *Theobroma cacao* | 1895 | Bronchodilator |
| Digoxin | Lanoxin | *Digitalis lanata* | 1930 | Heart disease |
| Quinine | Qualaquin | *Cinchona calisaya* | 1936 | Antimalarial |
| Reserpine | Diupres | *Rauvolfia serpentina* | 1954 | Antihypertensive |
| Artemisinin | Artemisin | *Artemisia annua* | 1987 | Antiparasitic |
| Paclitaxel | Taxol | *Taxus brevifolia Nutt* | 1993 | Anticancer |
| Masoprocol | Actinex | *Larrea divaricatta* | 1993 | Anticancer |

## 1.3 Cancer

Cancer is a class of diseases in which a cell or group of cells show uncontrolled growth (division beyond the normal limits), invasion (intrusion into and destruction of adjacent tissues), and sometimes metastasis (spread to other locations in the body via lymph or blood). These three malignant properties of cancers differentiate them from benign tumours, which are self-limited, and do not invade or metastasis. Most cancers form a tumour but some, like leukaemia, do not. Two factors primarily cause cancer: external factors, such as chemicals, radiation, tobacco and infectious organisms, and internal factors such as hormones, immune conditions, inherited mutations and mutations that occur from metabolism. These factors also act together or in sequence to initiate and develop cancers (Goyal, 2012). The study data revealed that there were 6.7 million deaths, 24.6 million people living with cancer, and 10.9 million new patients around the world (Parkin *et al*., 2005). The international burden of cancer doubled between 1975 and 2000 and is expected to double again by 2020 and nearly triple by 2030 (Kaplan, 2013). According to the WHO 2010 data, it was expected that approximately 84 million people died due to cancer. The WHO reported that in 2016, there were 14 million new cases and 6.2 million deaths worldwide and it is expected that these figures will rise to 22 million new cases within the two next decades. By 2030, there will be more than 13 million deaths from cancer worldwide and approximately 21 million diagnosed cases every year. According to WHO statistics, in 2050, it is estimated that 17 million new cases of cancer will be diagnosed in developed countries and 7 million new cases of cancer will occur in more developed countries (Schwartsmann *et al.*, 2002, Ferlay *et al.,* 2015, McGuire, 2016).

In Libya, cancer is the main health problem, but accurate continuous incidence studies are lacking and epidemiological data in the country is sparse. Previous studies have covered only part of Libya such as the eastern or western part. For instance, data were collected retrospectively from the Tripoli Medical Centre during 2008. The study

revealed that a total of 1051 cancer cases was found (50.1% males and 49.9% females). In males, they were lung (15.6%), colorectal (12.3%) and prostate (9.9%) cancers, whereas, in females, most common cancers were breast (23.7%), colorectal (9.4%) and uterine (8.6%). Age-wise, 31% were younger than 15 years, 64.6% between 15 and 64 years and 4.2% above 64 years old, but in females, there were two peaks (in the age group 40-44 and those older than 75) (Benyasaad *et al.*, 2017, Alramah *et al.*, 2019). On the other hand, 'The Benghazi Cancer Registry' has managed to collect data on all new cases diagnosed in Eastern Libya and also data from medical and mortality records from multiple other sources. The leading cancers in males were found to be lung, colorectal and bladder, while in females, the leading malignancy was breast, followed by colorectal and uterine cancers. Lung and breast cancers were the most common causes of cancer deaths in adults. In the paediatric age group, the most frequently occurring cancer was identified as lymphoid leukaemia (El Mistiri *et al.*, 2015).

Bray *et al.* (2012) evaluated the changing patterns of cancer according to varying levels of the Human Development Index (HDI). The study used four levels (low, medium, high, and very high) of HDI, and the study used an indicator of gross domestic product, education and life expectancy per person. In 2008, the study found Libya to be in medium HDI regions. They reported that the number of cancer incidence in cervical and stomach was decreased compared to increasing incidence of cancers of breast (female), prostate, and colorectum. (Figure 1.1) (Bray *et al.*, 2012). In addition, the Global Cancer Observatory (May 2019) provided new cancer statistics for Libya and found that lung cancer in males was most common 18.9% while leukaemia was 4.7%. On the other hand, female breast cancer showed the highest cases 23.8% while ovarian cancer the lowest 4.6% as shown in Tables 1.2 and 1.3.
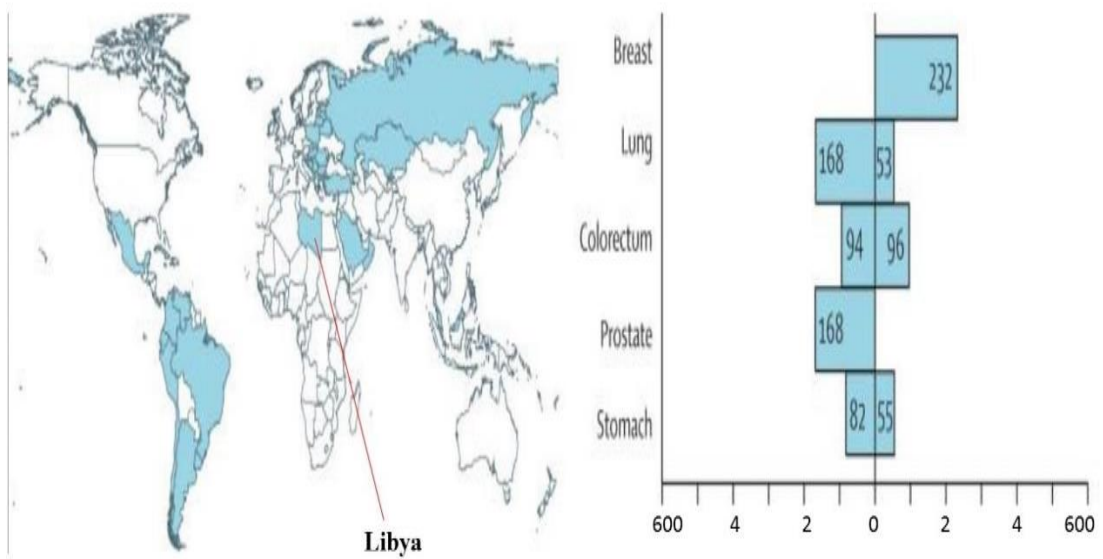
**Figure 1.1:** Five most frequently diagnosed cancers in terms of incidence in 2008, by the Human Development Index Level Map. The map shows only countries included in the analysis as Libya, and the image taken from (Bray *et al*., 2012).

**Table 1.2:** Number of new cancer cases in 2018, both sexes, all ages in Libya

| Males | | | Females | | |
|---|---|---|---|---|---|
| Lung | 595 | 18.9% | Breast | 753 | 23.8% |
| Bladder | 334 | 10.6% | Colorectum | 366 | 11.6% |
| Prostate | 317 | 10.1% | Cervix uteri | 319 | 10.1% |
| Colorectum | 309 | 9.8% | Leukaemia | 158 | 5% |
| Leukaemia | 174 | 4.7% | Ovary | 145 | 4.6% |
| Other cancers | 1447 | 46% | Other cancers | 1418 | 44.9% |
| Total | 3149 | 100% | Total | 3 159 | 100% |

6

**Table 1.3:** Summary of cancer statistics in 2018 for Libya

| | Males | Females | Both sexes |
|---|---|---|---|
| Population | 3 261 156 | 3 209 801 | 6 470 957 |
| Number of new cancer cases | 3 149 | 3 159 | 6 308 |
| Age-standardized incidence rate (World) | 135.3 | 109.4 | 120.3 |
| Risk of developing cancer before the age of 75 years (%) | 14.6 | 11.4 | 12.8 |
| Number of cancer deaths | 1 887 | 1 488 | 3 375 |
| Age-standardized mortality rate (World) | 85.3 | 55.9 | 69.1 |
| Risk of dying from cancer before the age of 75 years (%) | 9.3 | 6.1 | 7.6 |
| 5-year prevalent cases | 6 116 | 7 611 | 13 727 |
| Top 5 most frequent cancers excluding non-melanoma skin cancer (ranked by cases) | Lung Bladder Prostate Colorectum Leukaemia | Breast Colorectum Cervix uteri Leukaemia Ovary | Breast Colorectum Lung Bladder Cervix uteri |

## 1.3.1 Anticancer natural products

Many studies in the last few decades on the discovery and characterisation of anticarcinogenic compounds from medicinal plants and marine sources have revealed a great diversity (Newman and Cragg, 2016a). Some researchers have suggested that natural anticancer agents may belong to any of the following main class of compounds. The major emphasis has been laid on the flavonoids, coumarins, phenolics, terpenoids, carotenoids, anthraquinones, saponins, tannins, and many others all of which are secondary plant metabolites. More than 500 compounds belonging to at least 25 chemical classes have been reported to contain anticarcinogenic properties (Chouhan *et al.*, 2016).

The annual deaths worldwide according to the American Cancer Society accounts for roughly more than 3 million cancer deaths. Current research is being carried out throughout the globe to look for active cancer treatments. Medicinal plants are used to treat cancer using extracts and isolated compounds with antioxidant and anticancer activities that are known to inhibit or kill carcinogenic cells (Priya *et al.*, 2015).
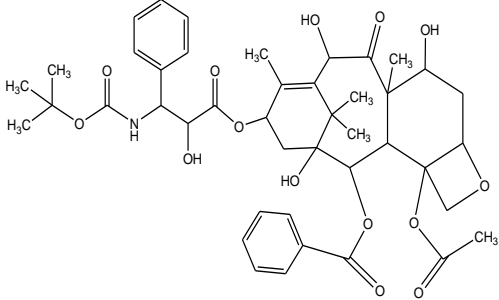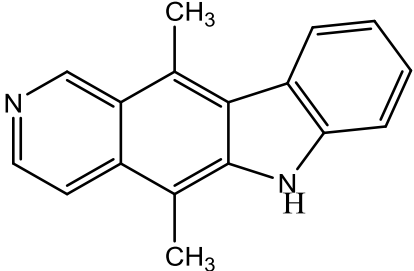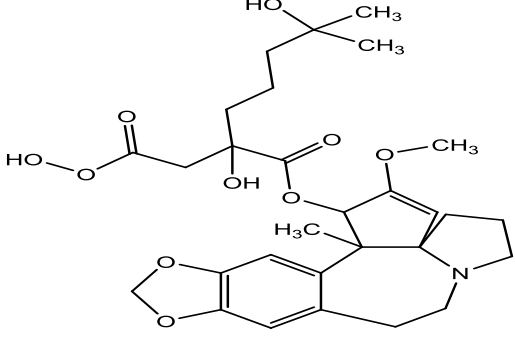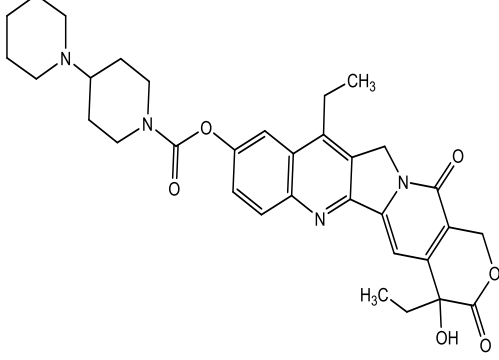
Cragg and Newman (2005) reported that plants are a source of anticancer agents, divided into three groups:

The first group contains plant-derived anticancer agents in clinical use (Table1.4) such as docetaxel **(1)** used for breast, lung cancer; ellipticine **(2)** and homoharringtonine **(3)** used for the treatment of acute and myelogenous leukaemia; irinotecan **(4)** used for the treatment of colorectal cancers; paclitaxel **(5)** used for the treatment of ovarian, breast and non-small-cell lung cancer; podophyllotoxin **(6)** used for the treatment of skin cancers and warts; topotecan **(7)** used for the treatment of ovarian and small-cell lung cancers; while vinblastine and vincristine **(8)** are used in the treatment of breast, lung, lymphomas, leukaemias and testicular cancers.

The second group includes plant-derived anticancer agents in clinical development (Table 1.5) such as combretastatin **(9)**, flavopiridol **(10)** and roscovitine **(11)**.

Finally, the third group includes plant-derived antitumour agents in preclinical development (Table 1.6) such as betulinic acid **(12)**, bruceantin **(13)**, β-lapachone **(14),** maytansine **(15)** and pervilleine A **(16)** (Cragg and Newman, 2005, Kaur *et al.*, 2011, Bhanot *et al.*, 2011, Newman and Cragg, 2016b).

**Table 1.4:** Plant-derived anticancer agents in clinical use (Cragg and Newman, 2005)

| Name of drug | Plant source | Chemical structure |
|---|---|---|
| Docetaxel (Taxotere®) **(1)** | *Taxus species* (Family: Taxaceae). |  |
| Ellipticine **(2)** | *Bleekeria vitensis* A.C. Sm. (Family: Apocynaceae). |  |
| Homoharringtonine (Ceflatonin®) **(3)** | *Cephalotaxus harringtonia var.drupacea* (Sieb and Zucc.) (Family: Cephalotaxaceae). |  |
| Irinotecan (Camptosar®) **(4)** | *Camptotheca acuminate* Decne. (Family: Nyssaceae). | (Djeddi et al., 2013)(Djeddi et al., 2013)(Djeddi et al., 2013)  |

| Paclitaxel (Taxol®) **(5)** | *Taxus brevifolia* Nutt. (Family: Taxaceae). |  |
| --- | --- | --- |
| Podophyllotoxin **(6)** | *Podophyllum species* (Family: Podophyllaceae). |  |
| Topotecan (Hycamtin®) **(7)** | *Camptotheca acuminate* Decne. (Family: Nyssaceae) |  |
| Vinblastine and Vincristine **(8)** | *Catharanthus roseus* G. Don. (Family: Apocyanaceae). |  |
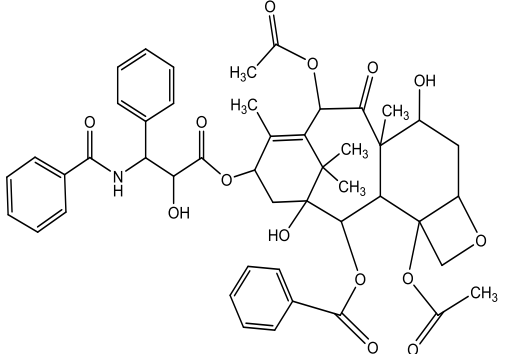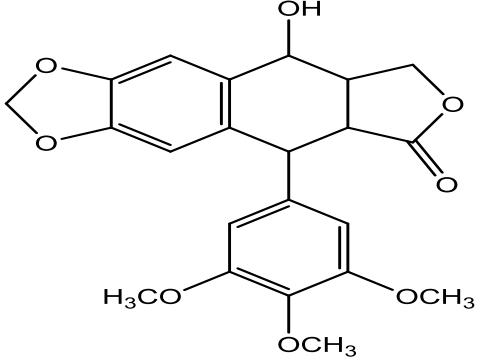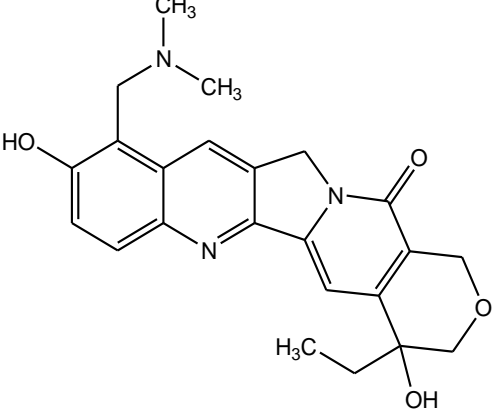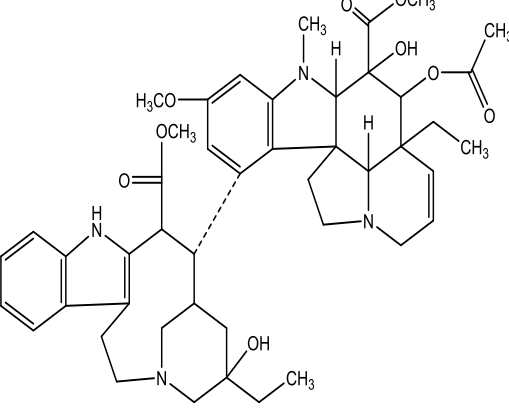
**Table 1.5:** Plant-derived anticancer agents in clinical development (Cragg and Newman, 2005)
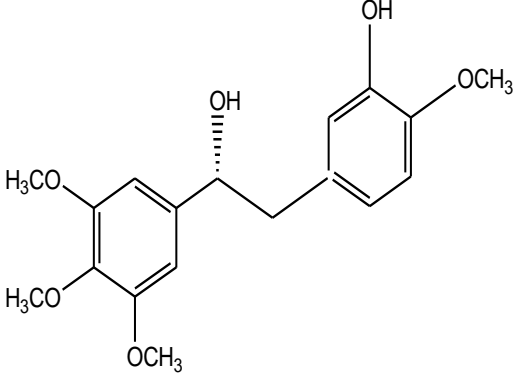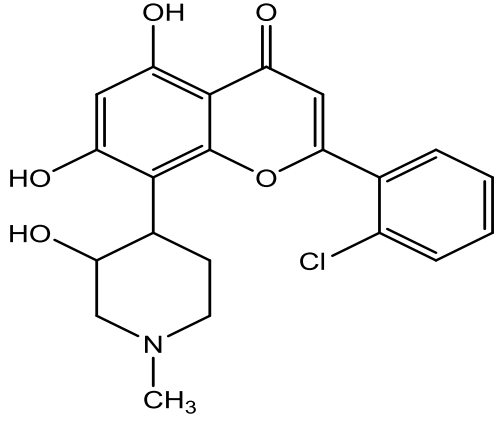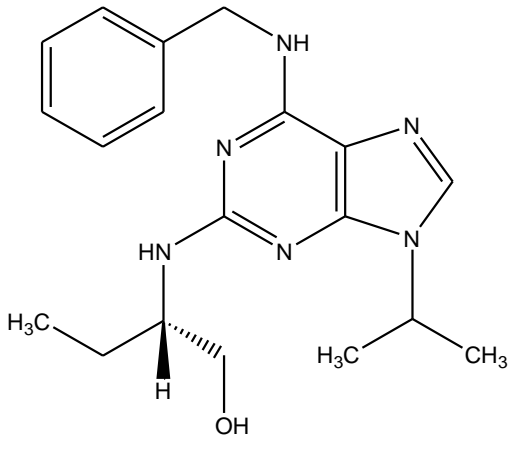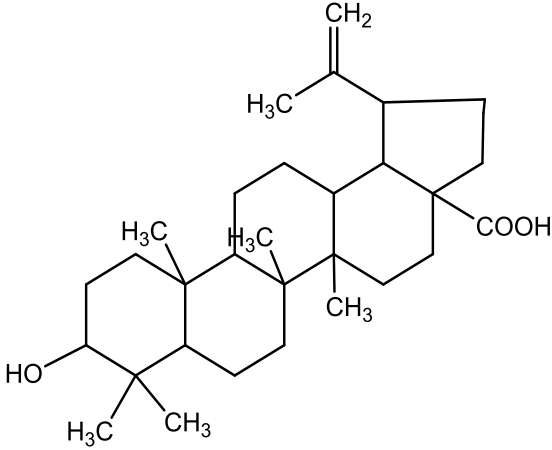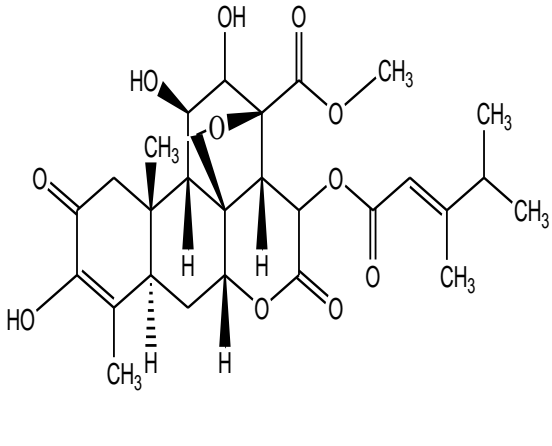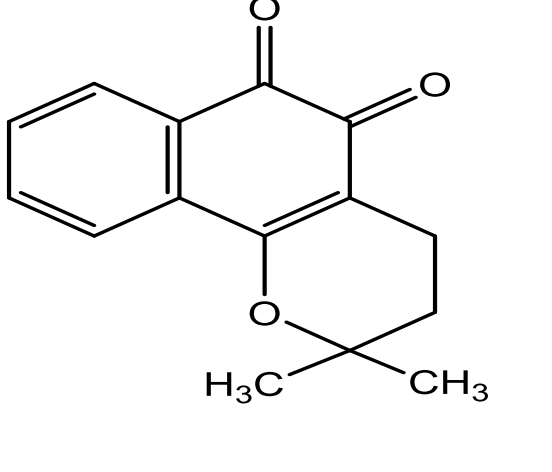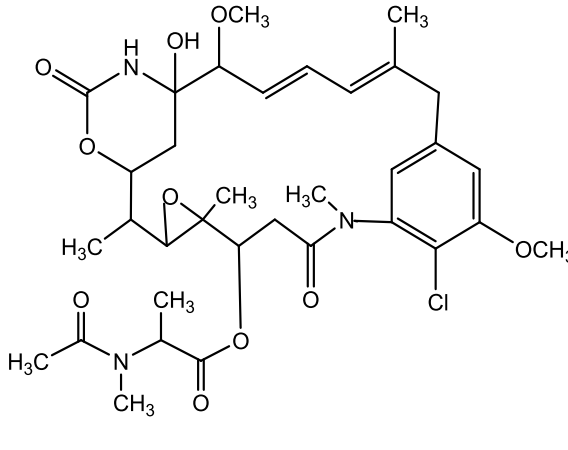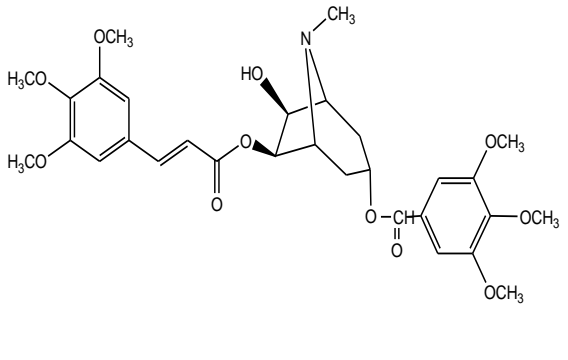
| Name of drug | Plant source | Chemical structure |
|---|---|---|
| Combretastatin (9) | *Combretum caffrum* (Eckl. & Zeyh.) Kuntze (Family: Combretaceae). |  |
| Flavopiridol or Alvocidib (10) | *Dysoxylum binectariferum* Hook. f. (Family: Meliaceae). |  |
| Roscovitine or Seliciclib (11) | *Raphanus sativus* L. (Family: Brassicaceae). |  |

**Table 1.6:** Plant-derived antitumour agents in preclinical development (Cragg and Newman, 2005).

| Name of drug | Plant source | Chemical structure |
|---|---|---|
| Betulinic acid **(12)** | *Betula species* (Family: Betula ceae). | |
| Bruceantin **(13)** | *Brucea antidysenter-ica* J.F.Mill. (Family: Simaroubaceae). | |
| β-Lapachone **(14)** | *Tabebuia species* (Family: Bignoniaceae). | |

| Name of drug | Plant source | Chemical structure |
|---|---|---|
| Maytansine **(15)** | *Maytenus serrata* (Hochst. Ex A. Rich.) Wilczek (Family: Celastraceae). |  |
| Pervilleine A **(16)** | *Erythroxylum pervillei* Baill. (Family: Erythroxylaceae). |  |

The present research is focussed on investigating anticancer activity in plants that are grown in Libya, which may contain compounds with significant cytotoxic effects on cancer.

## 1.4 Medicinal plants in Libya

Libya occupies a remarkably large area of Northern Africa, covering an area of 1,759, 540 Km², with a Mediterranean shore-line of about 93000 Km². This location enables an enormous wealth of vegetation distributed in various proportions in three major zones (Figure1.2) Fezzan (Saharan region), Cyrenaica and Tripolitania (Mediterranean regions). The Libyan Mediterranean coast has only moderate biodiversity when compared with the in-land Saharan flora (Mukassabi *et al.*, 2012).

As a result, Libyan traditional medicine consists of significant natural sources of medicinal plants which have protective and therapeutic properties. The recording of Libyan flora and/or vegetation started with the plant collector Cervelli, in 1811-12 in Cyrenaica, followed by many collectors during the Turkish Empire, but without a precise scientific procedure until Italian scholars occupied Libya in 1911 (such as Béguinot and Trotter in 1912- 1913, and Grande in 1914 in northern Fezzan and Tripolitania) (Cuccuini *et al.*, 2015). Despite many studies, new records of some plant species are still to be made in some areas of Libya due to their being previously poorly known (Saaed *et al*., 2019). On the other hand, some medicinal plants are threatened with extinction due to many influences including overgrazing and overexploitation which has led to deforestation (Ben-Mahmoud *et al.*, 2003), and desertification which transpires due to climate change (LE HOUEROU, 2004) and as a result of the increase of development activities without regulation (Elshatshat and Mansour, 2014). Finally, poor awareness of the importance of medicinal plants and shortage of strict policies that would regulate their uses and protect them from these degradation factors lead to a shortage of suitable use of medicinal plants (Louhaichi *et al.*, 2011).



**Figure 1.2:** Map showing the location of the major vegetation regions of Libya and the image taken from https://fanack.com/libya/geography-of-libya/ Attribution – Share Alike 4.0 International (CC BY-SA 4.0).

### 1.4.1 *Bougainvillea spectabilis* **Willd: (Paper flowers)**

*B. spectabilis* Willd (Figure 1.3) is called Almajnona or Aljohannamia in Arabic. The plant is a perennial shrub spreading horizontally or hanging downward. It can be grown as a tree or as ground cover, and its trunk tends to be crooked (Balasadasivam and Walker, 1998).

It is a climbing plant with spines and showy flowers, the colour of which range from orange, white, yellow, various shades of red to purple and violet (Shaiq Ali *et al.*, 2005). It is widely cultivated as an ornamental because it flowers throughout the year, and is easily propagated by stem-cutting: a favourite garden plant with many varieties, as a result of this property, the shrub is suitable for decorating fences and as side-walls of buildings and hedging plants in gardens.



**Figure 1.3:** Variety of *Bougainvillea spectabilis* flowers and image of the plant taken from https://candidegardening.com/GB/plants/27bfe2b6-fa17-4c26-b70a-8195e07cdae5 Starr 030418-0058 *Bougainvillea spectabilis* by Forest &amp; Kim Starr (CC BY 3.0).

### 1.4.1.1 Traditional uses

In the Northern region of Nigeria, especially by the Nupe people in Niger State, the crude extract of the leaves of *B. spectabilis* is still consumed as a herbal drug for diabetes (Malomo *et al.*, 2006), while its stem has been used in folk medicine for hepatitis (Chang *et al.*, 1993). However, in Libya, the plant has been used for a long time as an ornamental plant and there is no reported traditional medicinal use.

**1.4.1.2 Active ingredients and biological activities**

Rashid *et al*. (2013) analysed the phytochemical constituents of the dried powdered plant parts extracted using aqueous and organic solvents ethanol (EtOH), methanol (MeOH), chloroform (CHCl$_3$) and acetone (CH$_3$COCH$_3$). Phytochemical analysis demonstrated the presence of glycosides, tannins, alkaloid, flavonoids, saponins, steroids, terpenoids and phlobotannins in distilled water, EtOH, MeOH, CHCl$_3$ and CH$_3$COCH$_3$ extracts of leaves, stems and flowers. The extracts were found to have antimicrobial activity against *Salmonella typhi* using a paper disc diffusion method. Different parts of the stem extracts showed higher activity for MeOH extracts. Leaf extract showed the highest activity followed by flowers and stem. Also, leaf EtOH extracts revealed the highest activity, while flower EtOH and MeOH extracts showed the highest activity for both (Rashid *et al.*, 2013). Ahmed (2009) analysed the MeOH extract of *B. spectabilis* leaves which led to isolation and identification of three new triterpenoid saponins. The structures of the isolated compounds (**Bs-7**, **Bs-8** and **Bs-9**) were identified using a range of spectroscopic techniques (Table: 1.7) (Ahmed, 2009). In addition, Jawla *et al*. (2013) analysed the MeOH extract of stem bark. The powder of the stem bark was suspended in water and extracted with dichloromethane (CH$_2$Cl$_2$), ethyl acetate (EtOAc), and butanol (BuOH) sequentially. The EtOAc fraction was loaded on to a column packed with silica gel and eluted with a gradient of CHCl$_3$: MeOH, and water yielding five fractions (A - E). Chemical constituents were isolated by repeated column chromatography of these fractions. The results revealed that the column chromatography of fractions B and C afforded four compounds (**Bs-1**, **Bs-4**, **Bs-5** and **Bs-6**) (Table 1.7) which were identified by different spectroscopic techniques (Jawla *et al.*, 2013). Equally, Do *et al.* (2016) dissolved the EtOH extract of the stem bark in water and consecutively partitioned it with hexane and EtOAc. The EtOAc extract was subjected to various chromatographic methods to isolate eight new peltogynoids, bougainvinone A-H (**Bs-10**) (Table: 1.7) (Do *et al.*, 2016).

Besides, thirty-nine components, accounting for 97.2% of *B. spectabilis* oil, were identified from the aerial parts of *B. spectabilis* as analysed by gas chromatography (GC) and gas chromatography-mass spectroscopy (GC-MS). These consisted of 11 esters (27.1%), 7 monoterpenes (25.9%), 5 norisoprenoides (23.5%), 5 sesquiterpenes (10.4%), 2 diterpenes (2.5%), 2 aromatic compounds (2.1%), 4 aldehydes (0.7%), 1 ketone of non-terpenic type (0.7 %) and 2 acids (0.7%). The foremost compound was methyl salicylate (21.8%). Within the monoterpene fraction, terpinolene (8.2%) was identified as the chief compound, while α-copaene (4.9%) and aromadendrene (4.7%) were the most prevalent sesquiterpenes. α-(E)-ionone (9.8%) and dihydroedulan II (5.6%) were the main compounds from the group of norisoprenoides. Additionally, a fairly high concentration of the diterpenephytol (1.6%) was found (Vukovic *et al.*, 2013).

**Table 1.7:** Selection of phytochemicals isolated previously from *B. spectabilis*.
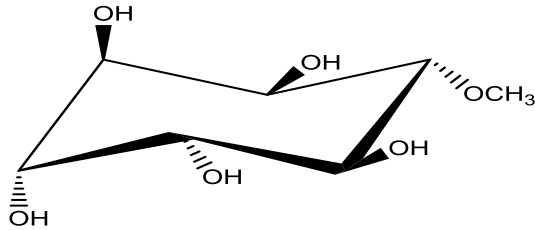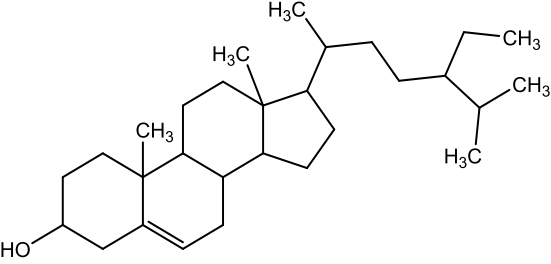
| Compound | Code | Parts of the plant | Reference |
|---|---|---|---|
| Pinitol  | **Bs-1** | Stem bark of *B. spectabilis* | (Jawla *et al.*, 2013) |
| β-sitosterol.  | **Bs-4** | Stem bark of *B. spectabilis* | (Jawla *et al.*, 2013) |

**Table 1.7 (continued):** Selection of phytochemicals isolated previously from
*B. spectabilis*.
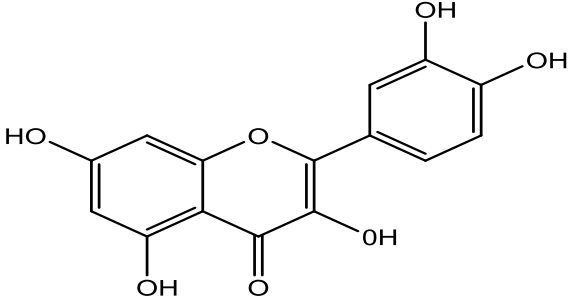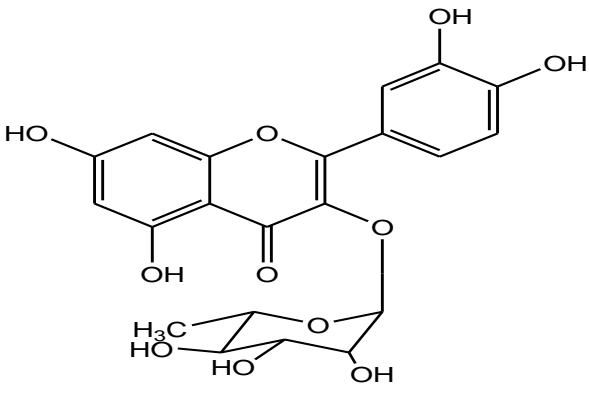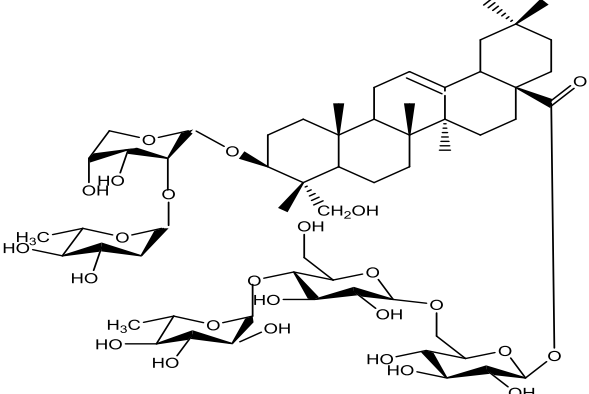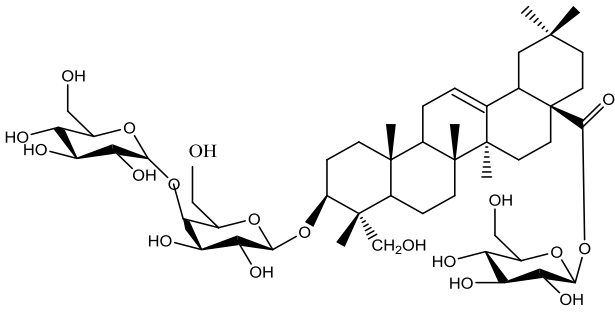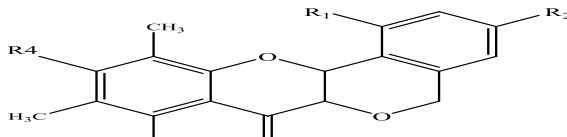
| Compound | Code | Parts of the plant | Reference |
|---|---|---|---|
| Quercetin.<br> | **Bs-5** | Stem bark of *B. spectabilis* | (Jawla *et al.*, 2013) |
| Quercitrin.<br> | **Bs-6** | Stem bark of *B. spectabilis* | (Jawla *et al.*, 2013) |
| 3,23-dihydroxy-12 - oleanen-28-oic acid, 3 – O - [α – L – rhamnop yrosyl-(1→2)-α-L-arabino pyranoside]-28-O-[α-L-rhamnopyrosyl (1→4) -β-D-glucopyranosyl-(1→6)-β-D-glucopyranoside.<br> | **Bs-7** | Leaves of *B. spectabilis* | (Ahmed, 2009) |

**Table 1.7 (continued):** Selection of phytochemicals isolated previously from

*B. spectabilis.*

| Compound | Code | Parts of the plant | Reference |
|---|---|---|---|
| 3-*O*-β-D-glucopyranosyl-1(1→2) -β-D- gluco pyranosyl-(1→4)-α-L-rhamnopyranosyl quinovic acid.<br><br> | **Bs-8** | Leaves of *B. spectabilis* | (Ahmed, 2009) |
| 3,23-dihydroxy-12-oleanen-28-oicacid-3-*O*-[α-D-glucopyranosyl-(1→4)-α-D-glucopyrano side]-28-O-[α-D-glucopyranoside].<br><br> | **Bs-9** | Leaves of *B. spectabilis* | (Ahmed, 2009) |
| Bougainvinones A-H<br><br> | **Bs-10** | Stem bark of *B. spectabilis* | (Do *et al.*, 2016) |

**1.4.1.2.1 Antimicrobial activity**

Umamaheswari *et al.* (2008) evaluated the antimicrobial activity of different solvent extracts of leaves from *B. spectabilis*. The qualitative analysis of phytochemicals and antibacterial activity was tested against Gram-positive and Gram-negative bacterial strains and the zones inhibition measured. The bacteria used in the Umamaheswari *et al.* (2008) study were *Bacillus subtilis, Escherichia coli, Klebsiella pneumoniae, Micrococcus luteus, Proteus vulgaris, Pseudomonas aeruginosa, Salmonella typhii, Serratia marcescens, Shigella flexneri, Staphycococcus aureus, Streptocococcus faecalis, and Vibrio cholerae.* The MeOH, CHCl$_3$, EtOAc and EtOH extracts showed maximum inhibitory effect on all tested bacteria except *V. cholerae* compared to the other solvent extracts. The alcoholic extracts were more active than CHCl$_3$ and EtOAc against both the Gram negative and Gram positive bacteria (Umamaheswari *et al.*, 2008). Similarly, Sudipta *et al.* (2012) evaluated the antibacterial and anti-fungal effects of various flowers extracts of *B. spectabilis* (CHCl$_3$, EtOAc, EtOH and H$_2$O). They found that the CHCl$_3$ and EtOH extracts of *B. spectabilis* were s highly active on *P. vulgaris* and *B. subtilis* at 40 µl but EtOAc and water extracts had moderate effect on *B. subtilis* while, the CHCl$_3$ and EtOH extracts of *B. spectabilis* had antifungal activity against *Aspergillus niger* and *Trichoderma viride* at 40 µl (Sudipta *et al.*, 2012).

In addition, Fawad *et al.* (2012) determined the antibacterial activity of EtOH and MeOH extracts of *B. spectabilis* and *B. variegata* leaves. The phytochemical constituents were tested qualitatively by the Harborne method (Harborne, 1998), while antimicrobial activities were determined by measuring the zone of inhibition on Mueller Hinton Agar. The results of this study revealed that the maximum inhibitory effects were obtained against Gram-negative microbes *P. vulgaris* and *S. marcescens* 16.00 ± 0.15 mm and 16.00 ± 0.06 mm, respectively, for the EtOH extract of *B. variegate*. While the maximum zone of inhibition for the MeOH extract of *B. spectabilis* against *S. typhimurium* was 17.26 ± 0.12 mm. However, the effects of the

MeOH extracts of *B. spectabilis* and *B. variegata* against Gram-positive microbe *S. aureus* was $28.54 \pm 0.18$ mm and $21.97 \pm 0.06$ mm respectively.

Both extracts of *B. spectabilis* and *B. variegate* did not show inhibitory activity against *E. faecalis*, *V. cholera* or *K. pneumonia* (Fawad *et al.*, 2012).

### 1.4.1.2.2 Antidiabetic activity

Jawla *et al.* (2012) evaluated the hypoglycaemic activity of *B. spectabilis* stem bark. The study was carried out to screen for the hypoglycaemic effects of extracts in albino rats (Wistar strain). EtOH extracts (100, 250 and 500 mg/Kg/day) of *B. spectabilis* were administered to both normal and alloxan-induced diabetic rats at defined time intervals. Blood glucose levels were tested at 0, 0.5, 1, 2, 4, 6 h, and on the 0, 1, 3, 5, 7th day after oral administration of the extracts. Of the doses tested, the highest anti-hyperglycemic effect was detected for the stem bark extract at 250 mg/kg after seven days treatment. The result of this study observed potent hypoglycaemic activity at different doses and intervals. The stem bark extract was found to be 22.2% more potent than the standard oral hypoglycaemic medication, glibenclamide 0.2 mg/kg (Jawla *et al.*, 2012).

### 1.4.1.2.3 Antihyperlipidemic activity

Adebayo *et al.* (2005) studied the effect of an EtOH extract of *B. spectabilis* leaves on serum lipid and haematological parameters in rats over 7 days oral administration at doses of 50,100 and 200 mg/kg body weight. The parameters evaluated included serum lipids, white blood cells (WBC) and red blood cell (RBC) indices. The results illustrated that the extract significantly ($p < 0.05$) reduced packed cell volume, haemoglobin concentration and RBC counts at a dose of 200 mg /kg body weight when compared with controls while other doses administered had a little significant effect on these parameters. Similarly, the extract significantly ($p < 0.05$) reduced WBC count at all doses administered when compared with the control. However, the extract had no significant effect on mean corpuscular haemoglobin, mean corpuscular

haemoglobin concentration, mean corpuscular volume and platelet count when compared with controls. Furthermore, the extract significantly ($p < 0.05$) reduced total serum cholesterol concentration, while it had no significant ($p > 0.05$) effect on serum HDL-cholesterol concentration at all doses administered when compared with controls. Nevertheless, the extract significantly ($p < 0.05$) increased serum triacylglycerol concentration at the dose of 50 mg/kg body weight while other doses administered had no significant effect. The study proposed that the extract may have a positive effect on serum cholesterol concentration reduction, while it probably has the potential of undesirably affecting haematological indices (Adebayo *et al.*, 2005).

### 1.4.1.2.4 Antifertility activity

Mishra *et al*. (2009) evaluated the effect of *B. spectabilis* on fertility of mice. The crude extract of *B. spectabilis* leaves were orally administered to Swiss Albino mice (800 mg/kg of body weight/day for 30 days) and the effects of the crude extract on reproductive organs and fertility were examined. The administration caused a diminished sperm count, and weight of testis, while histological examination showed a decrease in the size of seminiferous tubules along with the thickness of germinal epithelial cells, although some of the Leydig interstitial cells and epithelial cells exhibited hypertrophy. Furthermore, the lumen of the tubules was found to be devoid of sperm. In contrast, in treated females no histological changes could be detected, but there was a slight disturbance of the oestrus cycle having an extended metaestrus phase, which increased by 145.28%. The overall duration of the oestrous cycle was prolonged by more than one day. The *B. spectabilis* extract affected the hormonal profile with oestrogen and testosterone levels significantly reduced (Mishra *et al*., 2009). Similarly, Ikpeme *et al*. (2015) revealed mitigation in sperm count, viability, motility and increased sperm head abnormalities in rats caused by administration of a crude extract of *B. spectabilis* (Ikpeme *et al.*, 2015).

**1.4.1.2.5 Antioxidant activity**

Pintathong *et al*. (2012) analysed the phenolic antioxidants from *Bougainvillea spp*. In the study, the flower and bract parts of four different colours of *Bougainvillea spp*, pink, yellow, reddish-pink, and white, were tested for phenolic content and antioxidant capacity. The extraction process was performed by a conventional shaking method with different solvents; deionised water (DW), EtOAc, propylene glycol and EtOH. Extractable phenolic content of the extracts was investigated by the Folin-Ciocalteu method (Kumar and Kumar, 2008), while antioxidant capacity was determined by 2, 2- diphenyl-1-picrylhyrazyl (DPPH) radical scavenging activity and ferric reducing antioxidant power. The result showed that the different extracts had high natural antioxidant capacity (Pintathong *et al*., 2012).

**1.4.1.2.6 Cytotoxic activity**

Ahmed (2009) tested compounds (**Bs-7**, **Bs-8** and **Bs-9**) (Table 1.7) which were isolated from the MeOH extract of *B. spectabilis* leaves (section 1.4.1.2) for cytotoxic activity against H460 (human lung carcinoma), HeLa (human cervix carcinoma), U251 (human brain tumour), MCF7 (human breast carcinoma), HepG2 (human liver carcinoma) and EAC (Ehrlich ascites carcinoma) cell lines. Potential toxicity of the compounds was tested using the Skehan and Storeng method (Skehan *et al*., 1990). The results revealed that these compounds had no cytotoxic activity on these different type of cancer cell lines (Ahmed, 2009).

**1.4.2 *Alhagi graecorum* Boiss (Camel thorn)**

*Alhagi graecorum* Bioss (Figure 1.4) locally named as Al-Agool, Shouk Aljemal and Shwaika in Arabic is a wild plant belonging to the Fabaceae family. A shrubby evergreen perennial herb, with a woody base, erect to ascending to (60-100) cm high, thorny branched with about 1 inch long. The leaves are deciduous, simple, small, present at the base of each side twig, obovate to oblong, shortly petiolate, with a rounded tip, up to 2 cm.

Flowers are solitary or in pairs in axils and along with twigs, with deep red to purple papillionate petals. The fruit consists of a cylindrical pod, 1-3 cm, fairly thick straight, dark brown with constrictions between seeds; seeds consist of 3-8 kidney shaped, smooth and brown.



**Figure 1.4:** Aerial part of *Alhagi graecorum,* and image of the plant taken from http://earthclimatechange.blogspot.com/2011/06/alhagi-graecorum.html. Muhammed Bei, Earth Climate Change, Kuwait, 2011

### 1.4.2.1 Traditional uses

*A. graecorum* is traditionally used to treat constipation, jaundice, arthritis, with antimicrobial activity, and as a general tonic, blood purifier, and anthelmintic. Also, it is used against dysentery, upper respiratory system problems, wounds, haemorrhoids, and uterus problems.

It is now being recognised to help rheumatic pains, liver disorders, urinary tract infection, the decoction of its roots is used to relax the ureter and remove renal stones (Muhammad *et al.*, 2015).

### 1.4.2.2 Active ingredients and biological activities

Ibrahim (2015) investigated an 80% MeOH extract of the aerial parts of *A. graecorum* and the five phenolic compounds were identified as one hydrolysable tannin 6-*O*-galloyl-(α / β)-D-glucopyranose **(Ag-2)**, and four flavonol glycosides kaempferol 3-*O*-β-D-glucopyranoside **(Ag-3)**,kaempferol 3-*O*-(6"-*O*-galloyl) -β-D-glucopyranoside **(Ag-4)**, myricetin-4`-*O*-α-L-$^1$C$_4$ rhamnopyranoside **(Ag-5)** myricetin aglycone, the

structures were determined by spectroscopic methods (UV, ESI/MS,^{1}H- and ^{13}C NMR) (Ibrahim, 2015). El-Sayed *et al.* (1993) isolated compounds from the aerial parts of *A. graecorum* as tamarixetin 3-*O*-dirhamnoside (**Ag-6**) and isorhamnetin 3-*O*-glucosyl neohesperidoside (**Ag-7**) (Muhammad *et al.*, 2015).

**Table 1.8:** Selection of phytochemicals isolated previously from *A. graecorum*
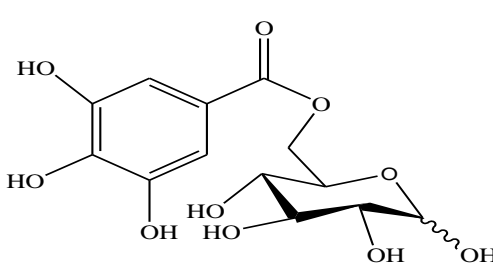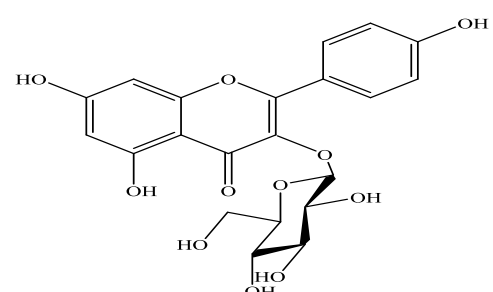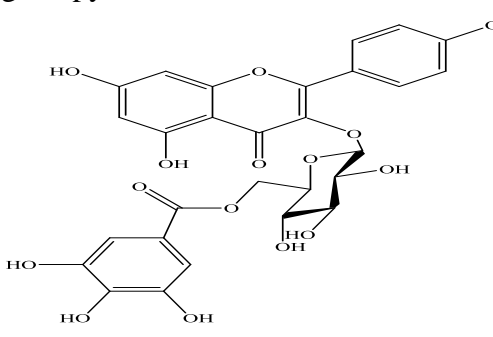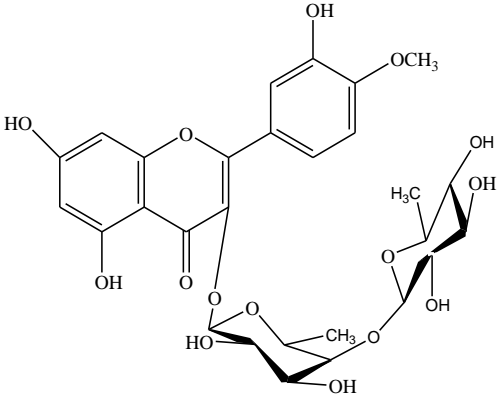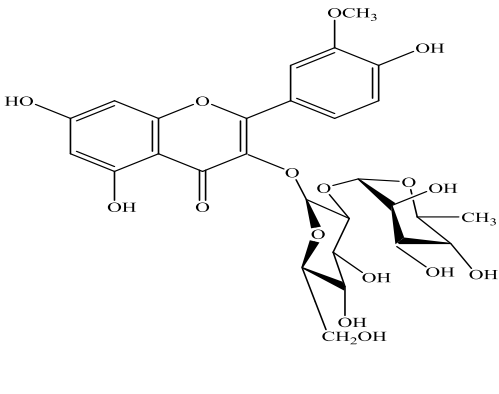
| Compound | Code | Parts of the plant | Reference |
|---|---|---|---|
| 6-*O*-Galloyl-(α / β)-D-glucopyranose<br> | **Ag-2** | Aerial parts of *A. graecorum* | (Ibrahim, 2015) |
| Kaempferol 3-*O*-β-D-glucopyranoside<br> | **Ag-3** | Aerial parts of *A. graecorum* | (Ibrahim, 2015) |
| Kaempferol 3-*O*-(6"-*O*-galloyl)-β-D-glucopyranoside<br> | **Ag-4** | Aerial parts of *A. graecorum* | (Ibrahim, 2015) |

**Table 1.8 (continued):** Selection of phytochemicals isolated previously from A. *graecorum.*

| Compound | Code | Parts of the plant | Reference |
|---|---|---|---|
| Myricetin-4`-*O*-α-L-$^1C_4$ rhamnopyranoside  | **Ag-5** | Aerial parts of *A. graecorum* | (Ibrahim, 2015) |
| Tamarixetin-3-*O*-dirhamnoside  | **Ag-6** | Aerial parts of *A. graecorum* | (Muhammad *et al.*, 2015) |
| Isorhamnetin-3-*O*- glucosyl Neohesperidoside  | **Ag-7** | Aerial parts of *A. graecorum* | (Muhammad *et al.*, 2015) |

### 1.4.2.2.1 Anti-inflammatory activity

Ibrahim (2015) evaluated the anti-inflammatory activity of an aqueous EtOH extract of the aerial part of *A. graecorum* using two animal inflammation models. The first model was a carrageenan-induced rat paw oedema, which was carried out by injecting 0.1 ml of 1% (w/v) carrageenan suspension in 0.9% (w/v) sterile saline into the plantar tissue of the left hind paw of all animals, one hour following oral administration of either control vehicle, diclofenac sodium or plant extract. The right paw served as a reference to measure the degree of inflammation in the left paw, the inhibition of oedema volume was calculated. The second model involved the use of cotton pellets to induce granuloma formation in a dose-dependent manner which was carried out by inserting 10 mg of sterile cotton pellets to all animals, one in each axilla. EtOH extract, control vehicle and diclofenac sodium were administered orally every day for 7 days. At the end, the cotton pellets were surgically removed and the moist pellets were weighed, dried at 60°C for 24 h and then re-weighed. The anti-inflammatory activity of the EtOH extract of *A. graecorum* was compared with diclofenac sodium, which was used as a positive control. The result showed that the plant possesses an anti-inflammatory effect which conforms to the traditional uses of *A. graecorum* for the treatment of inflammatory illnesses (Ibrahim, 2015).

### 1.4.3 *Retama raetam* (Forssk.) Webb & Berthel (White weeping broom)

*Retama raetam* (Forssk.) Webb & Berthel (Figure 1.5) or White weeping broom is a wild plant belonging to the Fabaceae family. It is a Mediterranean shrub that grows to about 3 metres high and may reach 6 metres. The plant is grey-green with slim, drooping branches. The young plant is flimsy with a single stem and a strong taproot. Its leaves are very small (about 6-7 mm long), narrow (only 1 mm wide), and they are rapidly dropped and the plant remains leafless along the year.

**Figure 1.5:** Aerial part of *Retama raetam*, and image of the plant taken from http://earthclimatechange.blogspot.com/2011/06/alhagi-graecorum.html. *Retama raetam* (Forssk.) Webb & Berthel.", Plants of the World Online, Royal Botanic Gardens, Kew, retrieved 2018-02-15. Attribution – Share Alike 4.0 International (CC BY-SA 4.0).

### 1.4.3.1 Traditional uses

The common uses of *R. raetam* are as abortifacient, anthelmintic, antiseptic, purgative and sedative (Benmiloud-Mahieddine *et al.*, 2011, Al-Tubuly *et al.*, 2011). Retama shrubs create natural barriers, which prevent the weakening of ecosystems and desertification. (Ben-Mahmoud *et al*., 2003, Louhaichi *et al*., 2011).

### 1.4.3.2 Active ingredients and biological activities

Xu *et al*. (2015) isolated two new furanoflavonoids retamasin A and retamasin B (**Rr-29**) and known flavonoids: ephedroidin (**Rr-3**), atalantoflavone (**Rr-4**), derrone (**Rr-5**) from a CHCl$_3$ extract of the aerial parts of *R. raetam* (Xu *et al.*, 2015). Djeddi *et al*. (2013) isolated flavonoids from a MeOH extract of the aerial parts of *R. raetam* by subjecting them to VLC using mixtures of CH$_2$Cl$_2$-MeOH of increasing polarity as eluents and the fractions were pooled into six groups and each group subjected to CC which yielded genistein (**Rr-7**), 6-hydroxygenistein (**Rr-8**), 3′methylorobol (**Rr-9**), pratensein (**Rr-10**), luteolin (**Rr-11**), kaempferol (**Rr-12**), 6-hydroxyapigenin (**Rr-13**), biochanin A (**Rr-14**) and *p*-coumaric acid (**Rr-15**) (Djeddi *et al.*, 2013).

Edziri *et al.* (2012) isolated the isoflavone derrone (**Rr-5**) and flavone licoflavone (**Rr-6**) from the EtOAc extract of the flower of *R. raetam* and the structures elucidated were based on the corresponding $^1H$-$^{13}C$-NMR data (Edziri *et al.*, 2012).

Awen *et al.* (2011) identified some components from the essential oil obtained by hydrodistillation from the flowers of *R. raetam* using GC/MS and the analysis revealed the presence of β-linalool (**Rr-17**), terpinolene (**Rr-20**), limonene (**Rr-25**), and 2-decen-1-ol (**Rr-26**) (Awen *et al.*, 2011).

Edziri *et al.* (2010) detected 50 components from the essential oil obtained by hydrodistillation from the flowers of *R. raetam* using GC and GC/MS analysis and found major components such as α-humulene (**Rr-16**), linalool (**Rr-17**), myrcene (**Rr-18**), β-carphyllene (**Rr-19**), terpinolene (**Rr-20**), α-terpinyl acetate (**Rr-21**), tridecanal (**Rr-22**), nonanal (**Rr-23**) and methyl anthranilate (**Rr-24**) (Edziri *et al.*, 2010).

Kacem *et al.* (2008) isolated pectin (**Rr-30**) from *R. raetam* when dried alcohol-insoluble residues of the plant were treated sequentially with DW, ammonium oxalate and basic solutions purified by ultrafiltration. The results exhibited that the extraction with ammonium oxalate solution gave the highest pectin yield (Kacem *et al*., 2008).

Kassem *et al.* (2000) isolated two new flavones from the aerial parts of *R. raetam,* luteolin 4′-O-neohesperidoside (**Rr-27**) and 5,4′- (dihydroxy - 3″,4″- dihydro -3″,4″-dihydroxy) -2″,2″- dimethylpyrano - (5″,6″:7,8)- flavone (**Rr-28**) and identified using spectroscopic methods (Kassem *et al*., 2000).

**Table 1.9:** Selection of phytochemicals isolated previously from *R. raetam.*
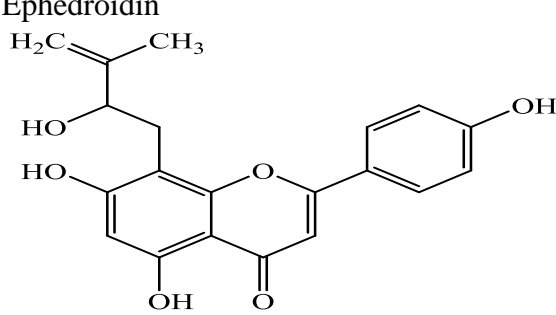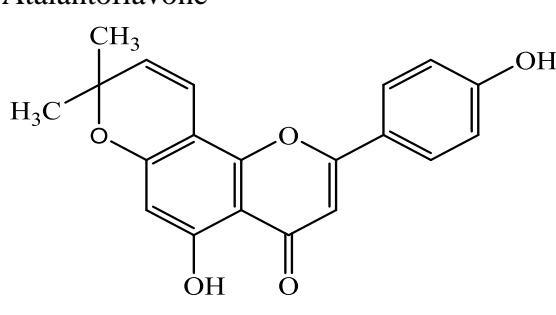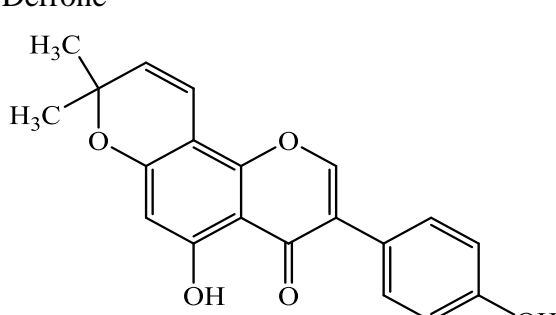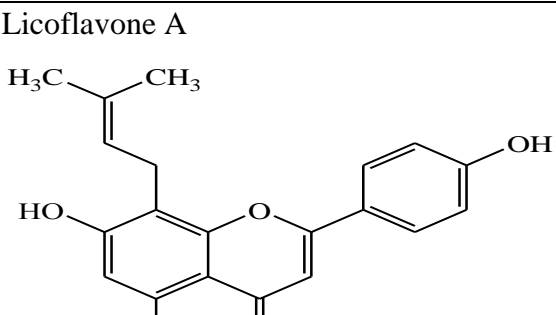
| Compound | Code | Parts of the plant | Reference |
|---|---|---|---|
| Ephedroidin  | **Rr-3** | Aerial parts of *R. raetam* | (Xu *et al.*, 2015) |
| Atalantoflavone  | **Rr-4** | Aerial parts of *R. raetam* | (Xu *et al.*, 2015) |
| Derrone  | **Rr-5** | Flowers of *R. raetam* | (Edziri *et al.*, 2012, Xu *et al.*, 2015) |
| Licoflavone A  | **Rr-6** | Flowers of *R. raetam* | (Edziri *et al.*, 2012, Xu *et al.*, 2015) |

**Table 1.9 (continued):** Selection of phytochemicals isolated previously from *R .raetam.*
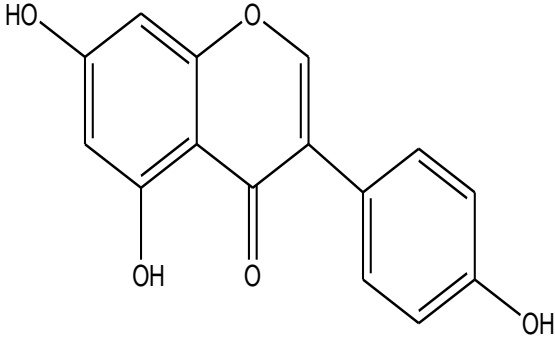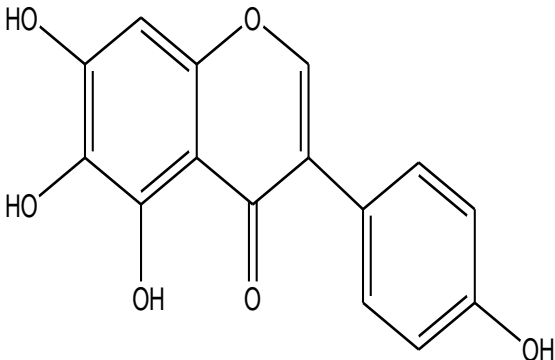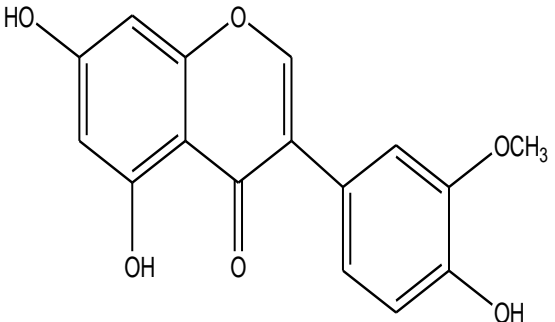
| Compound | Code | Parts of the plant | Reference |
|---|---|---|---|
| Genistein<br> | **Rr-7** | Aerial parts of *R. raetam* | (Djeddi *et al.*, 2013) |
| 6-Hydrogenistein<br> | **Rr-8** | Aerial parts of *R. raetam* | (Djeddi *et al.*, 2013) |
| 3′-Methylorobol<br> | **Rr-9** | Aerial parts of *R. raetam* | (Djeddi *et al.*, 2013) |

**Table 1.9 (continued):** Selection of phytochemicals isolated previously from *R. raetam.*
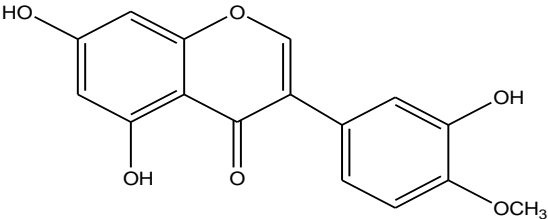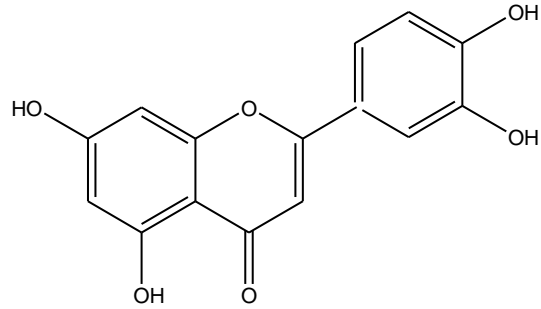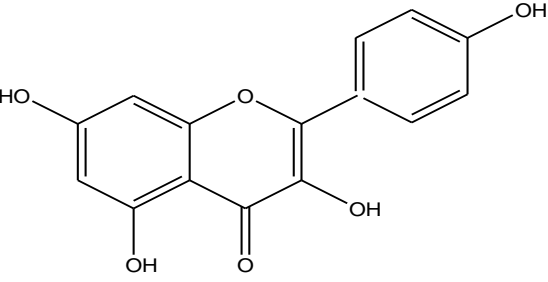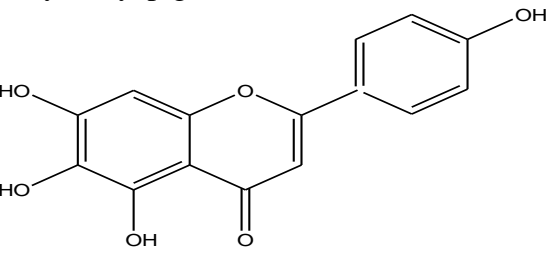
| Compound | Code | Parts of the plant | Reference |
|---|---|---|---|
| Pratensein  | **Rr-10** | Aerial parts of *R. raetam* | (Djeddi *et al.*, 2013) |
| Luteolin  | **Rr-11** | Aerial parts of *R. raetam* | (Djeddi *et al.*, 2013) |
| Kaempferol  | **Rr-12** | Aerial parts of *R. raetam* | (Djeddi *et al.*, 2013) |
| 6-Hydroxyapigenin  | **Rr-13** | Aerial parts of *R. raetam* | (Djeddi *et al.*, 2013) |

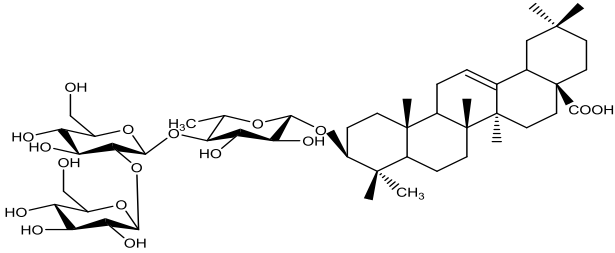**Table 1.9 (continued):** Selection of phytochemicals isolated previously from *R. raetam.*
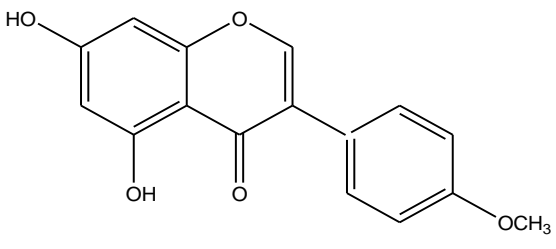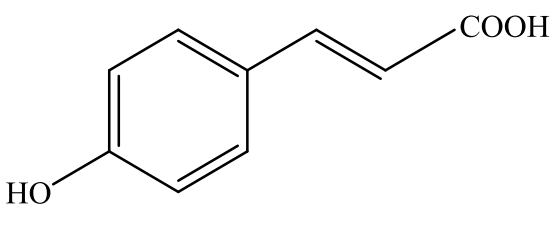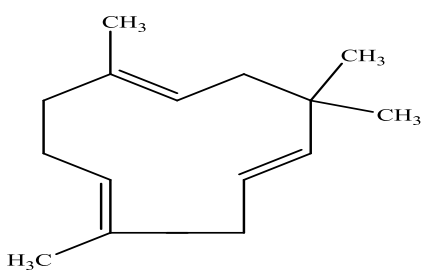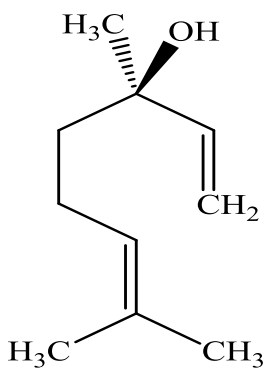
| Compound | Code | Parts of the plant | Reference |
|---|---|---|---|
| Biochanin<br> | **Rr-14** | Aerial parts of *R. raetam* | (Djeddi *et al.*, 2013) |
| *p*-Coumaric acid<br> | **Rr-15** | Aerial parts of *R. raetam* | (Djeddi *et al.*, 2013) |
| α-humulene<br> | **Rr-16** | Flowers of *R. raetam* | (Edziri *et al.*, 2010) |
| Linalool<br> | **Rr-17** | Flowers of *R. raetam* | (Edziri *et al.*, 2010, Awen *et al.*, 2011) |

**Table 1.9 (continued):** Selection of phytochemicals isolated previously from *R. raetam.*
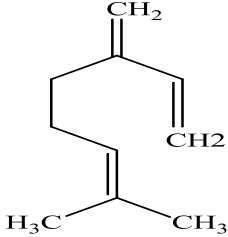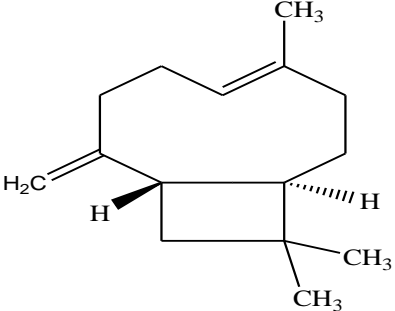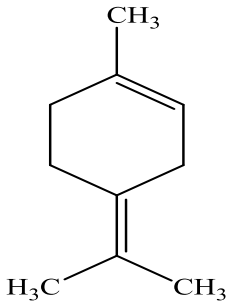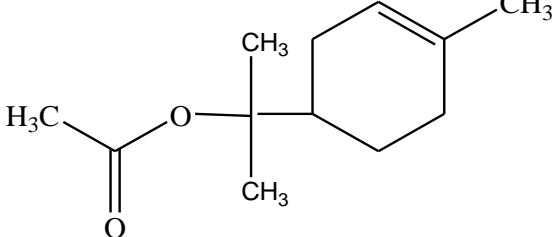
| Compound | Code | Parts of the plant | Reference |
|---|---|---|---|
| β-Myrcene  | **Rr-18** | Flowers of *R. raetam* | (Edziri *et al.*, 2010) |
| β-caryophyllene  | **Rr-19** | Flowers of *R. raetam* | (Edziri *et al.*, 2010) |
| Terpinolene  | **Rr-20** | Flowers of *R. raetam* | (Edziri *et al.*, 2010, Awen *et al.*, 2011) |
| α-terpinyl acetate  | **Rr-21** | Flowers of *R. raetam* | (Edziri *et al.*, 2010) |

**Table 1.9 (continued):** Selection of phytochemicals isolated previously from *R. raetam.*
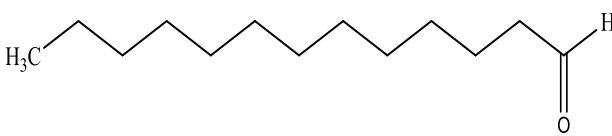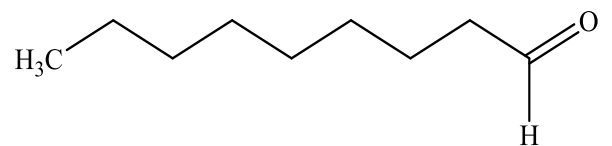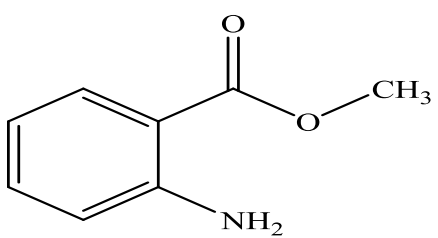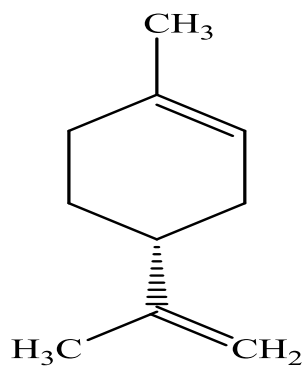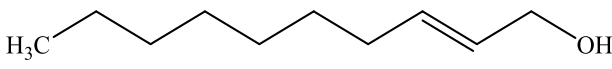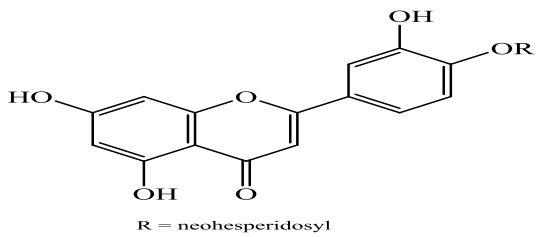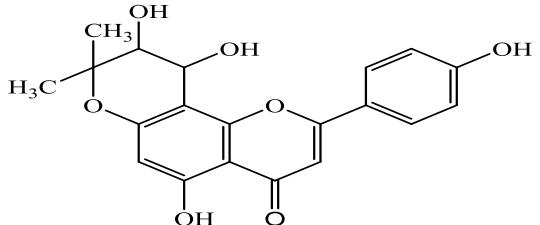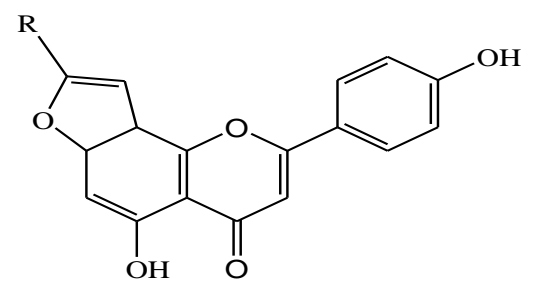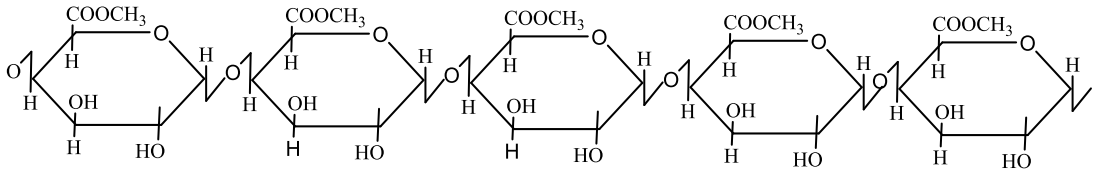
| Compound | Code | Parts of the plant | Reference |
|---|---|---|---|
| Tridecanal  | **Rr-22** | Flowers of *R. raetam* | (Edziri *et al.*, 2010) |
| Nonanal  | **Rr-23** | Flowers of *R. raetam* | (Edziri *et al.*, 2010) |
| Methyl anthranilate  | **Rr-24** | Flowers of *R. raetam* | (Edziri *et al.*, 2010) |
| Limonene  | **Rr-25** | Flowers of *R. raetam* | (Awen *et al.*, 2011) |
| 2-Decen-1-ol  | **Rr-26** | Flowers of *R. raetam* | (Awen *et al.*, 2011) |

**Table 1.9 (continued):** Selection of phytochemicals isolated previously from *R. raetam.*

| Compound | Code | Parts of the plant | Reference |
|---|---|---|---|
| Luteolin 4′-*O*-neohesperidoside<br><br>R = neohesperidosyl | **Rr-27** | Aerial parts of *R. raetam* | (Kassem *et al.*, 2000) |
| 5,4′-(dihydroxy-3″,4″-dihydro-3″,4″-dihydroxy)-2″,2″-dimethylpyrano-(5″,6″:7,8)-flavone<br> | **Rr-28** | Aerial parts of *R. raetam* | (Kassem *et al.*, 2000) |
| Furanoflavonoids<br><br>R = OH    Retamasin A<br>R = H     Retamasin B | **Rr-29** | Aerial parts of *R. raetam* | (Xu *et al.*, 2015) |
| Pectin<br> | **Rr-30** | Flowers of *R. raetam* | (Kacem *et al.*, 2008) |

### 1.4.3.2.1 Antimicrobial activity

Edziri *et al.* (2010) observed that the oil of *R. raetam* had a variation of minimal inhibitory concentrations (MIC) between 0.625 and 5 mg/ml against some bacteria and yeast using a microdilution assay. The oil had superior minimum bactericidal concentrations (MBC) to 5 mg/ml for most strains (Edziri *et al.*, 2010). Similarly, Awen *et al.,* (2011) reported that the oil obtained from *R. raetam* had antibacterial activity against microorganisms, such as *S. aureus*, with an inhibition zone value of 5.0 mm and MIC of 3.0 mg/ml (Awen *et al.*, 2011). In addition, Edziri *et al.* (2012) found that two flavonoid compounds (derrone and licoflavone) isolated from *R. raetam* had antibacterial activity against *E. coli* and *P. aeruginosa* with (MIC) 7.81–15.62 µg/ml using a microdilution method with standard antibiotics (amoxicillin, amphotericin, cefotaxim, oxacillin and ticarcillin). While derrone showed strong fungicidal action against *Candida* species with an inhibition zone of 7.81 µg/ml using disc a diffusion method with standard antibiotics (gentamycin and amphotericin B) (Edziri *et al.,* 2012).

### 1.4.3.2.2 Antidiabetic activity

Algandaby *et al.* (2010) tested for potential antihyperglycemic activity of *R. raetam* fruits by administering a MeOH extract to streptozotocin-induced diabetic rats. Oral $LD_{50}$ of the extract was found to be 1995 mg/kg. The extract was administered once orally to STZ-diabetic rats at three dose levels; 100, 250 or 500 mg/kg/day for 4 consecutive weeks. The result demonstrated that the extract at 250 or 500 mg/kg significantly lowered blood glucose levels at the 1$^{st}$ and 3$^{rd}$ week of treatment (Algandaby *et al.*, 2010).

### 1.4.3.2.3 Analgesic activity

Djeddi *et al.* (2013) evaluated the isolated compounds described in section 1.4.3.2 for their analgesic and antioxidant activities using the writhing test where Swiss mice under controlled conditions were divided into three groups of six mice each. The first group was treated with all compounds intra-peritoneally (i.p) at a dose of 1 mg/kg, while the second group was administered i.p aspirin (200mg/kg), and the third group served as a control treated with 10 ml/kg of saline (i.p). Following this, all the mice were injected with 10 ml/kg (i.p) of 1% (v/v) acetic acid 30 min after treatment and

the number of writing s was recorded for 30 min. The results showed analgesic activity of **Rr-7**, **Rr-8**, **Rr-9**, **Rr-10** and **Rr-14** isoflavones isolated from *R. raetam* (Djeddi *et al.*, 2013).

### 1.4.3.2.4 Antioxidant activity

Conforti *et al.* (2004) observed that the MeOH extract of *R. raetam* leaves had strong antioxidant activity compared with an extract of the seeds with an $IC_{50}$ value of 0.059% (w/v) and 0.122% (w/v) respectively using a DPPH free-radical scavenging assay and lipid peroxidation of liposomes assay (Conforti *et al.*, 2004). Also Edziri *et al.* (2010) found that the oil obtained from *R. raetam* showed antioxidant activity using the DPPH assay with an $IC_{50}$ value of 0.800 mg/ml compared to control butylated hydroxytoluene (BHT) with an $IC_{50}$ value of 20 mg/ml (Edziri *et al.*, 2010). On the other hand, Djeddi *et al.* (2013) observed that the extracts of *R. raetam* had very low antioxidant activity compared to the control BHT and lower hydrogen peroxide blocking activity than the positive control gallic acid using the DPPH assay and hydrogen peroxide scavenging activity (Djeddi *et al.*, 2013).

### 1.4.3.2.5 Cytotoxic activity:

Conforti *et al.* (2004) tested the MeOH extract of *R. raetam* leaves and seeds against COR-L23 cells (Human large cell carcinoma) using vinblastine (2 μg/ml) as the positive control. The MeOH extract of *R. raetam* subsp. Gussonei leaves showed cytotoxic activity with an $IC_{50}$ of 40 μg /ml (Conforti *et al.*, 2004).

In addition, Edziri *et al.* (2012) found that the two flavonoids derrone and licoflavone from *R. raetam* flowers showed strong cytotoxic activity against Hep-2 cells (human liver cell carcinoma) with $IC_{50}$ values of 9 μg/ml and 30 μg/ml respectively, using a MTT assay (Edziri *et al.*, 2012).

### 1.4.4 *Psoralea plicata*

The genus Psoralea includes about 130 species, mainly tropical and widely distributed in tropical and temperate regions such as Pakistan, India, Saudi Arabia, Egypt, Tunsia, and South of Africa and represented by two species in Libya, *P. plicata* and *P. bituminosa*. *P. plicata* (Delile) (Figure 1.6). It is known in Arabic as Annam and is a small shrub belonging to the Fabaceae family.

**Figure 1.6:** Aerial part of *Psoralea plicata*, and image of the plant taken from https://www.google.com/search?q=Psoralea+plicata,&rlz=1C1GCEU_enGB821GB822&sxsrf=AOaemvJaO0qSo6n__PLWcw58Bjc-vmALaA:1635803591708&source=lnms&tbm=isch&sa=X&ved=2ahUKEwi65oWgk_jzAhVMQUEAHRUwC74Q_AUoAXoECAEQAw&biw=1455&bih=717&dpr=1.1#imgrc=KISzv-pQ1z-nVM   Abohamam , 2017 website

### 1.4.4.1 Traditional uses

The common uses of *P. plicata* are as an anthelmintic, analgesic and, anti-inflammatory. The seeds decoction and powder are used to cure dermal diseases such as psoriasis. The roots of *P. plicata* are used as toothpicks (Cheikh *et al.*, 2015).

### 1.4.4.2 Active ingredients and biological activities

Rasool *et al.* (1989) isolated psoracinol (**Pp-6**) from the nonsaponifiable residue of an *n*-hexane-soluble fraction after extracting the plant material of *P. plicata* with EtOH at room temperature. The residue obtained from the EtOH extract was partitioned with $CHCl_3$ and $H_2O$. The *n*-hexane–soluble portion of the $CHCl_3$ fraction saponified with 5% alcoholic potash and worked up to the obtained compound. The nonsaponified fraction was subjected to silica gel column separation and eluted with solvents by increasing polarity and when oxidised **Pp-6** yielded psoracinone (**Pp-9**) (Rasool *et al*., 1989). In 1990, Rasool *et al.* extracted the plant with alcohol at room temperature. The residue obtained from the extraction was partitioned between $CHCl_3$ and water, and the *n*-hexane–soluble portion of the $CHCl_3$ fraction was subjected to silica gel column chromatography and eluted with solvents depending on polarity. The *n*-hexane: $CHCl_3$ (1:4) fraction was purified through preparative TLC that led to isolated two new phenolic cinnamates, plicatin A (**Pp-1**). The fraction *n*-hexane:$CHCl_3$ (5:3) was crystalised that led to plicatin B (**Pp-4**) being isolated (Rasool *et al*., 1990). Rasool *et al.* (1991) extracted the plant with EtOH then dissolved in water, extracted

with CHCl$_3$ and finally dried with Na$_2$SO$_4$. The *n*-hexane soluble fraction was subjected to the column using *n*-hexane and EtOAc as the eluant. The fraction *n*-hexane: EtOAc (3:7) led to isolation of plicadin (**Pp-7**) and fraction *n*-hexane: EtOAc (2:7) led to isolation of α-tocopherolquinone methyl ether (**Pp-25**) (Rasool *et al*., 1991). In 1997, Hamed *et al*. extracted *P. plicata* seeds by macerating with MeOH then the residue-free solvent was mixed with 100 ml water 50 ml MeOH, and partitioned between *n*-hexane, EtOAc and n-BuOH. The fractions of *n*-hexane, EtOAc and BuOH were subjected to column chromatography (CC). β-caryophyllene oxide (**Pp-15**), α-tocopherol(**Pp-13**), z-werneria (**Pp-14**), e-werneria (**Pp-16**) two furanocoumarins, bakuchicin (**Pp-23**) and psoralen (**Pp-2a**), plicatin B (**Pp-4**), Lupeol (**Pp-11**) and stigmasterol (**Pp-12**) were obtained from the *n*-hexane-soluble fraction and plicatin–A (**Pp-1**), 3-(-3-methyl-2,3-epoxybutyl)-p-coumaric acid methyl ester (**Pp-24**) and a new dimer α-diplicatin-B (**Pp-10**) were obtained from the EtOAc-soluble fraction. Roseside A (**Pp-18**), daidzein (**Pp-3**), isopsoralic acid–[4←1]*O-β*-D-gluco-pyranoside acetate (**Pp-19**) and isovitexin (**Pp-8**) were obtained from the BuOH-soluble fraction (Hamed *et al*., 1997). Likewise, in 1999, Hamed isolated three new benzofuran glycosides from a BuOH-soluble fraction of *P. plicata* seeds as (**Pp-19**), isocorylifonol [4←1]-*O-β*-D-glucopyranoside acetate (**Pp-20**), psoralic acid – [6←1]-*O- β* -D-gluco–pyranoside acetate (**Pp-21**) and corylifonol [6←1]-*O- β* -D-gluco-pyranoside acetate (**Pp-22**) (Hamed *et al*., 1999). El-Abgy *et al*. (2012) isolated flavonoid compounds from the MeOH of *P. plicata* dried aerial parts by maceration, concentrated it and mixed with MeOH the residue and H$_2$O. The solvent was separated and partitioned between *n*-hexane, EtOAc and BuOH. Each fraction was subjected to CC which was eluated with an *n*-hexane-EtOAc gradient. This method led to isolating psoralen (**Pp-2a**), analgicin (**Pp-2b**), plicatin-B (**Pp-4**), and chromen compounds isolated from the *n*-hexane soluble fraction. *p*-dimethylcoumaric acid (**Pp-26**), plicatin–A (**Pp-1**) and α-diplicatin-B (**Pp-10**) were isolated from the EtOAc soluble fraction while isovitexin (**Pp-8**), psoralic acid (**Pp-27**), roseside A (**Pp-18**) and daidzein (**Pp-3**) were isolated from the BuOH soluble fraction (El-Abgy *et al.,* 2012). Arfaoui *et al*. (2013) isolated some compounds from the MeOH soluble fraction of *P. plicata* seeds as a new cyclobutane ring system β-diplicatin-B (**Pp-17**), lolilide (**Pp-5**) and phloretic acid ethyl ester (**Pp-28**) (Arfaoui *et al*., 2013).

**Table 1.10:** Selection of phytochemicals isolated previously from *P. plicata.*

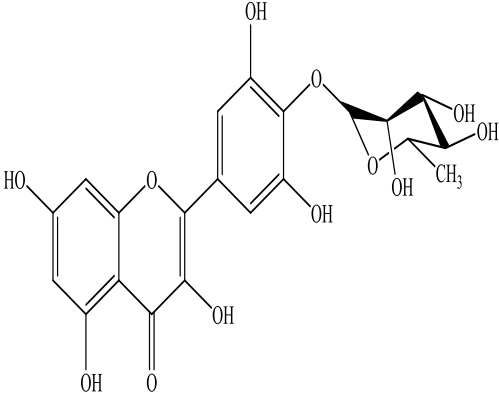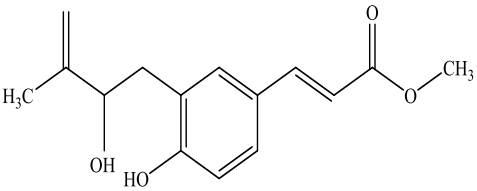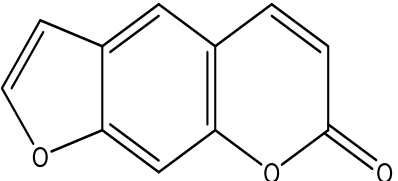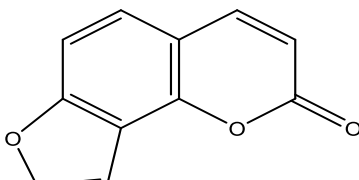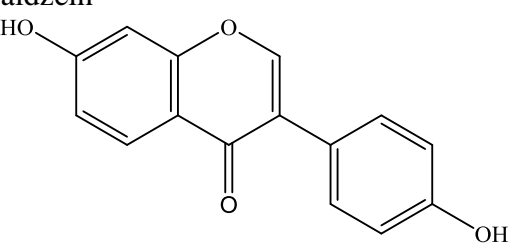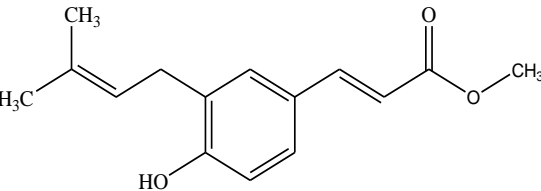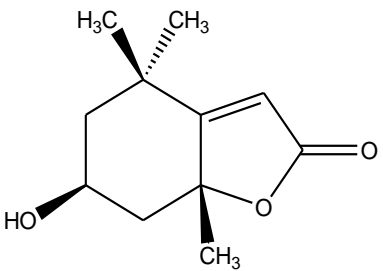| Compound | Code | Parts of the plant | Reference |
|---|---|---|---|
| Plicatin A | **Pp-1** | Aerial parts of *P. plicata* | (Rasool *et al.*, 1990, Hamed *et al.*, 1997) |
| Psoralen | **Pp-2a** | Aerial parts of *P. plicata* | (Hamed *et al.*, 1997) |
| Angelicin | **Pp-2b** | Aerial parts of *P. plicata* | (El-Abgy *et al.*, 2012) |
| Daidzein | **Pp-3** | Aerial parts of *P. plicata* | (Hamed *et al.*, 1997) |
| Plicatin B | **Pp-4** | Aerial parts of *P. plicata* | (Rasool *et al.*, 1990, Rasool *et al.*, 1991, Hamed *et al.*, 1997, Arfaoui et al., 2013) |
| Loliolide | **Pp-5** | Dried griended seeds of *P. plicata* | (Arfaoui *et al.*, 2013) |

**Table 1.10 (continued):** Selection of phytochemicals isolated previously from *P. plicata.*
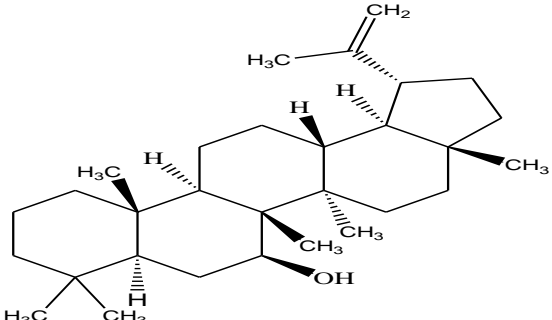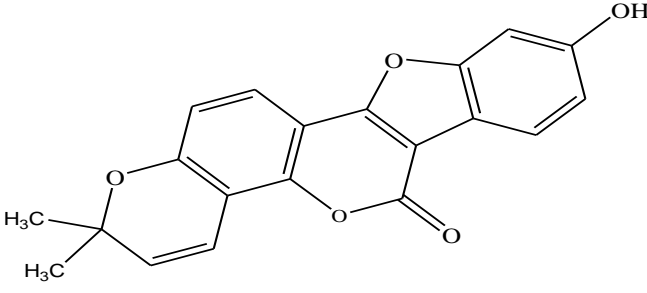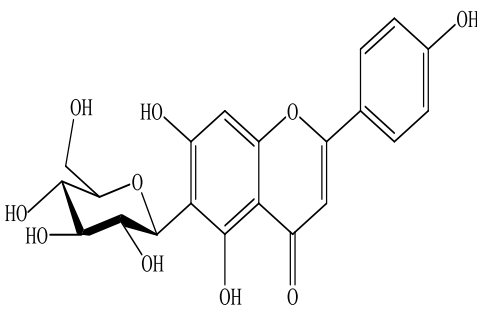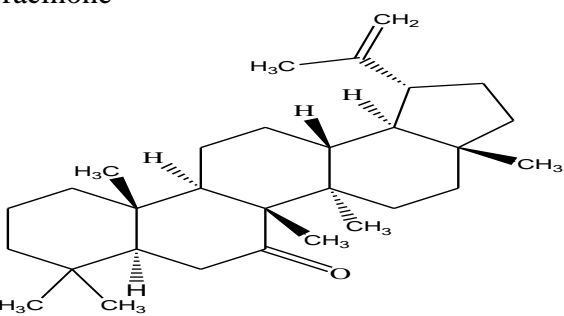
| Compound | Code | Parts of the plant | Reference |
|---|---|---|---|
| Psoracinol  | **Pp-6** | Aerial parts of *P. plicata* | (Rasool *et al.*, 1989) |
| Plicadin  | **Pp-7** | Aerial parts of *P. plicata* | (Rasool *et al.*, 1991) |
| Isovitexin  | **Pp-8** | Aerial parts of *P. plicata* | (Hamed *et al.*, 1997) |
| Psoracinone  | **Pp-9** | Aerial parts of *P. plicata* | (Rasool *et al.*, 1989) |

**Table 1.10 (continued):** Selection of phytochemicals isolated previously from *P. plicata.*
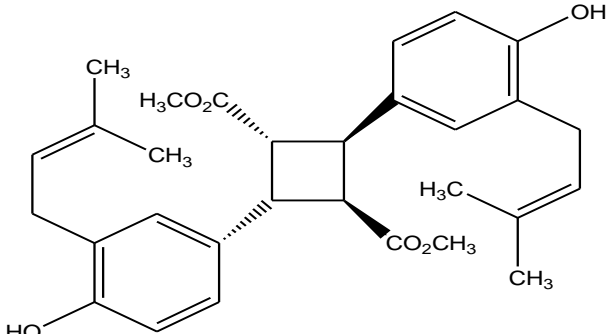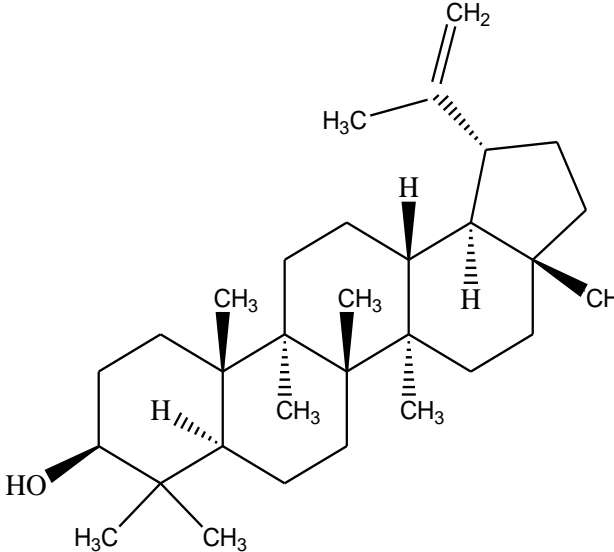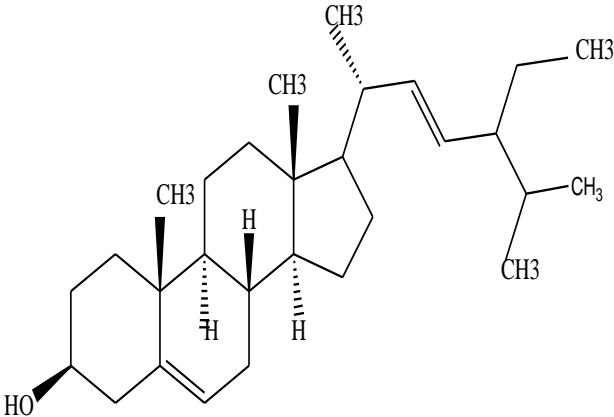
| Compound | Code | Parts of the plant | Reference |
|---|---|---|---|
| α-diplicatin B  | **Pp-10** | Aerial parts of *P. plicata* | (Hamed *et al.*, 1997) |
| Lupeol  | **Pp-11** | Aerial parts of *P. plicata* | (Hamed *et al.*, 1997) |
| Stigmasterol  | **Pp-12** | Aerial parts of *P. plicata* | (Hamed *et al.*, 1997) |

**Table 1.10 (continued):** Selection of phytochemicals isolated previously from *P. plicata.*
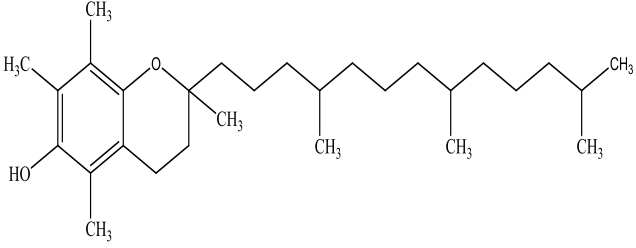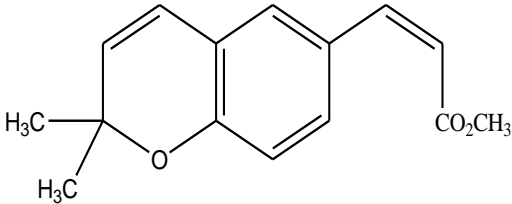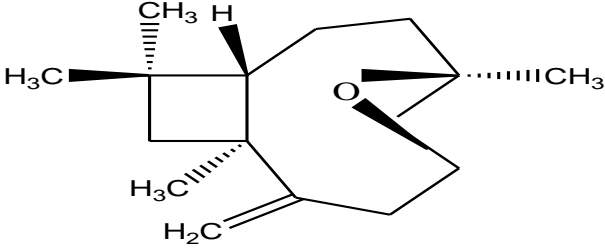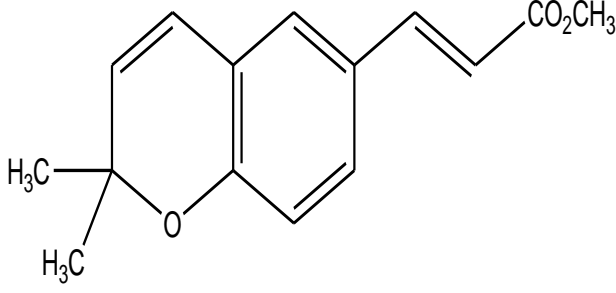
| Compound | Code | Parts of the plant | Reference |
|---|---|---|---|
| α-Tocopherol  | **Pp-13** | Aerial parts of *P. plicata* | (Hamed *et al.*, 1997) |
| Z-Werneria Chromenes  | **Pp-14** | Aerial parts of *P. plicata* | (Hamed *et al.*, 1997) |
| β-caryophyllene oxide  | **Pp-15** | Aerial parts of *P. plicata* | (Hamed *et al.*, 1997) |
| E-Werneria Chromenes  | **Pp-16** | Aerial parts of *P. plicata* | (Hamed *et al.*, 1997) |

**Table 1.10 (continued):** Selection of phytochemicals isolated previously from *P. plicata.*
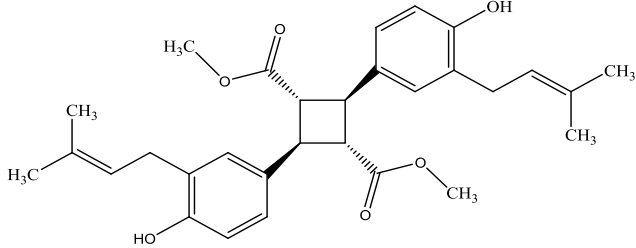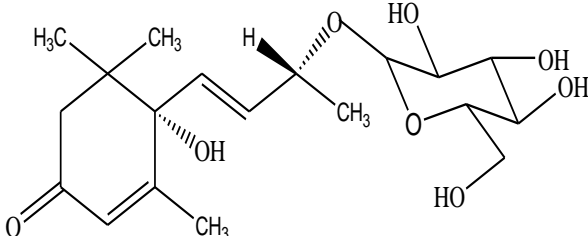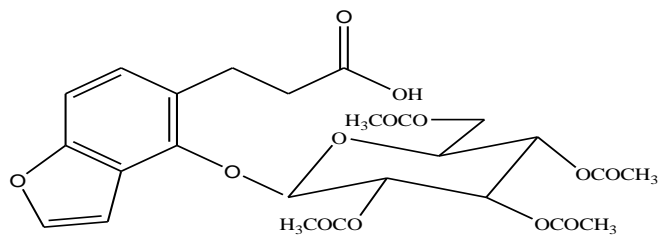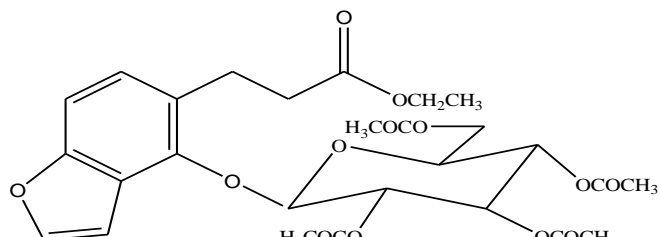
| Compound | Code | Parts of the plant | Reference |
|---|---|---|---|
| β-diplicatin B  | **Pp-17** | Aerial parts of *P. plicata* | (Arfaoui *et al.*, 2013) |
| Roseoside A  | **Pp-18** | Aerial parts of *P. plicata* | (Hamed *et al.*, 1997) |
| Isopsoralic acid -(4←1) *O-β*-D-gluco-pyranoside acetate.  | **Pp-19** | Aerial parts of *P. plicata*, Seeds of *P. plicata* | (Hamed *et al.*, 1997, Hamed *et al.*, 1999) |
| Isocorylifonol (4←1)- *O-β*-D-gluco-pyranoside acetate.  | **Pp-20** | Seeds of *P. plicata* | (Hamed *et al.*, 1999) |

**Table 1.10 (continued):** Selection of phytochemicals isolated previously from *P. plicata.*
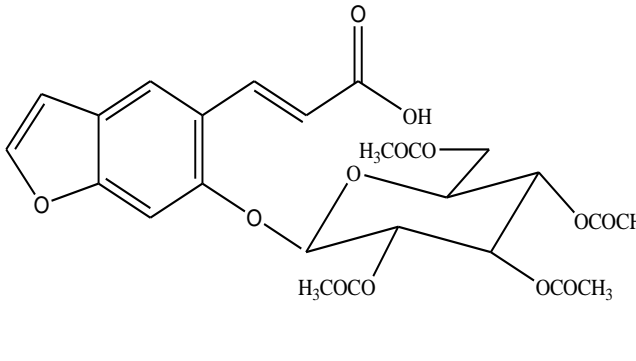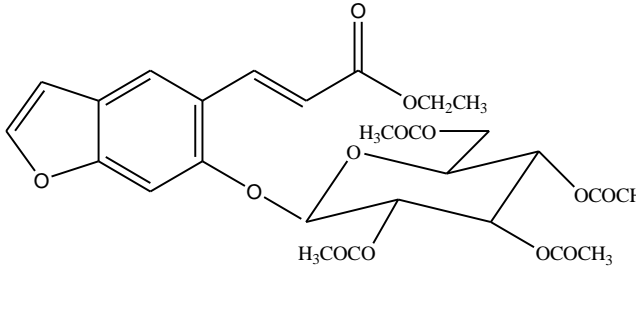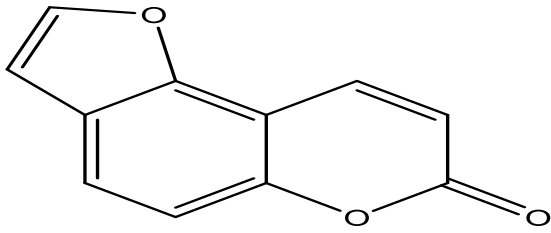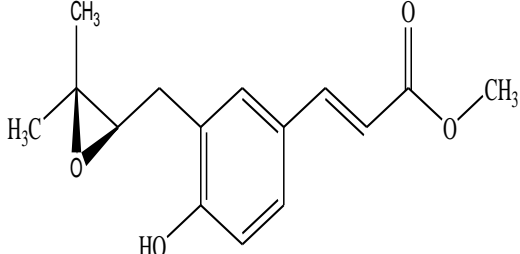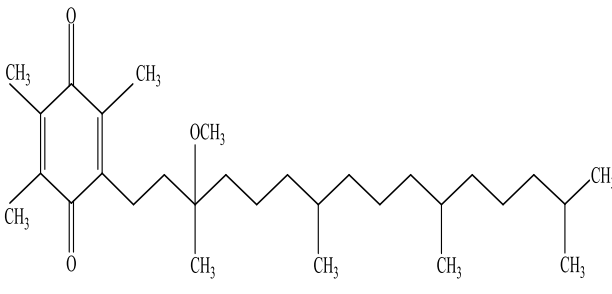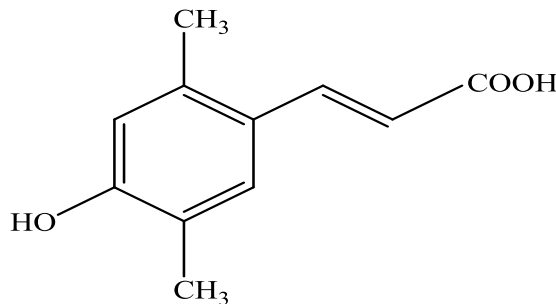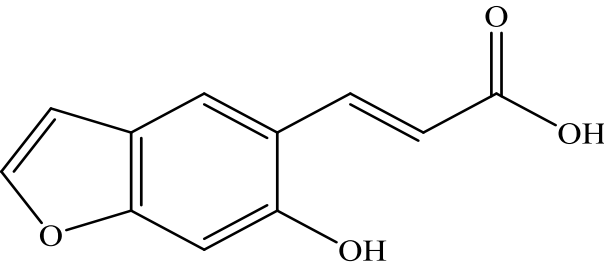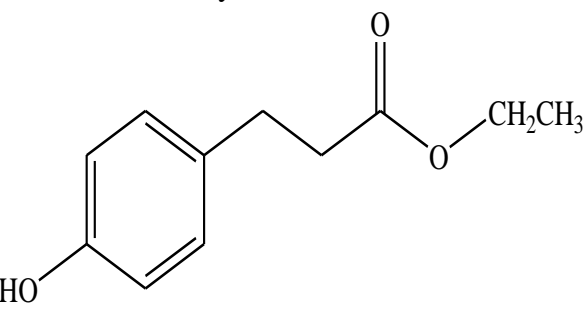
| Compound | Code | Parts of the plant | Reference |
|---|---|---|---|
| Psoralic acid - (6←1)-*O-β*-D-gluco-pyranoside acetate.  | **Pp-21** | Seeds of *P. plicata* | (Hamed *et al.,* 1999) |
| Corylifonol (6←1)-*O*-β-D-gluco-pyranoside acetate.  | **Pp-22** | Seeds of *P. plicata* | (Hamed *et al.*, 1999) |
| Bakuchicin  | **Pp-23** | Aerial parts of *P. plicata* | (Hamed *et al.*, 1997) |
| 3-(-3-methyl-2,3-epoxybutyl)-*p*-coumaric acid methyl ester  | **Pp-24** | Aerial parts of *P. plicata* | (Hamed *et al.*, 1997) |

**Table 1.10 (continued):** Selection of phytochemicals isolated previously from *P. plicata.*

| Compound | Code | Parts of the plant | Reference |
|---|---|---|---|
| α-Tocopherolquinone methyl ether  | **Pp-25** | Aerial parts of *P. plicata* | (Rasool *et al.,* 1991) |
| p-dimethylcoumaric acid  | **Pp-26** | Aerial parts of *P. plicata* | (El-Abgy *et al.,* 2012) |
| Psoralic acid  | **Pp-27** | Aerial parts of *P. plicata* | (El-Abgy *et al.,* 2012) |
| Phloretic acid ethyl ester  | **Pp-28** | Aerial parts of *P. plicata* | (Arfaoui *et al.,* 2013) |

## 1.4.4.2.1 Anti-mosquito activity

El-Abgy *et al.* (2012) evaluated the flavonoid compounds isolated from a MeOH extract of *P. plicata* leaves as an anti-mosquito agent. They found that the percentage of the hatchability larvae of *Culex pipiens pipiens* was decreased by chromene compound at concentration 0.0032 ppm with 43%, while 90% and 79% by plicatin-β (**Pp-4**) and isovitexin (**Pp-8**) respectively. But psoralen (**Pp-2a**) and α- diplicatine B (**Pp-10**) compounds did not effect on hatchability at 0.0032 and 0.0064 concentration. On the other hand, plicatin-β (**Pp-4**) and chromene showed highly effect against larvae duration and the percentage of the dead larvae of *C. pipiens pipiens* with 96.98 and 85.75% respectively. While psoralen (**Pp-2a**) and analgicin (**Pp-2b**) showed a moderate effect with 72.33% and 78.89% respectively, but α- diplicatine B (**Pp-10**) was less active against larvae duration (56.75%). Therefore, only plicatin B (**Pp-4**) and chromene showed the strongest insecticide activity (El-Abgy *et al.*, 2012).

## 1.4.3.2.2 Antioxidant activity

Cheikh *et al.* (2015) evaluated the antioxidant activity of fruit extracts of *P. plicata* by using a DPPH assay. The study illustrated that a MeOH extract showed antioxidant activity (288.32 µmol Trolox equivalent/100 g dry material) which is slightly higher to *P. plicata* aqueous extract (258,65 µmol Trolox equivalent/100 g dry material) (Cheikh *et al.*, 2015).

## 1.5 Aims and Objectives

The present study aimed to examine plants from Libya in search of cytotoxic agents which could be effective against cancer cells and not affect normal cells. Cancer was chosen because it is a very common disease and a leading cause of death in the world. The objectives of the work were to:

- Purify phytochemicals from selected plant extracts, using techniques such as TLC, VLC, CC, solvent extraction and PTLC.

- Elucidate the structures of isolated compounds using $^1$H and $^{13}$C nuclear magnetic resonance (NMR), including extensive two-dimensional $^1$H-$^1$H homonuclear (COSY, NOESY) and $^1$H - $^{13}$C heteronuclear (HMBC, HSQC) experiments and mass spectrometry (MS).

- Screen extracts and isolated compounds for activity against cancer cell lines HepG2 (hepatocarcinoma), A375 (melanoma), A549 (lung carcinoma), PANC-1 (pancreas carcinoma), MCF7 (breast adenocarcinoma), LNCaP (prostate carcinoma) and non-cancer PNT2 normal (prostate) using a resazurin assay.

- Further study to investigate whether any active extract(s) and compound(s) affected cell morphology, viability, adhesion, migration and invasion of cancer cells chosen from the screen above.

# Chapter 2

# *Materials and Methods*

## 2. Materials and methods

### 2.1 Solvents

Solvents listed below were used for the different methods of extraction, chromatographic separation and analytical TLC. All the solvents were stored at room temperature and transferred to 500 ml solvent bottles for routine use. Deuterated (99.9%) solvents ($CD_3COCD_3$, $CDCl_3$, DMSO-$d_6$ and $CD_3OD$) were utilised for the NMR analysis.

- *n*-Hexane (HPLC grade, VWR, UK Ltd)
- Acetone (Analytical grade, VWR, UK Ltd)
- Deuterated acetone ($CD_3COCD_3$) (Sigma-Aldrich, UK Ltd)
- Deuterated chloroform ($CDCl_3$) (Sigma-Aldrich, UK Ltd)
- Deuterated dimethyl sulfoxide (DMSO -$d_6$) (Sigma-Aldrich, UK Ltd)
- Deuterated methanol (methanol –$d_4$) (Sigma-Aldrich, UK Ltd)
- Ethanol (Analytical grade, VWR, UK Ltd)
- Ethyl acetate (HPLC grade, VWR, UK Ltd)
- Methanol (HPLC grade, VWR, UK Ltd)

### 2.2 Chemicals and materials

#### 2.2.1 Phytochemistry

- Anisaldehyde (FSA laboratory, UK)
- Anti-bumping granules (BDH, UK)
- Column grade silica gel (Silica gel 60, mesh size 20-200 μm (Merck, Germany)
- Lipophilic Sephadex LH-20 (Sigma Aldrich, UK)
- Non-adsorption cotton wool (Fisher Scientific, UK)
- Silica gel 60 H for TLC (Merck, Germany)
- Silica gel 60 0.063-0.200 mm for column chromatography (Merck, Germany)
- TLC grade silica gel (60H, Merck, Germany)
- TLC grade silica gel coated aluminium sheet (Precoated Silica gel PF254, Merck, Germany)

### 2.2.2 Biology

- 1% Virkon® (Antec International, UK)
- DMEM (Dulbecco's Modified Eagle's Medium) (Sigma Aldrich, UK)
- Foetal Bovine Serum (FBS) (Invitrogen, UK)
- L-glutamine (Thermo Fisher Scientific Inc, UK)
- $Mg^{2+}$- $Ca^{2+}$- free Hank's balanced salt solution (HBSS) (Invitrogen, UK)
- Non-essential amino acids (Thermo Fisher Scientific Inc, UK)
- Resazurin sodium salt (Sigma Aldrich, Germany)
- RPMI 1640 medium (Roswell Park Memorial Institute) (Sigma-Aldrich Ltd, UK)
- Sodium pyruvate (Thermo Fisher Scientific Inc, UK)
- Streptomycin/ Penicillin (Cambrex, UK)
- TrypLE Express (Invitrogen, UK)

## 2.3 Equipment

### 2.3.1 Phytochemistry

- A sintered glass Buchner filter funnel (Schott Duran, Germany)
- Avance DRX500 MHz NMR (Bruker, UK)
- Balance (Mettler Toledo, UK)
- Decon Sanicator (Decon laboratories, UK)
- Edwards freeze dryer ((Edwards, UK)
- Jeol Eclipse 400 MHz NMR spectrometer (Jeol, USA)
- LC-MS (Thermo fisher, UK)
- NMR tubes (5mm x178 mm, Sigma-Aldrich, UK)
- Orbitrap HRESI mass spectrometer (Thermo Fisher, UK)
- Rotary evaporator (Büchi, Switzerland)
- Safety Cabinet (Walker Safety Cabinets Ltd, UK)
- Soxhlet apparatus (Quickfit, UK)
- TLC tank
- UV-detector 254 nm and 364 nm UVGL-58 (UVP, USA)
- Water Bath (Grant Instruments Ltd, UK)

## 2.3.2 Biology

- - 80C freezer (Sanyo, CFC free)
- 25 cm$^2$ and 75 cm$^2$ sterile flask (Thermo Fisher, UK)
- 96 well plates (Sigma-Aldrich, UK)
- 0.22 μm filter unit (Millipore, UK)
- Centrifuge 5415D (Eppendorf, Germany)
- Cryovials (Cryotube TM vials, Nunc)
- CytoSelect™ 48-Well Cell Adhesion Assay (Fibronectin-Coated, Colorimetric Format) (Cell Biolabs, Inc, USA)
- CytoSelect™ 24-Well Cell Migration Assay (8μm, Colorimetric Format) (Cell Biolabs, USA)
- CytoSelect™ 24-Well Cell Invasion Assay (Basement Membrane, Colorimetric Format) (Cell Biolabs, USA)
- Decon (Decon laboratories, UK)
- Edwards freeze dryer (Edwards, UK)
- Forceps (Sigma-Aldrich, UK)
- Haemocytometer (Hawksley, UK)
- Microscope (Olympus, Japan)
- Safety Cabinet (Walker Safety Cabinets Ltd, UK)
- SpectraMax M5 Microplate Reader (Molecular Devices, USA)
- Water Bath (Grant Instruments Ltd, UK

## 2.4 Plant material

The aerial parts of plants were collected from different areas in Libya in 2015 (Table 2.1). The plant materials were identified by Prof. Mohamed Makhloof at the Herbarium of the Botany Department, Faculty of Science, Tripoli University, Tripoli, Libya. The plants were air-dried to prevent mould or any type of degradation. The dried plant materials were ground to a fine powder using a blender and stored at -20°C until analysed.

**Table 2.1:** Collection details of plants and amount used in the study.

| Plant Species | Location and Time | Plant Amount |
|---|---|---|
| *Bougainvillea spectabilis* | Ain Zara -Tripoli [1], Libya March 2015 | 500 g |
| *Alhagi graecorum* | Samno-Sebha [3], Libya December 2015 | 310 g |
| *Retama raetam* | Aljahawat-Alkhums [1], Libya April 2015 | 500 g |
| *Psoralea plicata* | Alfataeah – Derna [2], Libya June 2015 | 300 g |

Tripolitania[1], Cyrenica[2], Fezzan[3]

## 2.5 Extraction and Partitioning

### 2.5.1 Soxhlet extraction

The plant materials were extracted in a Soxhlet apparatus using different solvents starting with low to high polarity (*n*-hexane, EtOAc and finally MeOH or EtOH 3.5 L each) for days with each solvent. All extracts were evaporated at 40°C under vacuum using a rotary evaporator.

## 2.6 Fractionation work and isolation of compounds

Several chromatographic techniques were used for the isolation of compounds from the crude solvent extracts.

### 2.6.1 Analytical thin-layer chromatography (TLC)

TLC was used to screen crude extracts and fractions. It was also used to analyse the collected fractions from different separation methods. In addition, it was used to choose the elution system for mobile phases of other separation methods such as CC, and VLC. The fractions were dissolved in an appropriate solvent and spotted approximately 1cm above the bottom edge of a TLC grade silica gel coated aluminium sheet. Solvent combinations of *n*-hexane, *n*-hexane/EtOAc or EtOAc/MeOH were used as mobile phases depending on the expected polarity of the sample under analysis.

The filter paper was placed inside the tank to saturate the jar with solvent. Spotted TLC plates were then placed in the TLC tank to develop in an ascending direction. The TLC plates were taken out of the tank, the solvent front was marked with a pencil line and the plates air-dried immediately. Firstly, plates were examined under UV light using short ($\lambda$=254 nm) and long ($\lambda$=366 nm) wavelengths and subsequently sprayed with anisaldehyde-sulphuric acid spray (5 ml $H_2SO_4$, 85 ml MeOH, 10 ml glacial acetic acid and 0.5 ml anisaldehyde) and heated at 110°C for a min to allow the colour to develop. The R$f$ values for each spot were calculated by dividing the distance the spot travelled, by the distance of the solvent front. TLC was used to pool similar fractions together, which were then dried and further analysed by NMR to attempt to elucidate the structure of the compounds (Gray *et al.*, 2012).

### 2.6.2 Preparative TLC

This technique was mostly used for some fractions which required separating and purifying in low amounts. TLC plates $20 \times 20$ cm were used for fractions which were dissolved in a small amount of MeOH and spotted on TLC plates ($20 \times 20$ cm) as a narrow streak about 2.5 cm from the bottom. The plate was allowed to dry and then developed in an appropriate solvent system. After drying, the plate was observed under UV light (sometimes sprayed at one side with a suitable reagent if they were invisible), and the bands were marked by pencil and carefully cut using scissor into strips along with the absorbent. The strips attributed to each separate component were cut into small pieces and soaked in a polar solvent overnight for maximum recovery. After filtration and evaporation, the recovered components were analysed by NMR (Waksmundzka-Hajnos *et al*., 2008).

### 2.6.3 Size-Exclusion Chromatography (SEC)

This technique is also known as molecular sieve chromatography or gel filtration chromatography. The principle of SEC is the separation of molecules according to their molecular size. In this study, a slurry of Sephadex LH-20 (35 g) was added to a glass column of approximately 22 cm height and 2 cm diameter. The MeOH extract (2 g) was dissolved in a small quantity of MeOH to the top of the column. Elution was started with 100% MeOH and vials of 5 ml were used to collect different fractions. Also, SEC was carried out for some fractions to purify them.

### 2.6.4 Column Chromatography (CC)

This technique was used to fractionate polar and non-polar components, using an open glass column plugged with non-adsorption cotton wool. The glass column 55×3 cm was packed with 300 g silica gel 60 (mesh size 0.063-0.200 mm). Silica gel 60 was made into a wet slurry using the least polar solvent of the eluting system and then poured in a glass chromatography column of appropriate size. The hexane and EtOAc extracts were dissolved in a suitable solvent and adsorbed on a small amount of silica gel 60 then loaded at the top of the column. A cotton plug was applied over the sample to prevent any distortion in separation. The elution was started with low polar to high polar solvents and air bubbles were eliminated by taping. The eluent was passed through the column with gradient elution. The collected fractions were analysed by TLC and pooled according to similar chemical profiles.

### 2.6.5 Vacuum Liquid Chromatography (VLC)

VLC was used for rapid fractionation of crude extracts using a sintered glass funnel attached to a water pump. Silica gel 60 H (TLC grade) was loaded into the funnel and a vacuum was applied to compress the silica gel to a hard layer. The EtOAc or MeOH extracts were dissolved in an appropriate solvent, absorbed on a small amount of silica gel 60 (mesh size 0.063-0.200 mm) and dried to achieve a free-flowing powder. The powder was loaded and packed as a uniform thin layer on top of the compressed silica gel column and the thin layer was covered with a filter paper. N-Hexane and EtOAc were used as mobile phases in different ratios of increasing polarity. Each fraction was collected, evaporated to dryness at 40°C under vacuum using a rotary evaporator. Finally, the fractions were checked by TLC and pooled according to similar chemical profiles (Pelletier *et al.*, 1986).

**2.7 Spectroscopic examination**

**2.7.1 NMR**

1D ($^1$H and $^{13}$C) and 2D NMR experiments were carried out on a Jeol Eclipse 400 spectrometer at 400 MHz for $^1$H and 100 MHz for $^{13}$C and Distortionless Enhancement of Polarization Transfer (DEPT) spectra and a Bruker Avance DRX-500 (500 MHz) spectrometer 500 for heteronuclear single quantum coherence (HSQC) and heteronuclear multiple bond connectivity (HMBC). Each fraction was dissolved in about 500 µl of a suitable deuterated solvent (CD$_3$COCD$_3$, CDCl$_3$ or DMSO-$d_6$) and placed in 5 mm internal diameter NMR tubes. The structures of the compounds were elucidated from the resulting spectra. The NMR spectroscopic data were processed using MestReNova software 8.1.2 (Mestrelab Research, A Coruña, and Spain) and ChemBioDraw Ultra, Version 14 (PerkinElmer, Yokohama, Japan) were used to draw compound structures. Spectra obtained for known compounds were identified following comparison with spectral data published from previous studies.

**2.7.1.1 1D NMR**

This is the simplest technique used in structure elucidation. $^1$H NMR experiments were used for the determination of the types of protons in the compounds and $^{13}$C NMR for providing data on the number and kinds of carbon atoms in the compounds. Both $^1$H and $^{13}$C (1D) NMR spectra can be less informative than 2D NMR analysis especially in the case of some of the more complex organic molecules.

**2.7.1.2 2D NMR**

2D NMR includes Heteronuclear Multiple Bond Coherence (HMBC), Heteronuclear Single Quantum Coherence (HSQC), Correlation Spectroscopy (COSY), and Nuclear Overhauser Enhancement Spectroscopy (NOESY). HMBC provided the correlation between the chemical shift of the protons in the samples and the heteronucleus $^{13}$C through $^2J$ and $^3J$ coupling interaction between the nuclei (long-range H-X-C-C-C correlations). HSQC was used to identify the correlation between proton and carbon atoms in samples through the $^1J$ coupling between them. COSY displays $^1$H-$^1$H connectivities where the proton shifts are plotted on both axes with the contour plot along the diagonal of the square. NOESY records all the $^1$H-$^1$H NOE correlations occurring in a molecule.

### 2.7.2 Mass spectrometry (MS)

This technique was used to elucidate the elemental composition of a sample. One mg of each sample was dissolved in 1ml MeOH and 10 µl of the solution was then injected along with an infusion of 0.1% (v/v) formic acid in water (solution A) and 0.1% (v/v) formic acid in acetonitrile (solution B) at a flow rate of 300 µl/min. A gradient method was used for elution of the mobile phase starting with 10% (v/v) solution B in solution A to reach 100% of solution B then reduced again to 10% (v/v) solution B. Positive ion and negative ion mode electrospray ionization (ESI) experiments were carried out on a Dionex ultimate 5000 LC-Exactive Orbitrap mass spectrometer. MS data acquisition was carried out by Dr Tong Zhang (SIPBS, University of Strathclyde).

## 2.8 Biological examination

### 2.8.1 Tissue culture

#### 2.8.1.1 Preparation of complete culture medium

All procedures were carried out in a sterile environment and the medium for each cell line was prepared in a sterile flow hood and was then stored at 4°C until required (Table 2.2). Cells were grown in an incubator at 37°C, 100% humidity and 5% $CO_2$ and the medium changed or the cells subcultured every 3 days. All the cell lines used in this study were adherent with an epithelial morphology.

#### 2.8.1.2 Resuscitation of cells

To resuscitate the cell line, frozen cells (stored at -80°C or in liquid nitrogen) were thawed and transferred into a 25 $cm^2$ tissue culture flask containing 5 ml pre-warmed appropriate complete medium (Table 2.2) and incubated at 37°C, 100% humidity with 5% $CO_2$ to let the cells attach to the flask bottom. The medium was changed every 2 to 3 days.

#### 2.8.1.3 Sub-culture of cells

Cells were sub-cultured when the cells reached a minimum of 80% confluence. To detach the cells from the flask bottom, the medium was decanted into Virkon disinfectant and the cell layer was washed with 5 ml of $Mg^{2+}$-$Ca^{2+}$ free Hank's Balanced Salt Solution (HBSS) to clear the cell layer from the medium, dead cells and cell metabolites. After removing the HBSS, 1 ml of 0.25% (v/v) TryplE Express solution

was added to each 25 cm$^2$ flask for detaching the cells. The flask was incubated at 37°C, 100% humidity with 5% $CO_2$ for a maximum of 5 min. After complete detachment of the cells, approximately 330 µl of the cell suspension was transferred into each 75 cm$^2$ flask containing 10 ml appropriate complete medium (Table 2.2). The flask was returned to the incubator for further growth. The medium was changed when necessary.

**Table 2.2**: Cell culture media for the cell lines used in this study

| Cell lines | ECACC number | Complete Culture Medium |
|---|---|---|
| **1.  HepG2 cells** Human Caucasian hepatocyte carcinoma | 85011430 | 500 ml Dulbecco's Modified Eagle's Medium (DMEM) supplemented with 50 ml foetal calf serum, 5 ml penicillin/streptomycin and 5 ml L-glutamine. |
| **2.  A375 cells** Human malignant melanoma | 88113005 | |
| **3.  A549 cells** Human Caucasian lung carcinoma | 86012804 | |
| **4.  PANC-1 cells** Human Caucasian pancreas carcinoma | 87092802 | |
| **5.  MCF7 cells** Human Caucasian breast adenocarcinoma | 86012803 | |
| **6.  LNCaP cells** Human Caucasian prostate carcinoma | 89110211 | 500 ml Roswell Park Memorial Institute (RPMI 1640) medium supplemented with 50 ml foetal bovine serum, 5 ml penicillin /streptomycin, 5 ml L-glutamine and 5 ml sodium pyruvate. |
| **7.  PNT2 cells** Human normal prostate | 95012613 | |

### 2.8.1.4 Storage of cells

All cell lines were stored at a cell density of $1\times10^5$ cells/ml suspended in 1 ml cryopreservation medium (appropriate complete medium containing 5 %, v/v, DMSO). The cell solution was then transferred into cryovials and stored in a -80°C freezer. For longer term preservation, the cryovials were transferred to liquid nitrogen.

### 2.8.1.5 Plant sample preparation

One gram of crude extract or pure compound was dissolved in 1 ml of DMSO (for use in cell culture analysis) to give a stock solution of 10 mg/ml and was kept on -20°C. Further dilution of the required starting concentration was carried out using the appropriate complete cell culture medium.

### 2.8.1.6 Resazurin solution preparation

Resazurin sodium salt (5 mg) was dissolved in 50 ml distilled water. The solution was filter sterilised using a 0.22 μm filter unit and placed into a 50 ml centrifuge tube, protected from light by wrapped with tin foil and stored in the fridge until required.

### 2.8.2 Resazurin cell viability assay

This assay includes a colourimetric/ fluorometric growth indicator, based on the detection of metabolic activity. Resazurin is an oxidation-reduction (REDOX) indicator that permits observation of metabolic activity by both fluorescent and colourimetric detection.

The REDOX indicator is reduced by mitochondria of living cells in the presence of nicotinamide adenine dinucleotide dehydrogenase (NADH) which causes the indicator to change from resazurin, the oxidised, non-fluorescent, blue form to resorufin, the reduced, fluorescent, red form (Figure 2.1). The fluorescence is measured at the excitation and emission wavelengths of 560 nm and 590 nm, respectively.
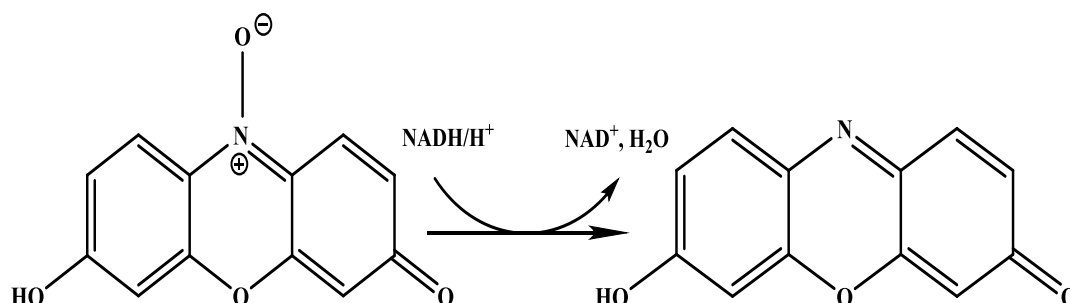


**Figure 2.1:** Reduction of resazurin to resorufin in living cells.

The cytotoxicity of the crude extracts and compounds were determined using 0.01% (w/v) resazurin solution (section 2.8.1.6) and the number of cells required for the cytotoxicity bioassay was $1 \times 10^5$ cells/ml per plate (i.e. $1 \times 10^4$ cells in 100 µl /well). For the crude extracts and compounds, plant sample was prepared (section 2.8.1.5) and diluted 1:9 with complete medium to give 1mg/ml of plant extract or compound in 5% (v/v) DMSO. On the first day, the cell plates were prepared with numbers of cells required then incubated for 24 h at $37^oC$, 100% humidity, 5% $CO_2$, before the samples were added. On the second day, a 1:1 serial dilution of each sample was performed in a dilution plate to give a concentration range from 500 µg/ml to 3.9 µg/ml. The diluted test sample (100 µl) was transferred to the corresponding assay well in the cell plate to give a final assay volume of 200 µl. The final serial dilution was from 250 µg/ml to 1.9 µg/ml. Controls (serial dilutions of 0.5% up to 50% DMSO as solvent controls) were added to the appropriate control wells, then the plate was incubated for 24 h at $37^oC$ in a humidified atmosphere containing 5% $CO_2$. On the third day, 20 µl of 10% (v/v) resazurin solution was added to each well and the assay plate was wrapped with tin foil and returned to the incubator under the previous conditions. Fluorescence intensity was measured after 24 h using a SpectraMax M5 microplate reader at the excitation and emission wavelengths of 560 nm and 590 nm, respectively.

Each sample was tested in triplicate and the results expressed as cell viability as a percentage of the cell only control. The equation used to determine the cell viability is shown below:

$$\% \text{ Cell Viability} = \frac{\text{Mean of Sample (OD560-590)} \times 100}{\text{Mean of Control (OD560-590)}}$$

Extract or compound was considered to be toxic if it caused a reduction in cell viability by at least 50% or more. Statistical analysis was carried out using analysis of variance (ANOVA) with a Dunnet's post-test using MiniTab 16 and graphs were plotted using GraphPad Prism software version 5.0.
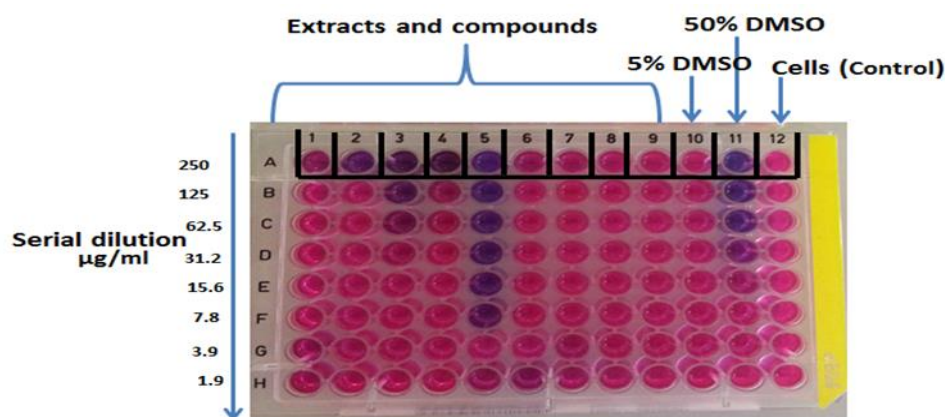
**Figure 2.2:** Template of a cytotoxicity plate layout.

## 2.8.3 Adhesion of LNCaP and MCF7 cells to Fibronectin using a CytoSelect™ 48 -Well Cell Adhesion Assay.

Following the manufacturer's instructions and under sterile conditions, the adhesion plate was warmed up at room temperature for 10 min. After which, 150 µl of a cell suspension containing $0.5 \times 10^6$ cells/ml in serum-free medium with the samples (Rr-1 and PpFr-2) at a final concentration of 250-31.25 µg/ml, respectively were added to a 48 well plate (containing 40 Human Fibronectin-coated wells and 8 BSA-coated wells as the negative control) and incubated at 37ºC in a humidified atmosphere with 5% $CO_2$. After 90 min, the medium was carefully discarded from each well. Each well was washed 4 times with 250 µl PBS, then the PBS was aspirated from each well. A 200 µl of cell stain solution was added to each well and incubated for 10 min at room temperature. The cell stain solution was discarded from the wells, which were then gently washed 4 times with 500 µl deionised water (DW). The DW was discarded and the wells left to air dry. Then, 200 µl of extraction solution was added to each well and incubated for 10 min. Subsequently, 150 µl from each extracted sample was transferred to a 96-well microtitre plate. A SpectraMax M5 microplate reader was used to measure the absorbance at 560 nm.

## 2.8.4 Migration assay using a Cytoselect™ 24-well Cell Migration Assay

Following the manufacturer's instructions, the migration plate was warmed up at room temperature for 10 min. Then, 300 µl of a cell suspension containing $0.5 \times 10^6$ cells/ml in serum-free medium with the samples (Rr-1 and PpFr-2, separately) at a final

concentration of 125-15.62 μg/ml, respectively were added to the inside of each insert (polycarbonate membrane, 8 μm pore size to assay the migratory properties of cells) in a 24 well plate. Appropriate culture medium (500 μl) containing 10% (v/v) foetal bovine serum (chemoattractant) was added to the lower chamber of the migration plate. The cells were incubated for 24 h at 37ºC in a humidified atmosphere with 5% $CO_2$. After 24 h, the non-migratory cells inside the insert were removed using ends of 2-3 wet flattened cotton-tip swabs by pressing them against a clean hard surface and gently, swabbing the interior of the inserts. The inserts were transferred by forceps to a clean well containing 400 μl of cell stain solution and incubated at room temperature for 10 min. The stained inserts were washed in a beaker of DW several times and allowed to air dry. The inserts were transferred to empty wells containing 200 μl of extraction solution and incubated at room temperature for 10 min. Finally, 100 μl from the extracted sample was transferred to a 96-well plate and the absorbance was measured at 560 nm using a SpectraMax M5 microplate reader. The results were calculated as % migration of the untreated control, which was considered 100% migration.

## 2.8.5 Invasion assay using a Cytoselect™ 24-well Cell Invasion Assay

Following the manufacturer's instructions, the invasion plate was warmed up at room temperature for 10 min. Hence, 300 μl of a cell suspension containing $0.5 \times 10^6$ cells/ml in serum-free medium with the samples (Rr-1 and PpFr-2, separately) at two concentrations of 15.62 μg/ml and 62.5 μg/ml, respectively were added to the inside of each insert. Similarly, the assay protocol was completed as for migration (section 2.8.4), except the basement membrane layer of the cell culture inserts was rehydrated first by adding 300 μl of warm serum-free media to the inner compartment and incubated at room temperature for 1 h. The difference between the invasion and migration assay kit is the inserts are coated with a uniform layer of dried basement membrane matrix solution in the invasion assay, which serves as a barrier to discriminate invading from non-invading cells. The results were calculated as a % invasion of the untreated control, which was considered 100% invasion.

# Chapter 3


# *Results*

**Part 1: Phytochemical results**

## 3.1 Solvent extraction and yield

Solvent extraction using a Soxhlet apparatus was carried out to obtain crude extracts from the flower of *B. spectabilis*, the leaves and stems of *R. raetam*, the leaves, stems and roots of *A. graecorum*, and the leaves and stems of *P. plicata*.

Table 3.1 shows the yields of the extracts obtained from the extractions calculated using the formula:

$$\% \text{ yield} = \frac{\text{Weight of the crude extract (g)} \times 100}{\text{Total weight of plant powder (g)}}$$

**Table 3.1:** Yields of extracts

| Plant Name and Part | Amount of Plant Material (g) | Weight of Plant Extract (g) Hexane | EtOAc | MeOH | Yield (%) Hexane | EtOAc | MeOH |
|---|---|---|---|---|---|---|---|
| *B. spectabilis* flowers | 500 | 6.0 | 12.0 | 60.0 | 1.2 | 2.4 | 12.0 |
| *R. raetam* leaves & stems | 500 | 7.5 | 14.0 | 95.0 | 1.5 | 2.8 | 19.0 |
| *A.graecorum* leaves, stems & roots | 310 | 7.9 | 3.4 | 28.4 | 2.5 | 1.1 | 9.2 |
| Plant Name and Part | Amount of Plant Material (g) | Weight of Plant Extract (g) EtOH | | | Yield (%) EtOH | | |
| *P.plicata* leaves & stems | 300 | 30.0 | | | 10.0 | | |

## 3.2 Fractionation of *B. spectabilis* crude extracts

*B. spectabilis* MeOH extract (60 g) was fractionated using three different methods. A VLC column was used (section 2.6.5) to fractionate 20.0 g. $^{1}$H NMR enabled elucidation of one compound, coded **Bs-1** (30 mg). A further 2 g was subjected to Sephadex CC (section 2.6.3) and led to the identification of **Bs-2** (15 mg).

Finally, 10.0 g was subjected to CC, which led to the isolation of **Bs-3** (3 g). No compounds were obtained from the fractionations of *B. spectabilis* *n*-hexane and EtOAc extracts using CC and VLC and the [1]NMR spectra of these crude extracts revealed that the signals indicated a mixture of fats.

### 3.2.1 Characterisation of Bs-1 as pinitol
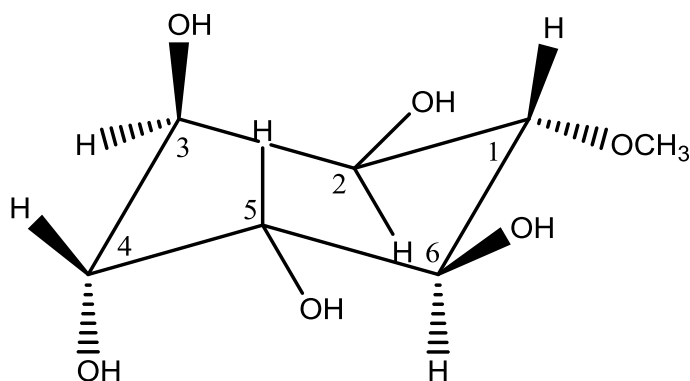


**Figure 3.1** Structure of Bs-1.

The compound **Bs-1** (Figure 3.1) was isolated from the MeOH extract of *B. spectabilis* flowers using VLC. On TLC with 50% hexane in 50% EtOAc, a yellow spot was observed (R$f$ = 0.56) after spraying with *p*-anisaldehyde-sulphuric acid reagent and heating.

The ^{1}H NMR (400 MHz) spectrum of **Bs-1** in DMSO-$d_6$ (Table 3.2) showed protons between 3.00 and 3.65 ppm. The methoxy group at $\delta_H$ 3.44 (3H, s, 1-OCH$_3$) integrated for 3H, while the protons at $\delta_H$ 3.02 (3H, t,H-1), 3.52 (1H, dd , H-2), 3.65 (1H, d , H-3), 3.65 (1H, d, H-4), 3.46 (1H, d , H-5), and $\delta_H$ 3.36 (1H, t, H-6) for a cyclic polyol.

The ^{13}C NMR (100 MHz) spectrum of the compound in DMSO-$d_6$ (Table 3.2) showed the presence of seven carbons at $\delta$c 83.6 (C-1), 70.3 (C-2), 72.0 (C-3), 72.5 (C-4), 71.1 (C-5), 72.8 (C-6) and 59.8 ppm (OCH$_3$).

Using HMBC spectrum (Figure 3.5) the compound was characterised as follows: the long-range interaction of the proton at $\delta_H$ 3.02 (H-1) showed [2]J correlation to the carbons at $\delta$c 70.3 (C-2), 72.8 (C-6) and [3]J correlation to the carbon of the methoxy (- OCH$_3$) group. The protons at $\delta_H$ 3.51 (H-2) and 3.36 (H-6) showed [2]J correlations

to the carbon at $\delta_C$ 83.6, while the protons at $\delta_H$ 3.65 (H-3) and 3.46 (H-5) showed $^3J$ correlations to the same carbon and was therefore assigned C-1.

The HRESI-MS spectrum of the compound in negative ion mode gave an [M-H]⁻ ion at $m/z$ 193.0716 (Calc $C_7H_{13}O_6$, 193.0712) which indicated that the molecular formula of this compound was $C_7H_{14}O_6$. The $^1H$ and $^{13}C$ NMR spectral data were in agreement with literature reports.

This compound was isolated previously from *Pisonia alba* (Nyctaginaceae) (Poongothai and Sripathi, 2013). Based on the above data, **Bs-1** was identified as pinitol.
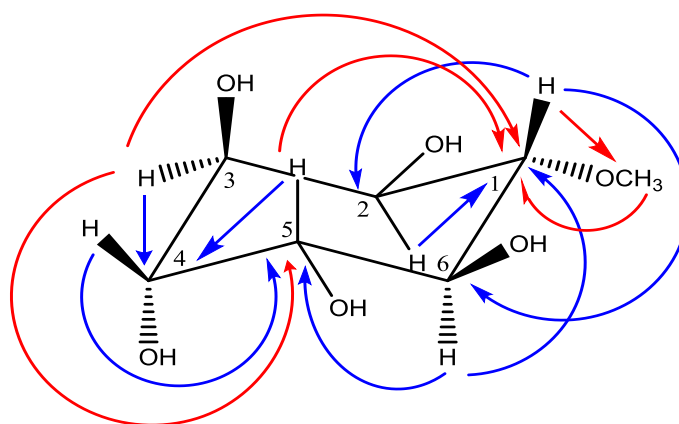


**Figure 3.2:** Structure of Bs-1 with key COSY ( ▬▬ ) and HMBC $^2J$ ( ⌒→ ) and $^3J$ ( ⌒→ ) correlations.

**Table 3.2:** $^1H$ (400 MHz), $^{13}C$ (100 MHz), HMBC and COSY data of Bs-1 in DMSO-$d_6$.

| Position | $^1H$ (δ ppm) (Mult, $J$ (Hz)) | $^{13}C$ (δ ppm) (Mult) | HMBC | | COSY |
|---|---|---|---|---|---|
| | | | $^2J$ | $^3J$ | |
| 1 | 3.02 (t) | 83.6 (CH) | C-2, C-6 | 1-OCH$_3$ | H-2, H-6 |
| 2 | 3.52 (dd) | 70.3 (CH) | C-1, C-3 | C6 | H-1 |
| 3 | 3.65 (d) | 72.1 (CH) | C-4 | C-1, C5 | - |
| 4 | 3.65 (d) | 72.5 (CH) | C-5 | - | - |
| 5 | 3.46 (m) | 71.1 (CH) | C-4 | C-1 | - |
| 6 | 3.36 (t) | 72.8 (CH) | C-1, C-5 | - | H-1 |
| 1-OCH$_3$ | 3.44 (s) | 59.8 (CH$_3$) | - | C-1 | - |
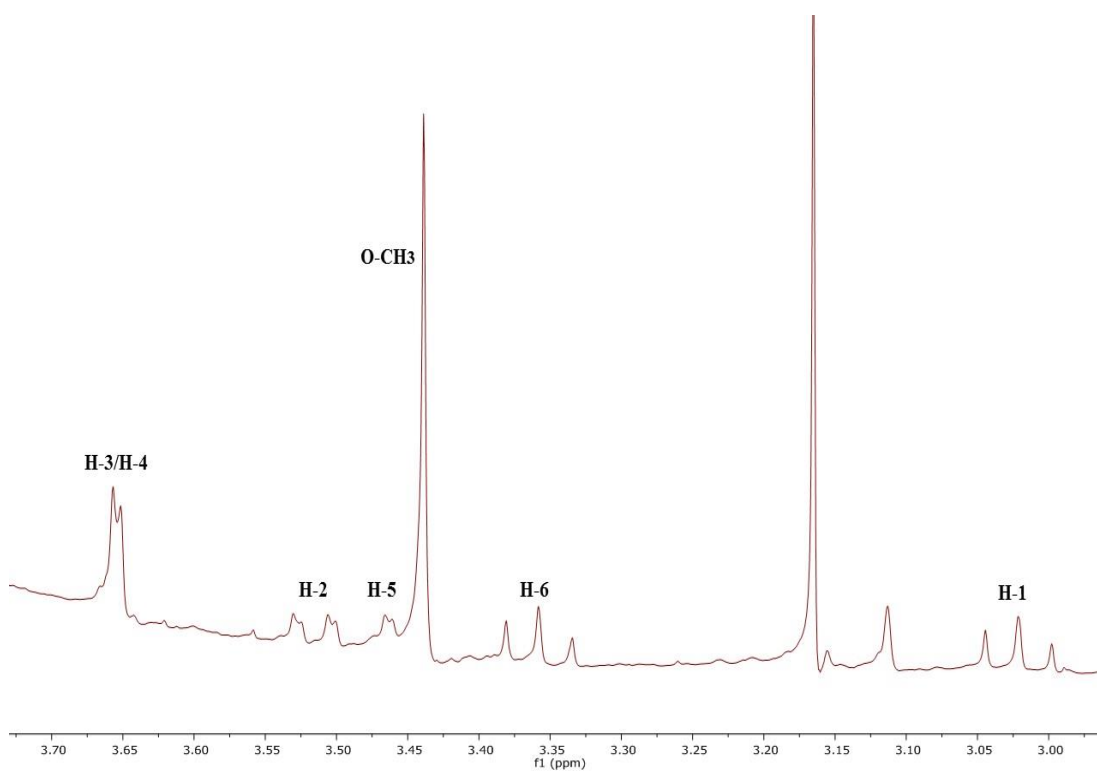
**Figure 3.3:** $^1$H NMR spectrum (400 MHz) of Bs-1 in DMSO-$d_6$.
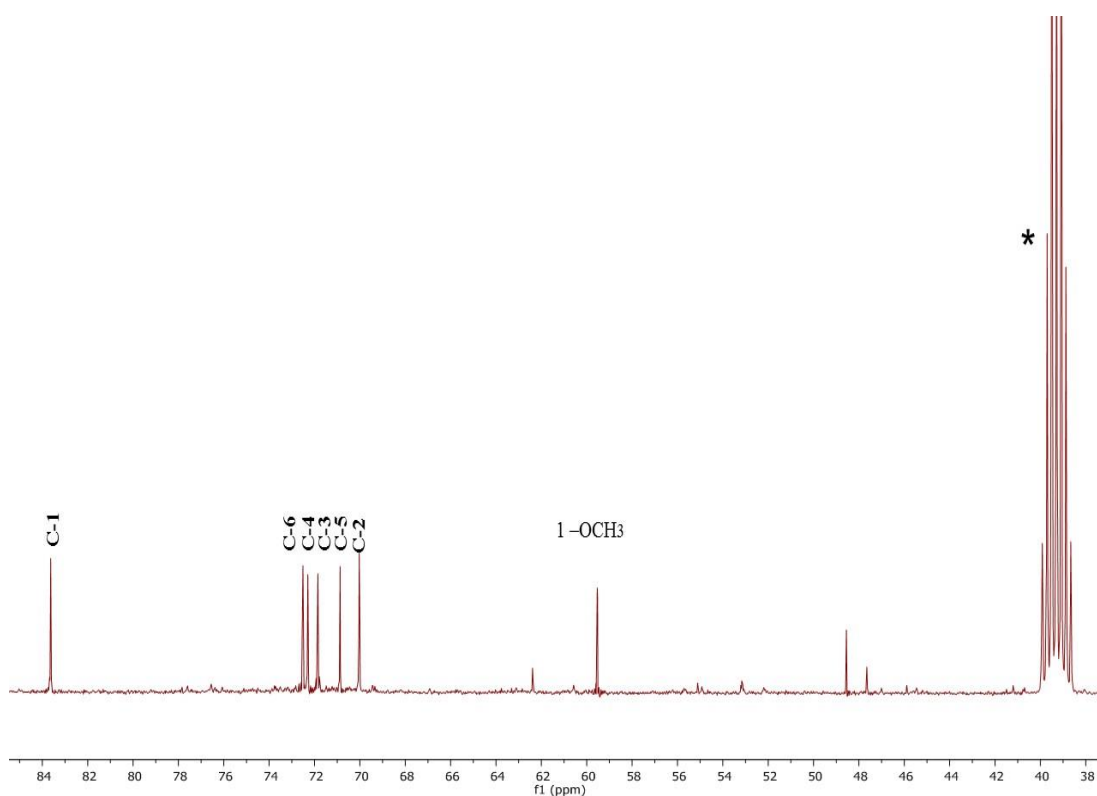


**Figure 3.4:** $^{13}$C NMR spectrum (100 MHz) of Bs-1 in DMSO-$d_6$*.
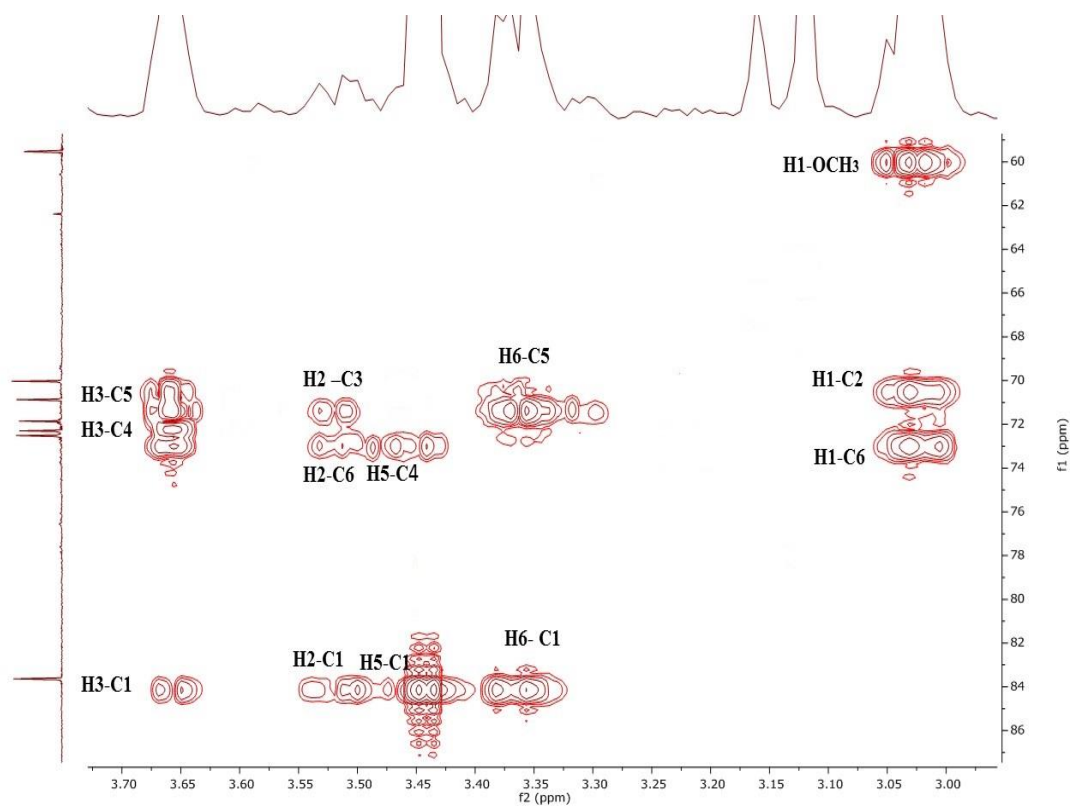
**Figure 3.5:** HMBC (DMSO-*d₆*) spectrum of Bs-1.
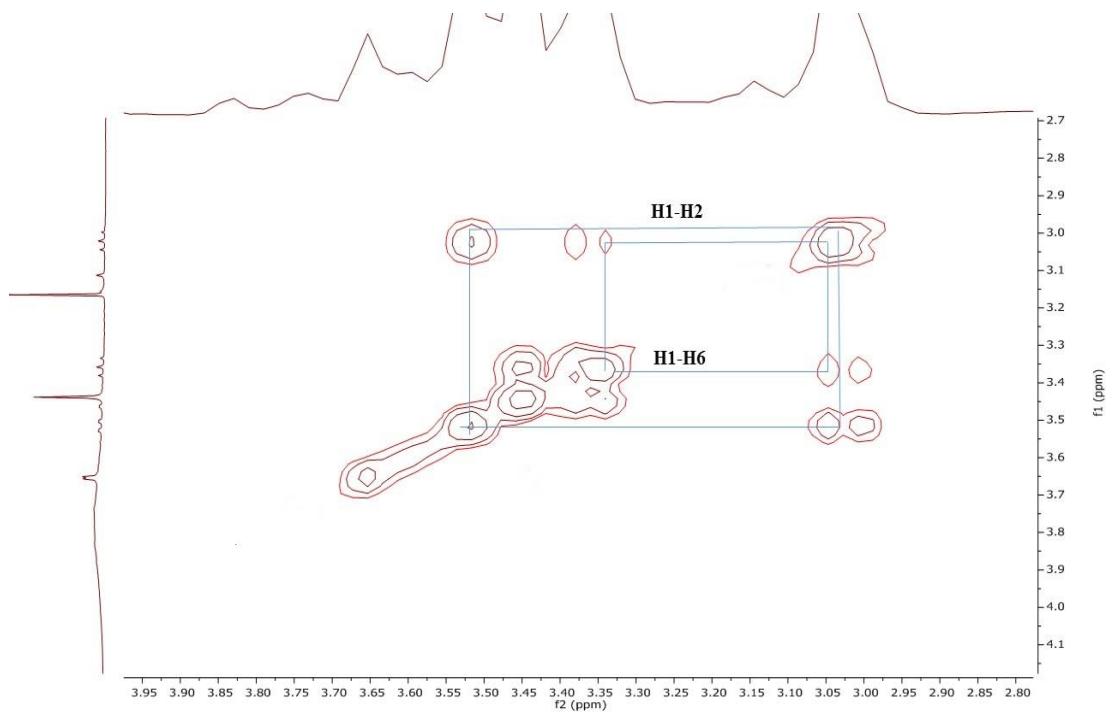


**Figure 3.6:** COSY spectrum of Bs-1 in DMSO-*d₆*

### 3.2.2 Characterisation of Bs-2 as allantoin
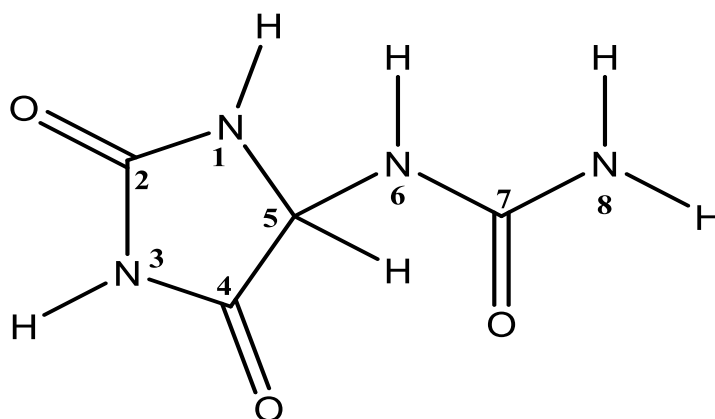


**Figure 3.7:** Structure of Bs-2.

The compound **Bs-2** (Figure 3.7) was isolated from the MeOH extract of *B. spectabilis* flower using Sephadex CC. On TLC with 50% hexane in 50% EtOAc, a yellow spot was observed (R$f$ = 0.64) after spraying with *p*-anisaldehyde-sulphuric acid reagent and heating. The $^1$H NMR (500 MHz) spectrum of **Bs-2** in DMSO-$d_6$ (Figure 3.9) showed two singlets at $\delta_H$ 8.05, and 5.82 and were assigned H-3 and H-8, respectively. Furthermore, it showed the presence of two doublets at $\delta_H$ 6.98 (d, H-1) which correlated with another doublet at $\delta_H$ 5.24 (d, H-5) in the $^1$H -$^1$H COSY. Additionally, the later proton also showed a correlation with the singlet signal at $\delta_H$ 8.05 (s, H-3) in $^1$H -$^1$H COSY spectrum ($^4J$-coupling). Furthermore, a broad proton singlet was observed at $\delta_H$ 10.57 ppm and was assigned H-6.

The $^{13}$CNMR (125 MHz) spectrum of the compound (Table 3.3) in DMSO-$d_6$ (Figure 3.10) showed the presence of four carbon atoms which were classified by DEPT into three carbonyl carbon atoms at $\delta_C$ 157.9 (C-2), 157.2 (C-4), and 174.0 (C-7), and one methine carbon at 62.8 (C-5).

The structure was confirmed by analysis of its HMBC spectrum as follows: the most important correlations were observed between the proton at $\delta_H$ 6.98 (H-1) with $^2J$ correlation to the carbons at $\delta_C$ 157.9 (C-2) and 62.8 (C-5). Protons at 8.05 (H-3) and

at 5.24 (H-5) showed $^2J$ correlation to carbon 157.2 (C-4) and $^3J$ correlation to carbons 62.8 (C-5) and 174.0 (C-7), respectively.

Based on these data, compound **Bs-2** was identified as allantoin. This compound has been isolated previously from *P. grandis* (Nyctaginaceae) (Sripathi *et al.*, 2011) but this is the first report of allantoin from *B. spectabilis*.

The HRESI-MS spectrum showed a molecular ion [M-H]$^-$ at *m/z* 157.0365 (Calc $C_4H_5N_4O_3$, 157.0361) suggesting a molecular formula of $C_4H_6N_4O_3$.
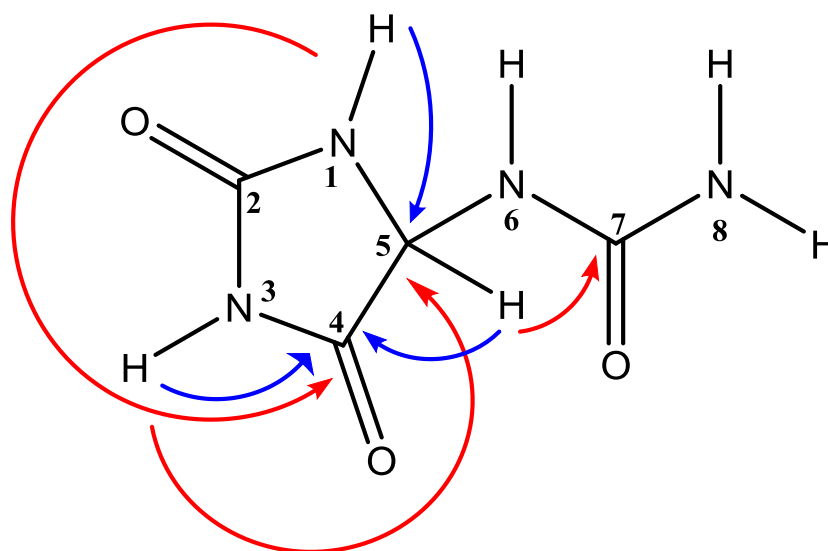


**Figure 3.8:** Structure of Bs-2 with key HMBC $^2J$ ( ⌒ ) and $^3J$ ( ⌒ ) correlations.

**Table 3.3:** $^1H$ (500 MHz), $^{13}C$ (125 MHz), HMBC and COSY data of Bs-2 in DMSO-$d_6$

| Position | $^1H$ (δ ppm) (Mult, *J* (Hz)) | $^{13}C$ (δ ppm) (Mult) | HMBC | | | COSY |
| | | | $^2J$ | $^3J$ | $^4J$ | - |
|---|---|---|---|---|---|---|
| 1 | 6.98 (d, *J* = 8.2 Hz) | - | C-5 | C-4 | C-7 | H-5 |
| 2 | - | 157.9 (C) | - | - | - | - |
| 3 | 8.05 (s) | - | C-4 | C-5 | - | H-5 |
| 4 | - | 157.2 (C) | - | - | - | - |
| 5 | 5.24 (d, *J* = 8.2 Hz ) | 62.8 (CH) | C-4 | C-7 | - | H-1, H-3 |
| 6 | 10.57 (br , s) | - | - | - | - | - |
| 7 | - | 174.0 (C) | - | - | - | - |
| 8 | 5.82 (s) 2H | - | - | - | C-5 | - |
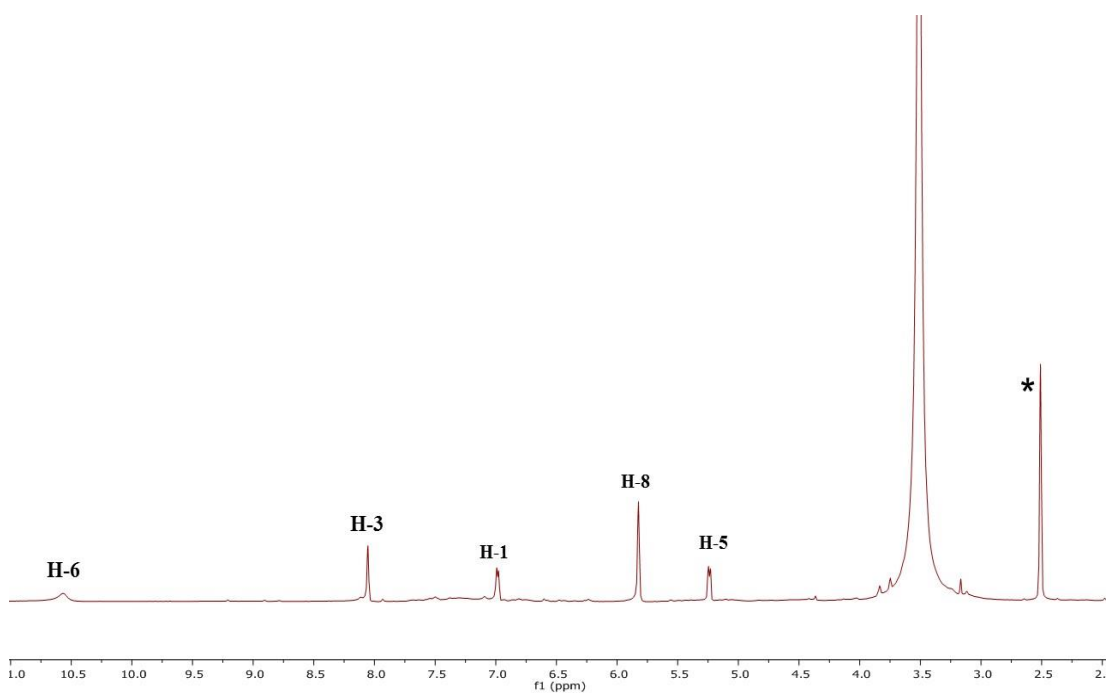
**Figure 3.9:** $^1$H NMR spectrum (500 MHz) of Bs-2 in DMSO-$d_6$*.
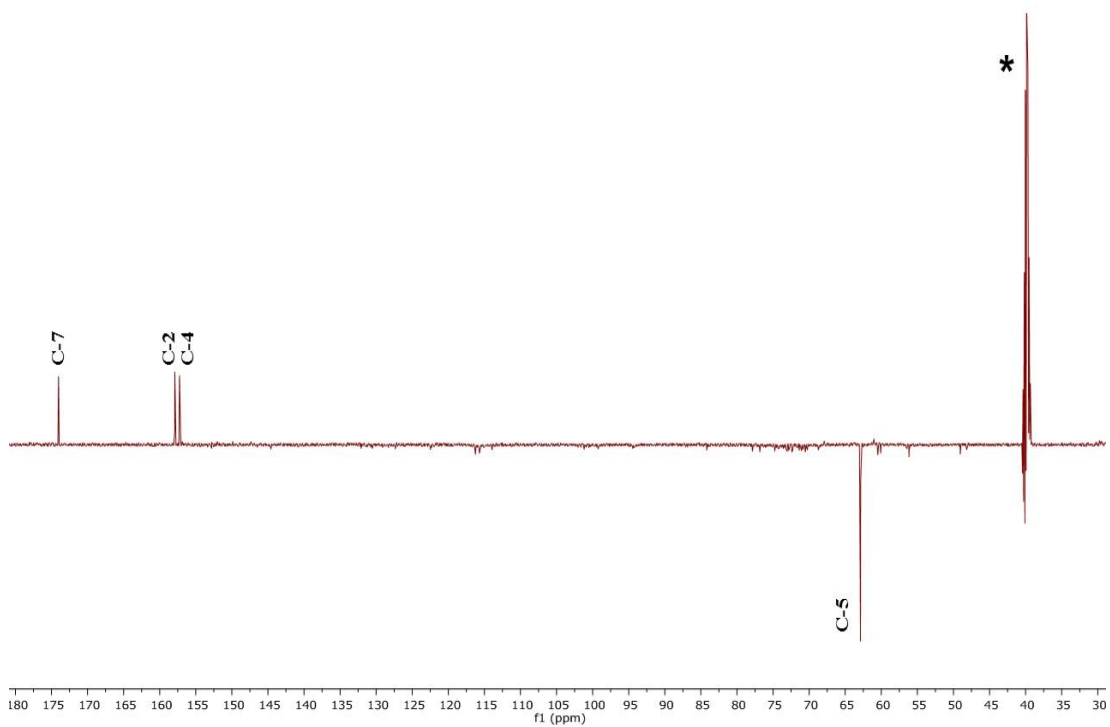


**Figure 3.10:** DEPTq-135 (125 MHz) NMR Spectrum of Bs-2 in DMSO-$d_6$*.
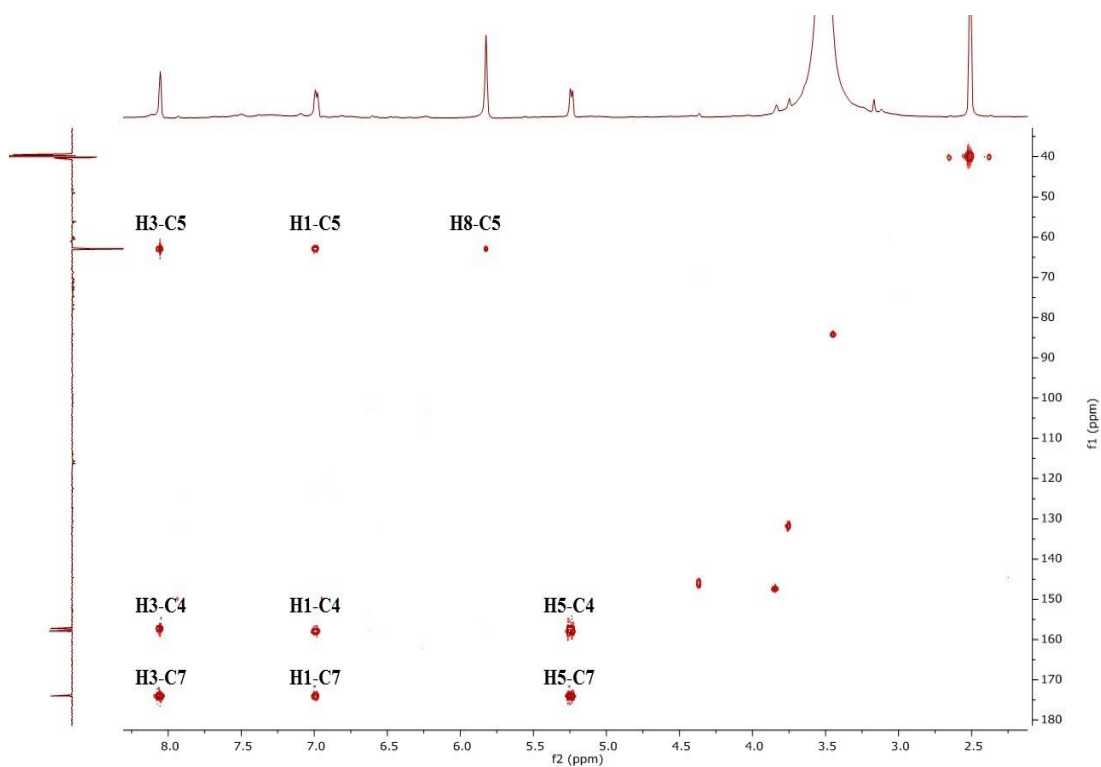
**Figure 3.11:** HMBC (DMSO-*d₆*) spectrum of Bs-2.
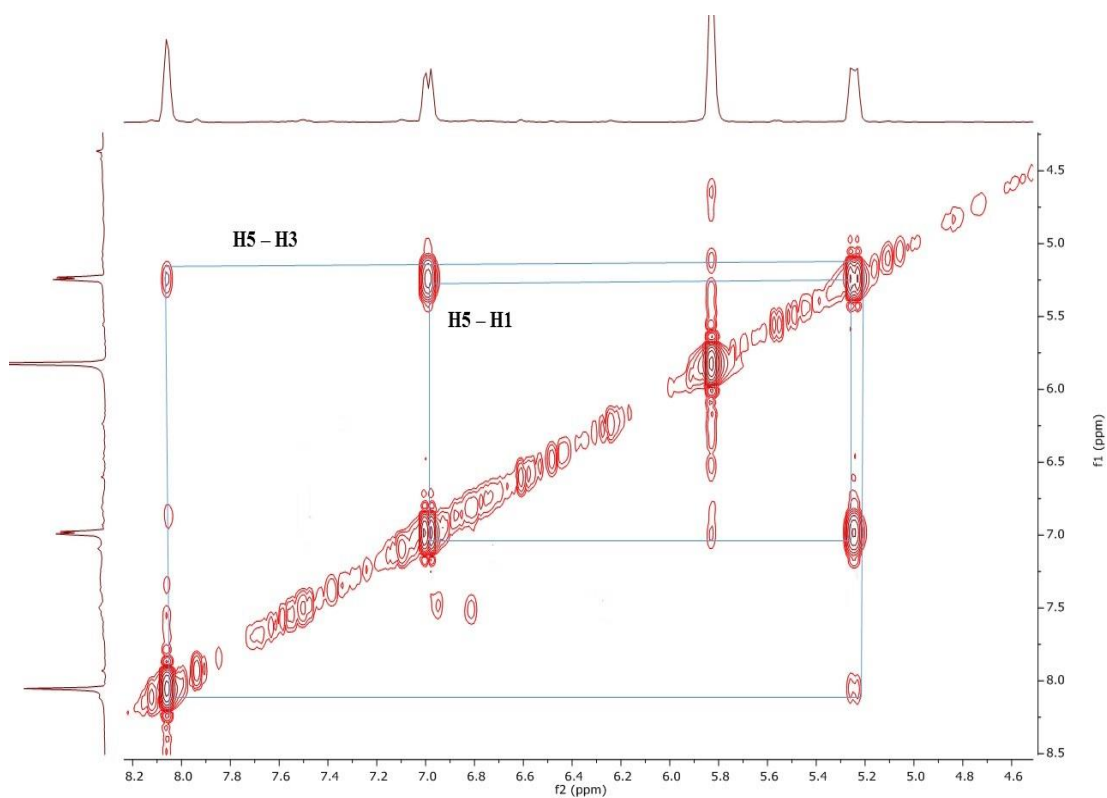


**Figure 3.12:** COSY (DMSO-*d₆*) spectrum of Bs-2.

### 3.2.3 Characterisation of Bs-3 as trigonelline
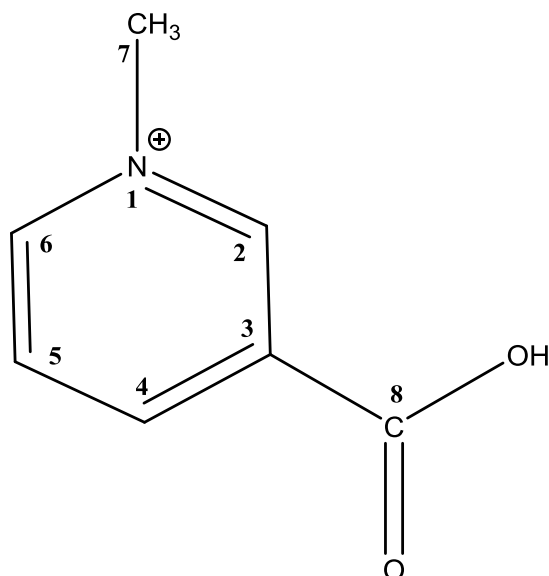


**Figure 3.13:** Structure of Bs-3.

The compound **Bs-3** (Figure 3.13) was obtained from fraction 8 of the CC of the MeOH extract of *B. spectabilis* as a black amorphous solid. On TLC with 50% (v/v), MeOH in EtOAc it gave a brown spot (R$f$ = 0.61) after spraying with *p*-anisaldehyde-sulphuric acid reagent and heating.

The $^1$H NMR spectrum (Figure 3.15) showed protons at $\delta_H$ 9.13 (1H, s, H-2), 8.74 (1H, d, H-4), 8.02 (1H, t, H-5), 8.92 (1H, d, H-6) and 4.37 (3H, s, CH$_3$). While the $^{13}$C NMR (100 MHz) spectrum of the compound in DMSO-$d_6$ (Figure 3.16) revealed the presence of carbons at $\delta_C$ 146.2 (C-2), 139.2 (C-3), 144.5 (C-4), 127.3 (C-5), 145.5 (C-6), 47.7 (C-7) and 163.7 (C-8).

Using HMBC NMR the compound was characterised as follows: the proton at $\delta_H$ 8.02 (H-5) showed $^3J$ correlation to $\delta_C$ 139.4 (C-3) and $^2J$ correlation to $\delta_C$ 145.5 (C-6). The protons at $\delta_H$ 8.74 (H-4) and 8.92 (H-6) showed $^2J$ correlation to the carbon at $\delta_C$ 127.3 (C-5). Also protons 9.13 (H-2) and at 8.74 (H-4) showed $^3J$ correlation to the carbonyl carbon at $\delta_C$ 163.7 (C-8).

The HRESI-MS spectrum showed a molecular ion [M+H]$^+$ at *m/z* 138.0546 (Calc C$_7$H$_8$NO$_2$, 138.0555) and indicated a molecular formula of C$_7$H$_7$NO$_2$. Thus, **Bs-3** was identified as trigonelline, which has been previously isolated from *Doliocarpus dentatus* (Jagessar *et al.*, 2013), but this is the first report from *B. spectabilis*.
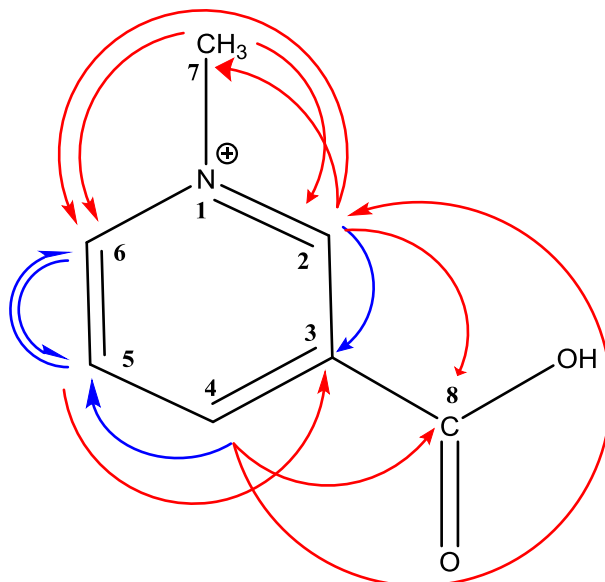


**Figure 3.14:** Structure of Bs-3 with key HMBC $^2J$ (⌒→) and $^3J$ (⌒) correlations.

**Table 3.4:** $^1$H (400 MHz), $^{13}$C (100 MHz), HMBC and COSY data of Bs-3 in DMSO-$d_6$.

| Position | $^1$H ($\delta$ ppm) (Mult, *J* (Hz)) | $^{13}$C ($\delta$ ppm) (Mult) | HMBC | | COSY |
|---|---|---|---|---|---|
| | | | $^2J$ | $^3J$ | - |
| 1 | - | - | - | - | - |
| 2 | 9.13 (1H, s) | 146.2 (CH) | C-3 | C-6, C7, C8 | CH$_3$ |
| 3 | - | 139.4 (C) | - | - | - |
| 4 | 8.74 (1H, d *J* = 7.7) | 144.5 (CH) | C-5 | C-2, C8 | H-5 |
| 5 | 8.02 (1H, d *J* = 6.7) | 127.3 (CH) | C-6 | C-3 | H-4, H-6 |
| 6 | 8.82 (1H, d *J* = 6.0) | 145.5 (CH) | C-5 | - | H-5, **CH$_3$** |
| 7 | 4.37 (3H, s) | 48.16 (N- CH$_3$) | - | C-2, C-6 | H-2, H-6 |
| 8 | - | 163.7 (C) | - | - | - |
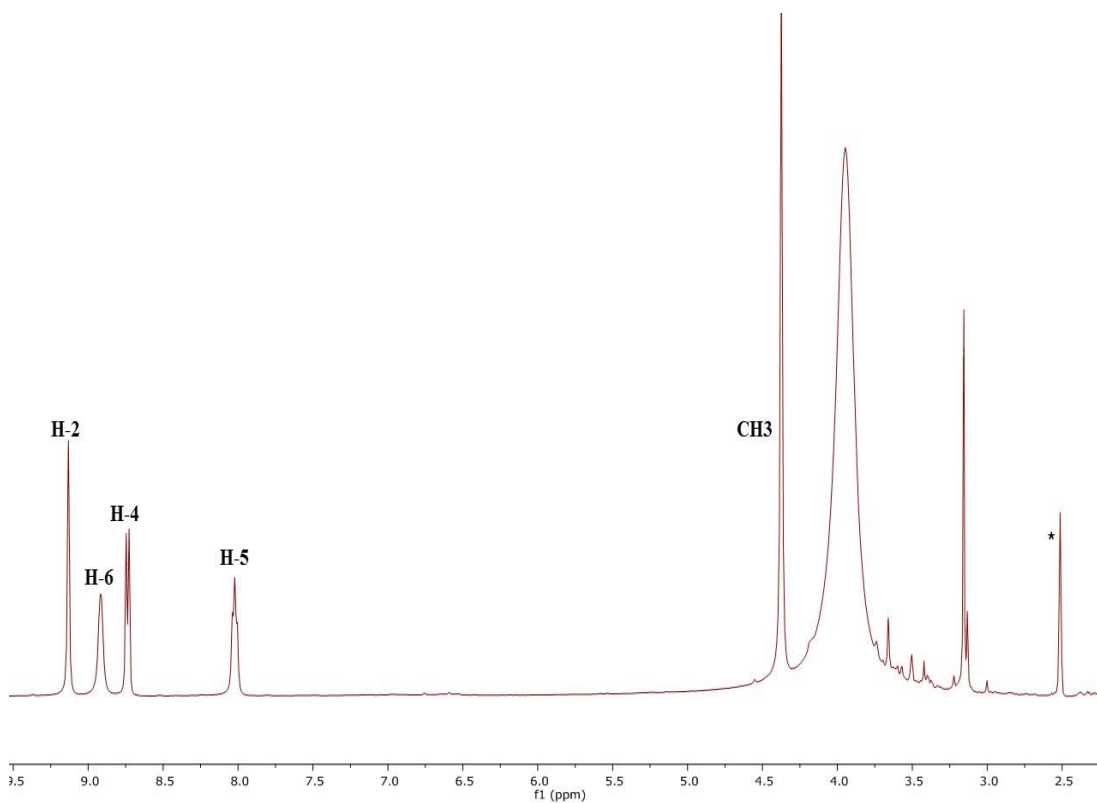
**Figure 3.15**: ¹H NMR spectrum (400 MHz) of Bs-3 in DMSO-$d_6$ *.
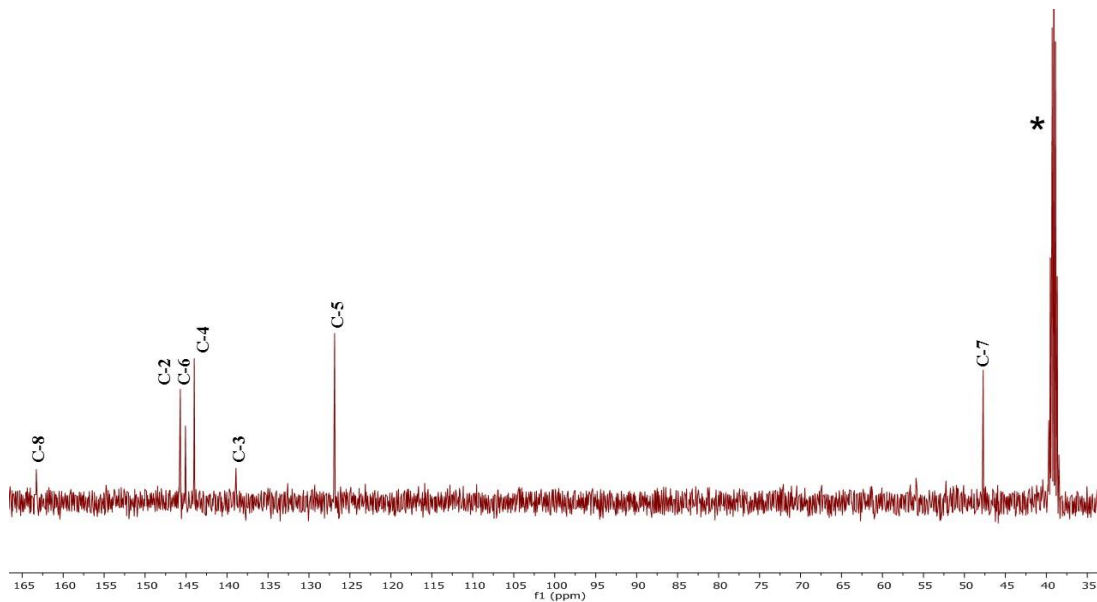


**Figure 3.16:** Full ¹³C NMR spectrum (100 MHz) of Bs-3 in DMSO-$d_6$ *.
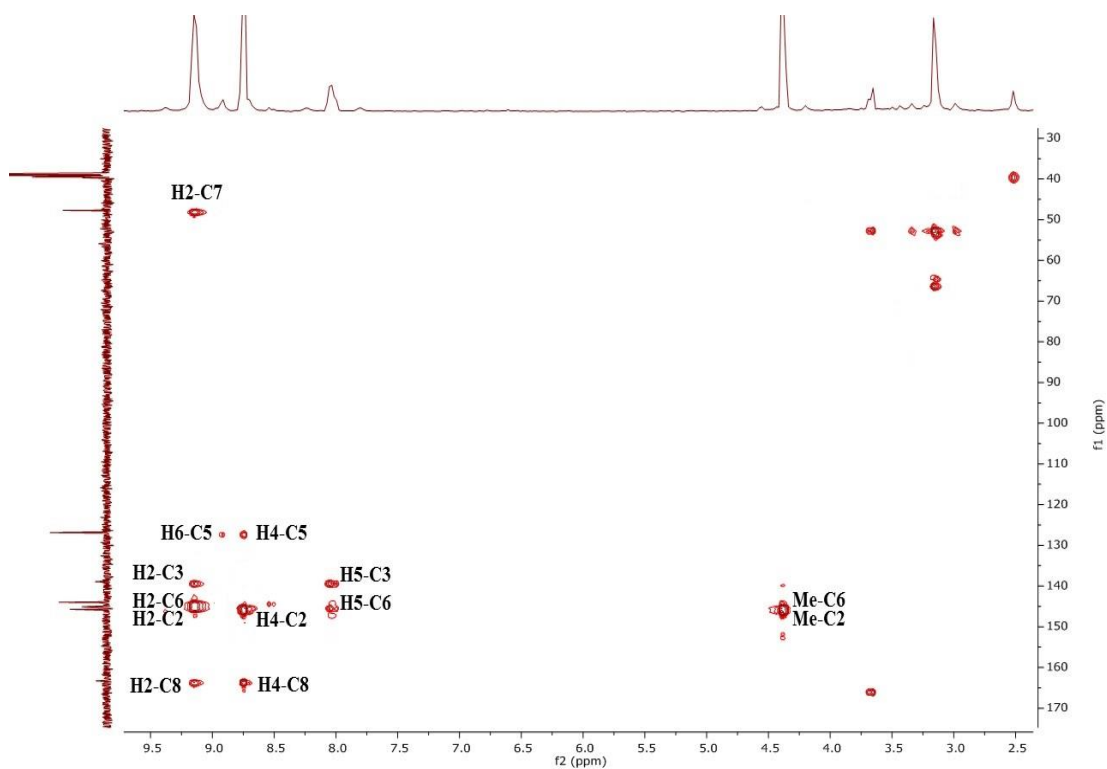
**Figure 3.17:** HMBC (DMSO-*d₆*) spectrum of Bs-3.
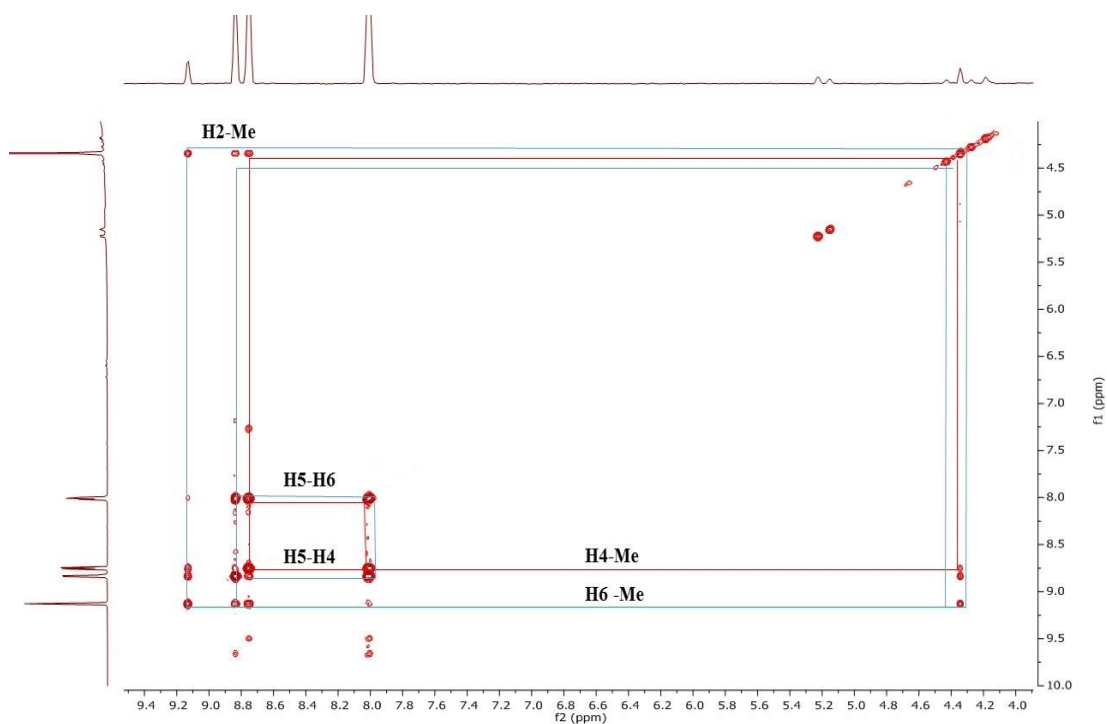


**Figure 3.18:** COSY (DMSO-*d₆*) spectrum of Bs-3.

### 3.3 Fractionation of *A. graecorum* crude extracts

The *A. graecorum* MeOH extract (28.41 g) was further fractionated. About 10.0 g was subjected to VLC (section 2.6.5) and eluted with hexane and increasing the polarity with EtOAc and up to 40% MeOH. The fractions from VLC were collected and their contents assessed using NMR and depending on their TLC profiles were combined and further fractionated by SEC. Fraction 7 from VLC of *A. graecorum* MeOH extract (2 g) was subjected to Sephadex CC and lead to the isolation of one compound coded **Ag-1** (16 mg). No compounds were identified from the fractionation of the hexane and EtOAc extracts of *A. graecorum* using CC and the ^{1}HNMR spectrum of these crudes revealed that the signals indicated a mixture of fats.

### 3.3.1 Characterisation of Ag-1 as narcissin
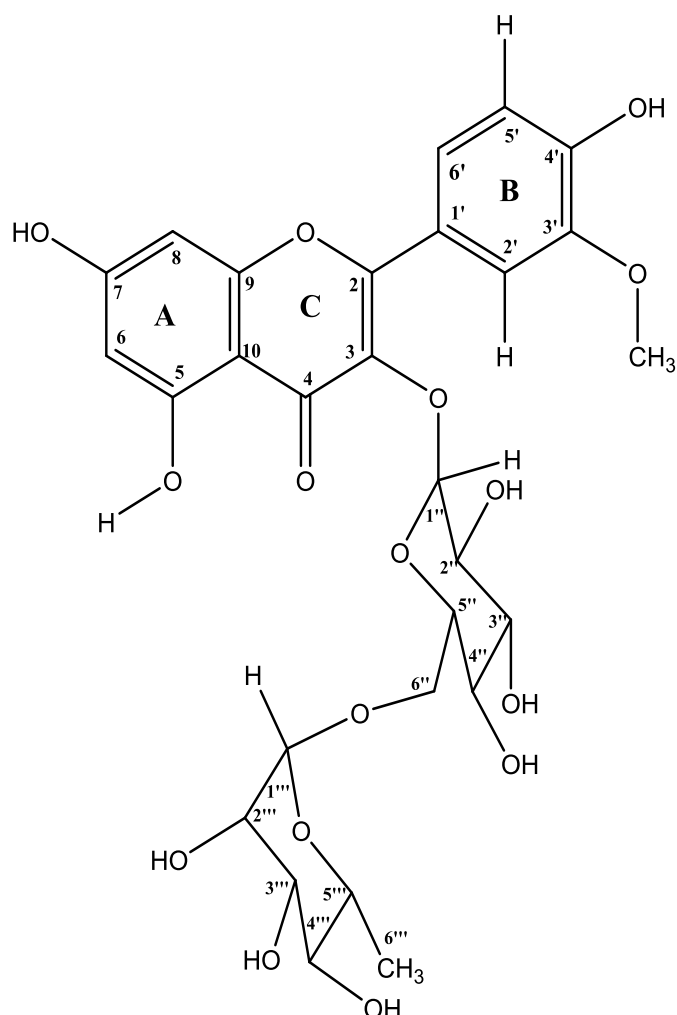


**Figure 3.19:** Structure of Ag-1.

Compound **Ag-1** (Figure 3.19) was isolated from the MeOH extract of *A. graecorum* leaves using Sephadex CC. On TLC with 50% EtOAc in 50% MeOH, it gave a yellow spot (R$f$ = 0.52) after spraying with *p*-anisaldehyde-sulphuric acid reagent and heating. ¹H NMR spectrum of the compound (Table 3.5) in (CD₃COCD₃, Figure 3.21) showed two doublets at $\delta_H$ 6.30 (1H, *d*, *J* = 2.0 Hz, H-6) and $\delta_H$ 6.55 (1H, d, *J* = 2.1Hz, H-8) together with a proton doublet at $\delta_H$ 6.98 (1H, *d, J* = 8.4 Hz, H-5') and an overlapped proton signal at $\delta_H$ 7.66 (1H, *d, J* = 8.4, H-6') and these patterns were typical of a flavonoid moiety.

In addition, the ¹H-NMR spectrum showed two protons resonating at d 5.38 (d, H-1″) and 4.58 (d, H-1‴) assigned to the anomeric β-glucopyranosyl proton and α-rhamnopyranosyl protons, respectively.

While the ¹³C NMR (125MHz) spectrum of the compound (Table 3.5) in (CD₃COCD₃, Figure 3.22) revealed the presence of 15 carbon signals for the substituted-flavonol moiety of the aglycon and 12 carbon resonances belonging to two sugar moieties, in addition, there was one carbon signal indicating the presence of one methoxy group. The anomeric carbons were observed at 103.6 (C-1″) and 100.4 (C-1‴).

In the HMBC spectrum (Figure 3.23), the proton at $\delta_H$ 6.30 (H-6) showed $^3J$ correlations to carbons at $\delta_C$ 93.7 (C-8), 104.5 (C-10) and $^2J$ correlations to 162.1 (C-5). The proton at $\delta_H$ 6.55 (H-8) showed $^3J$ correlations to the carbons 98.7 (C-6), 104.5 (C-10) and $^2J$ correlations to 164.6 (C-7), 157.1 (C-9).

The proton at $\delta_H$ 8.20 (H-2') in ring B showed $^2J$ correlations to carbon 122.5 (C-1') and oxygen-bearing aromatic carbon at 147.6 (C-3'). The protons at 6.98 (H-5') showed $^3J$ correlations at 122.5 (C-1'), 147.6 (C-3') and $^2J$ correlations to carbon at 149.6 (C-4').

Furthermore, the methoxy group at $\delta_H$ 3.98 (3H, s) showed $^3J$ correlation to the carbon at 147.6 (C-3') proving its connectivity to ring B. The anomeric proton of β-D-glucose at $\delta_H$ 5.38 (H-1″) showed $^3J$ correlations to carbon at 134.2 (C-3) proving its connectivity at that position.

The HRESI-MS spectrum showed a molecular ion [M-H] $^-$ at *m/z* 623.1630 (Calc C$_{28}$H$_{31}$O$_{16}$, 623.1612) suggesting a molecular formula of C$_{28}$H$_{32}$O$_{16}$.

Based on these results, **Ag-1** was identified as isorhamnetin 3-*O*-rutinoside (narcissin). This compound was isolated previously from *Peucedanum aucheri* Boiss (Apiaceae) (Dehaghani *et al.*, 2017), however, this is the first report of narcissin from *A. graecorum* (Fabaceae).
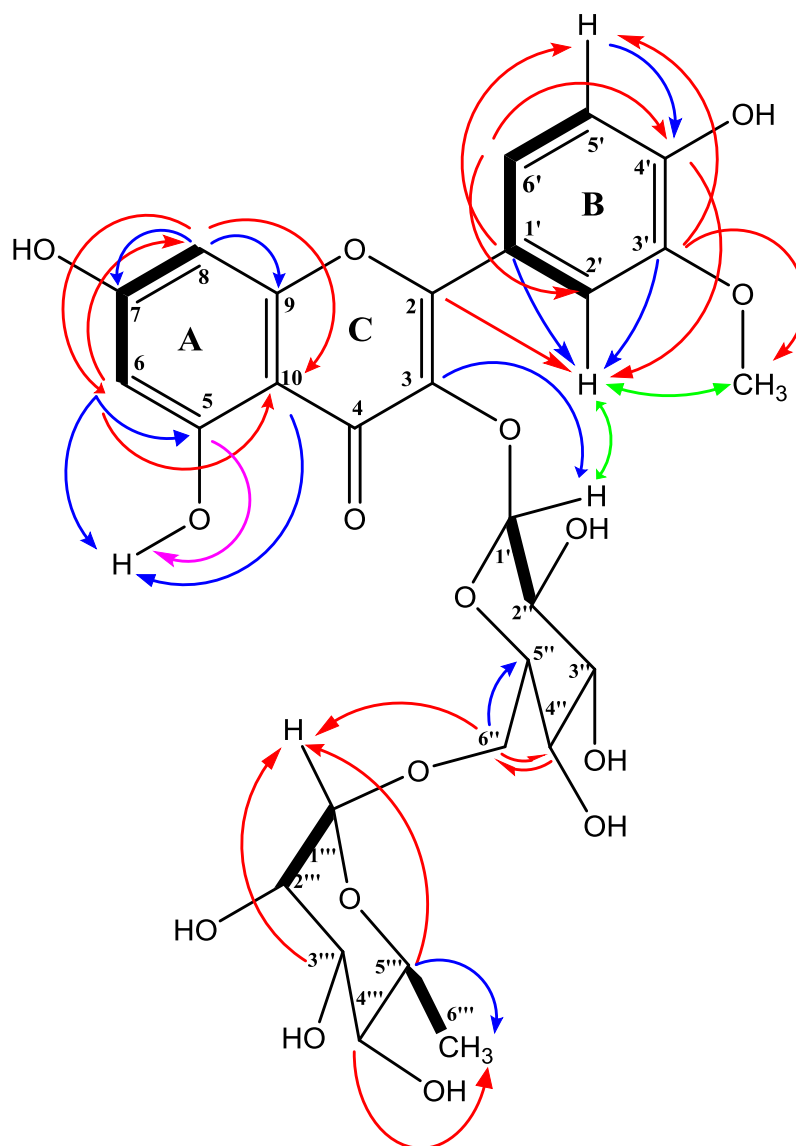


**Figure 3.20:** Structure of Ag-1 with key NEOSY ( ), COSY ( ), HMBC $^2J$ ( ) and $^3J$ ( ) correlations.

**Table 3.5:** $^1$H (500 MHz), $^{13}$C (125 MHz), HMBC and COSY data of Ag-1 in CD$_3$COCD$_3$

| Position | $^1$H (δ ppm) (Mult, $J$ (Hz)) | $^{13}$C (δ ppm) (Mult) | HMBC | | COSY |
| | | | $^2J$ | $^3J$ | - |
|---|---|---|---|---|---|
| 1 | - | - | - | - | - |
| 2 | - | 157.1 (C) | - | - | - |
| 3 | - | 134.2 (C) | - | - | - |
| 4 | - | 180.6 (C) | - | - | - |
| 5 | - | 162.1 (C) | - | - | - |
| 6 | 6.30 (1H, dd, $J$ = 2.0) | 98.7 (CH) | C-5 | C-8, C-10 | - |
| 7 | - | 164.6 (C) | - | - | - |
| 8 | 6.55 (1H, d, $J$ = 2.1) | 93.7 (CH) | C-7, C-9 | C-6, C-10 | - |
| 9 | - | 157.1 (C) | - | - | - |
| 10 | - | 104.5 (C) | - | - | - |
| 1′ | - | 121.7 (C) | - | - | - |
| 2′ | 8.20 (1H, d, $J$ = 2.1) | 113.6 (CH) | C-1′, C-3′ | C-4′, C-2 | - |
| 3′ | - | 147.6 (C) | - | - | - |
| 4′ | - | 149.6 (C) | - | - | - |
| 5′ | 6.98 (1H, d $J$ = 8.4) | 114.8 (CH) | C-4′ | C-1′, C-3′ | H-6′ |
| 6′ | 7.66 (1H, d $J$ = 8.4,2.1) | 122.3 (CH) | - | C-2′, C-4′ | H-5′ |
| Glu | | | | | |
| 1″ | 5.38 (d, $J$ = 7.8) | 103.6 (CH) | - | C-3 | H-2″ |
| 2″ | 3.83 (m) | 72.2 (CH) | - | - | H-1″ |
| 3″ | 3.77 (t, $J$ = 6.3) | 77.4 (CH) | - | - | - |
| 4″ | 3.50 | 74.1 (CH) | - | C-6″ | - |
| 5″ | 3.69 | 73.9 (CH) | - | - | - |
| 6″ | 3.83 / 3.51 (dd) | 65.8 (CH$_2$) | C-5″ | C-4″ | - |
| Rha | | | | | |
| 1‴ | 4.58 (d, $J$ = 1.7) | 100.4 (CH) | - | C-3‴, C-5‴, C-6″ | 2‴ |
| 2‴ | 3.61 (br, m) | 70.9 (CH) | - | - | 1‴ |
| 3‴ | 3.49 (m) | 71.5 (CH) | - | - | - |
| 4‴ | 3.30 (m) | 72.8 (CH) | - | - | - |
| 5‴ | 3.56 (m) | 68.2 (CH) | - | - | H-6‴ |
| 6‴ | 1.14 (3H, d $J$ = 6.1) | 17.2 (CH$_3$) | C-5‴ | C-4‴ | H-5‴ |
| 5 – OH | 12.47 (s) | - | C-5 | C-6, C-10 | - |
| 3′ - OCH$_3$ | 3.98 (3H, s) | 55.7 (CH$_3$) | - | C-3′ | - |
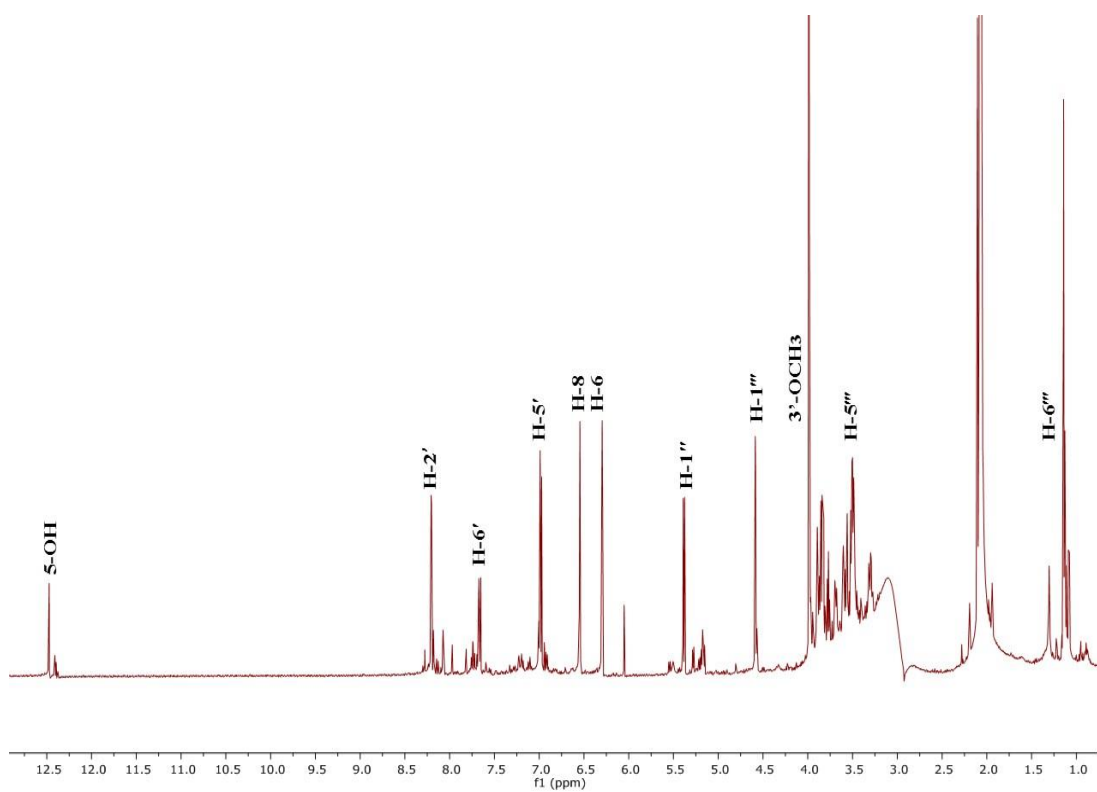
**Figure 3.21:** $^1$H NMR spectrum (500 MHz) of Ag-1 in CD$_3$COCD$_3$.
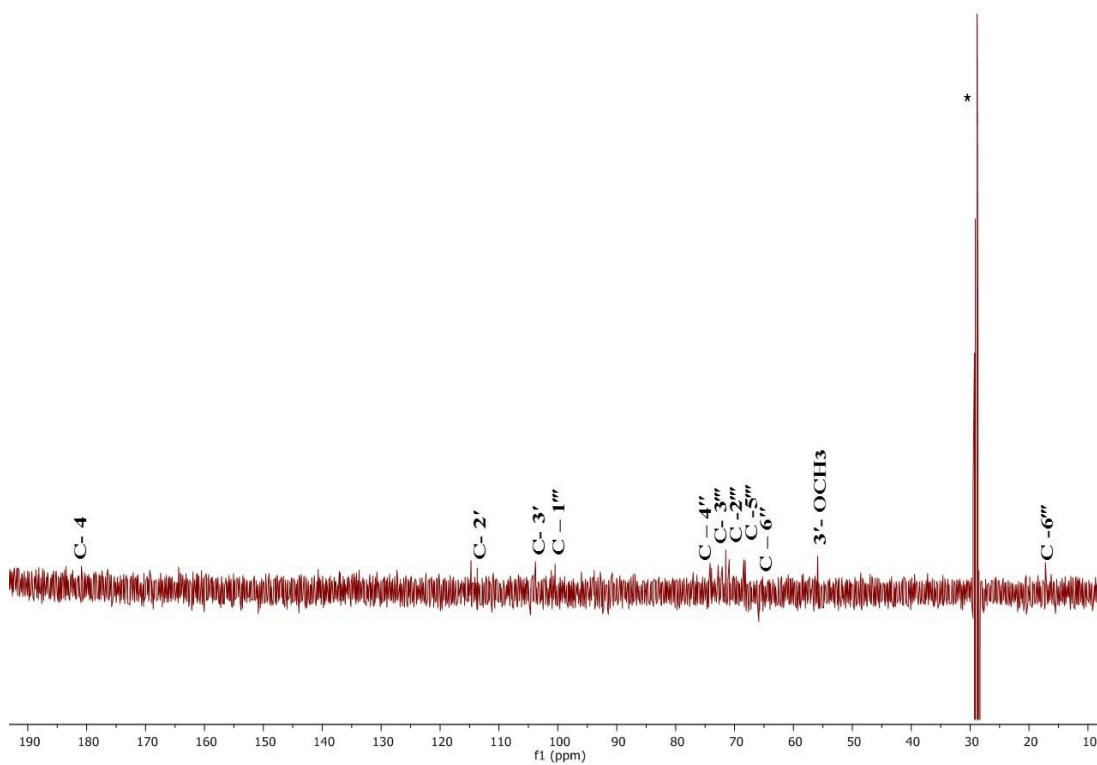


**Figure 3.22:** Full $^{13}$C NMR spectrum (125 MHz) of Ag-1 CD$_3$COCD$_3$*.
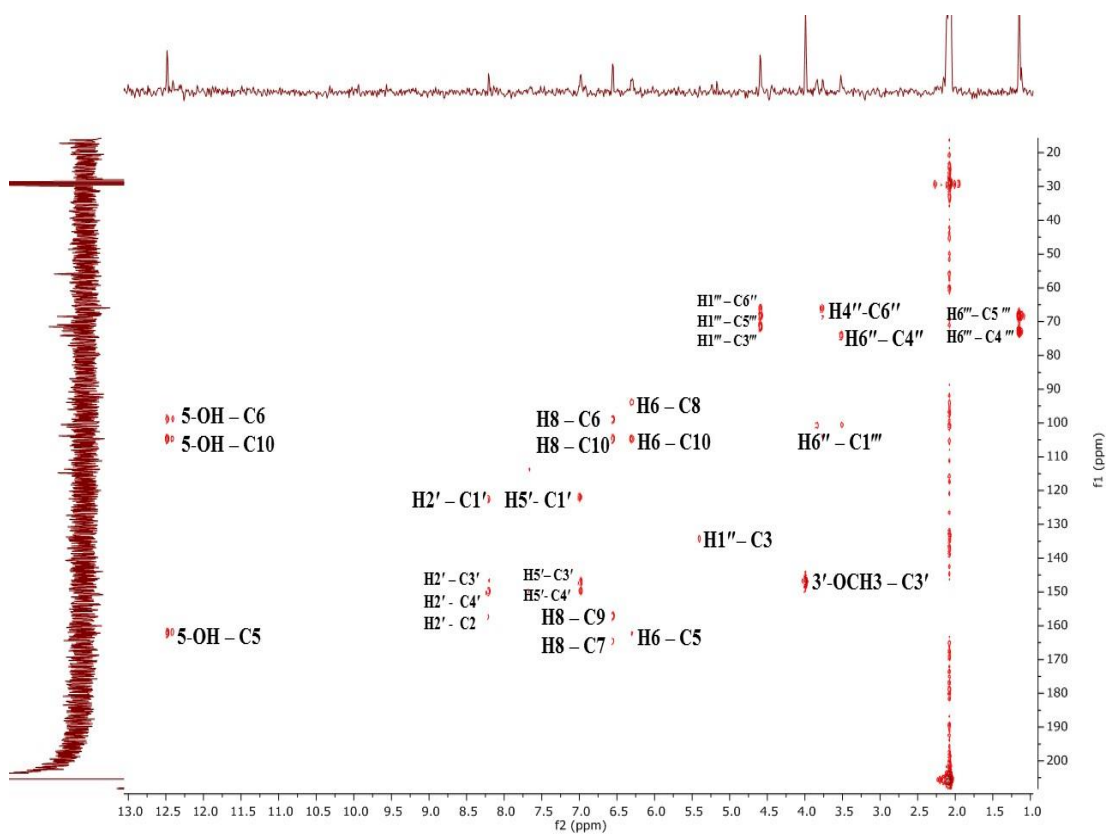
**Figure 3.23:** HMBC (CD₃COCD₃) spectrum of Ag-1.
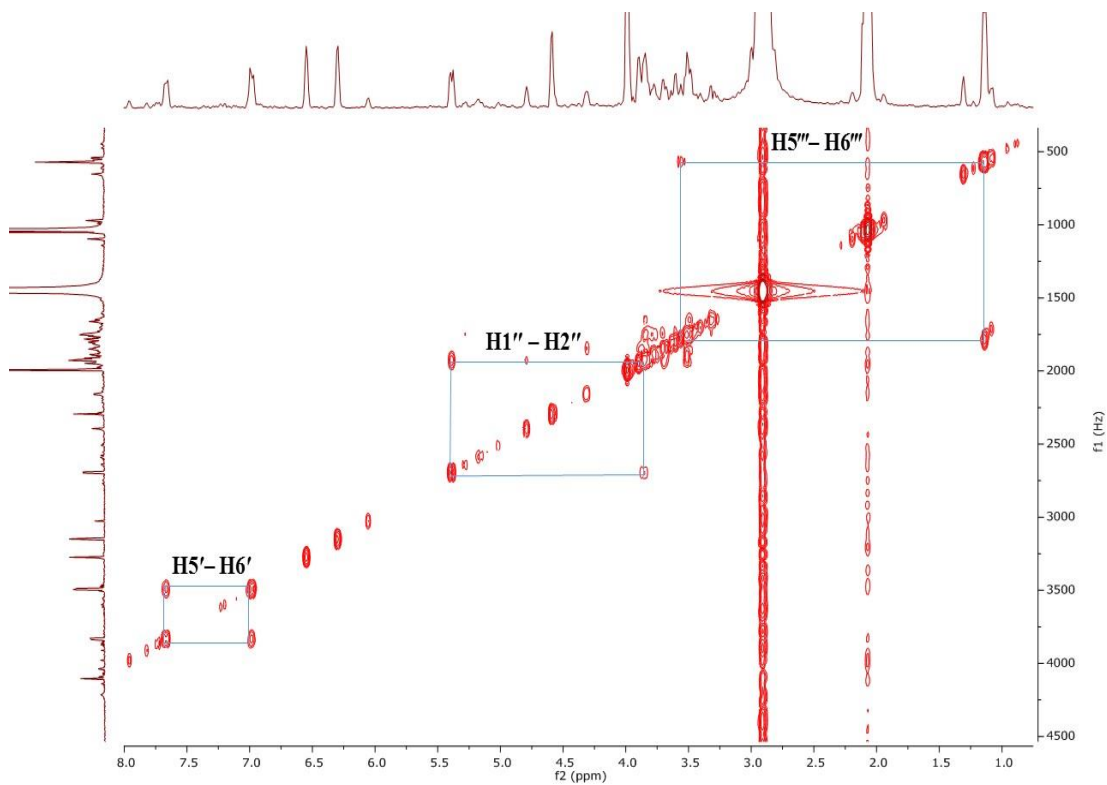


**Figure 3.24:** COSY (CD₃COCD₃) spectrum of Ag-1.
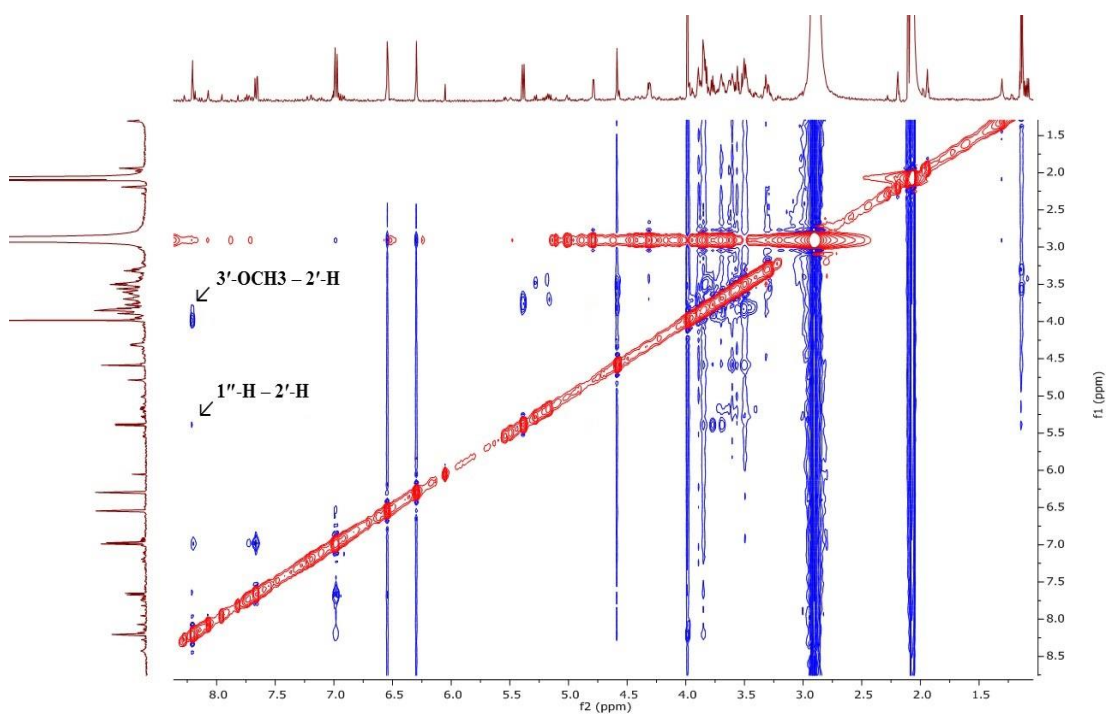
**Figure 3.25:** NEOSY (CD$_3$COCD$_3$) spectrum of Ag-1.

## 3.4 Fractionation of *R. raetam* crude extracts

The EtOAC extract (14.0 g) of *R. raetam* was further fractionated by two methods. In the first, 10 g was subjected to fractionation using CC (Section 2.6.4). Fraction 2 was obtained as a black solid containing a single compound (500 mg) which was identified using NMR and enabled elucidation of the structure **Rr-1**. The second method involved subjecting 2.0 g, to fractionation using Sephadex CC (Section 2.6.3) and led to the identification of compound **Rr-3** (25 mg).

Besides, 2.0 g of the MeOH extract of *R. raetam* was subjected to fractionation using a Sephadex CC. TLC was used applied to pool similar fractions. A Sephadex CC was used to fractionate the pooled fractions (25-35); 11 vials were collected and their contents were assessed using NMR and enabled elucidation of compound **Rr-2** from vial 5 (10 mg), The $^1$HNMR spectrum of the hexane extract of *R. raetam* showed signals suggesting the presence of mixtures of triglycerides and fats.

### 3.4.1 Characterisation of Rr-1 as alpinumisoflavone
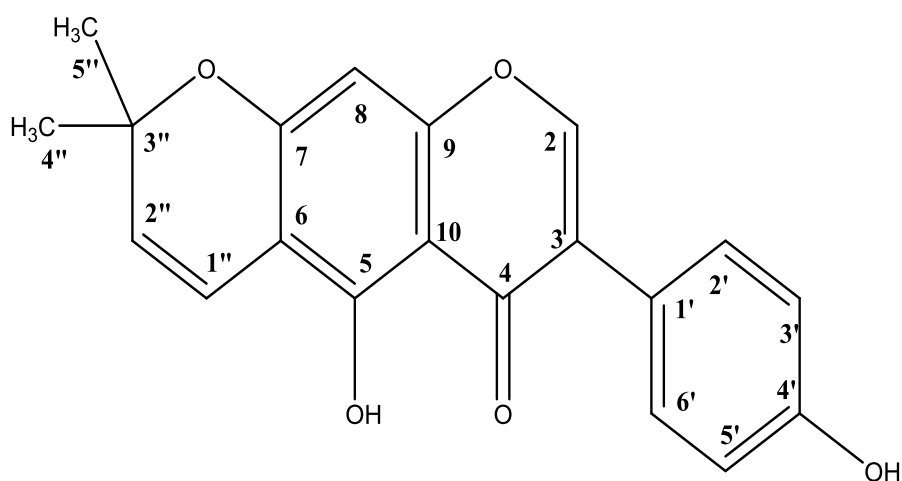


**Figure 3.26:** Structure of Rr-1.

The compound **Rr-1** (Figure 3.26) was obtained from the EtOAc extract of *R. reatam*. On TLC, the compound gave a green spot with R*f* = 0.68 in hexane: EtOAc (1:1) after spraying with *p*-anisaldehyde-sulfuric acid reagent and heating.

The $^1$H NMR (400 MHz) spectrum of the compound in CDCl$_3$ (Figure 3.21) showed signals typical of an isoflavone moiety having a pyrone ring. Two doublets were observed at $\delta_H$ 5.62 ($J = 10.0$ Hz, H-2″) and 6.72 ($J = 10.0$ Hz, H-1″) ppm usually for cis-diene protons and six methyl protons at $\delta_H$ 1.47 ppm (2 x CH$_3$). These signals were assigned to a 2, 2- dimethylchromene ring system.

The characteristic H-2 proton of the isoflavone was observed as a singlet at $\delta_H$ 7.80 ppm. Also observed in the spectrum were a pair of doublets, each integrated for two protons, at $\delta_H$ 6.89 ($J = 8.6$ Hz) and 7.38 ($J = 8.6$ Hz), which were due to H-3/H-5′ and H-2′/ H-6′ of a paradisubstituted aromatic nucleus.

The downfield resonance of H-3′ and H-5′ ($\delta_H$ 6.89) suggests the presence of an oxygenated substituent at C-4′. This was confirmed by the presence of a broad singlet at $\delta_H$ 5.04 (1H, H-4′), due to a hydroxyl group proton. The remaining signals at $\delta_H$ 6.32 (1H, s) was attributed to H-8, and the one at $\delta_H$ 13.13 (1H,s), to the chelated hydroxyl proton at C-5.

The DEPTq-135 NMR (100 MHz) spectrum (Figure 3.29) indicated the presence of 20 carbon atoms including a carbonyl at $\delta$c 181.1 (C-4) and six aromatic CH at $\delta_C$ 152.0, 95.0, 130.4, 115.6, 115.6 and 128.3 ppm.

The HRESI-MS spectrum showed a molecular ion [M-H]$^-$ at $m/z$ 335.0932 (Calc C$_{20}$H$_{15}$O$_5$, 335.0919) which indicated a molecular formula of C$_{20}$H$_{16}$O$_5$.

Based on the above spectral data and by comparison with previous reports, the identity of compound **Rr-1** was confirmed as alpinumisoflavone, previously isolated from *Cudrania tricuspidata* (Han *et al*., 2005). This is the first report of alpinumisoflavone from *R. raetam*.
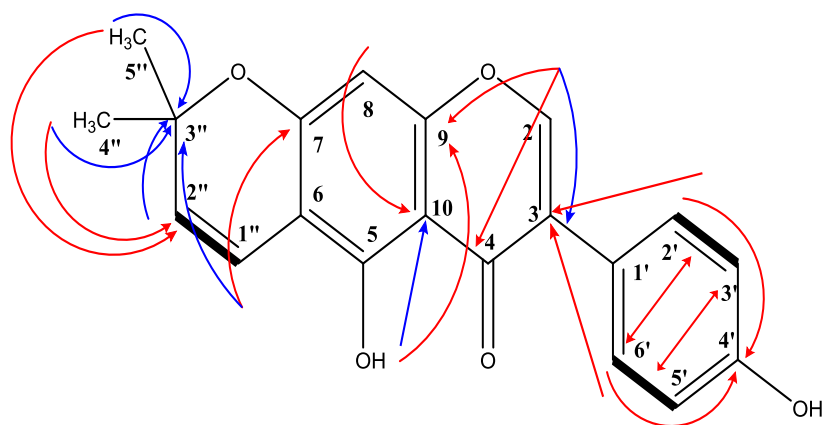
**Figure 3.27:** Structure of Rr-1with key COSY (▬▬) and HMBC $^2J$ ( ⌒ ) and $^3J$ ( ⌒ ) correlations.

**Table 3.6:** $^1H$ (400 MHz), $^{13}C$ (100 MHz), HMBC and COSY data of Rr-1 in CDCl$_3$

| Position | $^1H$ (δ ppm) (Mult, $J$ (Hz)) | $^{13}C$ (δ ppm) (Mult) | HMBC $^2J$ | HMBC $^3J$ | COSY - |
|---|---|---|---|---|---|
| 1 | - | - | - | - | - |
| 2 | 7.80 (1H, s) | 152.0 (CH) | C-3 | C-9, C-4 | - |
| 3 | - | 123.59(C) | - | - | - |
| 4 | - | 181.1(C) | - | - | - |
| 5 | - | 157.0 (C) | - | - | - |
| 6 | - | 105.7 (C) | - | - | - |
| 7 | - | 160.5 (C) | - | - | - |
| 8 | 6.32 (1H, s) | 95.0 (CH) | - | C-10 | - |
| 9 | - | 157.3 (C) | - | - | - |
| 10 | - | 106.3(C) | - | - | - |
| 1′ | - | 122.9(C) | - | - | - |
| 2′ / 6′ | 7.38 (2H,d, $J$ = 8.5 Hz) | 130.4 (CH) | - | C-3,C-4′,C6′/2′ | H-3′ / H-5′ |
| 3′ / 5′ | 6.89 (2H,d, $J$ = 8.6 Hz) | 115.6 (CH) | - | C-1′, C-5′/C-3′ | H-2′ / H-6′ |
| 4′ | - | 156.3 (C) | - | - | - |
| 1″ | 6.72 (1H,d, $J$ = 10.0 Hz) | 116.1(CH) | - | C-7, C-3″ | H-2″ |
| 2″ | 5.62 (1H,d, $J$ = 10.0 Hz) | 128.3 (CH) | C-3″ | C-6 | H-1″ |
| 3″ | - | 78.2 (C) | - | - | - |
| 4″ | 1.47 (s) | 28.15 (CH$_3$) | C-3″ | C-2″ | - |
| 5″ | 1.47 (s) | 28.15 (CH$_3$) | C-3″ | C-2″ | - |
| 5 - OH | 13.13 (1H,s) | - | C-10 | C-9 | - |
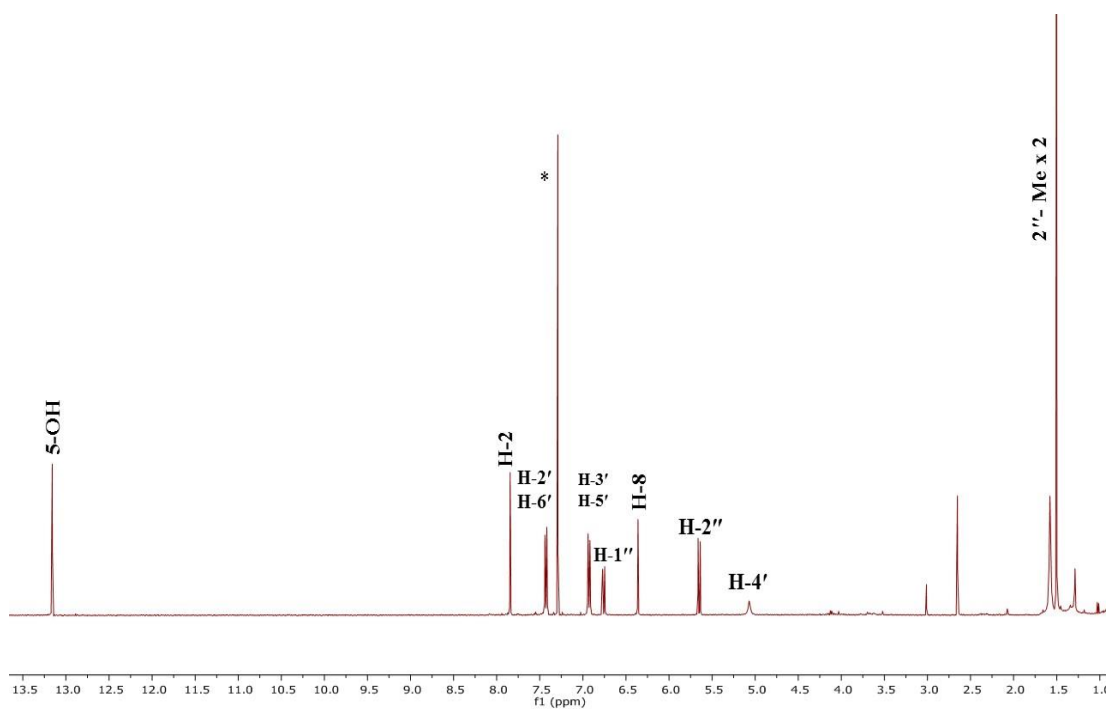
**Figure 3.28:** ¹H NMR spectrum (400 MHz) of Rr-1 in CDCl$_3$.*
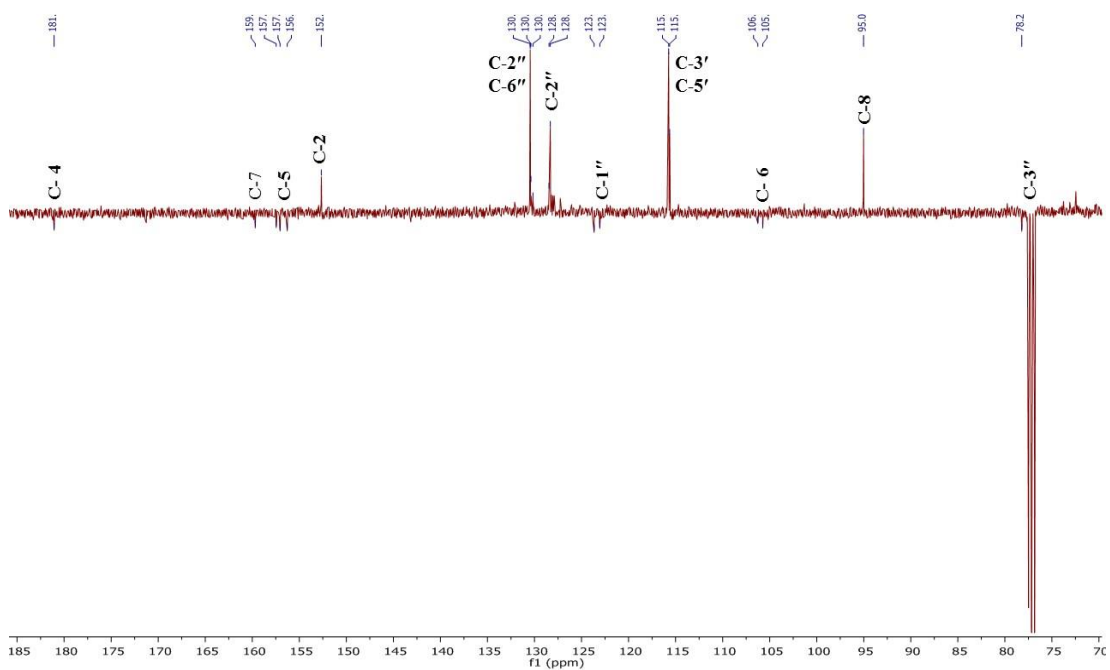


**Figure 3.29:** DEPTq-135 (100 MHz) NMR Spectrum of Rr-1 CDCl$_3$.
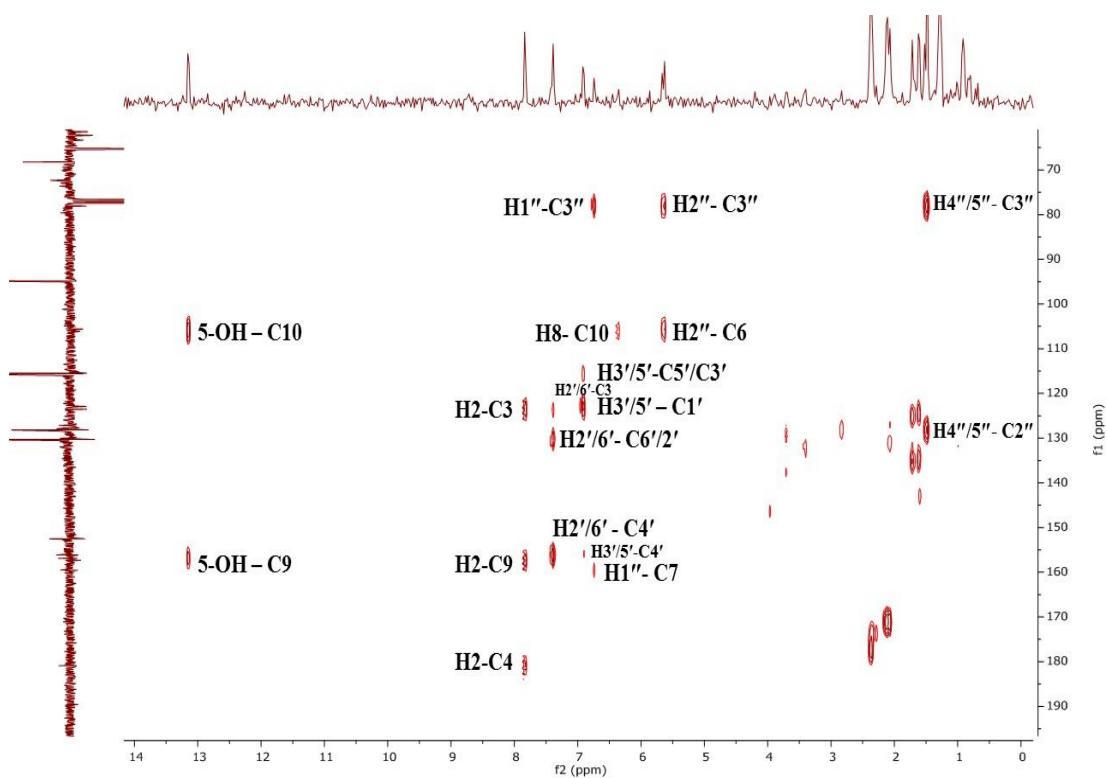
**Figure 3.30:** HMBC (CDCl₃) spectrum of Rr-1.
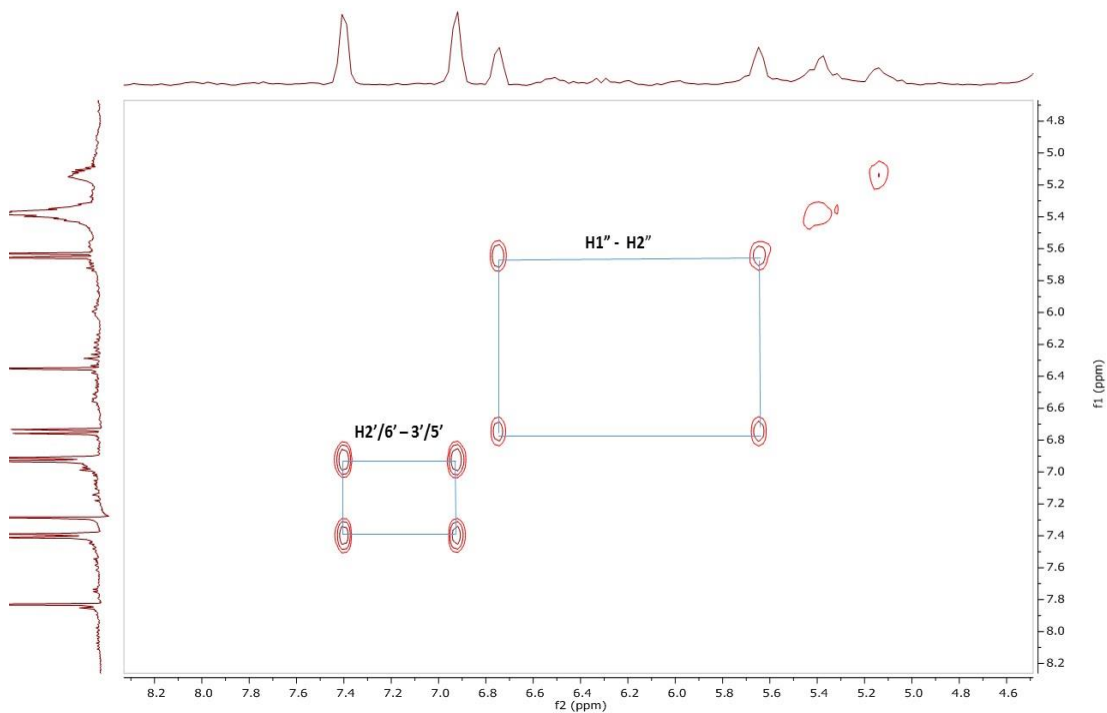


**Figure 3.31:** COSY (CDCl₃) spectrum of Rr-1.

### 3.4.2 Characterisation of Rr-2 as 8-*β*-D-glucopyranosylgenistein
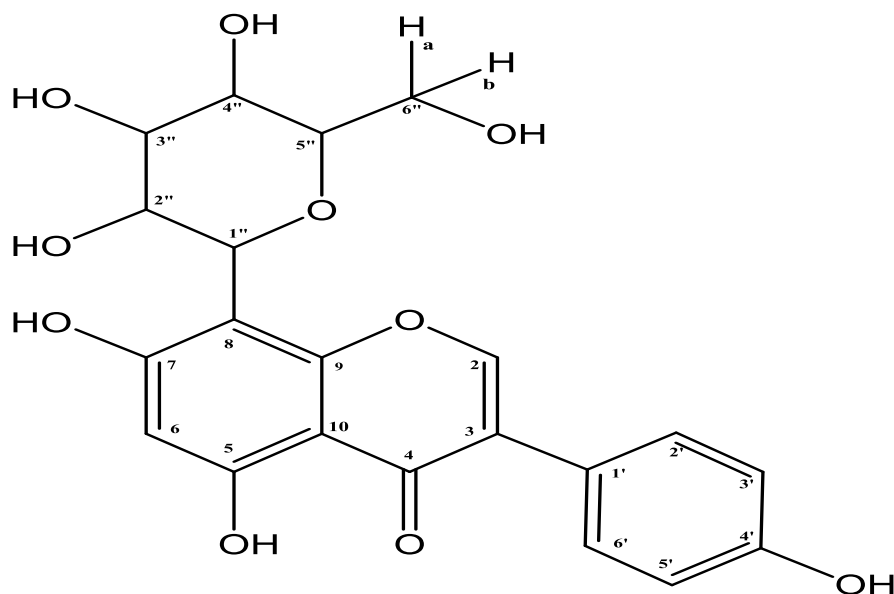


**Figure 3.32:** Structure of Rr-2.

The compound **Rr-2** (Figure 3.32) was isolated from the MeOH extract of *R. raetam* leaves using Sephadex CC. On TLC using a mixture of 10% MeOH, 40% EtOAc and 50% hexane, it gave one spot (R*f* = 0.53) which after spraying with *p*-anisaldehyde - sulfuric acid reagent and heating turned to violet.

The $^1$H NMR spectrum (Figure 3.34; Table 3.7) indicated a 1, 2, 3, 5 -tetrasubstituted ring A of a flavonoid moiety. Two aromatic protons were observed at $\delta_H$ 8.21 (1H, s, H-2), 6.27 (1H,s, H-6) while two ortho - coupled doublets at $\delta_H$ 6.91 (2H, d, *J* = 8.9 Hz, H-3′/5′), 7.46 (2H, d, *J* = 8.9 Hz, H-2′/6′) for a 1,4-para disubstituted ring B. The sugar unit showed an anomeric proton at $\delta_H$ 5.05 (1H, d, *J* = 9.9 Hz, H-1″) and a methyl doublet at $\delta_H$ 3.88 (3H, d, *J* = 3.4 Hz, H-6″). Although the multiplicity of H-4″ could not be determined due to signal overlap, the large coupling constant (*J* = 9.9 Hz) observed for H-3″ led to the assignment of H-3″ and H- 4″ as transdiaxial protons and thus the sugar unit was identified as *β*-D-glucopyranosyl.

In the HMBC spectrum (Figure 3.35; Table 3.7), the proton at $\delta_H$ 6.27 (H-6) showed $^2J$ correlation to two phenolic carbons at $\delta_C$ 163.3 (C-5), 162.9 (C-7) and a $^4J$ (W) coupling to the carbonyl carbon at $\delta_C$ 181.0 (C-4).

The protons at $\delta_H$ 7.46 (H-2'/6') and 6.91 (H-3'/5') showed $^3J$ and $^2J$ correlations respectively to another phenolic carbon at $\delta_C$ 157.5 (C-4') establishing the presence of an -OH substituent at C-4' on the ring B of the flavonoid. The protons at $\delta_H$ 7.46 (H-2'/6') also showed $^3J$ correlations to carbon at $\delta_C$ 122.8 (C-3). The position of the attachment of the glucose unit was established from the HMBC spectrum (Figure 3.36) as the anomeric proton at $\delta_H$ 5.05 (H-1") showed a $^2J$ correlation to C-8 ($\delta_C$ 103.1).

The HRESI-MS spectrum showed a molecular ion [M-H]$^-$ at *m/z* 431.0978 (Calc $C_{21}H_{19}O_{10}$, 431.0978) suggesting a molecular formula of $C_{21}H_{20}O_{10}$. Based on these results and comparison with previous data, **Rr-2** was identified as 8-*β*-D-glucopyranosylgenistein (Jesus *et al*., 2014).
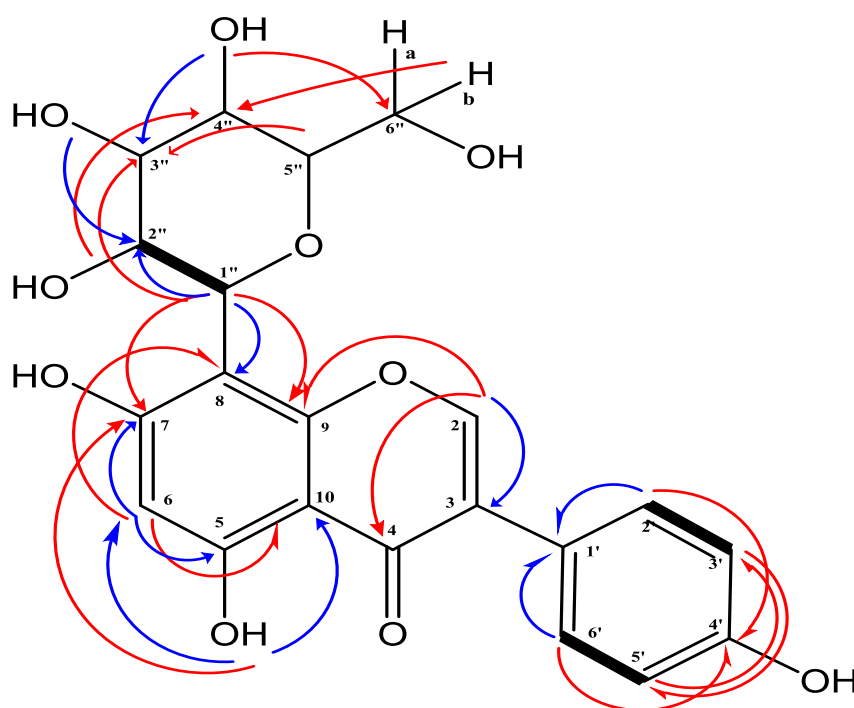


**Figure 3.33:** Structure of Rr-2 with key COSY ( ▬ ) and HMBC $^2J$ ( ⌒ ) and $^3J$ ( ⌒ ) correlations.

**Table 3.7:** $^1$H (500 MHz), $^{13}$C (125 MHz), HMBC and COSY data of Rr-2 in CD$_3$COCD$_3$

| Position | $^1$H (δ ppm) (Mult, *J* (Hz)) | $^{13}$C (δ ppm) (Mult) | HMBC | | COSY |
|---|---|---|---|---|---|
| | | | $^2J$ | $^3J$ | - |
| 1 | - | - | - | - | - |
| 2 | 8.21 (1H,s) | 153.0 (CH) | C-3 | C-9, C-4 | - |
| 3 | - | 122.8 (C) | - | - | - |
| 4 | - | 181.0 (C) | - | - | - |
| 5 | - | 162.3 (C) | - | - | - |
| 6 | 6.27 (1H,s) | 99.7 (CH) | C-5, C-7 | C-10, C-8 | - |
| 7 | - | 162.9 (C) | - | - | - |
| 8 | - | 103.1 (C) | - | - | - |
| 9 | - | 155.7 (C) | - | - | - |
| 10 | - | 105.3 (C) | - | - | - |
| 1′ | - | 122.0 (C) | - | - | - |
| 2′ / 6′ | 7.46 (1H, d, *J* = 8.9) | 130.4 (CH) | C-1′ | C-4′, C-3 | H-3′ / H-5′ |
| 3′ / 5′ | 6.91 (2H, d, *J* = 8.9) | 115.1 (CH) | - | C-5′ | H-2′ / H-6′ |
| 4′ | - | 157.5 (C) | - | - | - |
| 1″ | 5.05 (d, *J* = 9.9) | 74.8 (CH) | C-2″, C-8 | C-3″,C-9, C-7 | H-2″ |
| 2″ | 3.88 (1H, d, *J* = 9.9) | 72.7 (CH) | - | C-4″ | H-1″ |
| 3″ | 3.62 (1H, td, *J* = 9.9) | 78.4 (CH) | C-2″ | - | - |
| 4″ | 3.69 (1H, td, *J* = 9.93) | 69.9 (CH) | C-3″ | C-6″a,b | - |
| 5″ | 3.56 (1H,td, *J* = 2.9) | 70.3 (CH) | - | C-3″ | - |
| 6″a,b | 3.88 (2H, d, *J* = 3.4) | 61.0 (CH) | - | C-4″ | - |
| 5 - OH | 13.19 (1H,*s*) | - | C-6,C-10 | C-7 | - |
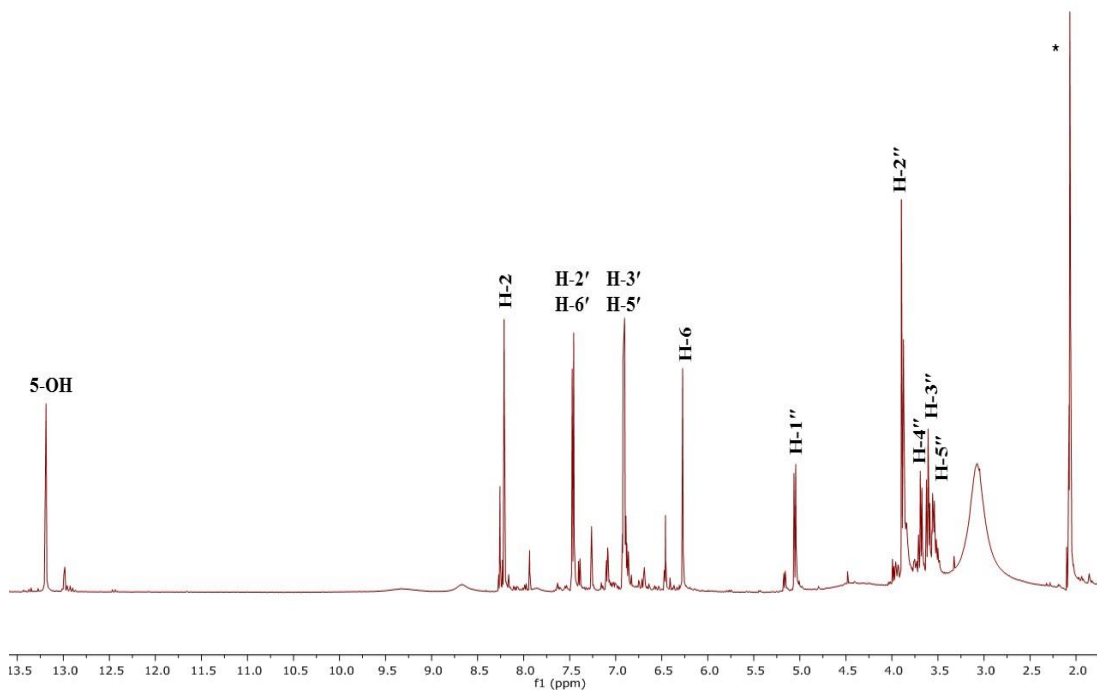
**Figure 3.34:** ¹H NMR spectrum (500 MHz) of Rr-2 in CD₃COCD₃*.
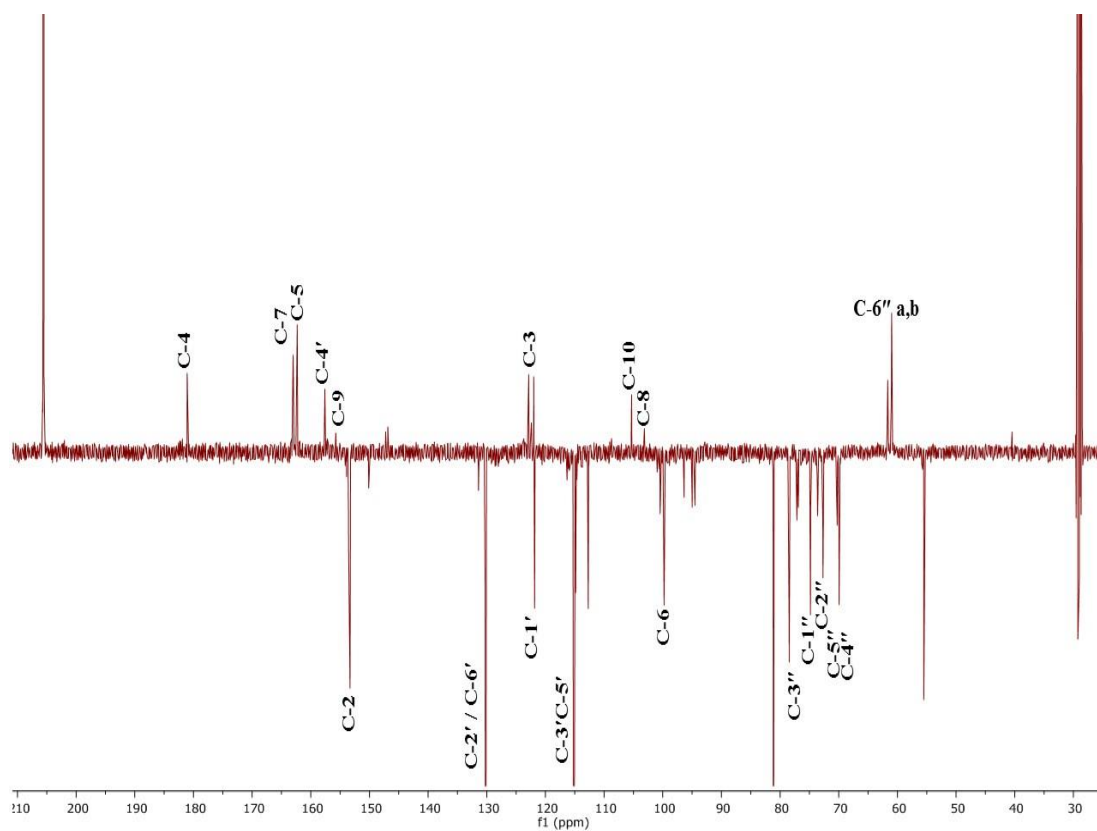


**Figure 3.35:** DEPTq-135 (125 MHz) NMR Spectrum of Rr-2 in CD3COCD3.
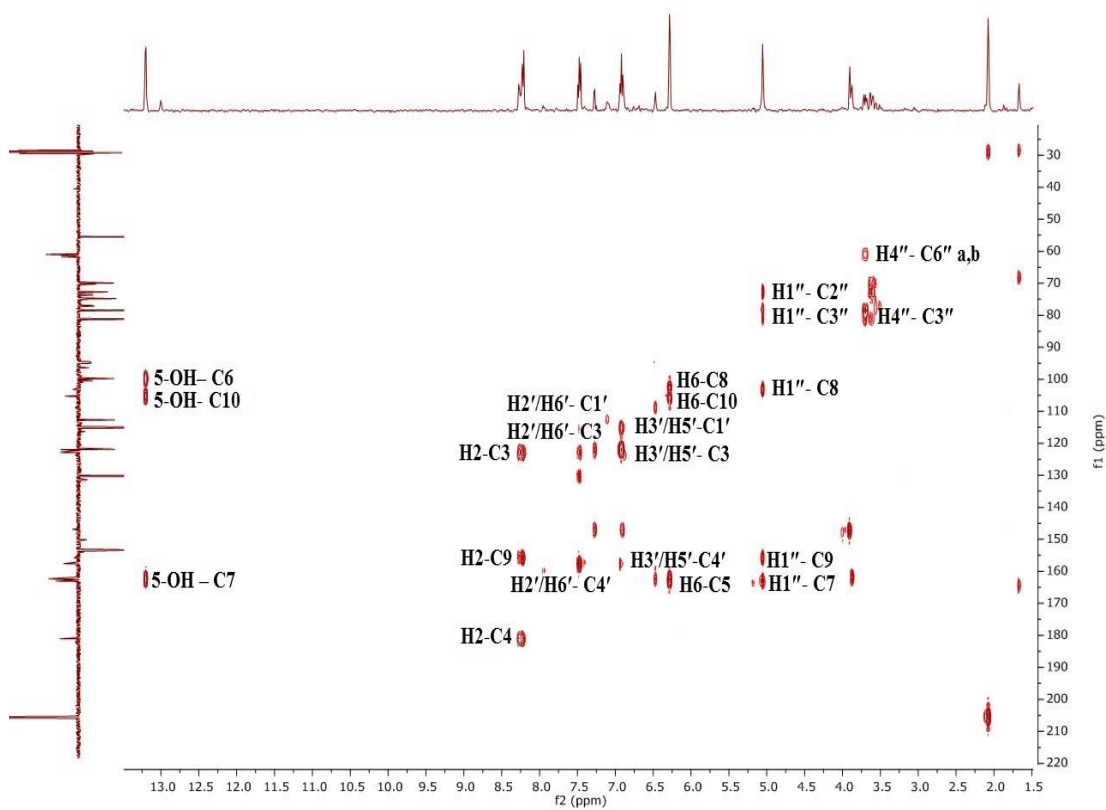
**Figure 3.36:** HMBC (CD₃COCD₃) spectrum of Rr-2.
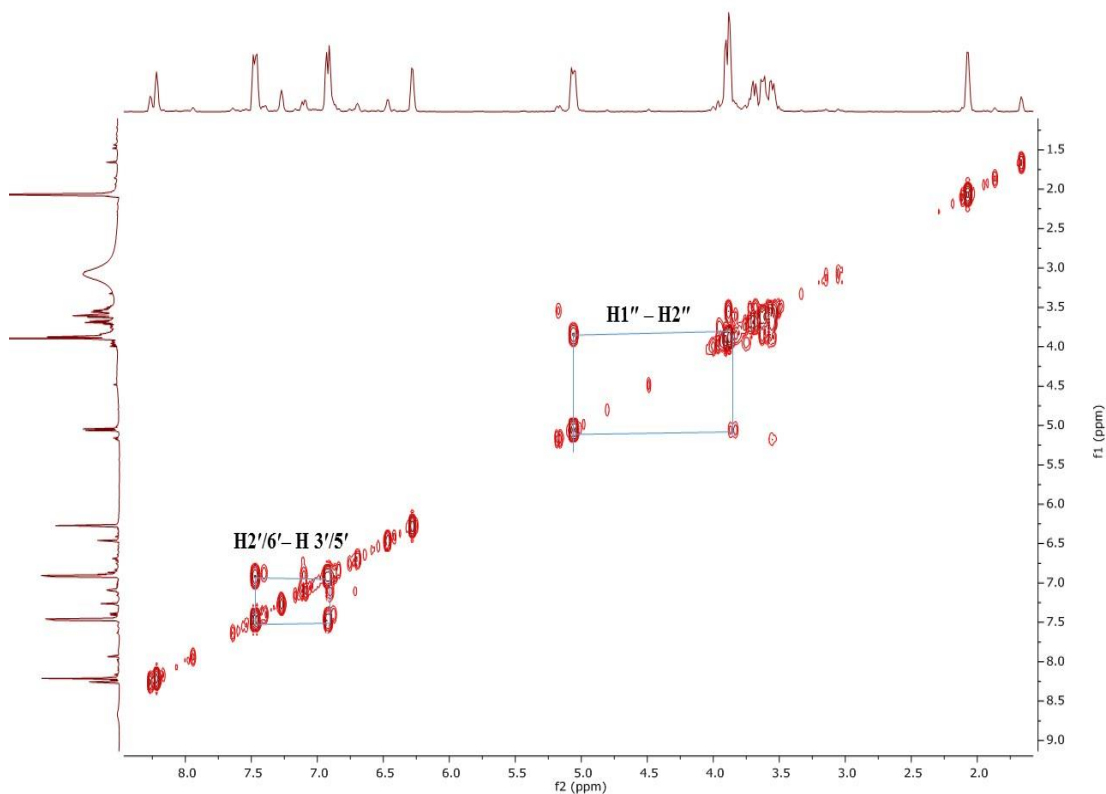


**Figure 3.37:** COSY (CD₃COCD₃) spectrum of Rr-2.

## 3.4.3 Characterisation of Rr-3 as ephedroidin
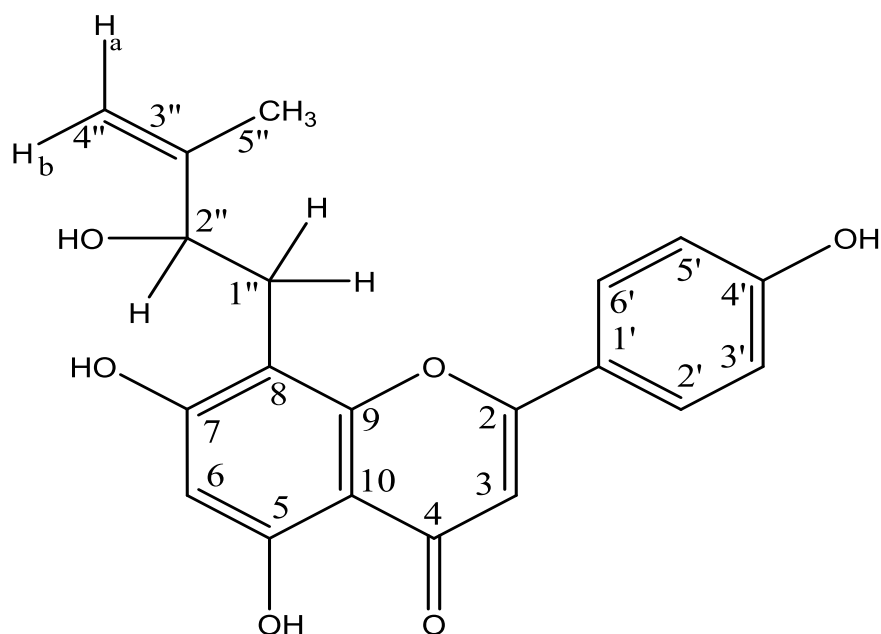


**Figure 3.38:** Structure of Rr-3.

Compound **Rr-3** (Figure 3.38) was also isolated from the MeOH extract of *R. raetam* leaves using Sephadex CC. On TLC in 10% MeOH, 40% EtOAc and 50% hexane, it gave a green spot ($Rf = 0.35$) after spraying with *p*-anisaldehyde-sulfhuric acid reagent and heating.

In the ^{1}H NMR spectrum (Figure 3.39; Table 3.8), a 1,2,3,5-tetrasubstituted benzene ring A of a flavonoid moiety was observed with one proton singlet at $\delta_H$ 6.64 (1H,*s*, H-3) while another proton singlet was observed at 6.30 (1H,s, H-6) and two ortho-coupled doublets at $\delta_H$ 7.98 (2H, d, $J = 8.7$ Hz, H-2′/6′), 7.04 (2H, d, $J = 8.6$ Hz, H-3′/5′) suggesting a 1,4-para disubstituted ring B. Also observed were two olefinic protons at 4.81 and 4.99, methyl singlet at 1.86, an oxymethine proton at 4.51 and two methylene protons at 3.10 ppm.

In the HMBC spectrum (Figure 3.42), both protons at $\delta_H$ 6.30 (H-6) showed $^2J$ correlations to two highly-deshielded oxygen-bearing quaternary carbons at $\delta_C$ 160.9 (C-5), 162.8 (C-7) and $\delta_C$ 158.6 (C-9), 166.0 (C-7), respectively. The proton at $\delta_H$ 6.30 (H-6) also showed a $^4J$ 'W' coupling to the carbonyl carbon. The protons at $\delta_H$ 7.98 (H-2′/6′) and 7.04 (H-3′/5′) showed $^3J$ and $^2J$ correlations, respectively to one oxygen-

bearing carbon at $\delta_C$ 160.6 (C-4′) establishing the presence of an -OH substituent at C-4′ on the B-ring. Protons at $\delta_H$ 7.98 (H-2′/6′) also showed $^3J$ correlation to carbon at $\delta_C$ 164.0 (C-2).

The presence of a side chain at C-8 was indicated by the absence of long-range correlations from H-6 to $\delta_C$ 104.5 (C-8) and the correlations from H-2″ to C-8. The length of the side chain using COSY and HMBC spectra was found to be 3-hydroxy-2-methylpentenyl group. Long-range correlations from H-1″ to C7, C-9 and C-3″ as well as H5″ to C-3″, C-2″ and C-4″ gave further proof of its structure and point of attachment.

The HRESI-MS spectrum showed a molecular ion [M-H]$^-$ at $m/z$ 353.1028 (Calc $C_{20}H_{17}O_6$, 353.1025) suggesting a molecular formula of $C_{20}H_{18}O_6$.

The $^1H$ and $^{13}C$ NMR spectral data were in agreement with previous reports (Pistelli *et al.*, 1998) and **Rr-3** was identified as ephedroidin previously isolated from *R. raetam*
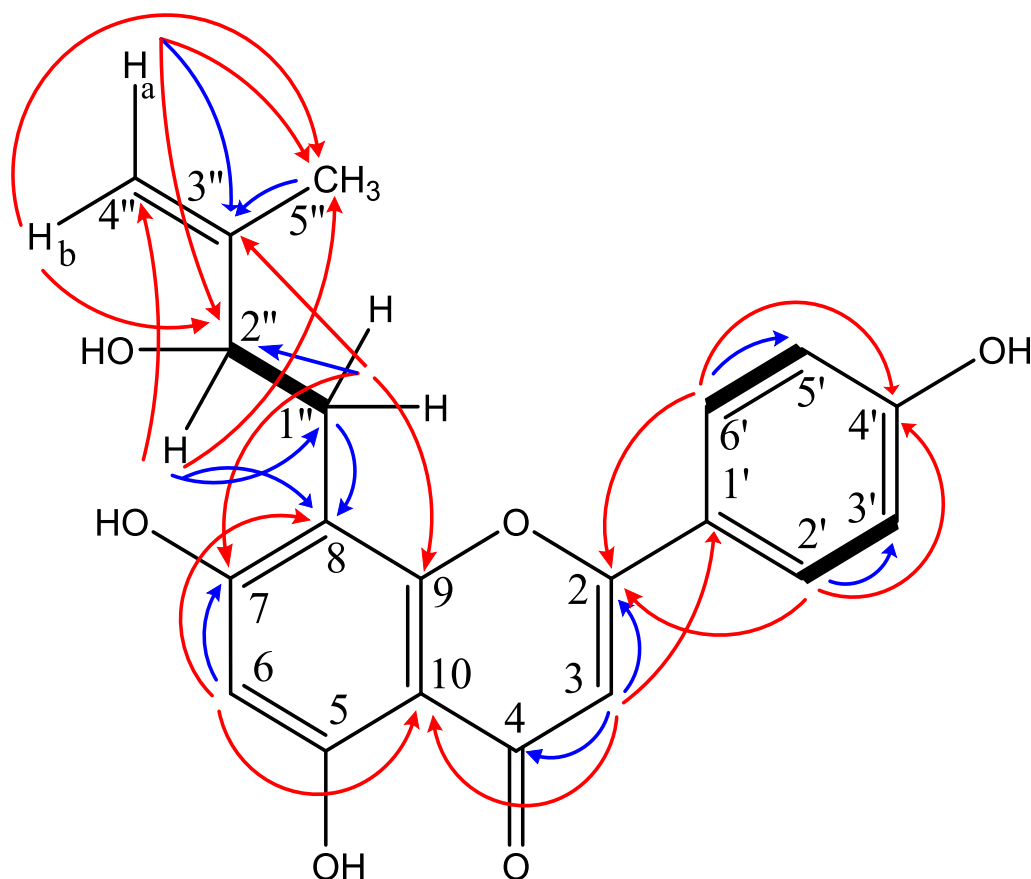


**Figure 3.39:** Structure of Rr-3 with key COSY ( ▬▬ ), HMBC $^2J$ ( ⌒ ) and $^3J$ ( ⌒ ) correlations.

**Table 3.8:** $^1H$ (500 MHz), $^{13}C$ (125 MHz), HMBC and COSY data of Rr-3 in CD$_3$COCD$_3$

| Position | $^1$H (δ ppm) (Mult, *J* (Hz)) | $^{13}$C (δ ppm) Mult | HMBC $^2J$ | $^3J$ | COSY - |
|---|---|---|---|---|---|
| 1 | - | - | - | - | - |
| 2 | - | 164.0 (C) | - | - | - |
| 3 | 6.64 (1H, s). | 103.0 (CH) | C-2,C-4 | C-1′,C-10 | - |
| 4 | - | 182.5 (C) | - | - | - |
| 5 | - | 160.9 (C) | - | - | - |
| 6 | 6.30 (1H, s) | 99.9 (CH) | C-7 | C-8,C10 | - |
| 7 | - | 162.8 (C) | - | - | - |
| 8 | - | 104.5 (C) | - | - | - |
| 9 | - | 155.5 (C) | - | - | - |
| 10 | - | 104.4 (C) | - | - | - |
| 1′ | - | 122.7 (C) | - | - | - |
| 2′ / 6′ | 7.98 (1H, d, *J* = 8.7 H) | 128.5 (CH) | C-3′/5′ | C-2,C-4′ | H3′/5′ |
| 3′ / 5′ | 7.04 (1H, d, *J* = 8.6) | 115.6 (CH) | - | - | H2′/6′ |
| 4′ | - | 160.6 (C) | - | - | - |
| 1″ | 3.10 (2H, dd, *J* = 14.4, 8.4). | 29.5 (CH) | C-2″,C-8 | C-3″,C-7 ,C-9 | H1″ |
| 2″ | 4.51(1H, dd, *J* = 8.4, 3.8). | 75.3 (CH) | C-1″, | C-8,C-5″ ,C4″ | H2″ |
| 3″ | - | 148.5 (C) | - | - | - |
| 4″a | 4.99 (1H, s) | 109.7 (CH) | C-3″ | C-2″,C-5″ | H5″ |
| 4″b | 4.81(1H, s) | 109.7 (CH) | - | C-2″,C-5″ | H5″ |
| 5″ | 1.86 (3H, s) | 17.1 (CH$_3$) | C-3″ | - | H4″a / b |
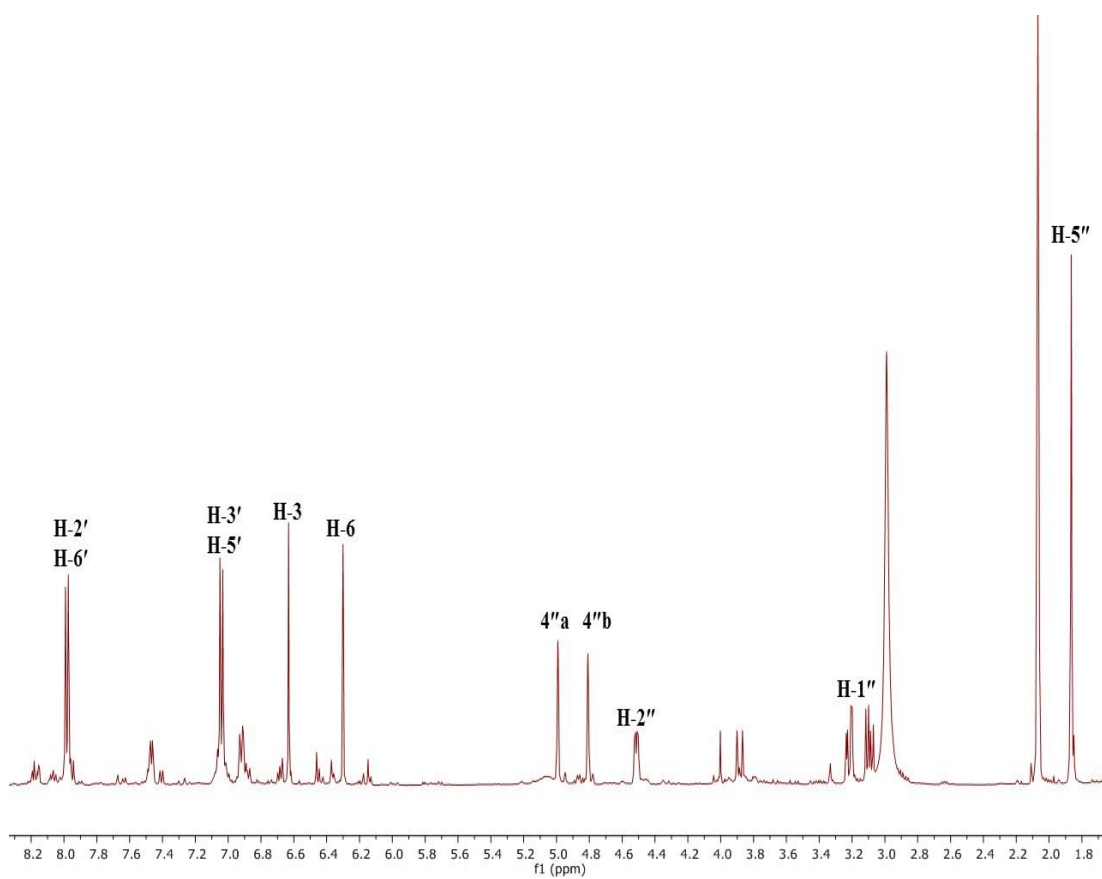
**Figure 3.40:** ¹H NMR spectrum (500 MHz) of Rr-3 in CD₃COCD₃.
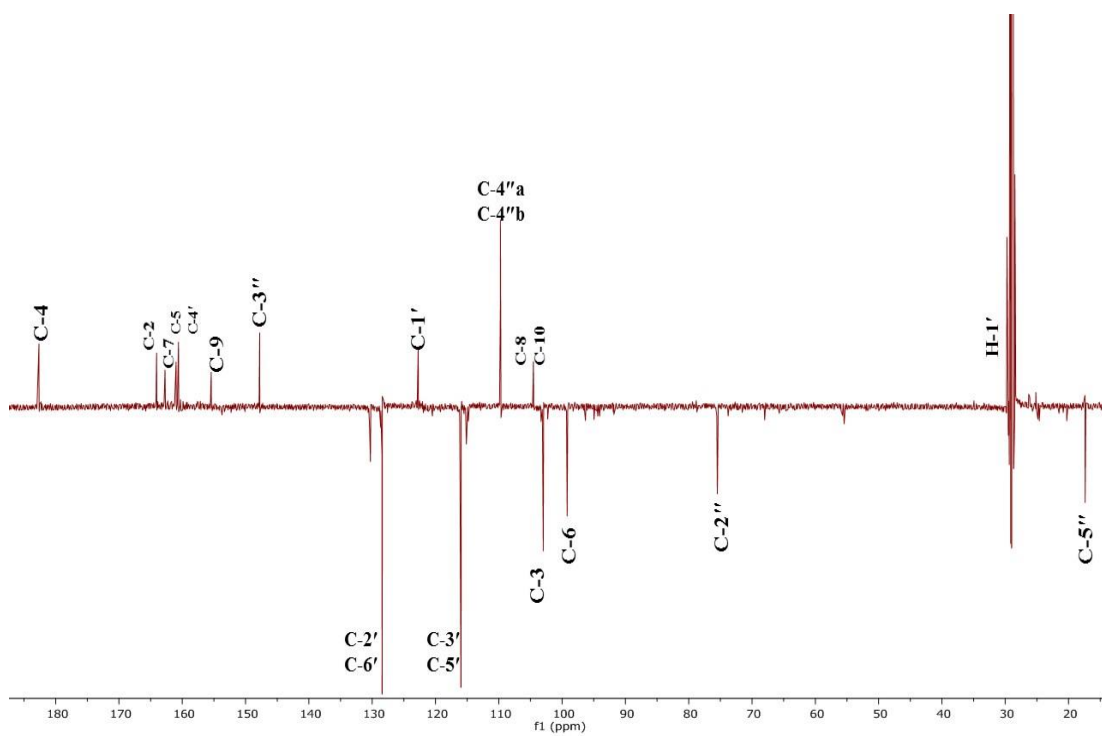


**Figure 3.41:** DEPTq-135 (125 MHz) NMR Spectrum of Rr-3 in CD₃COCD₃.
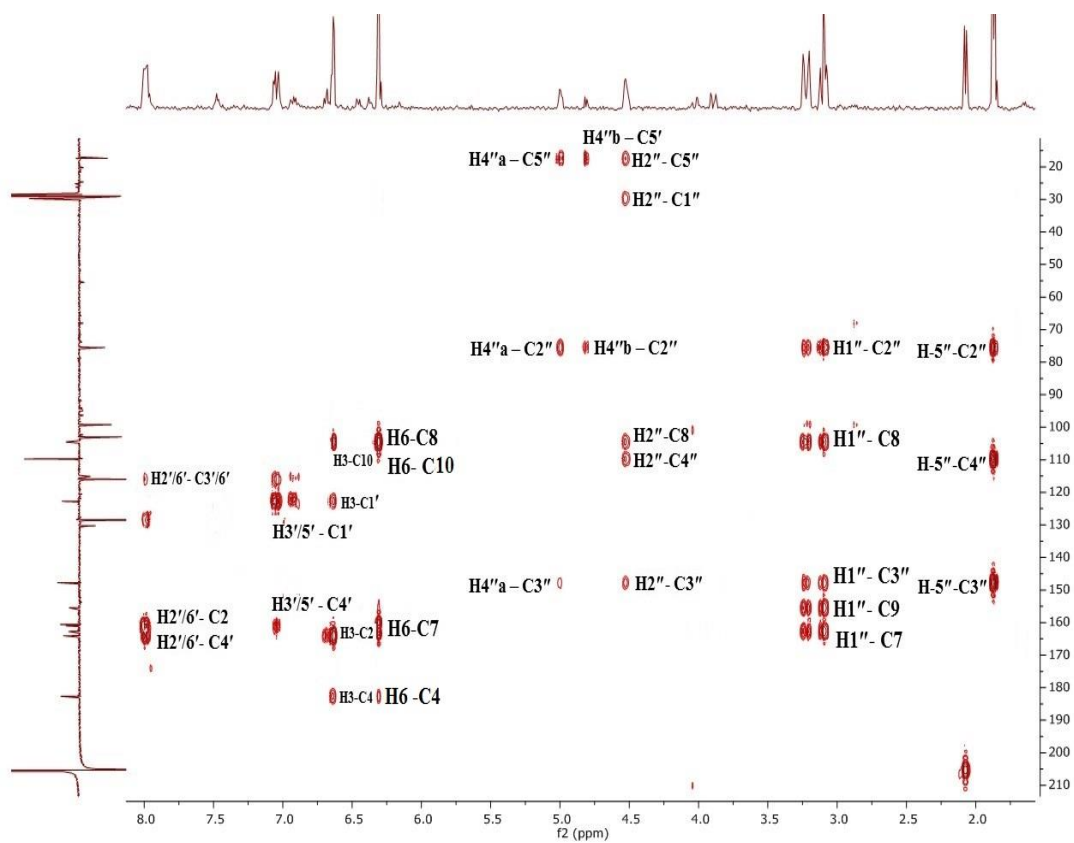
**Figure 3.42:** HMBC (CD3COCD3) spectrum of Rr-3.
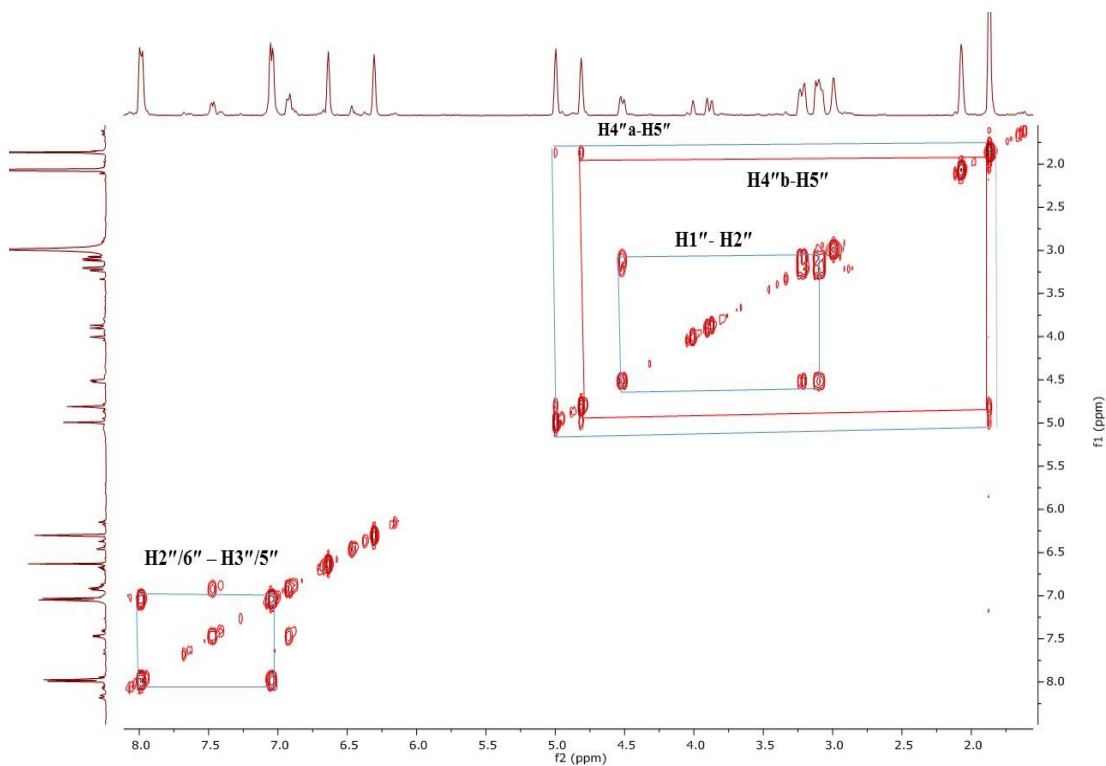


**Figure 3.43:** COSY (CD3COCD3) spectrum of Rr-3.

## 3.5 Fractionation of *P. plicata* crude extracts

*P. plicata* EtOH extract (30 g) was subjected to fractionation using CC (section 2.6.4). The five fractions were examined using NMR and combined for further fractionation. About 2.0 g from the second fraction (5.0 g) was subjected to fractionation using Sephadex CC (section 2.6.3). The fractions collected were examined using NMR and enabled elucidation of three compounds **Pp-1** (6.0 mg), **Pp-2** (7.0 mg) and **Pp-3** (5.0 mg) No compounds were identified from the fractionation of the other four fractions of *P. plicata* EtOH extracts using PTLC and Sephadex CC.

### 3.5.1: Characterisation of Pp-1 as plicatin A
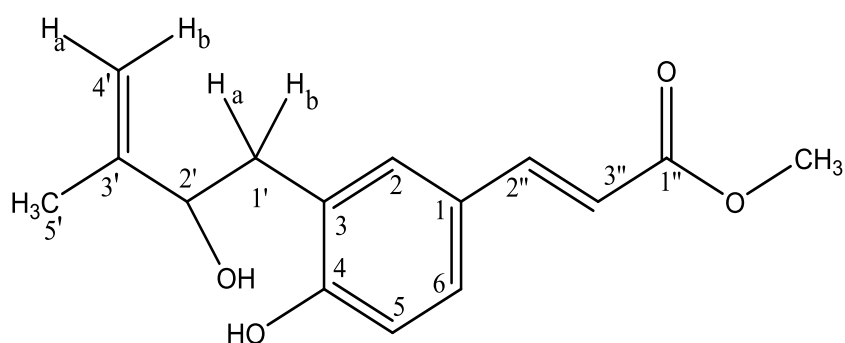


**Figure 3.44:** Structure of Pp-1.

Compound **Pp-1** (Figure 3.44) was isolated from the EtOH extract of *P. plicata* leaves using Sephadex CC. On TLC 10% MeOH and 40% EtOAc and 50% hexane, it gave a blue spot (R$f$ = 0.64) after spraying with *p*-anisaldehyde-sulphuric acid reagent and heating.

The $^1$HNMR spectrum of the compound showed signals for three ABX coupled aromatic protons at $\delta_H$ 7.49 (d, $J$ = 2.1 Hz, H-2), 6.88 (d, $J$ = 8.3 Hz, H-5) and 7.38 (dd, $J$ = 8.4, Hz, H-6). Two trans coupled olefinic protons were indicated by the presence of two doublets at $\delta_H$ 7.60 (1H, d, $J$ = 15.86 Hz, H-2″) and 6.36 (1H, d, $J$ = 15.9 Hz, H-3″). Also, a singlet was observed at $\delta_H$ 3.74 for a methoxy group, two geminal methylene protons at 2.92 (td, $J$ = 14.2, 9.0 Hz, H-1′), and one oxymethine proton at 4.78 (1H, s, H-4′a) and 4.97 (d, $J$ = 2.1 Hz, H-4′b). A methyl group attached to a double bond was shown by the presence of a singlet at $\delta_H$ 1.82 while another methyl group attached to an ester was observed at $\delta_H$ 3.74 ppm.

The $^{13}$CNMR spectrum showed the presence of 15 carbon atoms. The multiplicity of each carbon atom was determined using DEPT experiments, which showed the presence of two methyls, two methylenes and six methines and five quaternary carbon atoms.

Using the 2D NMR spectrum the structure of the compound was confirmed as follows: long-range correlations (HMBC) from H-2″ to C-2 and C-6 revealed that the transolefinic side chain was attached to C-1 of the aromatic ring. Also, correlations from the same proton to C-1″ and from the methyl group at 3.74 to a carbonyl at 166.9 (C-1″) indicated the propyl side chain to be an ester. Hence, the compound must be a para- coumaric acid derivative. The presence of a side chain at C-3 was confirmed by correlations from H-1′ to C-2 and C-4 and H-2 to C-1′. The length and structure of this side chain were established from its COSY and long-range correlations between the protons and carbons as given in Table 3.9.

The HRESI-MS for **Pp-1** showed a molecular ion [M-H] $^{-}$ at *m/z* 261.1136 (Calc C$_{15}$H$_{17}$O$_4$, 261.1126) suggesting a molecular formula of C$_{15}$H$_{18}$ O$_4$.

Based on the above spectral data and by comparison with previous reports, the identity of the compound was confirmed as plicatin A and has been previously isolated from *P. plicata* (Rasool *et al*., 1990).
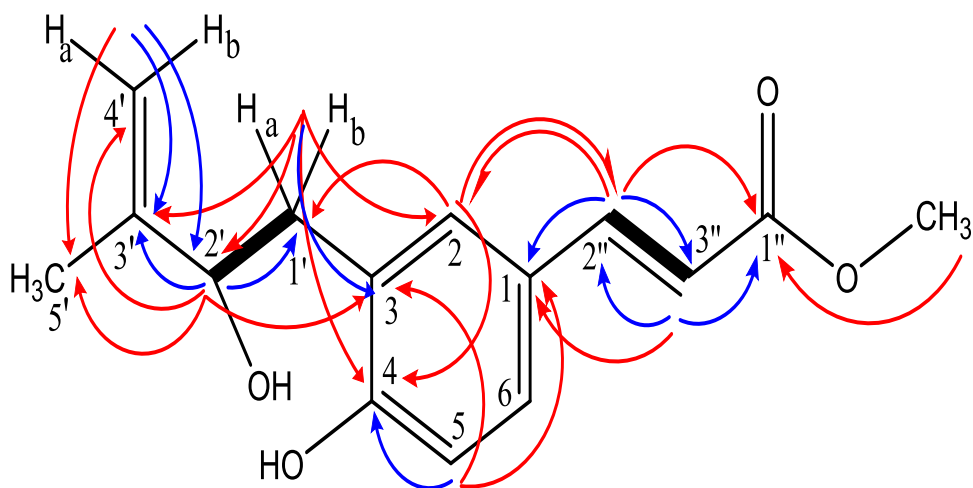


**Figure 3.45:** Structure of Pp-1 with key COSY (▬▬), HMBC $^2J$ (⌒) and $^3J$ (⌒) correlations.

**Table 3.9:** $^1H$ (500 MHz), $^{13}C$ (125 MHz), HMBC and COSY data of Pp-1 in CD$_3$COCD$_3$

| Position | $^1H$ (δ ppm) (Mult, $J$ (Hz)) | $^{13}C$(δppm) Mult | HMBC $^2J$ | $^3J$ | COSY - |
|---|---|---|---|---|---|
| 1 | - | 126.5 (C) | - | - | - |
| 2 | 7.49 (1H, d, $J$ = 2.1). | 131.8 (CH) | - | C-1′, C-2″,C-4 | H-5 |
| 3 | - | 126.5 (C) | - | - | - |
| 4 | - | 158.4 (C) | - | - | - |
| 5 | 6.88 (1H, d, $J$ = 8.3 ) | 116.9 (CH) | C-4 | C-1, C-3 | H-2 |
| 6 | 7.38 (1H, dd, $J$ = 8.4,) | 131.0 (CH) | - | - | - |
| 1′a | 2.92 (1H, td, $J$ = 14.7, 9.0) | 37.7 (CH) | C-2′,C-3 | C-2, C-3′, C-4 | H-2′ |
| 1′b | 2.92 (1H, td, $J$ = 14.2, 9.0) | 37.7 (CH) | C-2′,C-3 | C-2, C-3′, C-4 | H-2′ |
| 2′ | 4.44 (1H, dd, $J$ = 8.0, 4.1) | 75.8 (CH) | C-1′,C-3′ | C-3, C-4′, C-5′ | H-1′a, b |
| 3′ | - | 147.6 (C) | - | - | - |
| 4′a | 4. 78 (1H, s) | 109.8 (CH) | - | C-2′, C-5′ | H-5′,4′ b |
| 4′b | 4.97 (1H, d, $J$ = 2.1) | 109.8 (CH) | C-3′ | C-2′, C-5′ | H-5′,4′ a |
| 5′ | 1.82 (3H, s) | 17.5 (CH$_3$) | C-3′ | C-2′, C-4′ | H-4′a,b |
| 1″ | - | 166.9 (C) | - | - | - |
| 2″ | 7.60 (1H, d, $J$ = 15.86) | 144.6 (CH) | C-1,C-3″ | C-2, C-1″ | H-3″ |
| 3″ | 6.36 (1H d, $J$ = 15.9) | 114.3 (CH) | C-1″,C-2″ | C-1 | H-2″ |
| 1′- OCH$_3$ | 3.74 (s) | 50.4 (CH$_3$) | - | C-1″ | - |
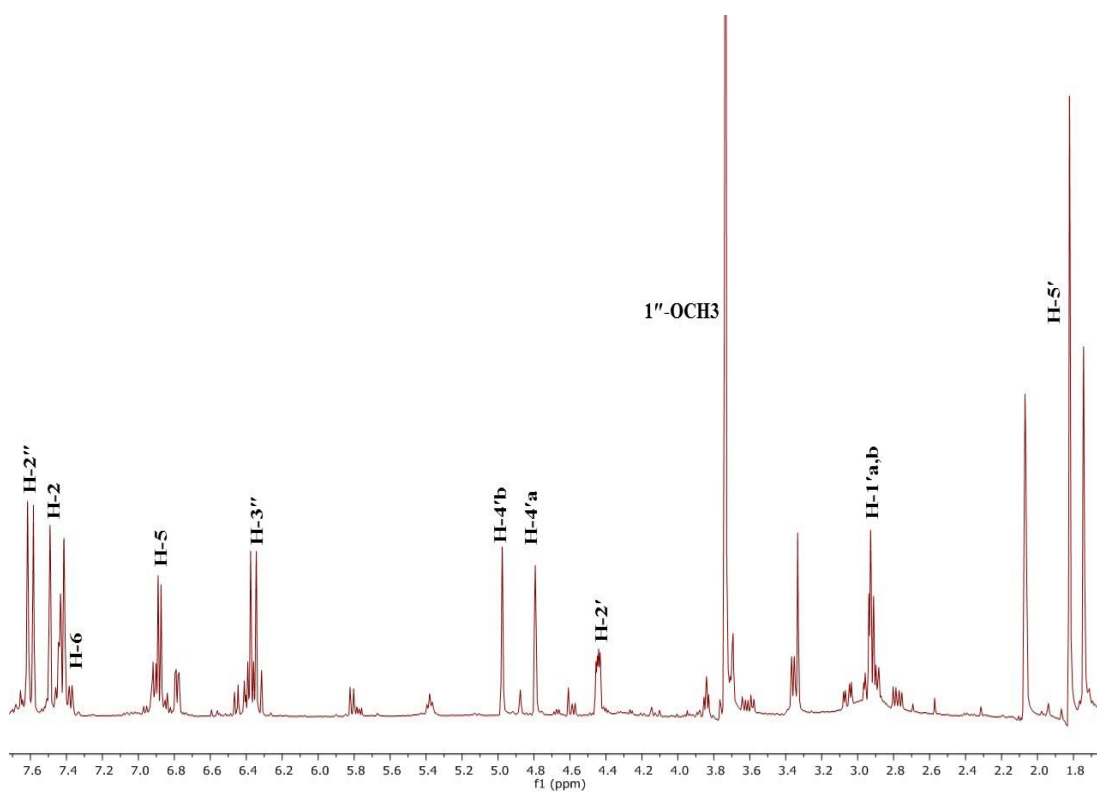
**Figure 3.46:** ¹H NMR spectrum (500 MHz) of Pp-1 in CD₃COCD₃.
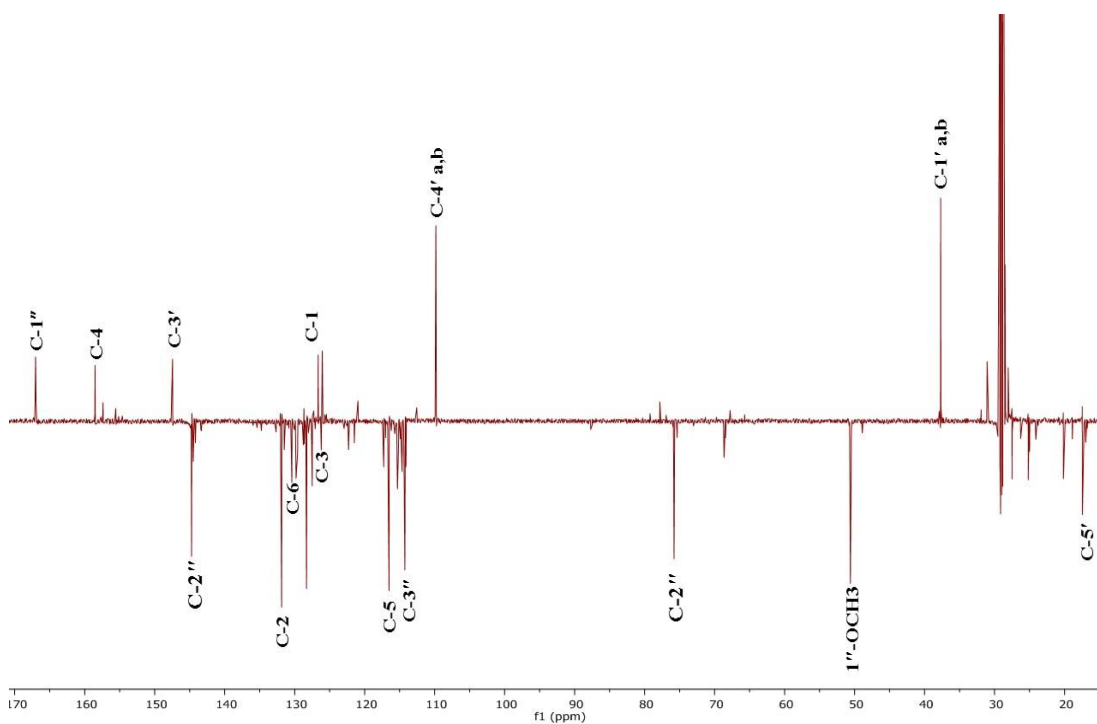


**Figure 3.47:** Full ¹³C NMR spectrum (125 MHz) of Pp-1 in CD₃COCD₃.
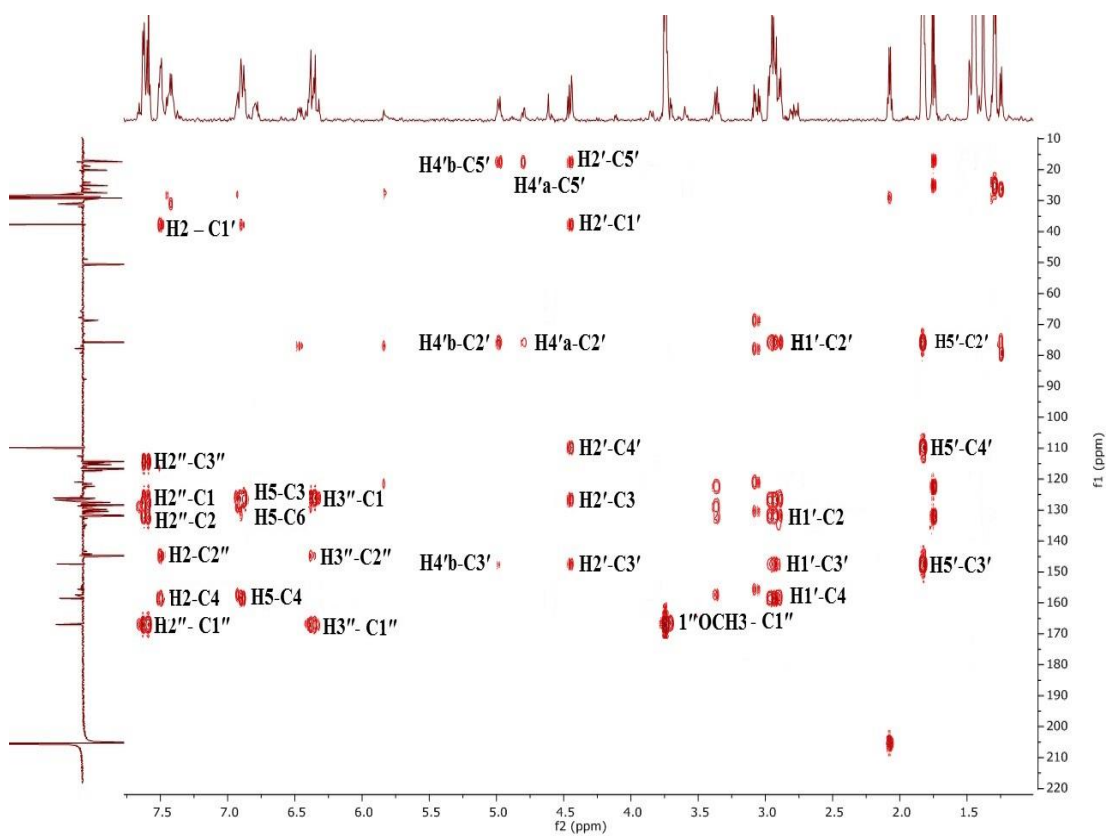
**Figure 3.48:** HMBC (CD$_3$COCD$_3$) spectrum of Pp-1.
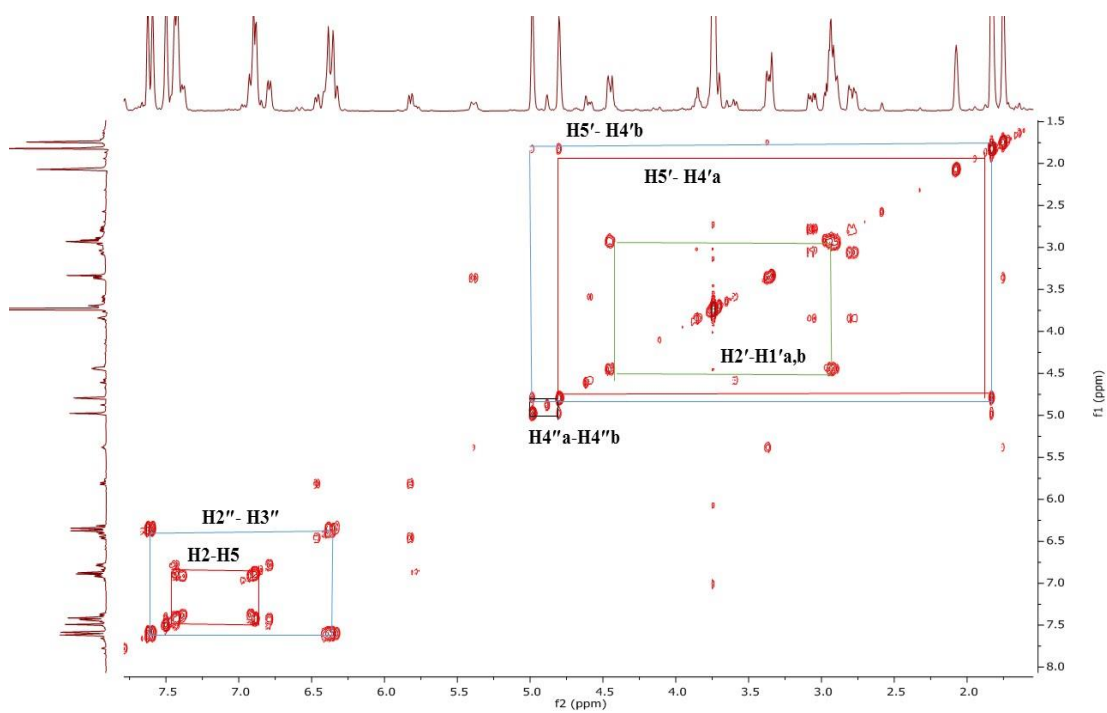


**Figure 3.49:** COSY (CD$_3$COCD$_3$) spectrum of Pp-1.

### 3.5.2 Characterisation of a mixture of Pp-2a as psoralen and Pp-2b as angelicin
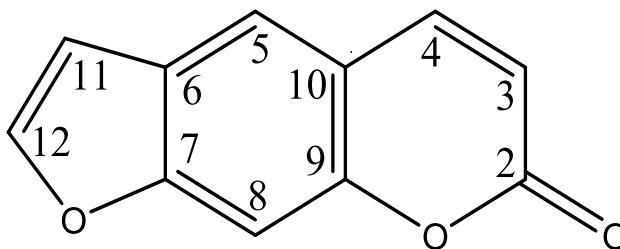


**Figure 3.50:** Structure of Pp-2a.
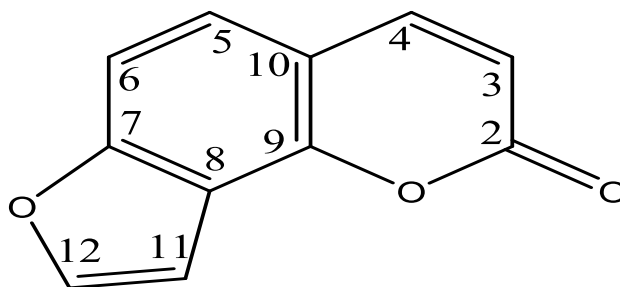


**Figure 3.51:** Structure of Pp-2b.

The mixture of compounds **Pp-2a** (Figure 3.50) and **Pp-2b** (Figure 3.51) was obtained from the EtOH extract of *P. plicata* leaves using Sephadex CC. On TLC with 10% MeOH and 40% EtOAc and 50% hexane, a yellow spot was observed (R$f$ = 0.58) after spraying with *p*-anisaldehyde-sulphuric acid reagent and heating.

The $^1$H NMR spectrum of the minor compound **Pp-2a** (Figure 3.54, Table 3.10) showed the presence of two cis coupled olefinic protons at $\delta_H$ 6.35 (1H, d, $J$ = 9.7 Hz, H-3), 8.06 (1H, d, $J$ = 9.6 Hz, H-4), and two aromatic protons $\delta_H$ 7.95 (1H, d, $J$ = 2.2 Hz, H-5) and 7.53 (1H, s, H-8). The spectrum also showed the presence of two other aromatic protons at $\delta_H$ 7.01 (1H, d, $J$ = 2.3 Hz, H-11) and 7.94 (1H, d, $J$ = 2.3 Hz, H-12) and the low coupling constant were indicative of a furan ring.

The DEPTq-135 NMR spectrum (Figure 3.55, Table 3.10) showed the presence of carbon atoms representing both compounds made up of atoms, comprising two carbonyl carbons, four quaternary carbons at 125.0, 152.2, 156.5 and 115.7 ppm in addition of six CH carbons at 115.2, 145.2, 120.7, 99.0, 106.3 and 146.7 ppm. The signals for psoralen were distinct from those of angelicin and the 2D correlations were distinguishable.

In the HMBC spectrum (Figure 3.56, Table 3.11) the proton at 8.06 (H-4) for psoralen showed $^2J$ correlations to the carbon at 115.2 (C-3) and 115.7 (C-10) and $^3J$ correlations to the carbons at 160.2 (C-2) and 120.7 (C-5). The proton at 7.95 (H-5) showed $^3J$ correlations to the carbons at 145.2 (C-4), 152.2 (C-7), 156.5 (C-9) and 106.3 (C-11) and a $^2J$ correlation to the carbon at 125.0 (C-6) and 115.7 (C-10). In addition, the proton at 7.53 (H-8) showed a $^2J$ correlations to the carbons at 152.2 (C-7) and 156.5 (C-9), and a $^3J$ correlation to C-6 and C-10.

The HRESI-MS spectrum showed a molecular ion [M+H]$^+$ at $m/z$ 187.0388 (Calc $C_{11}H_7O_3$, 187.0395) suggesting the molecular formula of $C_{11}H_6O_3$. The above data suggests **Pp-2a** be psoralen. The spectral data were consistent with those reported in the literature and this compound has been isolated from the fruits of *Psoralea corylifolia L* (Lu *et al*., 2014). However, this is the first report of the isolation of psoralen from *P. plicata*.

Besides, the $^1$H and DEPTq-135 NMR (Table 3.10) spectra for the major compound **Pp-2b** (Figure 3.54; Figure 3.55) had identical patterns as that of **Pp-2a** except for the presence of a furan ring now fused at C-7 and C-8. The carbons at positions C-6, C-9 and C-11were shielded and were observed at 108.5, 148.6 and 103.6 ppm respectively compared to the same carbon signals for psoralen (Table 3.10).

Similarly, the proton signals for **Pp-2b** (Figure 3.54, Table 3.10) were similar to the same protons as that of **Pp-2a** except for the absence of H-8 and presence of H-6 at $\delta_H$ 7.52 (1H, d, $J$ = 8.6 Hz). Proton H-5 appeared at 7.60 (1H, $d$, $J$ = 8.6 Hz) compared with the same proton in **Pp-2a** which appeared at 7.95 ppm, and proton H-11 was deshielded and appeared at 7.19 (1H, $d$, $J$ = 2.2 Hz) compared with the same proton in **Pp-2a** observed at 7.01 ppm (Table 3.10).

In the HMBC spectrum (Figure 3.56, Table 3.11) the proton at 7.60 (H-5) showed $^3J$ correlations to the carbons at 145.6 (C-4), 157.5 (C-7) and 148.6 (C-9). The proton at $\delta_H$ 7.52 (H-6) showed a $^2J$ correlation to the carbon at 157.2 (C-7) and $^3J$ correlation at 116.6 (C-8) and 115.7 (C-10). In addition, the proton at 7.19 (H-11) showed $^2J$

correlations to the carbons at 116.6 (C-8) and 146.7 (C-12), and a $^3J$ correlation to C-7. Protons H-5, H-11 and H-12 showed $^3J$ while H-6 showed $^2J$ correlations to C-7.

The HRESI-MS spectrum also showed a molecular ion [M+H]$^+$ at m/z 187.0388 (Calc C$_{11}$H$_7$O$_3$, 187.0395) suggesting the molecular formula of C$_{11}$H$_6$O$_3$. Based on the spectral data, **Pp-2b** was identified as angelicin and is reported from *P. plicata* for the first time.
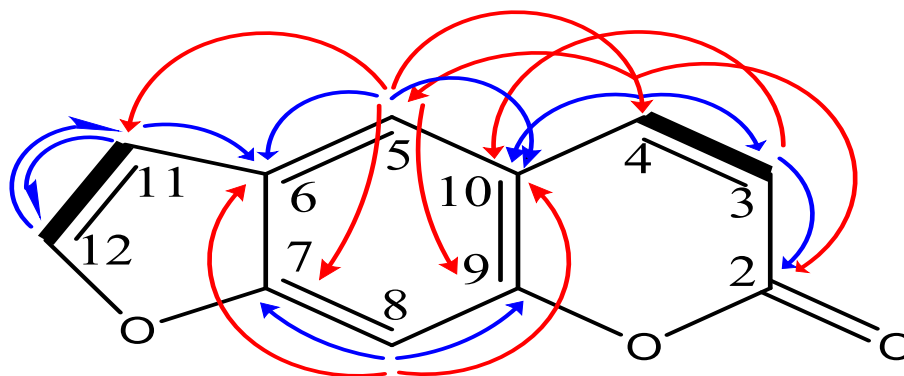


**Figure 3.52:** Structure of Pp-2a with key COSY ( ▬ ) and HMBC $^2J$ ( ⌒ ) and $^3J$ ( ⌒ ) correlations.
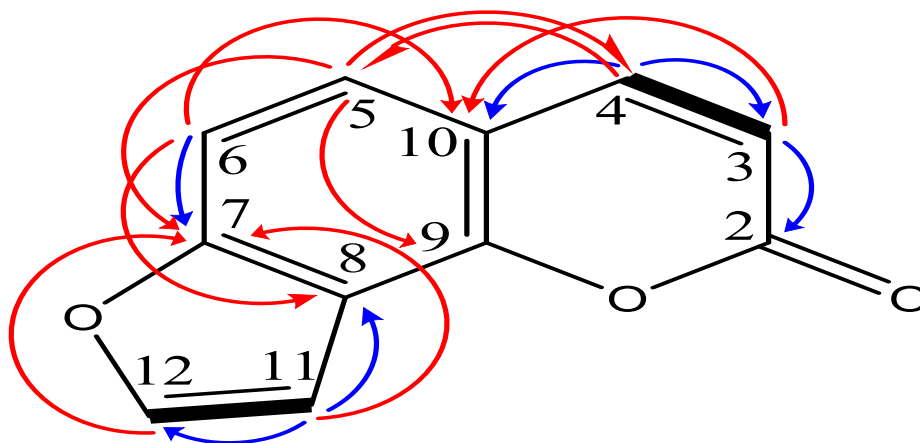


**Figure 3.53:** Structure of Pp-2b with key COSY ( ▬ ), HMBC $^2J$ ( ⌒ ) and $^3J$ ( ⌒ ) correlations.

**Table 3.10:** ¹H (500 MHz) and ¹³C (125 MHz) data of Pp-2a and Pp-2b in CD$_3$COCD$_3$

| Position | Pp-2a | | Pp-2b | |
|---|---|---|---|---|
| | ¹H (δ ppm) (Mult, *J* (Hz)) | ¹³C (δ ppm) Mult | ¹H (δ ppm) (Mult, *J* (Hz)) | ¹³C (δppm) Mult |
| 1 | - | - | - | - |
| 2 | - | 160.2 (C) | - | 160.5 (C) |
| 3 | 6.35 (1H, d, *J* = 9.7) | 115.2 (CH) | 6.37 (1H, d, *J* = 9.6) | 114.8 (CH) |
| 4 | 8.06 (1H, d, *J* = 9.6) | 145.2 (CH) | 8.07 (1H, d, *J* = 9.6) | 145.6 (CH) |
| 5 | 7.95 (1H, d, *J* = 2.2) | 120.7 (CH) | 7.60 (1H, d, *J* = 8.6) | 124.9 (CH) |
| 6 | - | 125.0 (C) | 7.52 (1H, d, *J* = 8.6) | 108.5 (CH) |
| 7 | - | 152.2 (C) | - | 157.2 (C) |
| 8 | 7.53 (1H, s) | 99.0 (CH) | - | 116.6 (C) |
| 9 | - | 156.5 (C) | - | 148.6 (C) |
| 10 | - | 115.7 (C) | - | 115.7 (C) |
| 11 | 7.01 (1H, d, *J* = 2.3) | 106.3 (CH) | 7.19 (1H, d, *J* = 2.2) | 103.6 (CH) |
| 12 | 7.94 (1H, d, *J* = 2.3) | 146.7 (CH) | 7.99 (1H, d, *J* = 2.2) | 146.7 (CH) |

**Table 3.11:** Selected HMBC and COSY correlations of Pp-2a and Pp-2b in CD$_3$COCD$_3$

| Position | HMBC | | | | COSY |
| --- | --- | --- | --- | --- | --- |
| | Pp-2a | | Pp-2b | | |
| | $^2J$ | $^3J$ | $^2J$ | $^3J$ | |
| 1 | - | - | - | - | - |
| 2 | - | - | - | - | - |
| 3 | C-2 | C-10 | C-2 | C-10 | H-4 |
| 4 | C-3, C-10 | C-5, C-2 | C-3, C-10 | C-5, C-9 | H-3 |
| 5 | C-6, C-10 | C-4, C-7, C-9, C-11 | - | C-4, C-9, C-7 | |
| 6 | - | - | C-7 | C-8, C-10 | - |
| 8 | C-7, C-9 | C-6, C-10 | - | - | - |
| 9 | - | - | - | - | - |
| 10 | - | - | - | - | - |
| 11 | C-6, C-12 | - | C-8, C-12 | C-7 | H-12 |
| 12 | C-11 | - | - | C-7 | H-11 |
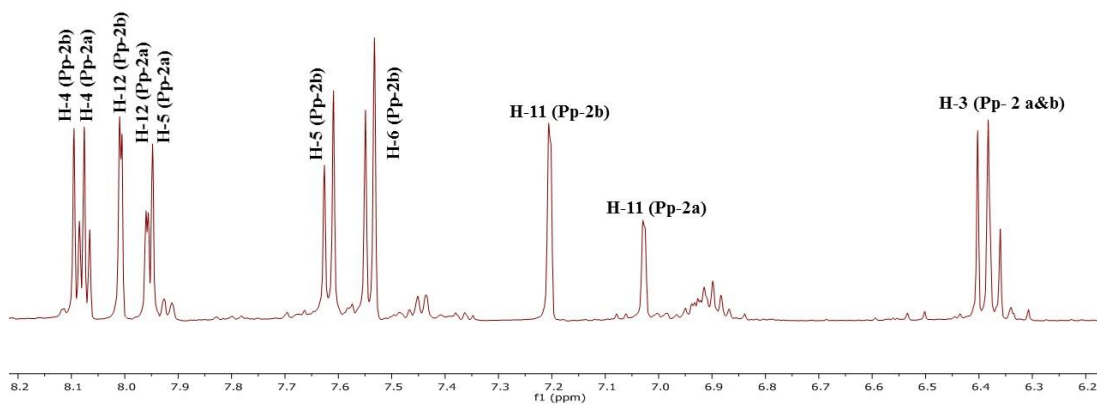


**Figure 3.54:** $^1$H NMR spectrum (500 MHz) of Pp-2a and Pp-2b in CD$_3$COCD$_3$.
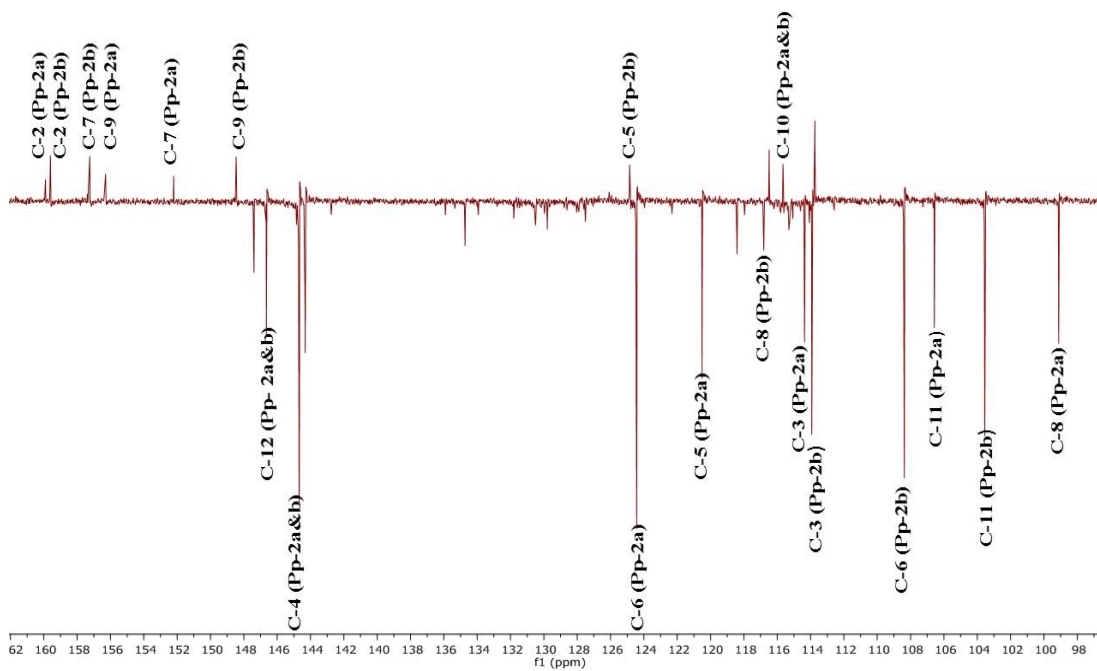
**Figure 3.55:** DEPTq-135 (125 MHz) NMR Spectrum of Pp-2a and Pp-2b in CD$_3$COCD$_3$.
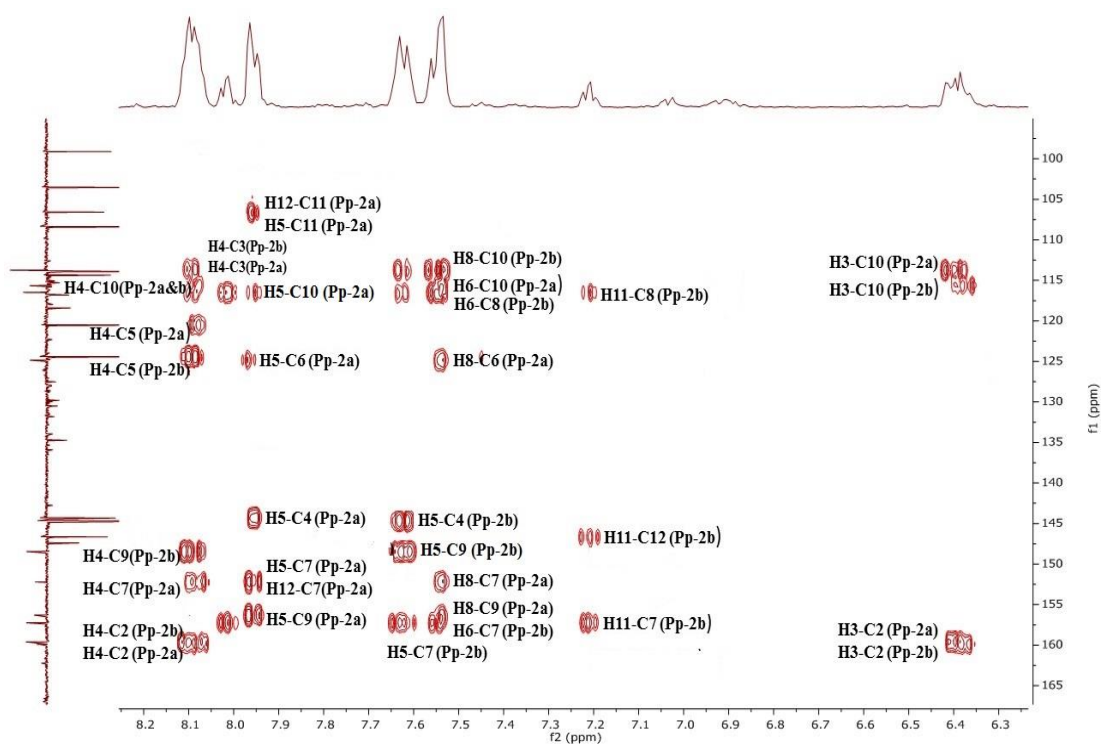


**Figure 3.56:** HMBC (CD$_3$COCD$_3$) spectrum of Pp-2a and Pp-2b.
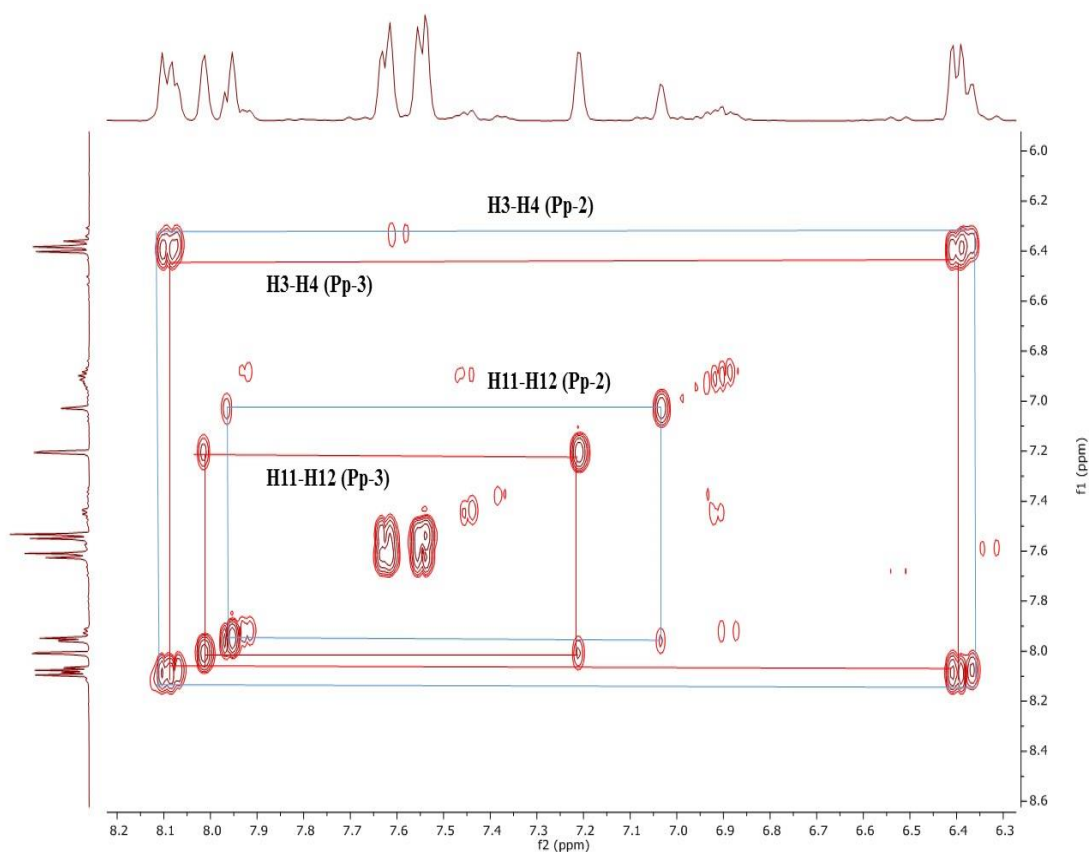
**Figure 3.57:** COSY (CD₃COCD₃) spectrum of Pp-2a and Pp-2b.

### 3.5.3 Characterisation of Pp-3 as daidzein
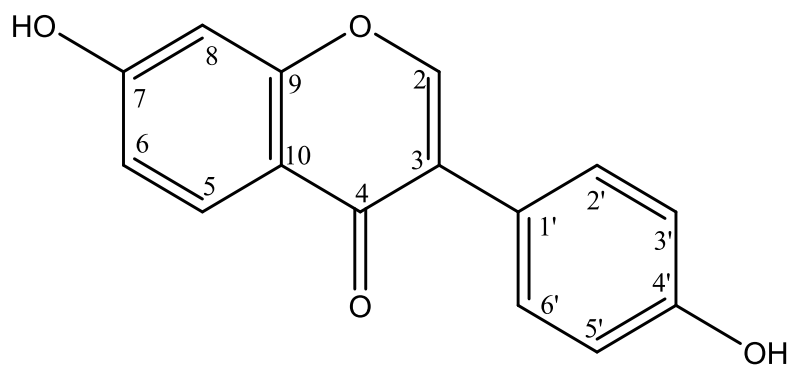


**Figure 3.58:** Structure of Pp-3.

Compound **Pp-4** (Figure 3.58) was isolated from the MeOH extract of *P. plicata* leaves using Sephadex CC. On TLC with 50% EtOAc and 50% MeOH, it gave a yellow spot (R*f* = 0.82) after spraying with *p*-anisaldehyde-sulfuric acid reagent and heating.

The $^1$H NMR (500 MHz) spectrum (Figure 3.60, Table 3.12) of Pp-3 showed protons of ring A meta and para-coupled protons at $\delta_H$ 7.01 (1H, dd, $J = 8.8$ Hz, H-6), 6.92 (1H, d, $J = 2.3$ Hz, H-8) and 8.08 (1H, d, $J = 8.7$ Hz, H-5) and the B ring with protons at 7.49 (1H, d, $J = 8.4$ Hz, H-2`/H-6`) and 6.81 (1H, d, $J = 8.6$ Hz, H-3`/H-5`) and proton singlet at 8.16 (1H, s) H-2 of ring C.

The $^{13}$C NMR (125 MHz) spectrum (Figure 3.61) indicated the presence of eight aromatic CH at $\delta_C$ 152.4, 127.7, 114.8, 102.2, 130.3, 114.8,130,3 and 114.8 ppm (C-2, C-5, C-6, C-8, C-2`, C-3`, C-6` and C-5`, respectively).

Other carbons especially the quarts were extracted from the HMBC spectrum (Figure 3.45), two quaternary carbons at $\delta$c117.9, and 123.5 ppm (C-10 and C-1`) and four phenolic carbons were observed at $\delta_C$130.6, 162.0, 157.9 and 157.5 ppm (C-3, C-7, C-9 and C-4`), respectively.

Using 2D NMR (HMBC and COSY) (Figure 3.62, Figure 3.63), the compound was confirmed as follows: The A ring protons at 7.01 (H-6) and $\delta_H$ 6.92 (H-8) both showed $^3J$ correlation to the same quaternary carbon at $\delta_C$117.9 (C-10). The proton at $\delta_H$ 6.92 (H-8) showed a $^2J$ coupling to the carbons at $\delta_C$ 162.0 (C-7), 157.4(C-9) and $^3J$ correlation to carbons at $\delta_C$ 114.8 (C-6), 117.9 (C-10).

The B ring protons at 7.49 (H-2′/ 6′) showed $^3J$ correlations to the quaternary carbon at $\delta_C$ 124.4 (C-3) and 157.5 (C-4′) and $^2J$ correlation to the carbon at $\delta_C$ 123.5 (C-1′).

The C ring proton at 8.16 (H-2) showed a $^3J$ correlations to the carbons at $\delta_C$ 123.5 (C-1′), 175.5 (C-4) and 157.9 (C-9) and $^2J$ coupling to carbon $\delta_C$124.4 (C-3). Protons at 8.16 (H-2) and 8.08 (H-5) had $^3J$ correlations to the carbon at $\delta_C$ 157.9 (C-9) and this confirmed the assignment of this signal to the C-9 of the aromatic ring C.

The HRESI-MS spectrum showed a molecular ion [M+H] $^+$ at $m/z$ 255.0645 (Calc $C_{15}H_{11}O_4$, 255.0657) suggesting a molecular formula of $C_{15}H_{10}O_4$.

Compound **Pp-4** was thus identified as daidzein and the spectral data agreed with a previous report by (Sordon *et al.*, 2017) who isolated it isolated from *A. coerulea* (Sordon *et al.*, 2017) However, this is the first report of daidzein from *P. plicata*. (Fabaceae).
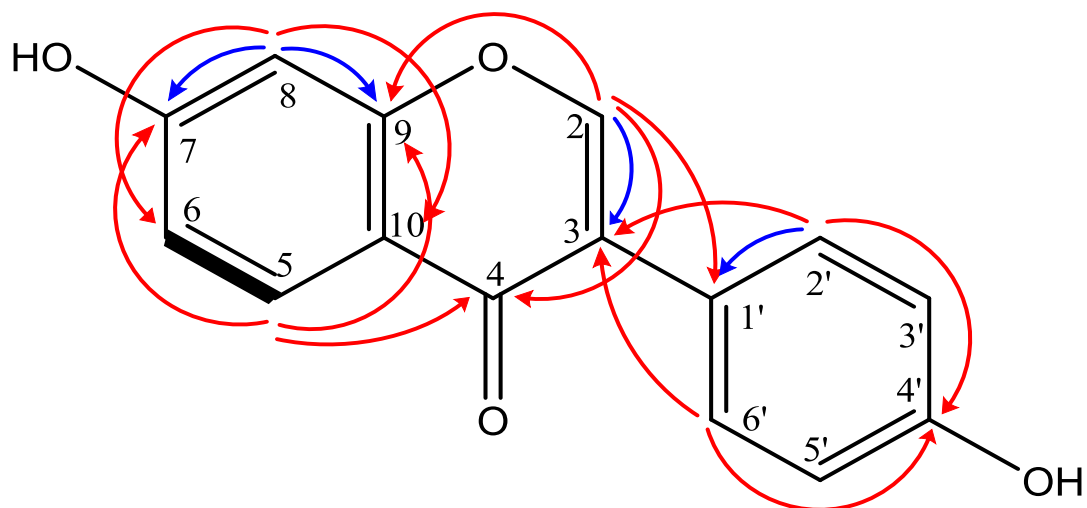


**Figure 3.59:** Structure of Pp-3 with key COSY (▬▬), HMBC $^2J$ ( ⌒ ) and $^3J$ ( ⌒ ) correlations.

**Table 3.12:** $^1$H (500 MHz), $^{13}$C (125 MHz), HMBC and COSY data of Pp-3 in CD$_3$COCD$_3$

| Position | $^1$H (δ ppm) (Mult, *J*) | $^{13}$C (δ ppm) Mult | HMBC $^2J$ | HMBC $^3J$ | COSY - |
|---|---|---|---|---|---|
| 1 | - | - | - | - | - |
| 2 | 8.16 (1H,s) | 152.5 (CH) | C-3 | C-1′,C-4, C-9 | - |
| 3 | - | 124.4 (C) | - | - | - |
| 4 | - | 175.2 (C) | - | - | - |
| 5 | 8.08 (1H, d, *J* = 8.7) | 127.7 (CH) | - | C-4, C-7, C-9 | H-6 |
| 6 | 7.01(1H, dd *J* = 8.8,2.3) | 114.8 (CH) | - | C-8, C-10 | H-5 |
| 7- OH | 10.80 | 162.0 (C) | - | - | - |
| 8 | 6.92 (1H, d, *J* = 2.3) | 102.2 (CH) | C-7, C-9 | C-6, C-10 | H-2′/6′ |
| 9 | - | 157.9 (C) | - | - | - |
| 10 | - | 117.9 (C) | - | - | - |
| 1′ | - | 123.5 (C) | - | - | - |
| 2′ / 6′ | 7.49 (2H, d, *J* = 8.4) | 130.3 (CH) | C-1′ | C-3, C-4′ | H-8 |
| 3′ / 5′ | 6.81 (2H, d, *J* = 8.6) | 114.8 (CH) | - | - | - |
| 4′- OH | 9.53 (1H, s) | 157.5 (C) | - | - | - |
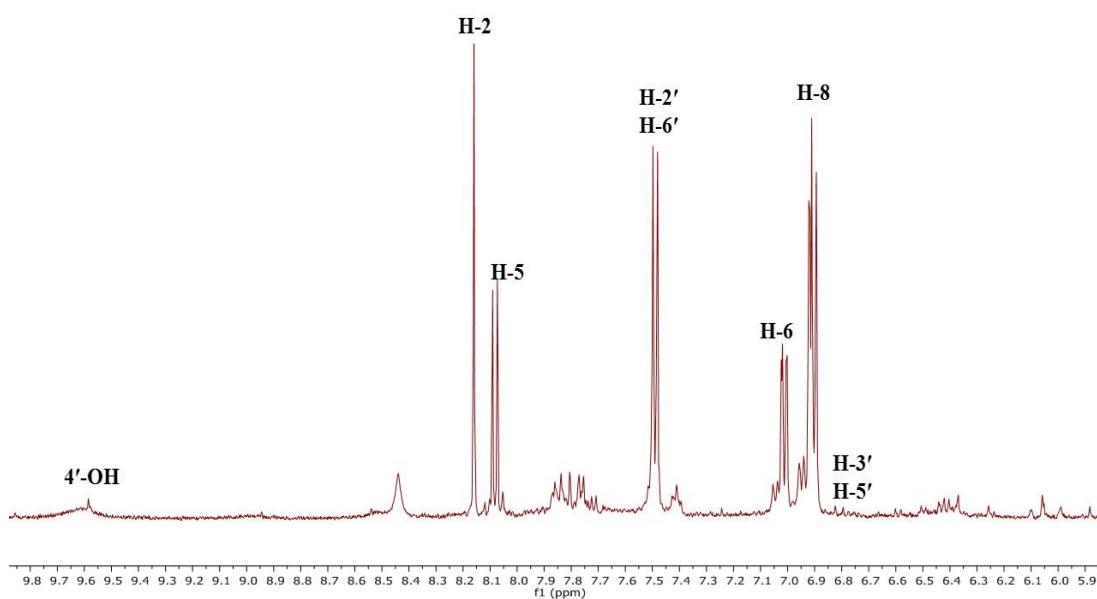
**Figure 3.60:** $^1$H NMR spectrum (500 MHz) of Pp-3 in CD$_3$COCD$_3$.
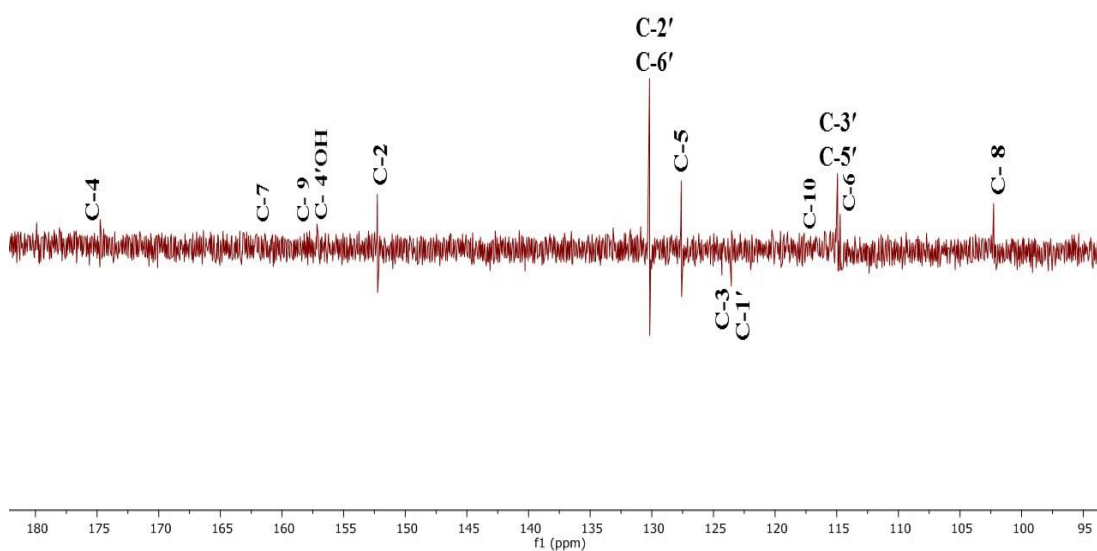


**Figure 3.61:** Full $^{13}$C NMR spectrum (125 MHz) of Pp-3 in CD$_3$COCD$_3$.
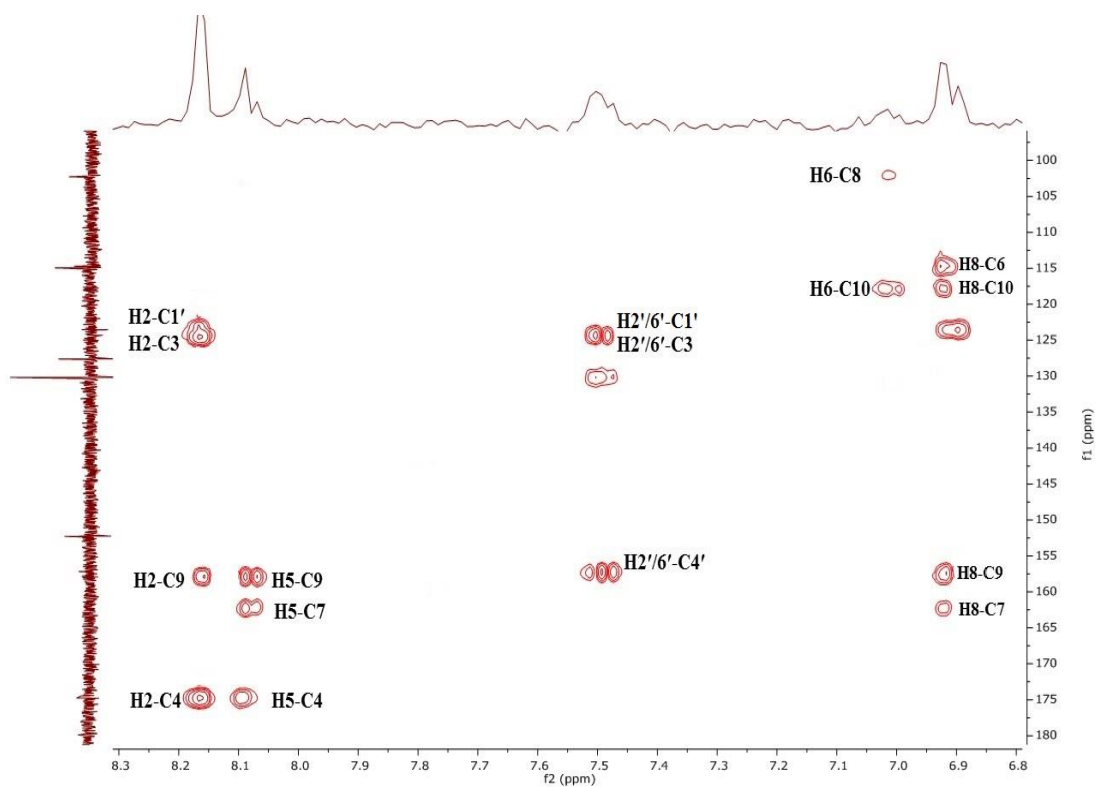
**Figure 3.62:** HMBC (CD₃COCD₃) spectrum of Pp-3.
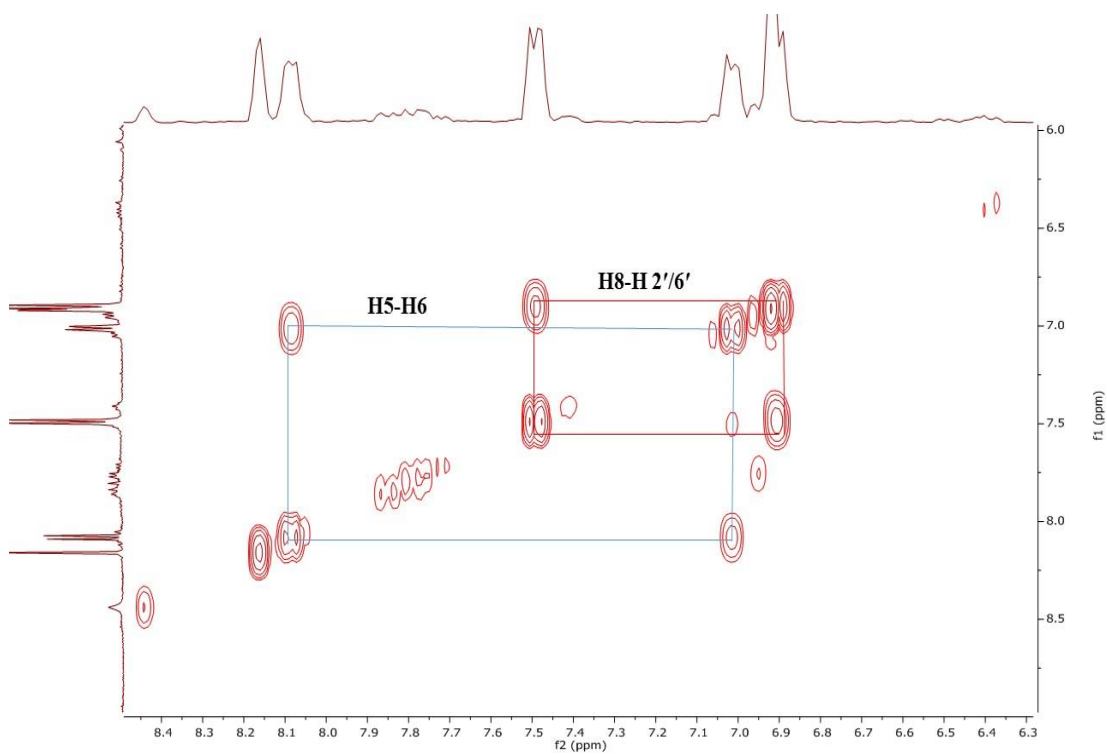


**Figure 3.63:** COSY (CD₃COCD₃) spectrum of Rr-3.

**Part 2: Biological Results**

## 3.6 Cytotoxicity screening of plant crude extracts and isolated compounds using a resazurin assay

A cytotoxicity assay was carried out against human cancer cell lines HepG2, A375, A549, PANC-1, MCF7 and LNCaP and non-cancer cell line PNT2 using a resazurin assay. It was used to assess the toxicity of extracts and isolated compounds from *B. spectabilis*, *A. graecorum, R. raetam* and *P. Plicata* (sections 3.6.1, 3.6.2, 3.6.3, and 3.6.4), respectively. Any test agent that caused cell viability to decrease to less than 50% was considered cytotoxic and the IC$_{50}$ for each was calculated. Furthermore, as shown in Figure 3.64, a 5 % (v/v) (63.99 µM) of DMSO was used to dissolve samples without killing the cells in contrast with a high concentration of DMSO (50 %, 639.95 µM) that had a cytotoxic effect on the cells (Table. 3.13).

**Table 3.13:** IC$_{50}$ of 50% DMSO on cancer and normal cell lines. The values are means ± SEM of at least three independent experiments performed in triplicate.

| Cell | IC$_{50}$ (µ M) |
|---|---|
| HepG2 cells | 63.47± 1.803 µg/ml (812.36) |
| A375 cells | 26.91± 1.430 µg/ml (344.45) |
| A549 cells | 38.54± 1.568 µg/ml (493.28) |
| PANC-1 cells | 51.80± 1.714 µg/ml (663.00) |
| MCF7 cells | 35.83± 1.554 µg/ml (458.59) |
| LNCaP cells | 66.27± 1.821µg/ml (848.20) |
| PNT2 cells | 72.94 ±1.890 µg/ml (933.57) |
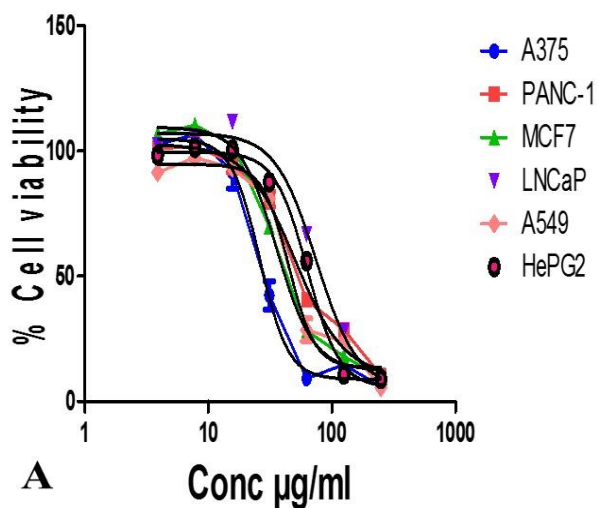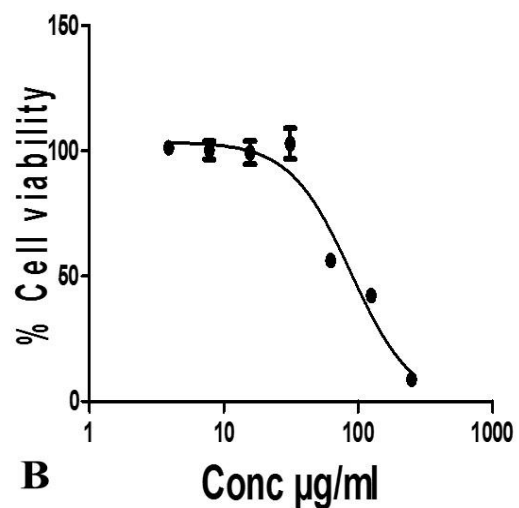
**Figure 3.64:** Effect of 50% DMSO on cell viability of (**A**) cancer cells and (**B**) normal cells after 48 h. Cell viability was measured using a resazurin assay at 560 nm and 590nm. Values represent the mean ± SEM of 3 readings.
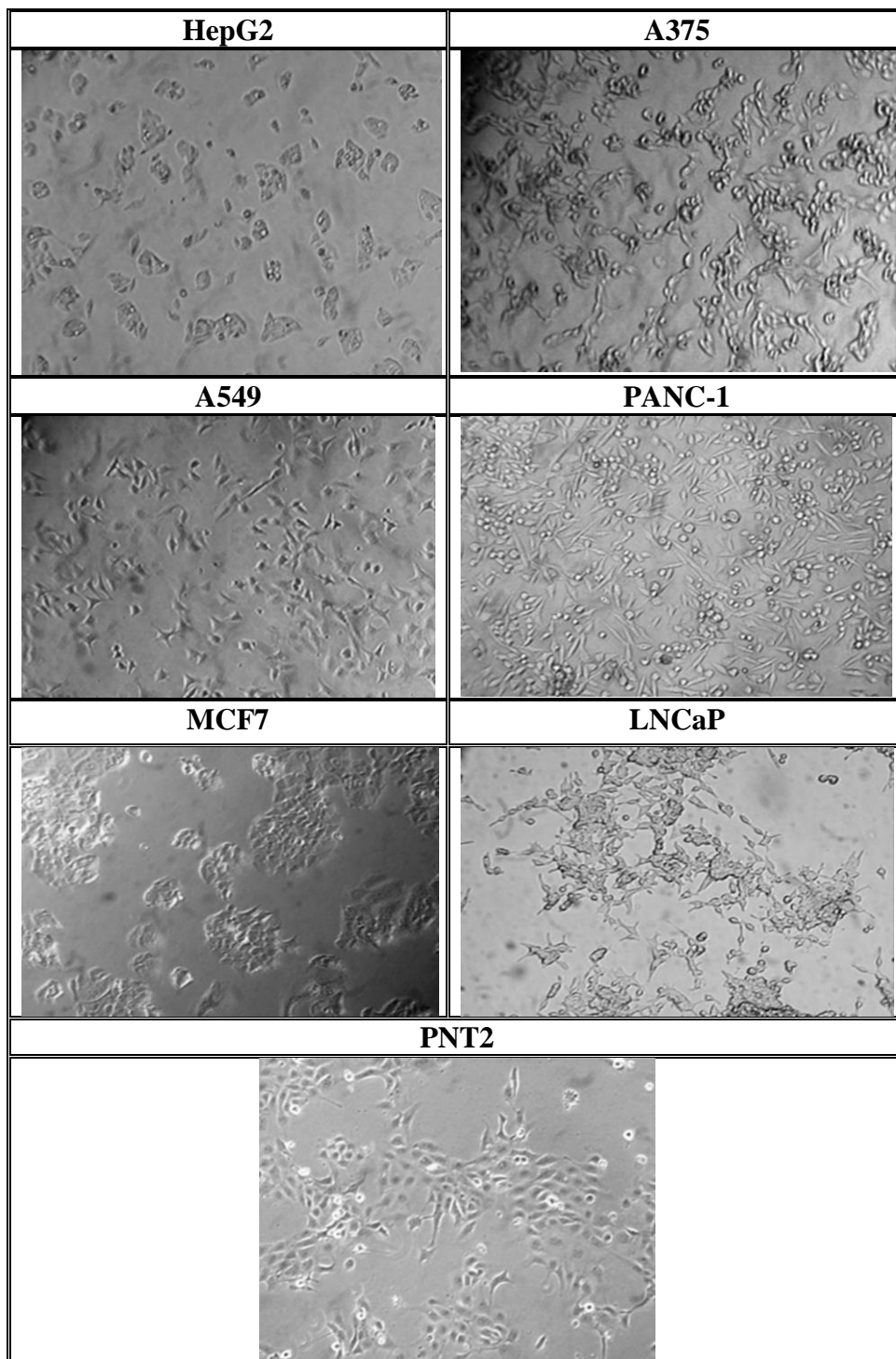
**Figure 3.65:** Morphology and substrate coverage of the cells for the cytotoxicity assay. The images show that $1\times10^5$ cells per well were chosen as an optimum number to be used in a 96 well plate. Objective lens x 10.

### 3.6.1 Cytotoxicity of *B. spectabilis* crude extracts and isolated compounds

None of the extracts or isolated compounds showed any cytotoxic activity on the cell lines. Results not shown.

### 3.6.2 Cytotoxicity of *A. graecorum* crude extracts and isolated compound

None of the extracts or isolated compound showed any cytotoxic activity on the cell lines. Results not shown.

### 3.6.3 Cytotoxicity of *R. raetam* crude extracts and isolated compounds

Results of the cytotoxic activity of *R. raetam* extracts and its constituents against cancer and normal cells are presented in Table 3.14. The *n*-hexane and methanol extracts of *R. raetam*, **Rr-2** and **Rr-3** showed no cytotoxic effects.

In contrast, *R. raetam* EtOAc extract was toxic to HepG2, A375, PANC-1 and PNT2 at 250 µg/ml with $IC_{50}$ values of 139.2 ± 2.14 µg/ml, 143.9 ± 2.15 µg/ml, 129.1 ± 2.11 µg/ml, and 154.30 ± 2.18 µg/ml, respectively and this extract was toxic to LNCaP at 125 µg/ml with an $IC_{50}$ value of 67.60 ± 1.83, but this extract was not toxic to A549 and MCF7 cells (Figure 3.66).

In addition, **Rr-1** was toxic against HepG2, A375, A549, PANC-1, MCF7 and PNT2 at 125 µg/ml with $IC_{50}$ values of 63.9 ± 1.80 µg/ml (190.021 µM), 64.24 ± 1.80 µg/ml (191.00 µM), 118.8 ± 2.07 µg/ml (353.22 µM), 64.14 ± 1.80 µg/ml (190.70 µM), 72.91 ± 1.86 µg/ml (272.71 µM), and 112.60 ± 2.05 µg/ml (334.79 µM) respectively, while it was highly toxic to LNCaP at 62.5 µg/ml with an $IC_{50}$ value of 43.63 ± 1.64 µg/ml (129.72 µM) (Figure 3.67).

**Table 3.14:** Summary of IC$_{50}$ of *R. raetam* extracts and compounds on the cell lines. The values are mean $\pm$ SEM of at least three independent experiments performed in triplicate, not active up to 250 µg/ ml.

| Extract or compound | Cancer cell lines | | | | | | Normal cell line |
|---|---|---|---|---|---|---|---|
| | HepG2 | A375 | A549 | PANC-1 | MCF7 | LNCaP | PNT2 |
| *R. raetam* Hexane extract | ---- | ---- | ---- | ---- | ---- | ---- | ---- |
| *R. raetam* EtOAc extract | 139.2 | 143.9 | ---- | 129.1 | ---- | 67.6 | 154.3 |
| *R. raetam* MeOH extract | ---- | ---- | ---- | ---- | ---- | ---- | ---- |
| *Alpinumisoflavone* **Rr-1** | 190.0 µM | 191.0 µM | 353.2 µM | 190.7 µM | 272.7 µM | 129.7 µM | 334.8 µM |
| *8-ß-D Glucopyranosylgenistein* **Rr-2** | ---- | ---- | ---- | ---- | ---- | ---- | ---- |
| *Ephedroidin* **Rr-3** | ---- | ---- | ---- | ---- | ---- | ---- | ---- |
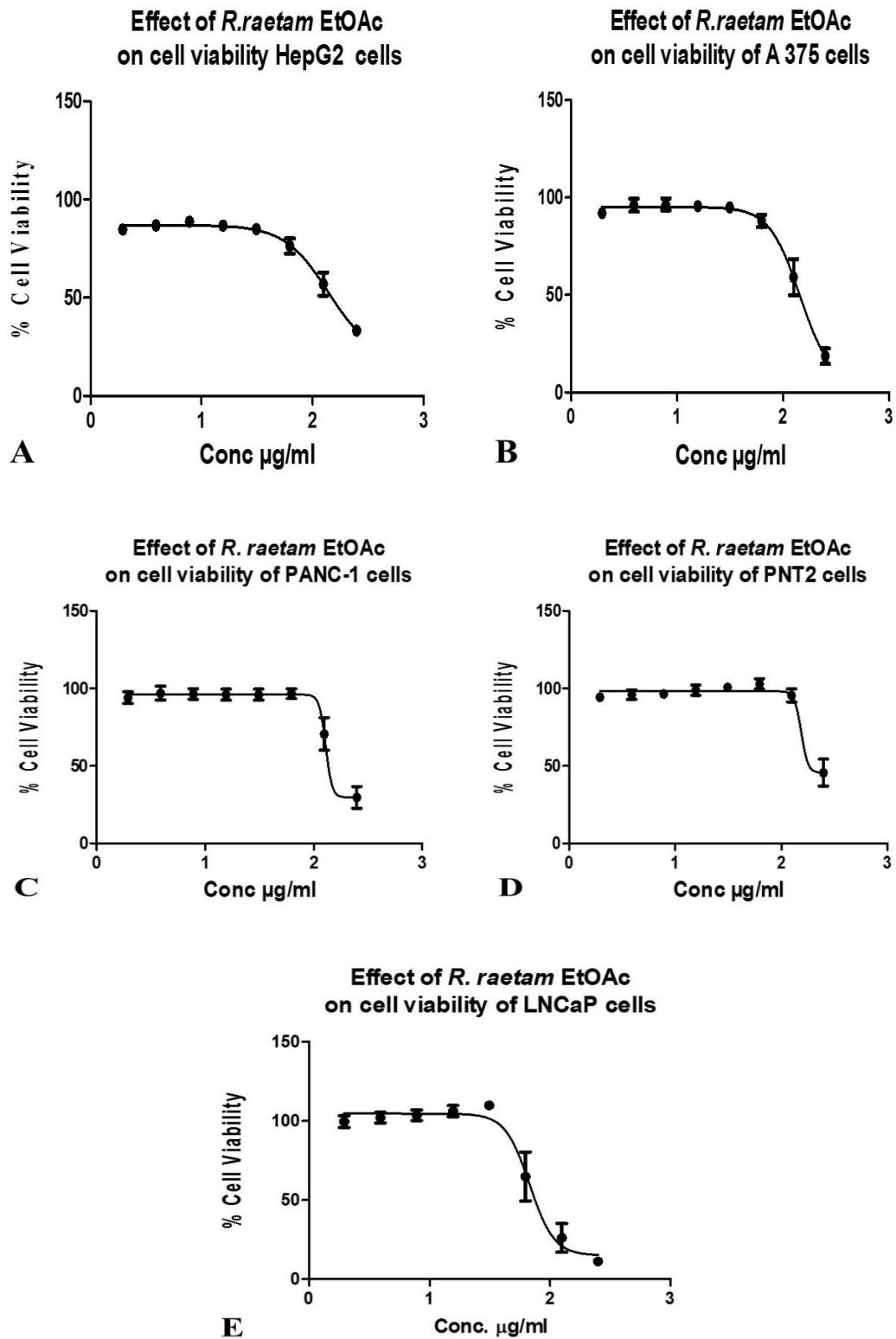
**Figure 3.66:** Effect of *R. raetam* EtOAc extracts on cell viability of **(A)** HepG2 cells, **(B)** A375 cells, **(C)** PANC-1 cells, **(D)** PNT2 cells, **(E)** LNCaP cells after 48 h. Cell viability was measured using a resazurin assay at 560 nm and 590 nm and calculated as a % of untreated controls. Values are the means of triplicate reading ± SEM. N= 3.
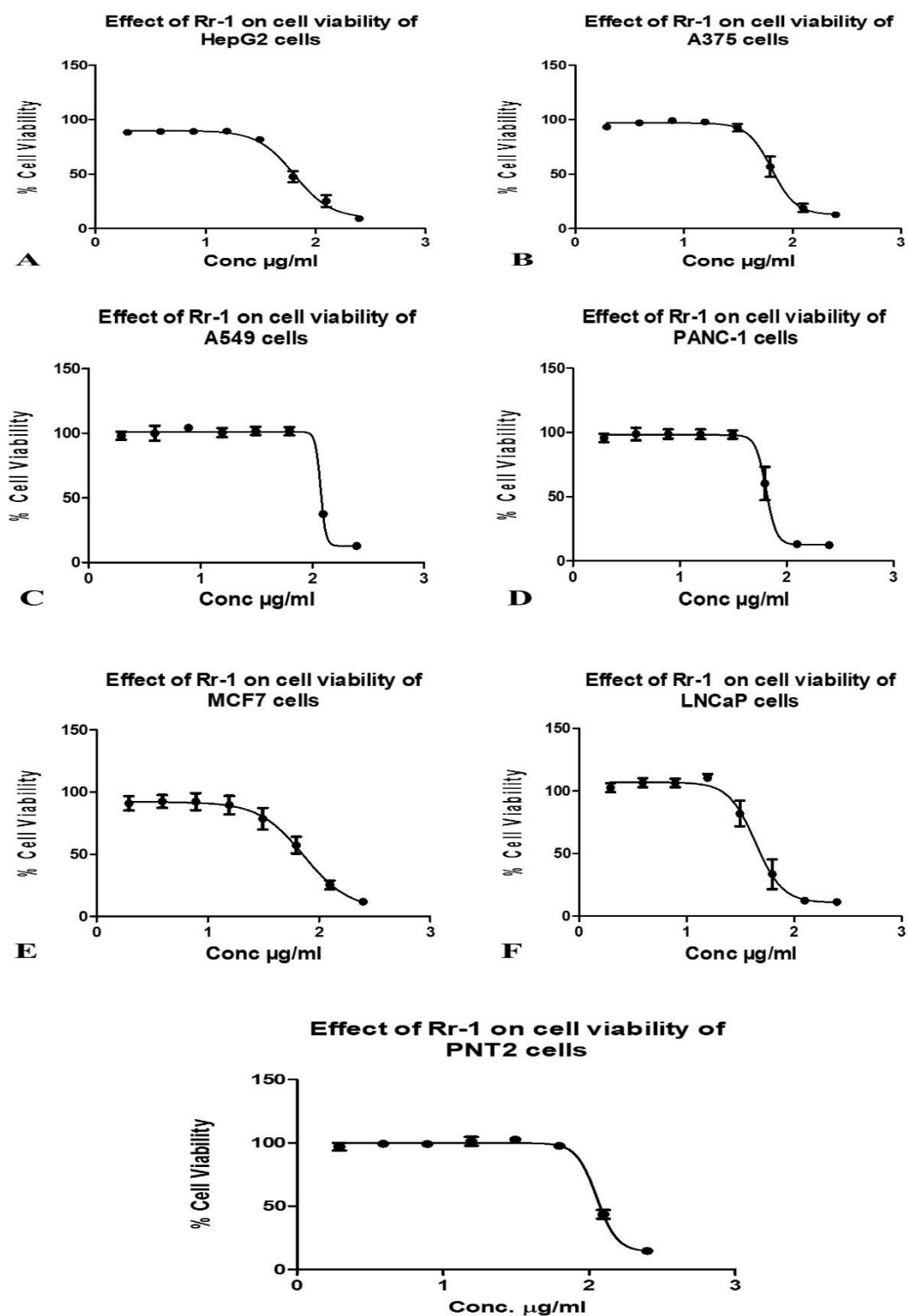
**Figure 3.67:** Effect of *R. raetam* EtOAc Fr-2 (**Rr-1**) on cell viability of (**A**) HepG2 cells, (**B**) A375 cells, (**C**) A549 cells, (**D**) PANC-1 cells (**E**) MCF7 cells (**F**) LNCaP cells and (**G**) PNT2 cells after 48 h. Cell viability was measured using a resazurin assay at 560 nm and 590 nm and calculated as a % of untreated controls. Values are the means of triplicate reading ± SEM. N= 3.

### 3.6.4 Cytotoxicity of *P. plicata* crude extract and its fractions

Results of cytotoxic activity of the ethanol extract of *P. plicata* against cancer and normal cells are presented in Table 3.15. Only fraction 2 **(PpFr-2)** was toxic against most of the cell lines, except A549. It was toxic to HepG2, PANC-1, and PNT2 at 250 µg/ml with $IC_{50}$ values of $161.50 \pm 2.20$ µg/ml, $125.9 \pm 2.10$ µg/ml, and $126.1 \pm 2.10$ µg/ml respectively, and was toxic against A375 at 125 µg/ml with $IC_{50}$ values of $118.0 \pm 2.07$ µg/ml, while it was highly toxic against MCF7 and LNCaP at 62.5 µg/ml with $IC_{50}$ values of $51.20 \pm 1.70$ µg/ml, $34.74 \pm 1.54$ µg/ml respectively (Figure 3.68).

**Table 3.15:** Summary of $IC_{50}$ of *P. plicata* EtOH extract and its fractions on each cell line. The values are means $\pm$ SEM of at least three independent experiments performed in triplicate. Not active up to 250 µg/ml.

| Extract or fraction | Cancer cell line | | | | | | Normal cell line |
|---|---|---|---|---|---|---|---|
| | HepG2 | A375 | A549 | PANC-1 | MCF7 | LNCaP | PNT2 |
| *P. plicata* EtOH | ---- | ---- | ---- | ---- | ---- | ---- | ---- |
| *P. plicata* EtOH Fr-2 **(PpFr-2)** | 161.5 | 118 | ---- | 125.9 | 51.2 | 34.7 | 126.1 |
| *P. plicata* EtOH Fr3 | ---- | ---- | ---- | ---- | ---- | ---- | ---- |
| *P. plicata* EtOH Fr4 | ---- | ---- | ---- | ---- | ---- | ---- | ---- |
| *P. plicata* EtOH Fr5 | ---- | ---- | ---- | ---- | ---- | ---- | ---- |
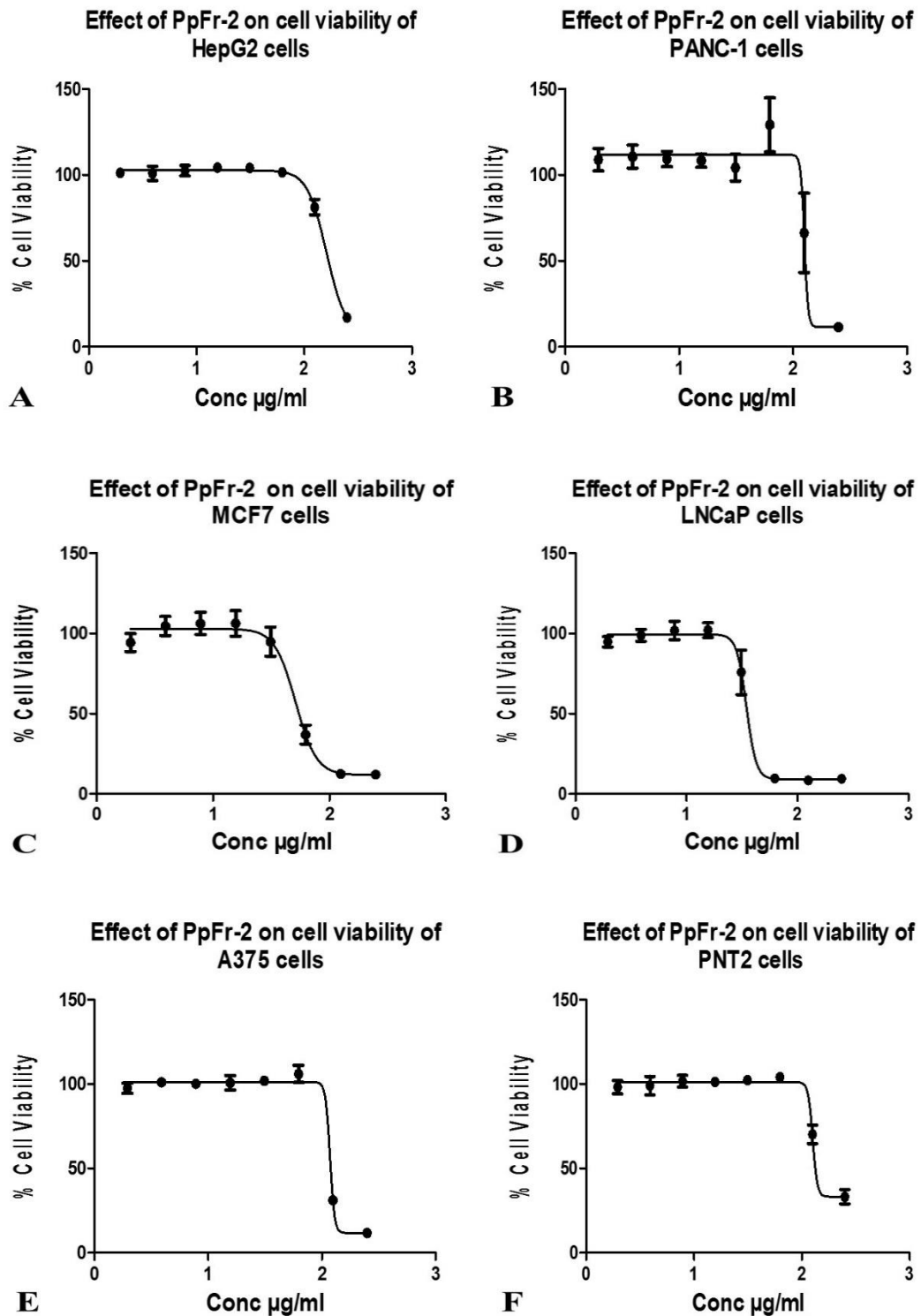
**Figure 3.68:** Effect of *P. plicata* EtOH Fr-2 **(PpFr-2)** on cell viability of **(A)** HepG2 cells, **(B)** PANC-1cells, **(C)** MCF7 cells, **(D)** LNCaP cells, **(E)** A375 cells and **(F)** PNT2 cells after 48 h. Cell viability was measured using a resazurin assay at 560 nm and 590 nm and calculated as a % of untreated controls. Values are the means of triplicate readings ± SEM. N= 3.

### 3.6.5. Effects of *R. raetam* EtOAc Fraction-2 (Rr-1) and *P. plicata* EtOH Fraction-2 (PpFr-2) on LNCaP and MCF7 cell lines.

The general aim of this section was to investigate the effect of Rr-1 and PpFr-2 on morphology, viability, adhesion, migration and invasion on LNCaP and MCF7 cell lines as these provided the best results in the preliminary cytotoxicity screening when compared with appropriate non-toxic concentrations of the normal cell.

### 3.6.5.1. Viability of Rr-1 and PpFr-2 on LNCaP and PNT2 cells after 48 h

The effect of different concentrations of Rr-1 on the viability of LNCaP cells and PNT2 cells was tested. Rr-1 was found to have an effect on the viability of the LNCaP cells at concentrations between 31.25 µg/ml to 250 µg/ml after 48 h but the viability of the PNT2 cells was affected ($p < 0.0001$) only at 125 and 250 µg/ml (Figure 3.69 **A** & **B**).

Similarly, the viability of the LNCaP cells and PNT2 cells was tested and PpFr-2 was found to have a significant ($p < 0.0001$) decrease on the viability of the LNCaP cells at concentrations between 31.25 µg/ml to 250 µg/ml after 48 h, but the viability of the PNT2 cells was affected ($p < 0.0001$) only at 125 and 250 µg/ml (Figure 3.69 **C** & **D**). Consequently, both concentrations 31.25 and 62.5 µg/ml of Rr-1 and PpFr-2 extracts were chosen for further investigation because they did not kill the normal cell line. This result was confirmed quantitatively with a resazurin assay.
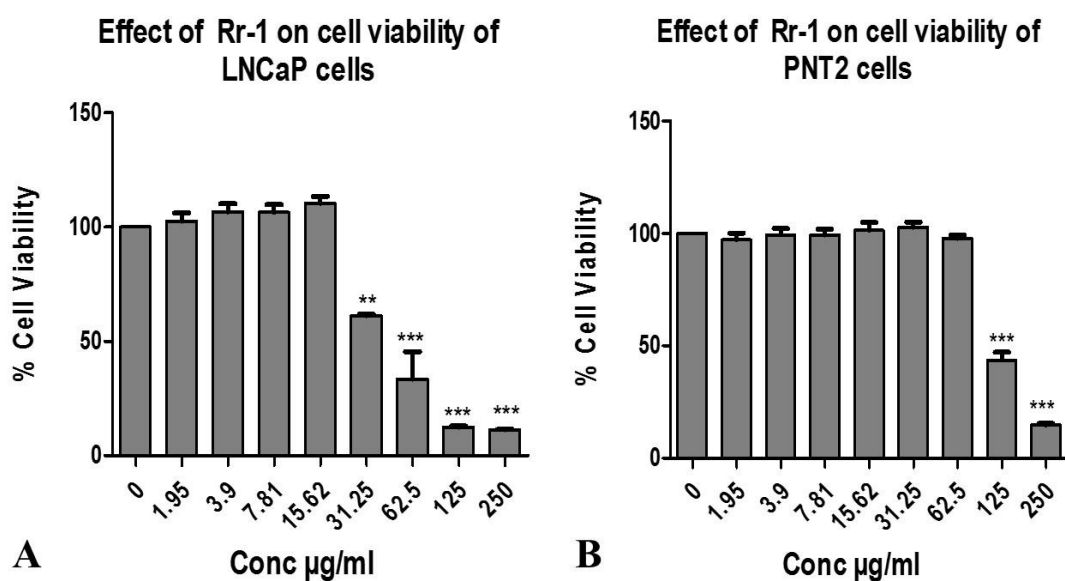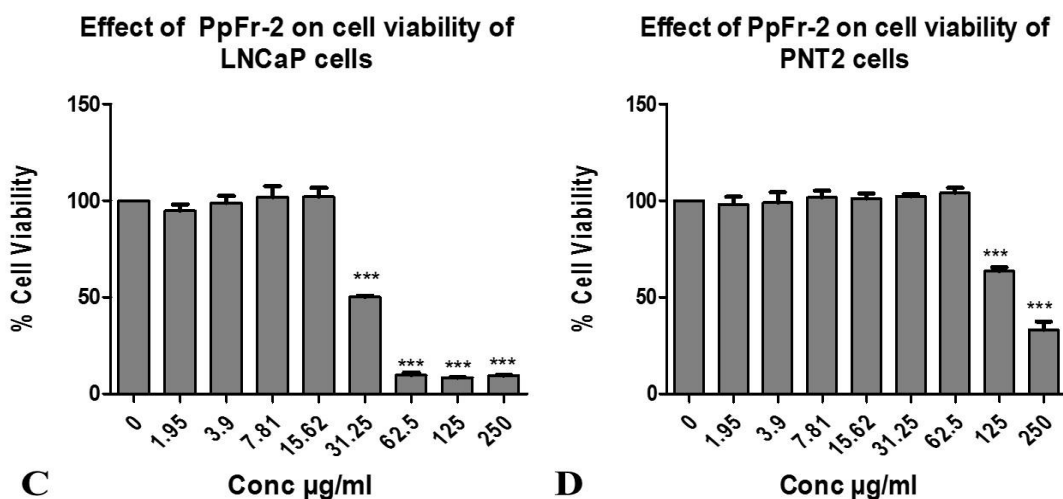
**Figure 3.69:** Effect of Rr-1 on the viability of **(A)** LNCaP cells and **(B)** PNT2 cells after 48 h, and effect of PpFr-2 on the viability of **(C)** LNCaP cells and **(D)** PNT2 cells after 48 h. Statistical analysis was performed using one way ANOVA with Tukey's Multiple Comparison Test. *** indicates significantly ($p < 0.0001$), lower values compared with the untreated control. (0 = untreated control).

### 3.6.5.1.1 Effect of Rr-1 and PpFr-2 on the morphology of LNCaP cells after 48 h

This test was carried out to determine the effect of Rr-1 and PpFr-2 at 62.5 μg/ml on the morphology of LNCaP cells after 48 h. There was a difference in the morphology after treatment with Rr-1 and PpFr-2 separately compared with non-treated cells which showed an epithelial tissue morphology with good attachment and spreading. While cells treated with Rr-1 and PpFr-2 at 62.5 μg/ml appeared changed in size and were poorly attached, suggesting there was an effect on adhesion of the cells (Figure 3.70).
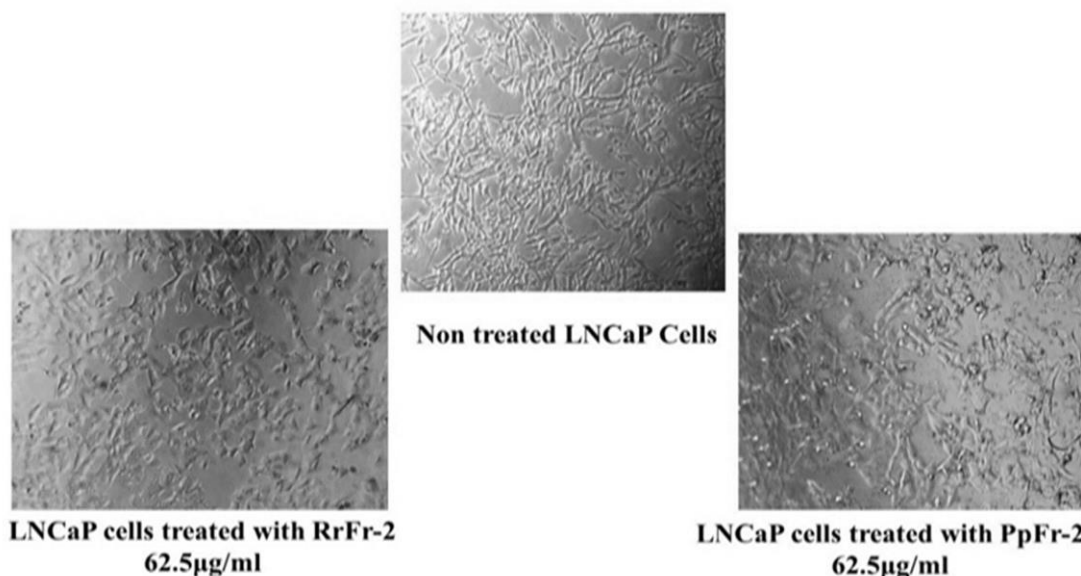
**Figure 3.70:** Morphology of LNCaP cells before and after treatment with Rr-1 and PpFr-2 after 48 h. Objective lens x 10.

**3.6.5.1.2 Effect of Rr-1 and PpFr-2 on adhesion, migration and invasion of LNCaP cells**

Cancer metastasis is the major cause of cancer illness and death and accounts for about 90% of cancer mortality. Cancer metastasis begins with the detachment of metastatic cells from the primary tumour, which then travel to different sites through blood / lymphatic vessels, settlement and growth of the cells at a distal site. Throughout the process, metastatic cells go through detachment, migration, adhesion and invasion. The metastatic steps are affected by numerous multi-biochemical factors including tumour microenvironment (such as extracellular matrix ECM, growth factors, chemokines, and matrix metalloproteinases) which play critical roles in cancer progression.

Besides this, ECM is mainly composed of collagen type IV and laminin. Also, the ECM consists of many non-collagenous molecules such as fibronectin and osteonectin. Fibronectin is a glycoprotein of the ECM, and together with collagen IV plays a major role in cell adhesion, growth, migration, and differentiation in cancer cells. Consequently, the purpose of this investigation was to evaluate the effect of Rr-1 and PpFr-2 on adhesion of LNCaP cells to fibronectin-coated plates.

**3.6.5.1.2.1 Effect of Rr-1 and PpFr-2 on adhesion of LNCaP cells to ECM (Fibronectin) using a Cytoselect™ 48-well Cell Adhesion Assay**

A large % of untreated LNCaP cells compared with treated cells was significantly ($p < 0.0001$) affected because the cells adhered and spread well on fibronectin, whereas cells treated with Rr-1 and PpFr-2, lost their adherence to fibronectin (Figure 3.71). Hence, Rr-1 extract concentrations 31.25 µg/ml to 250 µg/ml had greater significant ($p < 0.0001$) effect on adhesion (Figure 3.71 **A**) and the % of adhesion of LNCaP was 24% to 30%, respectively. Likewise, with PpFr-2, there was decreased adhesion of LNCaP cells to fibronectin in a dose-dependent manner and the % adhesion was 25% to 40% at 31.25 to 250 µg/ml (Figure 3.71 **B**).
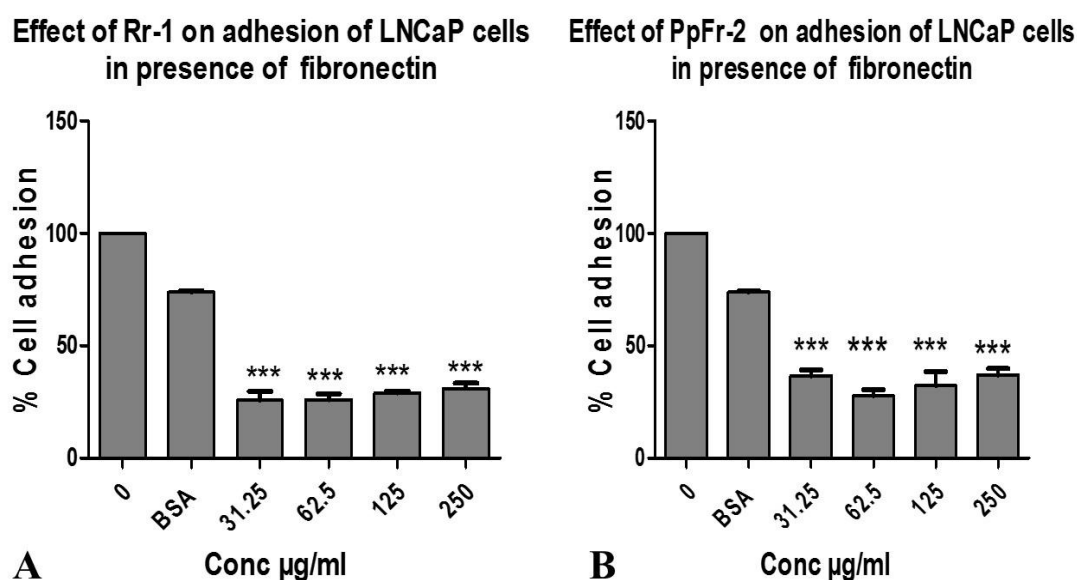


**Figure 3.71:** Effect of **(A)** Rr-1 and **(B)** PpFr-2 on adhesion of LNCaP cell coated plates of fibronectin, with BSA as a negative. The values are means ± SEM of 3 values. Statistical analysis was performed using one-way ANOVA with Tukey test, *** indicated significantly ($p < 0.0001$) lower values compared with the untreated control. (0 = untreated control).

### 3.6.5.1.2.2 Effect of Rr-1 and PpFr-2 on the migration of LNCaP cells using a Cytoselect™ 24-well Cell Migration Assay

Rr-1 had a significant (p < 0.0001) inhibitory effect on migration between 15.62 and 125 μg/ml and the % migration of LNCaP cells treated with Rr-1 was between 40% - 50% (Figure 3.72 **A**). While PpFr-2 inhibited the migration of LNCaP cells at 15.62 and 125 μg/ml and the % migration was between 30% - 32% (Figure 3.72 **B**).
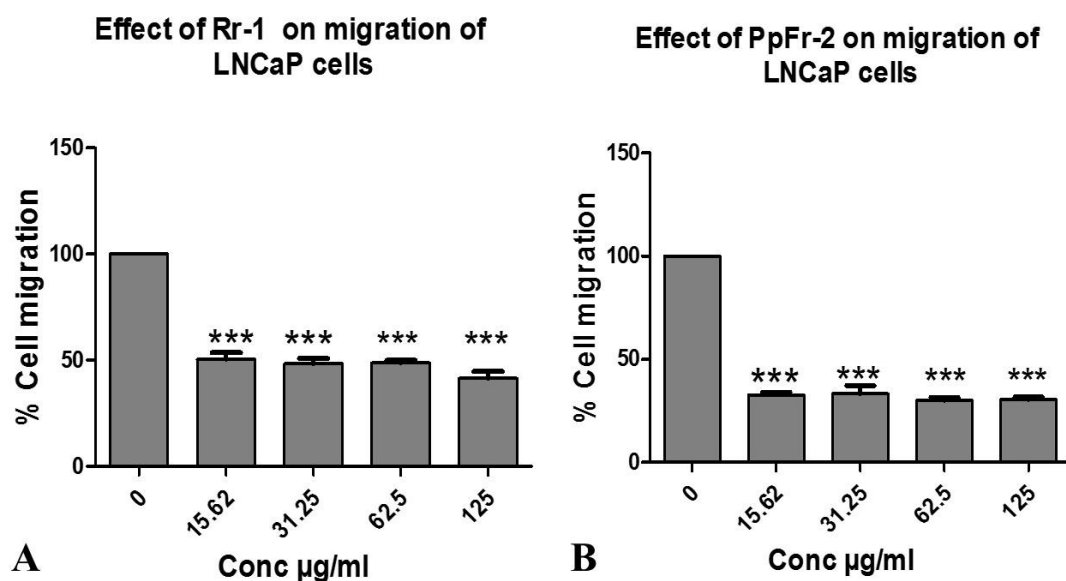


**Figure 3.72:** Effect of **(A)** Rr-1 and **(B)** PpFr-2 on the migration of LNCaP cells. The values are means ± SEM of 3 values. Statistical analysis was performed using one-way ANOVA with Tukey test, *** indicated significantly (p < 0.0001) lower values compared with the untreated control. (0 = untreated control).

### 3.6.5.1.2.3 Effect of Rr-1 and PpFr-2 on the invasion of LNCaP cells across the basement membrane using a Cytoselect™ 24-well Cell Invasion Assay

The effect of Rr-1 and PpFr-2 on the invasion of LNCaP cells across a basement membrane was assessed using a Cytoselect™ 24-well Cell Invasion Assay.

As shown in Figure 3.72 the number of LNCaP cells which invaded after exposure to Rr-1 was approximately the same as the untreated control. Rr-1 between 31.25 and 62.5 μg/ml slightly (p = 0.6938) inhibited the invasion of LNCaP cells across the basement membrane (Figure 3.73**A,** % invasion 80% - 95%).

Similarly, PpFr-2 between 31.25 and 62.5 μg/ml slightly (p = 0.4411) inhibited invasion (Figure 3.73**B,** % invasion 80% - 90%). Both Rr-1 and PpFr-2, between 31.25 and 62.5 μg/ml, did not kill normal cell (PNT2) hence, these concentrations are recommended for future work for treatment of LNCaP cells.
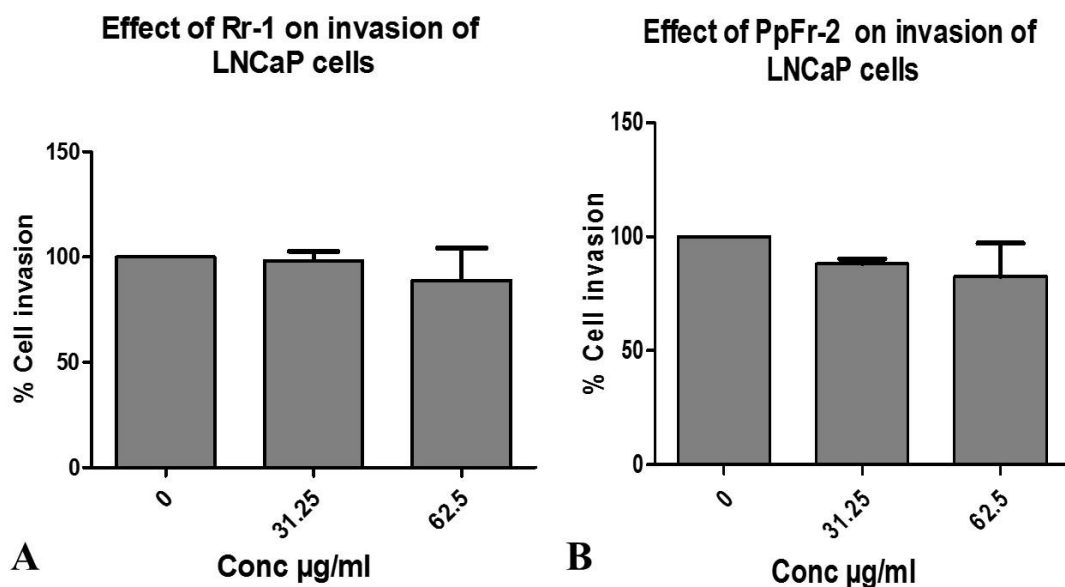


**Figure 3.73:** Effect of **(A)** Rr-1 and **(B)** PpFr-2 on the invasion of LNCaP cells. The values are means ± SEM of 3 values. Statistical analysis was performed using one-way ANOVA with Tukey test, Results indicated slightly (p = 0.6938, p = 0.4411) lower values compared with the untreated control, respectively, but these were not significant. (0 = untreated control).

### 3.6.5.2. Viability of Rr-1 and PpFr-2 on MCF7 and PNT2 cells after 48 h

The effect of different concentrations of Rr-1 on the viability of MCF7 cells and PNT2 cells were tested and found to have a significant (p < 0.0001) effect on the viability of the MCF7 cells at concentrations between 62.50 μg/ml to 250 μg/ml after 48 h but the viability of the PNT2 cells was affected significantly (p < 0.0001) only at 250 and 125 μg/ml (Figure 3.74 **A** & **B**).

Similarly, the viability of MCF7 cells and PNT2 cells were tested with PpFr-2 and found to have a significant (p < 0.0001) effect on the viability of the MCF7 cells between 62.50 μg/ml to 250 μg/ml after 48 h, but the viability of the PNT2 cells was affected (p < 0.0001) only at 125 and 250 μg/ml (Figure 3.74 **C** & **D**). As a result, the concentrations 31.25, 62.5 of both Rr-1 and PpFr-2 extracts were chosen for more investigations because they did not kill the normal cell line.
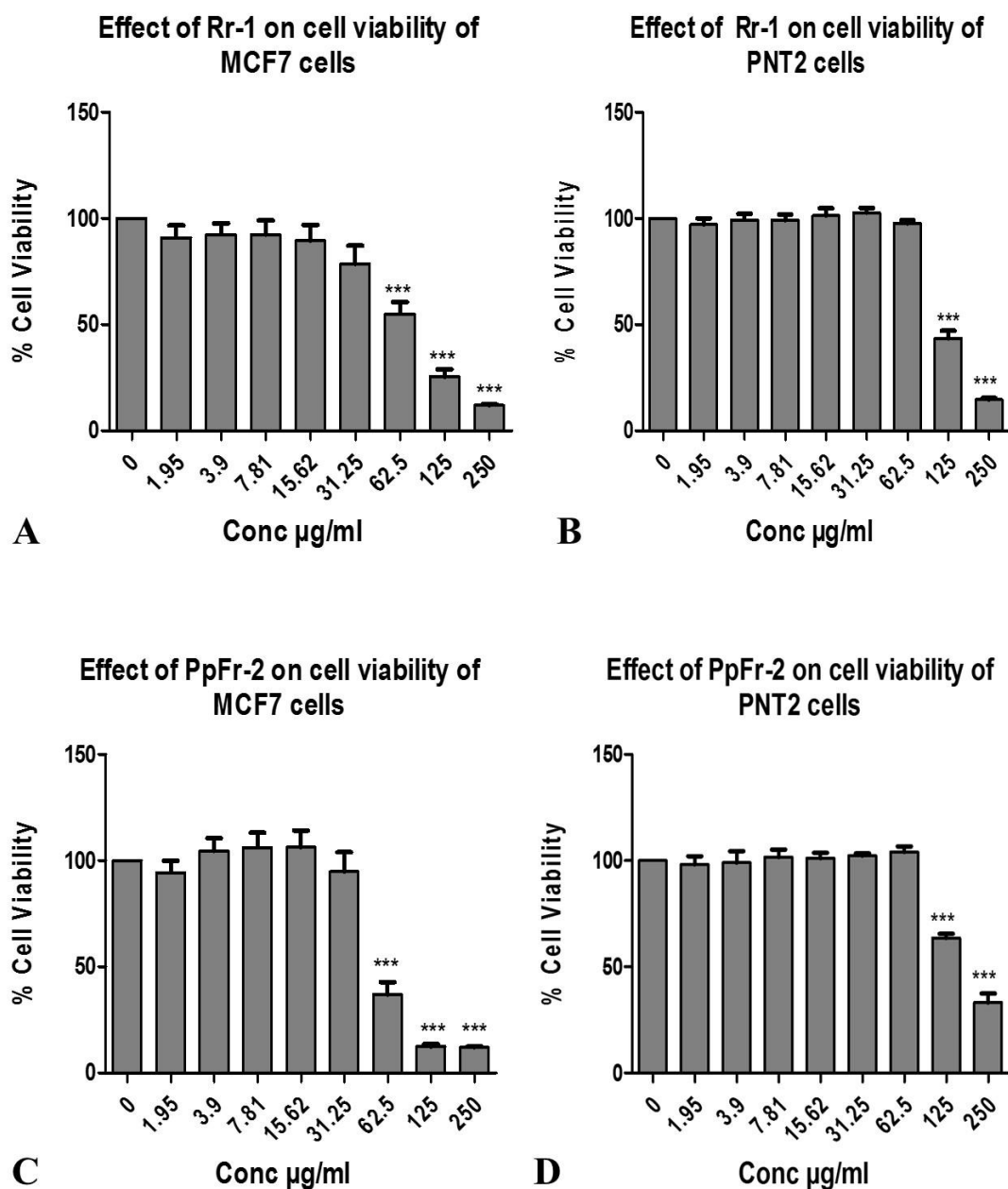
**Figure 3.74:** Effect of Rr-1 on the viability of **(A)** MCF7 cells and **(B)** PNT2 cells after 48 h and effect of PpFr-2 on the viability of **(C)** MCF7 cells and **(D)** PNT2 cells after 48 h. Statistical analysis was performed using one way ANOVA with Tukey test. *** indicates significantly ($p < 0.0001$) lower values compared with the untreated control. (0 = untreated control).

## 3.6.5.2.1 Effect of Rr-1 and PpFr-2 on the morphology of MCF7 cells after 48 h

There was a difference in the morphology of MCF7 cells after treatment with Rr-1 and PpFr-2 separately compared with the non-treated cells which displayed a rounded and

aggregated morphology with cell-cell contacts. While cells that were treated with Rr-1 appeared small and changed in size, but the cells treated with PpFr-2 showed poor attachment, suggesting there was an effect on adhesion of the cells (Figure 3.75).



**Non treated MCF7 Cells**

MCF7 cells treated with RrFr-2
62.5µg/ml

MCF7 cells treated with PpFr-2
62.5µg/ml
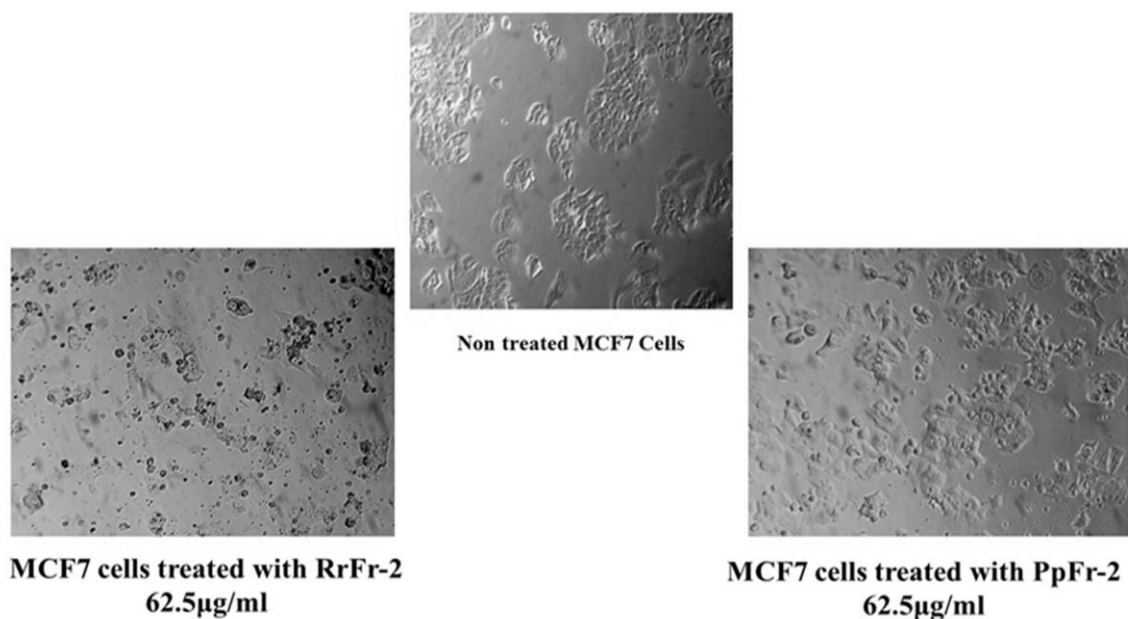
**Figure 3.75:** Morphology of MCF7 cells before and after treatment with Rr-1 and PpFr-2 after 48 h. Objective lens x 10

### 3.6.5.2.2 Effects of Rr-1 and PpFr-2 on adhesion, migration and invasion of MCF7cells

### 3.6.5.2.2.1 Effect of Rr-1 and PpFr-2 on adhesion of MCF7 cells to ECM (fibronectin) using a Cytoselect$^{TM}$ 48-well Cell Adhesion Assay

A large % of untreated MCF7 cells compared with treated cells was significantly ($p < 0.0001$) affected because the cells adhered and spread well on fibronectin. Cells treated with Rr-1 and PpFr-2, lost their adherence to fibronectin (Figure 3.76). Hence, Rr-1 extract concentrations 31.25 µg/ml to 250 µg/ml had greater significant ($p < 0.0001$) effect on adhesion (Figure 3.76 **A**) and the % of adhesion of MCF7 treated with 31. 25 to 250 µg/ml of Rr-1 was 20% to 50%. Also, with PpFr-2, there was decreased adhesion of MCF7 cells to fibronectin in a dose-dependent manner and the % adhesion was 22% to 52% at 31.25 to 250 µg/ml (Figure 3.76 **B**).
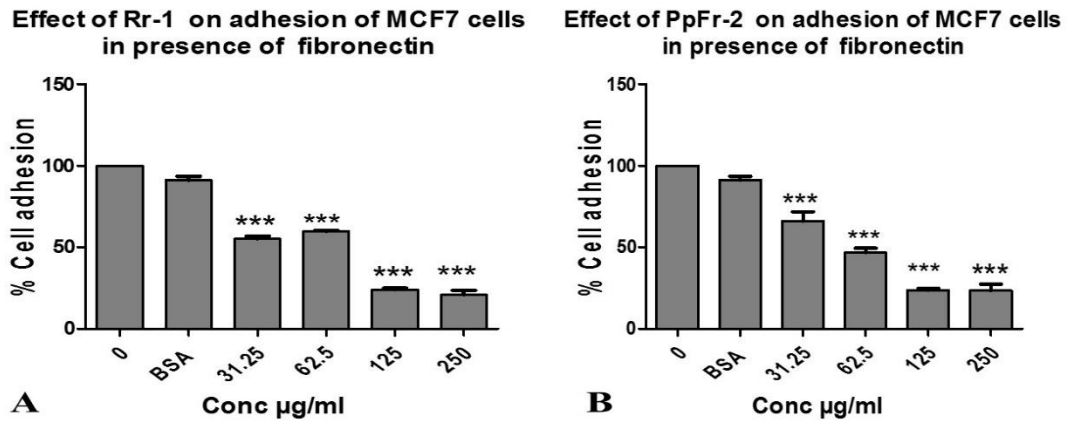
**Figure 3.76:** Effect of **(A)** Rr-1 and **(B)** PpFr-2 on adhesion of MCF7 cell coated plates of fibronectin, with BSA as a negative. The values are means ± SEM of 3 values. Statistical analysis was performed using one-way ANOVA with Tukey test, *** indicated significantly (p < 0.0001) lower values compared with the untreated control. (0 = untreated control).

### 3.6.5.2.2.2 Effect of Rr-1 and PpFr-2 on migration of MCF7 cells using a Cytoselect™ 24-well Cell Migration Assay

Rr-1 had a significant (p < 0.0001) inhibitory effect on migration between 15.62 and 125 µg/ml and the % migration of MCF7 cells treated with Rr-1 between 25% - 48% (Figure 3.77 **A**). While PpFr-2 inhibited the migration of MCF7 cells at 15.62 and 125 µg/ml and the % migration was between 10% - 25% (Figure 3.77 **B**).
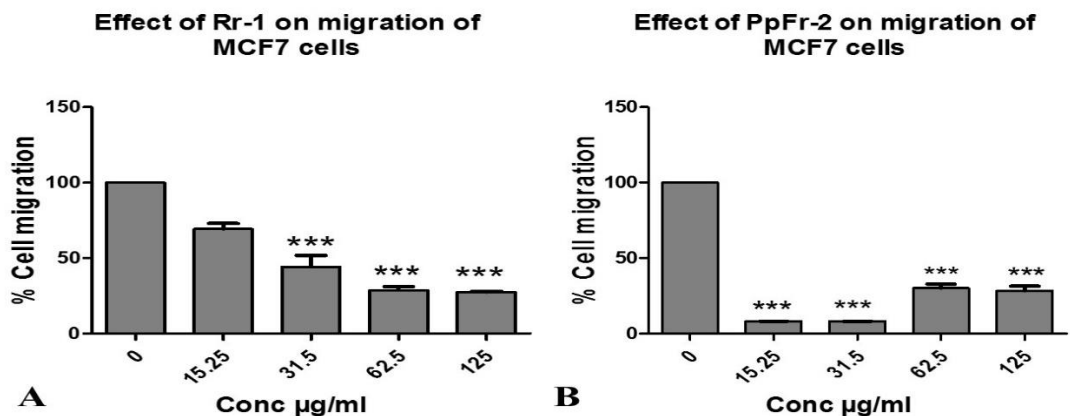


**Figure 3.77:** Effect of **(A)** Rr-1 and **(B)** PpFr-2 on the migration of MCF7 cells. The values are means ± SEM of 3 values. Statistical analysis was performed using one-way ANOVA with Tukey test, *** indicated significantly (p < 0.0001) lower values compared with the untreated control. (0 = untreated control).

### 3.6.5.2.2.3 Effect of Rr-1 and PpFr-2 on the invasion of MCF7 cells across the basement membrane using a Cytoselect™ 24-well Cell Invasion Assay

The effect of Rr-1 and PpFr-2 on the invasion of MCF7 cells across a basement membrane was assessed using a Cytoselect™ 24-well Cell Invasion Assay.

As shown in Figure 3.78 the number of MCF7 cells which invaded after exposure to Rr-1 was approximately the same as the untreated control. Rr-1 between 31.25 and 62.5 µg/ml ($p = 0.3840$) did not inhibit the invasion of MCF7 cells across the basement membrane (Figure 3.78 **A,** % invasion 100 %).

In contrast, PpFr-2 between 31.25 and 62.5 µg/ml slightly ($p = 0.1423$) inhibited invasion of MCF7 (Figure 3.78 **B,** % invasion 70% - 85%). Both of Rr-1 and PpFr-2 between 31.25 and 62.5 µg/ml, did not kill the normal cell line (PNT2) therefore, these concentrations are recommended for future work for treatment of MCF7 cells.
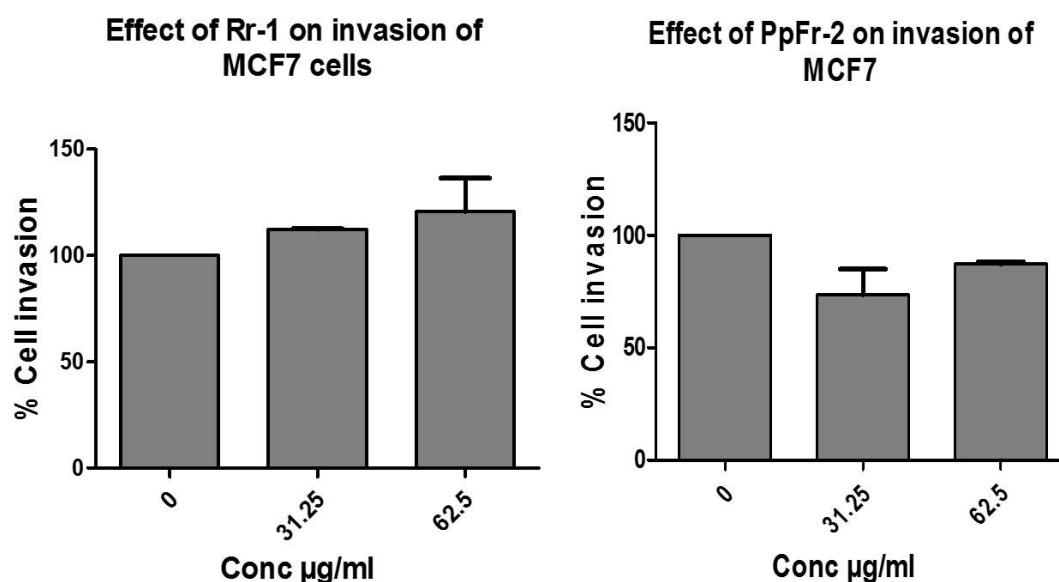


**Figure 3.78:** Effect of **(A)** Rr-1 and **(B)** PpFr-2 on the invasion of MCF7 cells. The values are means ± SEM of 3 values. Statistical analysis was performed using one-way ANOVA with Tukey test. The result indicated no effect with Rr-1 ($p = 0.3840$) while slightly lower values with PpFr-2 ($p = 0.1423$) compared with the untreated control, respectively, but these were not significant. (0 = untreated control).

# Chapter 4

## *Discussion, Future work and Conclusion*

## 4.1 Discussion

The main aim of this study was to examine four Libyan plants for their potential anticancer properties. Hence, isolation and identification of bioactive compounds from these plants was carried out followed by an investigation into their bioactivity.

To achieve this, the plants *B. spectabilis*, *A. graecorum. R. raetam* were extracted using Soxhlet apparatus by three successive solvents (*n*-hexane, EtOAc and MeOH) to obtain crude extracts while *P. plicata* was extracted using EtOH only because of time limitation. The crude extracts were subjected to many chromatographic and spectroscopic methods to isolate and identify compounds. Biological assays of the crude extracts and isolated compounds were tested to confirm previously reported observations and to understand the correlation between biological activities and traditional uses of these plants.

The crude extracts and isolated compounds in sufficient quantities were evaluated for potential cytotoxicity against the following human cancer cell lines: HepG2, A375, A549, PANC-1, MCF7, LNCaP and normal cell line PNT2. Two fractions (Rr-1 and PpFr-2) which were toxic to cancer cells and not toxic to normal cells were investigated for their effects on morphology, viability, adhesion, migration and invasion of two cancer cell lines (LNCaP and MCF7) based on the preliminary screening.

### 4.2 *In vitro* cytotoxicity activity assessment

### 4.2.1 Effects of crude extracts from *B. spectabilis* and its components on cell viability

Previous studies examining the chemical constituents of *B. specabtilis* revealed the presence of essential oils, glycosides, flavonoids, peltogynoids, saponins, steroids, terpenoids and phlobatannins (Table 1.6). In this study, the phytochemical examination of *B. specabtilis* flower extracts of $^1$H NMR spectra of the *n*-hexane and EtOAc extracts showed signals suggesting the presence of mixtures of β-sitosterol and stigmasterol compounds associated with fats (data not shown) but the $^1$H NMR spectra of MeOH extract and its fractions after being subjected to three different methods of

analytical chromatography showed some distinguishable signals which led to the isolation of three compounds Bs-1 which was isolated in a previous study from the stem part of this plant (Jawla *et al*., 2013), Bs-2 and Bs-3, which were isolated for the first time from *B. specabtilis*.

Studies have identified a range of potential biological properties for extracts from *B. specabtilis* such as antimicrobial (Umamaheswari *et al.*, 2008, Sudipta *et al.,* 2012, Fawad *et al.,* 2012), antidiabetic (Jawla *et al*., 2012), antihyperlipidemic (Adebayo *et al*., 2005), antifertility (Mishra *et al.,* 2009, Ikpeme *et al.,* 2015) and antioxidant activity (Pintathong *et al*., 2012).

In the present study, cytotoxicity activity of B. spectabilis flowers extracts and its constituents against cancer and normal cells has was absent. The results confirmed those of a previous study using cancer cell lines: HepG2, U251(model of glioblastoma), H460 (large cell lung carcinoma), HeLa, MCF7 that revealed the same result although it used a different plant part and a different assay (Ahmed, 2009). Similarly, Do *et al*. (2016) evaluated eight bougainvinones A-H that showed that bougainvinone G exhibited cytotoxicity against five cancer cell lines KB (ubiquitous keratin-forming tumor cell line), HT-29 (Human colorectal adenocarcinoma cell line), HeLa S-3 (clonal derivative of the parent HeLa line), MCF7 and HepG2, while bougainvinones B and C exhibited cytotoxicity against the KB cell line only and the others were inactive. Bougainvinones A, D, E, F and H replaced the hydroxyl group with a methoxy group that generally resulted in reduction or loss of activity. These results suggested that only those peltogynoids with C-5 and C-7 hydroxy substitution of bougainvinones B, C and G exhibited cytotoxic activity, and the replacement of the hydroxy group with a methoxy group of bougainvinones A, D, E, F and H generally resulted in reduction or loss of activity (Do *et al.*, 2016).

On the other hand, in this study, most of the *B. spectabilis* extracts and isolated compounds failed to exhibit this level of activity (less than 250 µg/ml) against the tested cancer cells. However, negative results do not mean that the plant extracts are inactive or that bioactive compounds are absent. Active compounds might be found in insufficient quantities in the crude extracts for them to exhibit activity with the concentrations assayed. For example, solubility issues became quite challenging in preliminary screening. None of the extracts showed activity up to 250 µg/ml against

all the tested cancer cells, which could have been due to the extracts of the plant having selective activity against particular cell lines. Furthermore, the different extraction methods for example in the present study which used soxhlet extraction could have affected the extraction of the plants. Further, selection of suitable extraction processes is recommended such as maceration to preserve the original compounds which may have a relatively unstable character (Zhang *et al.*, 2018). However, further phytochemical experiments or better alternative isolation methods such as HPLC are recommended for future use.

Therefore, the plant *B. spectabilis* has many traditionally uses with antidiabetic activity being the most common in traditional medicine. The present study though focussed on evaluating the anticancer activity. In the literature, pinitol was identified from this plant and reported as an anticancer agent (Lin *et al.*, 2013, Rengarajan *et al.*, 2014).

**Bs-1** is a major constituent of the soybean plant (*Glycine max L Merr.*) and is known to be an insulin mimicker. Poongothai and Sripathi (2013) reviewed that **Bs-1** was isolated from various plant families having different biological activities such as antidiabetic (Davis *et al.*, 2000), anti-inflammatory (Singh *et al.*, 2001), antioxidant (Orthen *et al.*, 1994), immunosuppressive potential (Chauhan *et al.*, 2011), anticancer (Lin *et al.*, 2013, Rengarajan *et al.*, 2014) and used in the treatment of hypertension, rheumatism, cardiovascular diseases, AIDS and neurological disorders (Ostlund and Sherman, 1996, Kim *et al.*, 2005).

**Bs-2** has been isolated previously from *Pisonia grandis* (Nyctaginaceae) (Sripathi *et al.*, 2011) and for the first time from *B. spectabilis.* It is used as a moisturiser to treat or prevent dry, rough, scaly, itchy skin and minor skin irritations (Scimeca *et al.*, 2008, Becker *et al.*, 2010, Navone *et al.*, 2014).

**Bs-3** was isolated previously from *Trigonella foenum graecum* (Al-Khateeb *et al.*, 2012) and *Doliocarpus dentatus* (Jagessar *et al.*, 2013) and for the first time from *B. spectabilis*; it has been used as a hypoglycaemic, and it has been shown to reduce diabetic auditory neuropathy and platelet aggregation (Zhou *et al.*, 2012).

## 4.2.2 Effects of crude extracts from *A. graecorum* and its component on cell viability

In this study, the phytochemical examination of *A. graecorum* leaf, stem and root extract demonstrated that the $^1$H NMR spectra of the hexane and EtOAc extracts

showed signals suggesting the presence of a mixture of fats. The MeOH extract was subjected to VLC were with increasing polarity of hexane up to 40% MeOH. The fractions from VLC further fractionated by Sephadex. None of the fractions showed compounds except the seventh fraction that was assessed using NMR and enabled elucidation of narcissin (**Ag-1**).

In this study, the cytotoxic activity of *A. graecorum* leaf, stem and root extract and its constituents against cancer and normal cells showed no cytotoxic activity. However, negative results of cytotoxic effects do not mean that the plant extracts are inactive or that there is an absence of bioactive compounds; they may be present in insufficient quantities in the crude extracts for them to show activity with the concentrations assayed. A previous study demonstrated that this plant possesses anti-inflammatory activity, which confirms the traditional uses of *A. graecorum* for the treatment of inflammatory illnesses (Ibrahim, 2015). **Ag-1** was identified as isorhamnetin 3-*O*-rutinoside also called narcissin and isolated for the first time from *A. graecorum* leaves, stems and root. It was isolated previously from the aerial part of *Peucedanum aucheri* Boiss (Dehaghani *et al.*, 2017). Ag-1 did not exhibit cell toxicity against any of the cancer cell lines used in the present study. There are no previous reported biological activities of this compound. Thus, for future work, screening of this compound for various biological activities needs to be carried out.

### 4.2.3 Effects of crude extracts from *R. raetam* and its components on cell viability

Fractionation of the EtOAc extract of *R. raetam* led to the isolation of two flavonoid compounds, alpinumisoflavone **(Rr-1)** and ephedroidin **(Rr-3)**. In addition, fractionation of the MeOH extract led to the isolation and characterisation of one flavonoid compound 8-*β*-D-Glucopyranosylgenistein **(Rr-2)**. The ^{1}HNMR spectrum of the hexane extract of *R. raetam* showed signals suggesting the presence of mixtures of triglycerides and fats. Rr-3 was isolated in a previous study from the aerial parts of this plant (Xu *et al.*, 2015) while the isolated compounds Rr-1 and Rr-3 in this study were identified for the first time from *R. raetam.*

Studies have identified a range of potential biological properties for extracts from *R. raetam* such as antimicrobial (Edziri *et al.*, 2010, Awen *et al.*, 2011, Edziri *et al.*, 2012), antidiabetic (Algandaby *et al.*, 2010), analgesic (Djeddi *et al.*, 2013) and antioxidant (Conforti *et al.*, 2004, Edziri *et al.*, 2010, Djeddi *et al.*, 2013).

In this study, the hexane extract of this plant showed no toxicity on both cancer and normal cells (Table 3.14). Also, the MeOH extract had no toxic effect compared to the previous study that used the protein-staining sulforodamine (SRB) assay to evaluate a MeOH extract of *R. raetam* leaves and seeds. This extract had a toxic effect against Caucasian lung large cell carcinoma (COR-L23) (Conforti *et al*., 2004). Generally, the difference in the results could be due to a different assay used by Conforti and his colleagues to measure cell viability in which they used a SRB is assay rather than a resazurin assay used in the present study. SRB is used to estimate cell number indirectly by providing a sensitive index of total cellular protein content which is linear to cell density.

In contrast, the EtOAc extract of *R. raetam* demonstrated toxic effects against HepG2 (liver), A375 (melanoma), PANC-1 (pancreas) and PNT2 (normal) at 250 μg/ml and this extract was toxic to LNCaP (prostate) at 125 μg/ml but this extract was not toxic to A549 (lung) and MCF7 (breast) cells.

The isolated compounds **Rr-2** and **Rr-3** had no toxicity on any of the tested cell lines, while **Rr-1** which was isolated from EtOAc of *R. raetam* extract. It was toxic against HepG2, A375, A549, PANC-1, MCF7 and PNT2 at 125 μg/ml, while it was highly toxic to LNCaP at 62.5 μg/ml.

**Rr-1** a natural prenylated isoflavonoid, identified as alpinumisoflavone was isolated for the first from *R. raetam.* It has been isolated previously from various plant families such as Leguminosae, Moraceae, Dilleniaceae and Apiaceae and is medicinally important by having biological activities such as antimicrobial, antioxidant, anti-inflammatory, antidiabetic, antiosteoporotic, anticancer, estrogenic, antiestrogenic, and neuroprotective (Ateba *et al*., 2019).

In this study, **Rr-1** showed strong cytotoxicity on all the cancer cells. A previous study reported an $IC_{50}$ that ranged from 5.91 μM towards leukaemia cell (CEM/ADR5000) to 65.65 μM towards drug-resistant breast adenocarcinoma cells (MDAMB-231-BCRP) (Kuete *et al*., 2016).

Consequently, the inhibitory effect, particularly against LNCaP cells, produced by the EtOAc extract was suggested to be related to the presence of **Rr-1** compound and/ or to unisolated phytochemical(s).

In addition, MeOH extract and its isolated compound **Rr-2** did not show toxicity on cancer cells which could be due to the presence of this flavonoid glycoside and/ or to other unidentified phytochemical(s); flavonoid glycosides of their attached sugar units are less active than the free flavonoid (Plochmann *et al*., 2007).

8-*β*-D-Glucopyranosylgenistein **(Rr-2)** was previously isolated from *Genista tenera* and this was the first report from *R. raetam.* Jesus *et al.* (2014) reported that **Rr-2** is a promising molecular entity for intervention in amyloid events of both diabetes and the frequently associated Alzheimer's disease (Jesus *et al*., 2014).

Daidzein (**Rr-3)** did not show any cytotoxicity, therefore, was not suitable in this study as a potential anticancer agent.

### 4.2.4 Effects of crude extracts from *P. plicata* and its components on cell viability

Previous studies examining the chemical constituents of the aerial parts or seeds of *P. plicata* have revealed the presence of isoflavonoids, chromenes, furanocoumarins, benzofuran glycosides, flavonoid glycosides, phenolic cinnamates, monoterpenoids and triterpenoids compounds (Table 1.9). In this study, the phytochemical examination of *P. plicata* leaf and stem extract was fractionated by increasing the polarity with hexane up to 40% MeOH that led to isolation of five fractions that were further fractionated by Sephadex CC. The $^1$H NMR spectra of the four fractions (Fr-1, Fr-3, Fr-4 and Fr-5) showed no compounds. Fraction 2 (*n*-hexane : EtOAc 50:50) of *P. plicata* ethanol extract **(PpFr-2)** was subjected to fractionation using Sephadex CC that led to the identification of two compounds coded Pp-1, Pp3 and mixture of Pp-2a and Pp-2b**.**

In the literature, the plant *P. plicata* has been identified to have some potential biological properties such as anti-mosquito activity (El-Abgy *et al.*, 2012) and antioxidant activity and is used to treat dermal diseases such as psoriasis (Cheikh *et al*., 2015). However, the cytotoxicity evaluation of this species of *Psoralea* has not been investigated previously but has been for other species such as *P. corylifolia* where Wang *et al.* (2011) evaluated the cytotoxicity of a MeOH extract of *P. corylifolia* L. seeds using a MTT assay that showed a dose-dependent anticancer effect on four cell lines of human oral carcinoma (KB, KBv200) and human erythroleukemia (K562, K562/ADM) (Wang *et al.*, 2011). Thus, this is the first report of cytotoxicity for *P. plicata.*

Consequently, the cytotoxicity activity of *P. plicata* EtOH extract and its fractionations against cancer and normal cells are presented in Table 3.16. Only fraction 2 **(PpFr-2)** was toxic against the normal and most of the cancer cell lines. It was toxic to HepG2, PANC-1, and PNT2 at 250 µg/ml and was toxic against A375 at 125 µg/ml, while it was highly toxic against MCF7 and LNCaP at 62.5 µg/ml, but this fraction was not toxic to A549 cells.

Therefore, the inhibitory effect, particularly in MCF7 and LNCaP cells, produced by PpFr-2 is thought to be attributable to the combined effects of these compounds Pp-1, Pp-3, and mixture of Pp-2a and Pp-2b and/or to unidentified phytochemical(s). Attempting to increase the quantities of these compounds, the remaining fractions were subjected to different chromatography columns to obtain sufficient quantities, but these further separation methods failed to obtain enough quantities of these compounds. Due to low quantities, it was difficult to purify them. Further work is required to separate the mixture of Pp-2a and Pp-2b to isolate the pure compounds in sufficient quantities, using another purification method such as HPLC, so that physical data for the pure substances can be obtained (e.g. melting point) and to enable biological tests to be carried out separately on the pure compounds. Furthermore, increasing the initial amount of the plant is required to improve the compound yield.

## 4.2.5 Rr-1 and PpFr-2 had an inhibitory effect on morphology, adhesion, migration and invasion of LNCaP and MCF7 cells.

From these preliminary findings, Rr-1 and PpFr-2 were chosen for further examination due to the selective cytotoxicity on LNCaP and MCF7 cells. Therefore, Rr-1 and PpFr-2 were chosen to investigate their anti-adhesion properties on LNCaP and MCF7 cells.

Cancer metastasis is a complex process which causes the spread of cancer cells from the primary tumour to surrounding tissues and distant organs (Gupta and Massague, 2006, Lv *et al.*, 2014). It is involved in the loss of cellular adhesion, increased migration and invasion, circulation through the vascular/lymphatic systems at distant sites (Chambers *et al.*, 2002). For metastasis to occur to new sites, cell adhesion molecules, migration and invasion are required (Keleg *et al.*, 2003). Degradation of the ECM and BM by proteolytic enzymes and invasion is essential for metastasis (Bogenrieder and Herlyn, 2003). ECM components have been revealed to play a

significant role in cancer cell invasion and metastasis (Müller-Pillasch *et al.*, 1997). The ECM is composed of two main classes of macromolecules: fibrous proteins and proteoglycans (Frantz *et al.*, 2010). Hence, this study focussed on the effect of Rr-1 and PpFr-2 viability, adhesion to ECM protein fibronectin, migration and invasion of LNCaP and MCF7 cells. Up to now, there has not been a study of the effect of Rr-1 and PpFr-2 on the morphology of LNCaP and MCF7 cells. Rr-1 and PpFr-2 had an effect on the morphology of the cells. It was revealed that these morphological changes were associated with the anti-adhesion properties of the Rr-1 and PpFr-2.

Morgan *et al*. (2000) reported that apoptosis in prostate cancer was shown to be influenced by external events including constituents of ECM because the ECM plays an important role in embryologic development, epithelial differentiation, cytolocomotion, and epithelial cells survival through suppression of apoptosis. The ECM consists of many non-collagenous molecules including fibronectin, tenascin, laminin, and collagen IV, which are present at the epithelial-mesenchymal interface of both benign and malignant tissues. Morgan *et al*. (2000) showed that fibronectin influences cell proliferation, apoptosis, and Bcl-2 expression similarly among LNCaP and PC-3 cell lines (Morgan *et al.*, 2000). Several ECM proteins are significantly deregulated and specific matrix components that stimulate tumour progression and metastasis in breast cancer. Fibronectin is an element of the mammary mesenchymal compartment of ECM in breast cancer and it is a primary component of the mammary mesenchymal compartment and undergoes dramatic changes during breast cancer development. Increased fibronectin expression is associated with invasive and metastatic breast cancer phenotype. Li *et al*. (2017) demonstrated that fibronectin causes an epithelial-mesenchymal transition (EMT)-like morphological change in MCF7 breast cancer cells. They found that fibronectin stimulation caused the downregulation of epithelial markers E-cadherin and tight junction protein ZO-1, and the upregulation of mesenchymal markers N-cadherin and vimentin (Li *et al*., 2017). Furthermore, fibronectin promoted cell migration and invasion in LNCaP and MCF7 cells, therefore fibronectin is a glycoprotein of the ECM, plays a major role in cell adhesion, growth, migration, and differentiation in cancer cells. Consequently, the purpose of this experiment was to assess the effect of Rr-1 and PpFr-2 on adhesion of LNCaP and MCF7 cells to fibronectin-coated plates.

To date, there has not been a study of the effect of **Rr-1** on the viability of LNCaP and MCF7 cells. **Rr-1** had an effect on the viability of the cells as explained in section 3.6.5. It was demonstrated that the viability and morphological changes were associated with the anti-adhesion properties of the **Rr-1**. The result of the current work is similar to the result by Nkengfack *et al.* (2001) who reported that **Rr-1** showed strong cytotoxicity against oral epidermoid carcinoma cells (KB) with $IC_{50}$ value 4.13 μg/ml using a MTT assay (Nkengfack *et al.*, 2001) and on murine leukaemia cells (P-388) with $IC_{50}$ value 4.31 μg/ml (Tjahjandarie and Tanjung, 2015). At a concentration of $10^{-5}$ M, **Rr-1** inhibited the growth of renal carcinoma cell (SN12C) by 32.67% (Amen *et al.*, 2013). Another study demonstrated that **Rr-1** showed moderate cytotoxicity on lung cancer cell lines (H2108, H1299, and MRC-5), with $IC_{50}$ values of 33.5, 38.8, and 52.5 μM, respectively (Namkoong *et al.*, 2011). Kumar *et al.* (2013) also found it to be more toxic against human leukaemia cell lines (HL-60, K-562, and MOLT-4) with $IC_{50}$ values of 19, 34, and 41 μM, respectively (Kumar *et al.*, 2013). To clarify that the actions of **Rr-1** on viability and morphology were due to their effect on adhesion because it acted on ECM. In addition, Gao *et al.* (2017) found that **Rr-1** inhibited cell adhesion, migration, and invasion in melanoma cells (A375 and SK-MEL-1) with 5 and 10 μM Rr-1 treatment by downregulating COX-2 via the miR-124/SPHK 1 axis; decreased number of lung metastases; decreased COX-2 and SPHK1 expression and increased miR-124 expression in metastatic tissues (Gao *et al.*, 2017). It has been shown *in vivo*, that the **Rr-1** treatment also reduced tumor growth in various xenograft mouse models in esophageal squamous cell carcinoma (KYSE30 and Eca109) with (50 and 100 mg/kg/day) and (20 mg/kg/day) respectively, after 30 consecutive days of treatment (Ateba *et al.*, 2019). A study by Wang *et al.* (2017) found that **Rr-1** caused suppression of cell growth; induction of apoptosis; and inhibition of cell invasion of clear cell renal cell carcinoma (ccRCC) by increased miR-101 expression; repression of RLIP76 expression and inhibition of Akt *in vivo* suppression of tumor growth and pulmonary metastasis. Therefore, the protein of ECM play an important role in tumour invasion and metastasis by degeneration of ECM proteins such as fibronectin (Wang *et al.*, 2017, Ateba *et al.*, 2019).

Therefore in this study the effect of **Rr-1** on interaction between fibronectin with LNCaP and MCF7 were studied.

In this study, a concentration between 31.25 μg/ml to 250 μg/ml, **Rr-1** caused significant (p < 0.0001) loss of cell adhesion 75% in LNCaP and 65% in MCF7 cell lines to fibronectin. It can be concluded the **Rr-1** is specific at least for the fibronectin receptor.

In this study, at concentrations of 15.62 and 125 μg/ml, inhibition of migration occurred and the % migration of LNCaP and MCF7 cells was 40% -50% and 25% - 48% respectively. The mechanism of action was through the inhibition effect of **Rr-1** on cell migration and it is likely due to the reduced attachment to fibronectin. The current work also demonstrated that **Rr-1** had an inhibitory effect on migration but not on invasion of LNCaP and MCF7 cell lines. This result was different to a study carried out by Wang *et al.* (2017), which demonstrated that the **Rr-1** at 10 μM inhibited the growth and invasion of the human clear-cell renal carcinoma ccRCC 786-O and Caki1 cells and were suppressed by 40% and 55%, respectively (Wang *et al.*, 2017). Another study revealed that **Rr-1** (10 μg/ml) demonstrated a low antiproliferative activity (30 – 40% inhibition) against human melanoma cells A375 and SK-MEL-1 after a 24h incubation and suppressed the adhesion, migration and invasion of these cell lines (Gao *et al.*, 2017). In contrast, in the present study the antiproliferative activity against LNCaP and MCF7 cells was suppressed by **Rr-1** on adhesion and migration, but not invasion. Therefore, the difference of the results of the invasion assay in the Gao *et al.* (2017) study and the current work may be attributed to the difference in mechanism of action based on the cell type and the invasion assay. However, the present a study used a Cytoselect$^{TM}$ 24-well cell invasion assay which has polycarbonate membrane, while, Gao *et al.* 2017 used 24 - Transwell inserts coated with matrigel, where the Corning Matrigel matrix is a solubilised BM prepared from the Engelbreth-Holm-Swarm (EHS) mouse sarcoma (Gao *et al.*, 2017). As a result, all previous studies demonstrate that alpinumisoflavone **(Rr-1)** could have a potential anticancer activity.

The cytotoxicity of *P. plicata* has not been studied before, although isolated compounds psoralen (Pp-2a) and isopsoralen (Pp-2b) isolated from *P. corylifolia* extracts (CHCl$_3$ and EtOH) showed cytotoxicity against an epithelial type 2 cell line (HEp-2) (Whelan and Ryan, 2003). Also, Pp-2a and Pp-2b induced apoptosis in cancer oral carcinoma cell lines (KB, KBv200), erythroleukemia cell lines (K562 and

K562/ADM) thus, confirming their anti-cancer potential. The $IC_{50}$ values of Pp-2a were 88.1, 86.6, 24.4 and 62.6, while Pp-2b were 61.9, 49.4, 49.6 and 72.0, respectively (Wang *et al.*, 2011). Jiang and Xiong (2014) tested Pp-2a on a hepatocarcinoma cell line (SMMC-7721), and found that it had inhibitory activity by inducing apoptosis, inhibited the growth of SMMC-7721 cells in a dose - and time-dependent manner and had a strong pro-apoptotic effect on these cells (Jiang and Xiong, 2014). However, there are no scientific studies of Pp-2a and Pp-2b on metastasis mechanisms (adhesion, migration and invasion).

In this study, the effect of PpFr-2 on the interaction between fibronectin with LNCaP and MCF7cells was studied. A concentration between 31.25 μg/ml to 250 μg/ml, **Rr-1** caused significant ($p < 0.0001$) loss of cell adhesion 75% in LNCaP and 65% in MCF7 cell lines to fibronectin and a concentration between 31.25 and 250 μg/ml, **PpFr-2** caused a loss of cell adhesion of 70% in both LNCaP and MCF7 cell lines to fibronectin in a dose-dependent manner. The current work also demonstrated that PpFr-2 at 15.62 and 125 μg/ml, had an inhibitory effect on migration and the % migration of LNCaP and MCF7cells was 30% - 32% and 10% -25% respectively. However, they did not prevent the invasion of LNCaP and MCF7cells.

Generally, in *in vitro* step-by-step protocol techniques, scientists have the challenge to determine and measure an extensive variety of cell motility parameters that relate to the migration process, for example wound area, velocity, healing speed, front cell velocity, travelled distance, invasion, and spreading rate (Pijuan *et al*., 2019). It seems that the results in the present work regarding invasion assays correlate with Hu *et al.* (2017) which showed that the higher incubation time was associated with the lower antiproliferative activity (Hu *et al.*, 2017). In addition, the long incubation times are often associated with the metabolism, decomposition, or precipitation of compounds (Ateba *et al.,* 2018). Moreover, Pijuan *et al.* (2019) found that the pore size of the membrane inserts may affect the invasion of cells due to cell type size (Pijuan *et al.*, 2019). Therefore, in this study the pore size of the membrane insert was 8μm which may be too large leading to the cells invading through the membrane.

Therefore, according to the aforementioned observations, the non-inhibition of invasion cells could be attributable to one or these combined effects of protocol

techniques of the experiment. Hence, further work is required to use smaller pore size (3-5 µm) and lower incubation times. Therefore, **Rr-1** and **PpFr-2** could be a promising target to treat prostate and breast cancer by inhibition of cell migration as a result of reduced or inhibited attachment to fibronectin.

## 4.3. Overall evaluation of the cytotoxicity activity of the crude extracts

The present study was undertaken with the objective to explore the anticancer activities of the plants *B. spectabilis*, *A. graecorum*, *R. raetam* and *P. plicata* against cancer cells because there are few scientific studies reporting anticancer activities for these plants. In summary, cytotoxicity activity in this study, the hexane, EtOAc and MeOH extracts of *B. spectabilis* and *A. graecorum* showed a lack of toxicity against cancer cells.

The isolated compounds were low in quantity with impurities. The purification work on these compounds has not yet been completed because of the limited quantities of plant materials. Hence, in subsequent studies, the same chromatographic techniques could be repeated with larger amounts of the fractions to improve the yields. Moreover, further separation and consequent purification have to be continued to purify the isolated compounds. However, the activity of the extracts containing these compounds was evaluated for cytotoxic effect as discussed earlier and the results were not very promising.

These findings may be attributed to the extraction methods and different seasonal variation of the plant; for instance, the time and areas of the collection could affect the compounds in the plant (Liu *et al*., 2016). As a result, further work is required to isolate and carry out the biological investigation of pure compounds for these plants.

On the other hand, the EtOAc extract of *R. raetam* was selective toward PC cells (LNCaP). The preliminary results for alpinumisoflavone (**Rr-1**) showed selective activity against LNCaP and MCF7. By considering all the aforementioned data, the anti-cancer activity of the EtOAc extract of the *R. raetam* could be attributed to the isolated compound Rr-1, and the results were very promising.

The EtOH extract of *P. plicata* was selective against cancer cells. This extract had anti-cancer activity against LNCaP and MCF7 cells by inhibiting adhesion on fibronectin in the ECM and inhibited their migration. The EtOH extract of *P. plicata* was mainly composed of furanocoumarins compounds. This activities of anti-adhesion, anti-

migration of this extract was probably due to the presence of Pp-1, Pp-3, Pp-2a and Pp-2b.

The present study indicated the toxicity of some of the plant extracts where this information was available. The method of preparation and administration by traditional medicine is the starting point to design experimental protocols aimed at finding scientific evidence of efficacy and toxicity. The ability to produce safe, standardised medicinal plant products for further clinical evaluation is a major stumbling block in most countries wishing to enhance the quality of their herbal medicines.

## 4.4 Recommendations for the future

The most significant issue in this study was the impact on the work of limited quantities of *A. graecorum*, dried plant stocks and the lack of fresh plant material. Hence, if further work is to be carried out large quantities of fresh plant material should be made available for an in-depth study. The lack of toxicity of this plant and its isolated compound could be due to time of collection of the plant thus; this plant could be collected from a different locality and time of year (season) and repeating what has been carried out here.

Further work could be focussed on *P. plicata* plant to separate the mixture of Pp-2a and Pp-2b to isolate the pure compounds in sufficient quantities, using another purification method such as HPLC.

It also recommended that the type of the invasion assay should be 24 - Transwell inserts coated with matrigel invasion assay, with suitable pore size (3-5 µm) and lower incubation times.

The PpFr-2 extract and pure compound Rr-1 may have an anti-metastatic effect on prostate and breast cancer and could be used for production of safer, natural and active antimetastatic lead candidate drugs, so future work could focus on three-dimensional (3D) *in vitro* models (Weiswald *et al*., 2015).

Furthermore, future work would need to focus on *in vivo* assessment, initially using a suitable rodent experimental model to improve prostate and breast cancer patient outcomes.

## 4.5 Conclusion

In the current project four medicinal plants from Libya were investigated for their phytochemical constituents and biological activities. A total of 10 compounds, including alkaloid, flavonoids, phenolics, furanocoumarin and flavonoid glycosides were isolated. Some of these compounds were isolated for the first time for these plants.

From *B. spectabilis* extracts a series of cycloalkane, phenolic and alkaloid were isolated. All crude extracts and compounds were tested for cytotoxicity activities. In conclusion, the three extracts and compounds did not show cytoxicity.

For *A. graecorum,* one flavonoid glycoside compound was isolated, which was tested for various cytotoxicity activity and showed none.

For *R. raetam*, a series of flavonoids was isolated. It can be concluded that the hexane and MeOH extracts of *R. raetam* showed no toxicity against normal and cancer cells but the EtOAc of *R. raetam* showed toxicity against HepG2, A375, PANC-1and PNT2 and high toxic to LNCaP and was not toxic to A549 and MCF7 cells. The isolated compound alpinumisoflavone (**Rr-1**) from *R. raetam* EtOAc extract presented some promising activities and it was toxic against hepatoma, melanoma, lung, pancreatic, breast and normal cells while it was highly toxic to prostate cells.

For *P. plicata,* the EtOH fractions showed no toxicity to the normal and cancer cells while fraction two (**PpFr-2**) was highly toxic against MCF7 and LNCaP, but this fraction was not toxic to A549 cells.

Due to the high toxicity of extract and compound on cells, therefore, **Rr-1** and **PpFr-2** were chosen to examine anti-metastatic activity against LNCaP and MCF7 cells. Both **Rr-1** and **PpFr-2** showed anti-adhesion and anti-migration activity against both cells lines, but not anti-invasion. So **Rr-1** and **PpFr-2** are promising anticancer therapeutics against LNCaP and MCF7 cells. Furthermore, it was possible to identify one lead compound from *R. raetam* with promising anticancer activity for prostate cancer. Thus, **Rr-1** could be a source of a promising treatment for prostate cancer in the future.

Generally, this result display that traditional medicinal plants such as these two have potential as a source of natural anticancer agents available to fight cancer. This study provided detailed scientific information about the cytotoxic activity and

phytochemistry of *R. raetam* and *P. plicata* that would serve as a benchmark towards anticancer drug development.

In conclusion, the results indicate that naturally occurring plant components, including pyranoisoflavone (alpinumisoflavone) and furanocoumarins (psoralen and angelicin), may be used as starting structures for the potential development of novel anticancer agents.

# APPENDICES
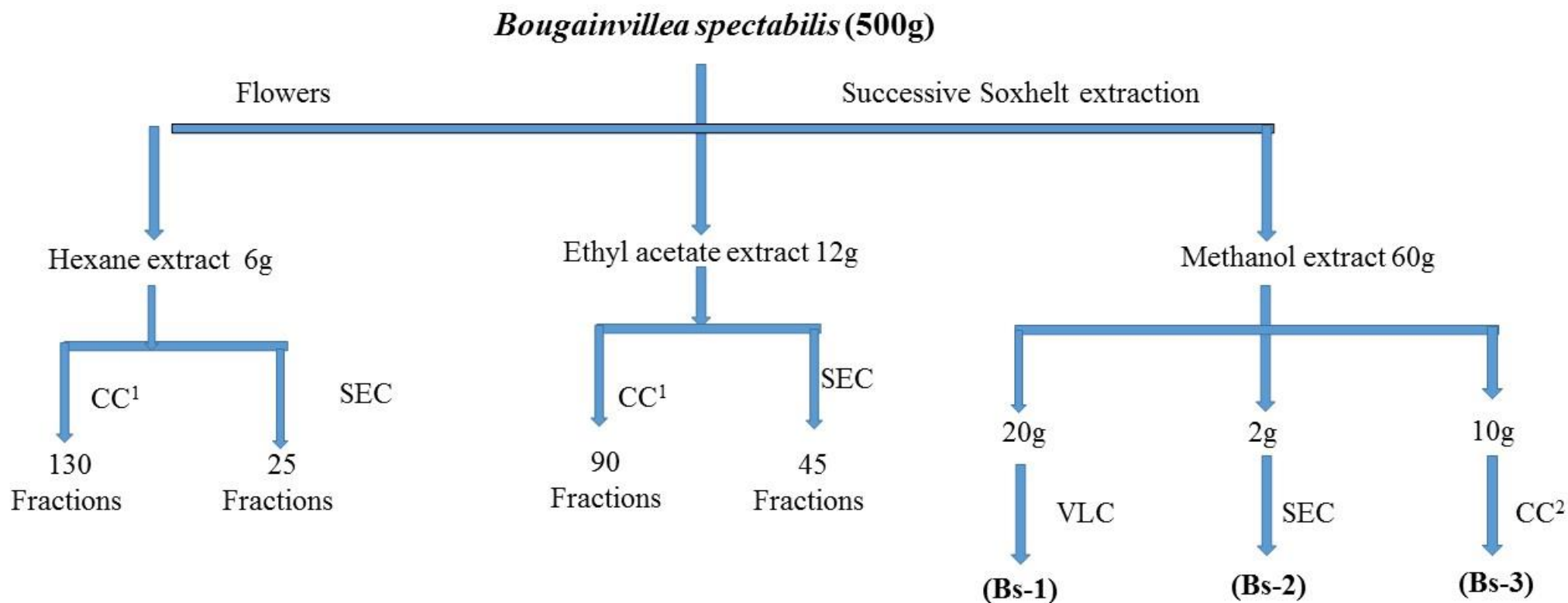
**Bougainvillea spectabilis (500g)**

Flowers

Successive Soxhelt extraction

Hexane extract 6g

CC¹

SEC

130 Fractions

25 Fractions

Ethyl acetate extract 12g

CC¹

SEC

90 Fractions

45 Fractions

Methanol extract 60g

20g

2g

10g

VLC

SEC

CC²

**(Bs-1)**

**(Bs-2)**

**(Bs-3)**

VLC: Vacuum liquid chromatography eluted with 100% *n*-hexane, with the gradual increase of EOAc, followed by the increase of MeOH then CC¹
CC¹ : Gradient column eluted with 10% n-hexane , increasing polarity by addition of EtOAc.
CC² : Open gradient column eluted with 10% n-hexane , increasing polarity by addition of EtOAc.
SEC: Size-exclusion chromatography with 100% methanol.

**Scheme I:** Isolation of compounds from the extracts of *Bougainvillea spectabilis*
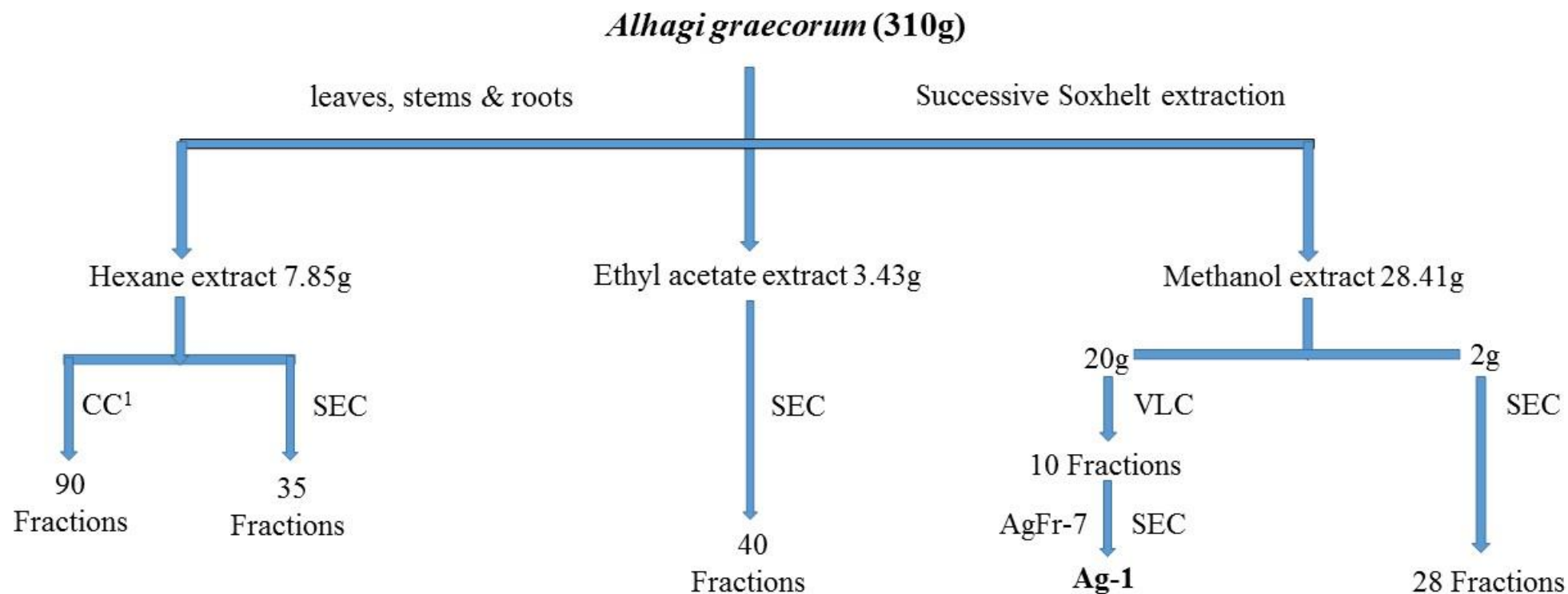
**Alhagi graecorum (310g)**

leaves, stems & roots

Successive Soxhelt extraction

Hexane extract 7.85g

Ethyl acetate extract 3.43g

Methanol extract 28.41g

CC¹

SEC

SEC

20g

VLC

2g

SEC

90 Fractions

35 Fractions

10 Fractions

40 Fractions

AgFr-7

SEC

28 Fractions

**Ag-1**

VLC: Vacuum liquid chromatography eluted with 100% *n*-hexane, with the gradual increase of EOAc and up to 40% MeOH.
CC¹ : Gradient column eluted with 10% *n*-hexane , increasing polarity by addition of EtOAc.
CC²: Open gradient column eluted with 10% n-hexane , increasing polarity by addition of EtOAc.
SEC: Size-exclusion chromatography with 100% methanol.

**Scheme II:** Isolation of compounds from the extracts of *Alhagi graecorum*
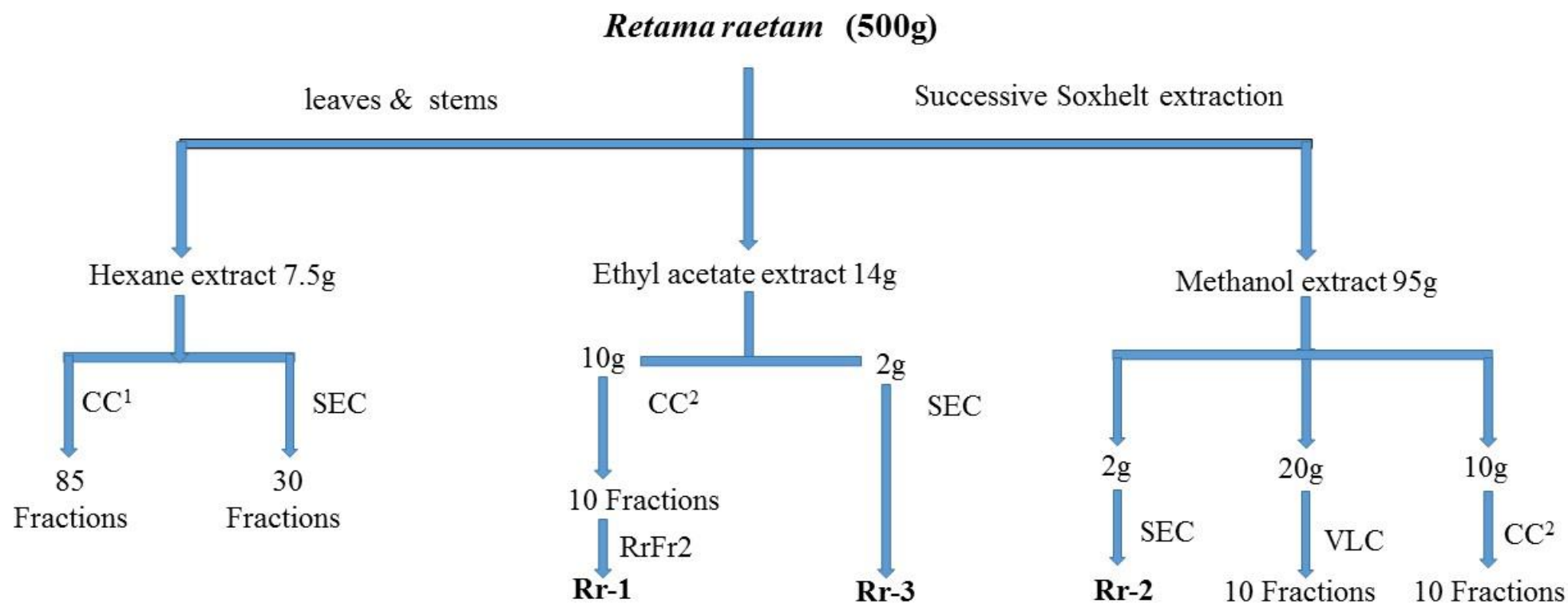
**_Retama raetam_ (500g)**

leaves & stems    Successive Soxhelt extraction

Hexane extract 7.5g          Ethyl acetate extract 14g          Methanol extract 95g

CC¹          SEC        10g        2g                         2g        20g        10g
                              CC²        SEC                       SEC      VLC       CC²

85          30          10 Fractions                            Rr-2     10 Fractions   10 Fractions
Fractions   Fractions
                         RrFr2

**Rr-1**                    **Rr-3**

VLC: Vacuum liquid chromatography eluted with 100% *n*-hexane, with the gradual increase of EOAc and up to 40% MeOH.
CC¹ : Gradient column eluted with 10% n-hexane , increasing polarity by addition of EtOAc.
CC² : Open gradient column eluted with 10% n-hexane , increasing polarity by addition of EtOAc.
SEC: Size-exclusion chromatography with 100% methanol.

**Scheme III**: Isolation of compounds from the extracts of *Retama raetam*

**Psoraela plicata (300g)**

leaves & stems     EtOH     Soxhelt extraction

30g

$CC^2$

| PpFr-1 | PpFr-2 | PpFr-3 | PpFr-4 | PpFr-5 |
| 2g | 2g | 2g | 2g | 2g |
| SEC PTLC | SEC | SEC PTLC | SECP TLC | SEC PTLC |
| 22 Fractions | **Pp-1 Pp-2a Pp-3 Pp-2b** | 26 Fractions | 24 Fractions | 28 Fractions |
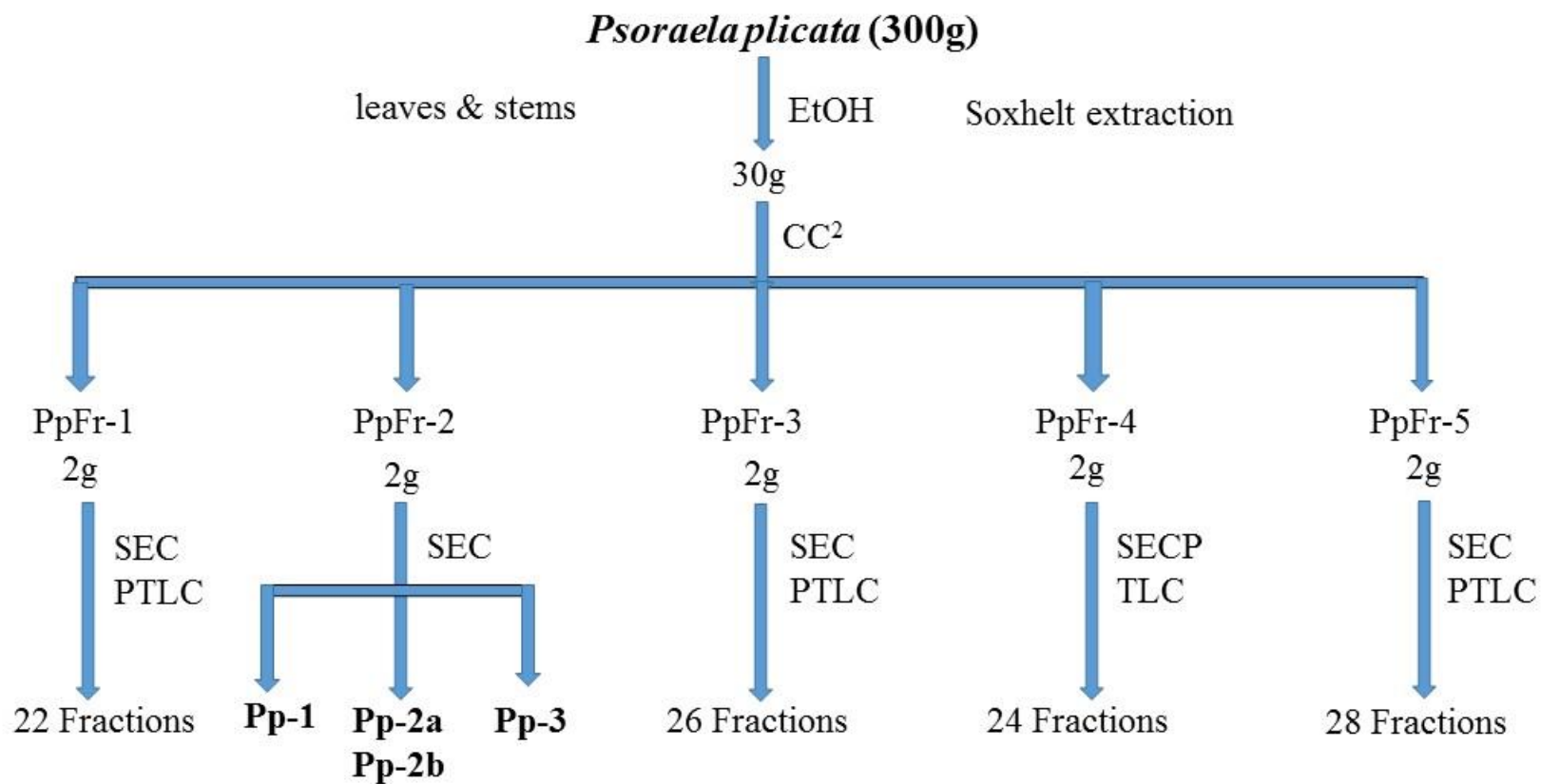
$CC^2$ : Open gradient column eluted with 10% n-hexane , increasing polarity by addition of EtOAc.
PTLC: Preparative thin layer chromatography.
SEC: Size-exclusion chromatography with 100% methanol.

**Scheme IV:** Isolation of compounds from the extracts of *Psoraela plicata*

# References

ADEBAYO, J. O., ADESOKAN, A. A., OLATUNJI, L. A., BUORO, D. O. & SOLADOYE, A. O. 2005. Effect of ethanolic extract of Bougainvillea spectabilis leaves on haematological and serum lipid variables in rats.

AGISHO, H., OSIE, M. & LAMBORE, T. 2014. Traditional medicinal plants utilization, management and threats in Hadiya Zone, Ethiopia. *J. Med. Plant,* 2**,** 94-108.

AHMAD, I., AQIL, F. & OWAIS, M. 2006. *Modern phytomedicine: Turning medicinal plants into drugs*, John Wiley & Sons.

AHMED, A. H. 2009. Biologically active saponins from Bougainvillea spectabilis growing in Egypt. *Asian Journal of Chemistry,* 21**,** 5510.

AL-KHATEEB, E., HAMADI, S. A., AL-HAKEEMI, A. A., ABU-TAHA, M. & AL-RAWI, N. 2012. Hypoglycemic effect of trigonelline isolated from Iraqi fenugreek seeds in normal and alloxan-diabetic rabbits. *Eur. Sci. J,* 8**,** 16-24.

AL-TUBULY, R. A., AUZI, A. A., AL-ETRI-ENDI, A. A., NAHAR, L. & SARKER, S. D. 2011. Effects of Retama raetam (Forssk.) Webb & Berthel.(Fabaceae) on the central nervous system in experimental animals. *Archives of Biological Sciences,* 63**,** 1015-1021.

ALGANDABY, M. M., ALGHAMDI, H. A., ASHOUR, O. M., ABDEL-NAIM, A. B., GHAREIB, S. A., ABDEL-SATTAR, E. A. & HAJAR, A. S. 2010. Mechanisms of the antihyperglycemic activity of Retama raetam in streptozotocin-induced diabetic rats. *Food and Chemical Toxicology,* 48**,** 2448-2453.

ALRAMAH, M. A., SAMAT, N. A. & MOHAMED, Z. 2019. Mapping Lung Cancer Disease in Libya using Standardized Morbidity Ratio, BYM Model and Mixture Model, 2006 to 2011: Bayesian Epidemiological Study. *Sains Malaysiana,* 48**,** 217-225.

AMEN, Y. M., MARZOUK, A. M., ZAGHLOUL, M. G. & AFIFI, M. S. 2013. Bioactive compounds from Tipuana tipu growing in Egypt. *J Am Sci,* 9**,** 334-9.

ARFAOUI, Y., AL-AYED, A. S., SAID, R. B. & HAMED, A. I. 2013. Experimental and Density Functional Theory Study of a New Dimer with Tetrasubstituted Cyclobutane Ring System Isolated from Psoralea plicata Seeds. *International Journal of Chemistry,* 5**,** 73.

ATEBA, S. B., MVONDO, M. A., DJIOGUE, S., ZINGUÉ, S., KRENN, L. & NJAMEN, D. 2019. A pharmacological overview of alpinumisoflavone, a natural prenylated isoflavonoid. *Frontiers in pharmacology,* 10**,** 952.

ATEBA, S. B., MVONDO, M. A., NGEU, S. T., TCHOUMTCHOUA, J., AWOUNFACK, C. F., NJAMEN, D. & KRENN, L. 2018. Natural terpenoids against female breast cancer: a 5-year recent research. *Current medicinal chemistry,* 25**,** 3162-3213.

AWEN, B. Z. S., UNNITHAN, C. R., RAVI, S., KERMAGY, A., SASIKUMAR, J., KHRBASH, A. S. & EKREEM, W. L. 2011. Essential oils of Retama raetam from Libya: chemical composition and antimicrobial activity. *Natural product research,* 25**,** 927-933.

BECKER, L. C., BERGFELD, W. F., BELSITO, D. V., KLAASSEN, C. D., MARKS, J. G., SHANK, R. C., SLAGA, T. J., SNYDER, P. W. & ANDERSEN, F. A.

2010. Final report of the safety assessment of allantoin and its related complexes. *International journal of toxicology,* 29**,** 84S-97S.

BEN-MAHMOUD, K., MANSUR, S. & AL-GOMATI, A. 2003. Land degradation and desertification in Libya. *Third Millennium. Swets and Zeitlinger Publishers. Lisse, the Netherland***,** 339-350.

BENMILOUD-MAHIEDDINE, R., ABIRACHED-DARMENCY, M., BROWN, S. C., KAID-HARCHE, M. & SILJAK-YAKOVLEV, S. 2011. Genome size and cytogenetic characterization of three Algerian Retama species. *Tree genetics & genomes,* 7**,** 987.

BENYASAAD, T., ALTRJOMAN, F., ENATTAH, N., ELTAIB, F., ASHAMMAKHI, N. & ELZAGHEID, A. 2017. Cancer incidence in Western Libya: First results from Tripoli. *Ibnosina Journal of Medicine and Biomedical Sciences,* 9**,** 37-45.

BHANOT, A., SHARMA, R. & NOOLVI, M. N. 2011. Natural sources as potential anti-cancer agents: A review. *International journal of phytomedicine,* 3**,** 09.

BOGENRIEDER, T. & HERLYN, M. 2003. Axis of evil: molecular mechanisms of cancer metastasis. *Oncogene,* 22**,** 6524-36.

BRAY, F., JEMAL, A., GREY, N., FERLAY, J. & FORMAN, D. 2012. Global cancer transitions according to the Human Development Index (2008–2030): a population-based study. *The lancet oncology,* 13**,** 790-801.

CALIXTO, J. 2000. Efficacy, safety, quality control, marketing and regulatory guidelines for herbal medicines (phytotherapeutic agents). *Brazilian Journal of medical and Biological research,* 33**,** 179-189.

CHAMBERS, A. F., GROOM, A. C. & MACDONALD, I. C. 2002. Dissemination and growth of cancer cells in metastatic sites. *Nat Rev Cancer,* 2**,** 563-72.

CHANG, W.-S., LEE, Y.-J., LU, F.-J. & CHIANG, H.-C. 1993. Inhibitory effects of flavonoids on xanthine oxidase. *Anticancer research,* 13**,** 2165-2170.

CHAUHAN, P. S., GUPTA, K. K. & BANI, S. 2011. The immunosuppressive effects of Agyrolobium roseum and pinitol in experimental animals. *International immunopharmacology,* 11**,** 286-291.

CHEIKH, A., SAMBA, M., HADOU, A., ISMAIL, A. & MINNIH, M. S. 2015. Ethnobotanic study, phytochemical screening and antioxidant activity of Psoralea plicata (Cullen plicatum) Delile. *Journal of Chemical and Pharmaceutical Research,* 7**,** 1743-1747.

CHOUHAN, A., KARMA, A., ARTANI, N. & PARIHAR, D. 2016. Overview on cancer: role of medicinal plants in its treatment. *World Journal Of Pharmacy And Pharmaceutical Sciences,* 5**,** 185-207.

CONFORTI, F., STATTI, G., TUNDIS, R., LOIZZO, M., BONESI, M., MENICHINI, F. & HOUGHTON, P. 2004. Antioxidant and cytotoxic activities of Retama raetam subsp. Gussonei. *Phytotherapy Research: An International Journal Devoted to Pharmacological and Toxicological Evaluation of Natural Product Derivatives,* 18**,** 585-587.

CRAGG, G. M. & NEWMAN, D. J. 2005. Plants as a source of anti-cancer agents. *Journal of ethnopharmacology,* 100**,** 72-79.

CUCCUINI, P., NEPI, C., ABUHADRA, M., CECCHI, L., FREITAG, H., LUCCIOLI, E., MAIER STOLTE, M., MARCUCCI, R., PERUZZI, L. & PIGNOTTI, L. 2015. The Lybian collections in FI (Herbarium Centrale

Italicum and Webb Herbarium) and studies on the Lybian flora by R. Pampanini–Part 1.

DAVIS, A., CHRISTIANSEN, M., HOROWITZ, J. F., KLEIN, S., HELLERSTEIN, M. K. & OSTLUND, R. E. 2000. Effect of pinitol treatment on insulin action in subjects with insulin resistance. *Diabetes care,* 23**,** 1000-1005.

DEHAGHANI, Z. A., ASGHARI, G. & DINANI, M. S. 2017. Isolation and Identification of Nicotiflorin and Narcissin from the Aerial Parts of Peucedanum aucheri Boiss. *Journal of Agricultural Science and Technology A,* 7**,** 45-51.

DJEDDI, S., KARIOTI, A., YANNAKOPOULOU, E., PAPADOPOULOS, K., CHATTER, R. & SKALTSA, H. 2013. Analgesic and antioxidant activities of Algerian Retama raetam (Forssk.) Webb & Berthel extracts. *Records of Natural Products,* 7**,** 169.

DO, L. T., AREE, T., SIRIPONG, P., PHAM, T. N., NGUYEN, P. K. & TIP-PYANG, S. 2016. Bougainvinones A-H, Peltogynoids from the Stem Bark of Purple Bougainvillea spectabilis and Their Cytotoxic Activity. *J Nat Prod,* 79**,** 939-45.

EDZIRI, H., MASTOURI, M., CHERAIF, I. & AOUNI, M. 2010. Chemical composition and antibacterial, antifungal and antioxidant activities of the flower oil of Retama raetam (Forssk.) Webb from Tunisia. *Natural product research,* 24**,** 789-796.

EDZIRI, H., MASTOURI, M., MAHJOUB, M. A., MIGHRI, Z., MAHJOUB, A. & VERSCHAEVE, L. 2012. Antibacterial, antifungal and cytotoxic activities of two flavonoids from Retama raetam flowers. *Molecules,* 17**,** 7284-7293.

EL-ABGY, E., EL-SHEREEF, M. & EL-MAHGOUP, F. 2012. Antimosquitoes principles isolated from the wild herb Psoralea plicata Del. *The Medical Journal of Cairo University,* 80**,** 165-168.

EL MISTIRI, M., SALATI, M., MARCHESELLI, L., ATTIA, A., HABIL, S., ALHOMRI, F., SPIKA, D., ALLEMANI, C. & FEDERICO, M. 2015. Cancer incidence, mortality, and survival in Eastern Libya: updated report from the Benghazi Cancer Registry. *Annals of epidemiology,* 25**,** 564-568.

ELSHATSHAT, S. & MANSOUR, A. 2014. Disturbance of flora and vegetation composition of Libya by human impacts: costal region of Al-Jabal Al-Akhdar area as model. *J Appl Sci Res,* 5**,** 286-292.

FAWAD, S. A., KHALID, N., ASGHAR, W. & SULERIA, H. A. R. 2012. In vitro comparative study of Bougainvillea spectabilis "stand" leaves and Bougainvillea variegata leaves in terms of phytochemicals and antimicrobial activity. *Chinese journal of natural medicines,* 10**,** 441-447.

FERLAY, J., SOERJOMATARAM, I., DIKSHIT, R., ESER, S., MATHERS, C., REBELO, M., PARKIN, D. M., FORMAN, D. & BRAY, F. 2015. Cancer incidence and mortality worldwide: sources, methods and major patterns in GLOBOCAN 2012. *International journal of cancer,* 136**,** E359-E386.

FRANTZ, C., STEWART, K. M. & WEAVER, V. M. 2010. The extracellular matrix at a glance. *J Cell Sci,* 123**,** 4195-200.

GAO, M., CHANG, Y., WANG, X., BAN, C. & ZHANG, F. 2017. Reduction of COX-2 through modulating miR-124/SPHK1 axis contributes to the antimetastatic effect of alpinumisoflavone in melanoma. *American journal of translational research,* 9**,** 986.

GOYAL, P. 2012. Cancer chemoprevention by natural products: current & future prospects. *J Integr Oncol,* 1**,** e101.

GRAY, A. I., IGOLI, J. O. & EDRADA-EBEL, R. 2012. Natural products isolation in modern drug discovery programs. *Natural Products Isolation.* Springer.

GUPTA, G. P. & MASSAGUE, J. 2006. Cancer metastasis: building a framework. *Cell,* 127**,** 679-95.

HAMED, A. I., SPRINGUEL, I., EL-EMARY, N. A., MITOME, H. & YAMADA, Y. 1997. A phenolic cinnamate dimer from Psoralea plicata. *Phytochemistry,* 45**,** 1257-1261.

HAMED, A. I., SPRINGUEL, I. V. & EL-EMARY, N. A. 1999. Benzofuran glycosides from the seeds of Psoralea plicata Del. *Studies in Plant Science.* Elsevier.

HAN, X. H., HONG, S. S., HWANG, J. S., JEONG, S. H., HWANG, J. H., LEE, M. H., LEE, M. K., LEE, D., RO, J. S. & HWANG, B. Y. 2005. Monoamine oxidase inhibitory constituents from the fruits ofCudrania tricuspidata. *Archives of pharmacal research,* 28**,** 1324.

HAQ, I. 2004. Safety of medicinal plants. *Pak J Med Res,* 43**,** 203-10.

HARBORNE, A. 1998. *Phytochemical methods a guide to modern techniques of plant analysis*, springer science & business media.

HU, Y., LI, Z., WANG, L., DENG, L., SUN, J., JIANG, X., ZHANG, Y., TIAN, L., WANG, Y. & BAI, W. 2017. Scandenolone, a natural isoflavone derivative from Cudrania tricuspidata fruit, targets EGFR to induce apoptosis and block autophagy flux in human melanoma cells. *Journal of Functional Foods,* 37**,** 229-240.

IBRAHIM, M. T. 2015. Anti-inflammatory effect and phenolic isolates of Alhagi graecorum Boiss (Family Fabaceae). *Journal of American Science,* 11.

IKPEME, E., EKALUO, U., UDENSI, O., EKERETTE, E. & PIUS, M. 2015. Phytochemistry and reproductive activities of male albino rats treated with crude leaf extract of great Bougainvillea (Bougainvillea spectabilis). *Asian Journal of Scientific Research,* 8**,** 367.

JAGESSAR, R., HOOLAS, G. & MAXWELL, A. 2013. Phytochemical screening, isolation of betulinic acid, trigonelline and evaluation of heavy metals ion content of Doliocarpus dentatus. *Journal of Natural Products,* 6.

JAWLA, S., KUMAR, Y. & KHAN, M. 2012. Hypoglycemic activity of Bougainvillea spectabilis stem bark in normal and alloxan-induced diabetic rats. *Asian Pacific Journal of Tropical Biomedicine,* 2**,** S919-S923.

JAWLA, S., KUMAR, Y. & KHAN, M. S. Y. 2013. Isolation of antidiabetic principle from Bougainvillea spectabilis Willd (Nyctaginaceae) stem bark. *Tropical Journal of Pharmaceutical Research,* 12**,** 761-765.

JESUS, A. R., DIAS, C., MATOS, A. M., DE ALMEIDA, R. F., VIANA, A. S., MARCELO, F., RIBEIRO, R. R. T., MACEDO, M. P., AIROLDI, C. & NICOTRA, F. 2014. Exploiting the therapeutic potential of 8-β-d-glucopyranosylgenistein: synthesis, antidiabetic activity, and molecular interaction with islet amyloid polypeptide and amyloid β-peptide (1–42). *Journal of medicinal chemistry,* 57**,** 9463-9472.

JIANG, Z. & XIONG, J. 2014. Induction of apoptosis in human hepatocarcinoma SMMC-7721 cells in vitro by psoralen from Psoralea corylifolia. *Cell biochemistry and biophysics,* 70**,** 1075-1081.

KACEM, I., MAJDOUB, H. & ROUDESLI, S. 2008. Physicochemical properties of pectin from retama raetam obtained using sequential extraction. *Journal of Applied Sciences,* 8**,** 1713-1719.

KAPLAN, W. 2013. Background Paper 6.5 Cancer and Cancer Therapeutics. *World Health Organization (ed) Priority medicines for Europe and the world: update***,** 6.5-1.

KASSEM, M., MOSHARRAFA, S., SALEH, N. & ABDEL-WAHAB, S. 2000. Two new flavonoids from Retama raetam. *Fitoterapia,* 71**,** 649-654.

KAUR, R., KAPOOR, K. & KAUR, H. 2011. Plants as a source of anticancer agents. *J Nat Prod Plant Resour,* 1**,** 119-24.

KELEG, S., BUCHLER, P., LUDWIG, R., BUCHLER, M. W. & FRIESS, H. 2003. Invasion and metastasis in pancreatic cancer. *Mol Cancer,* 2**,** 14.

KIM, J.-I., KIM, J., KANG, M.-J., LEE, M.-S., KIM, J.-J. & CHA, I.-J. 2005. Effects of pinitol isolated from soybeans on glycaemic control and cardiovascular risk factors in Korean patients with type II diabetes mellitus: a randomized controlled study. *European journal of clinical nutrition,* 59**,** 456-458.

KUETE, V., MBAVENG, A. T., NONO, E. C., SIMO, C. C., ZEINO, M., NKENGFACK, A. E. & EFFERTH, T. 2016. Cytotoxicity of seven naturally occurring phenolic compounds towards multi-factorial drug-resistant cancer cells. *Phytomedicine,* 23**,** 856-863.

KUMAR, S. & KUMAR, D. 2008. Evaluation of antioxidant potential, phenolic and flavonoid contents of hibiscus liliaceous flowers.

KUMAR, S., PATHANIA, A. S., SAXENA, A., VISHWAKARMA, R., ALI, A. & BHUSHAN, S. 2013. The anticancer potential of flavonoids isolated from the stem bark of Erythrina suberosa through induction of apoptosis and inhibition of STAT signaling pathway in human leukemia HL-60 cells. *Chemico-biological interactions,* 205**,** 128-137.

LE HOUEROU, H. N. 2004. An agro-bioclimatic classification of arid and semiarid lands in the isoclimatic Mediterranean zones. *Arid land research and management,* 18**,** 301-346.

LI, C. L., YANG, D., CAO, X., WANG, F., HONG, D. Y., WANG, J., SHEN, X. C. & CHEN, Y. 2017. Fibronectin induces epithelial-mesenchymal transition in human breast cancer MCF-7 cells via activation of calpain. *Oncology letters,* 13**,** 3889-3895.

LIN, T.-H., TAN, T.-W., TSAI, T.-H., CHEN, C.-C., HSIEH, T.-F., LEE, S.-S., LIU, H.-H., CHEN, W.-C. & TANG, C.-H. 2013. D-pinitol inhibits prostate cancer metastasis through inhibition of $\alpha V\beta 3$ integrin by modulating FAK, c-Src and NF-$\kappa$B pathways. *International journal of molecular sciences,* 14**,** 9790-9802.

LIU, W., YIN, D., LI, N., HOU, X., WANG, D., LI, D. & LIU, J. 2016. Influence of environmental factors on the active substance production and antioxidant activity in Potentilla fruticosa L. and its quality assessment. *Scientific reports,* 6**,** 28591.

LOUHAICHI, M., SALKINI, A., ESTITA, H. & BELKHIR, S. 2011. Initial assessment of medicinal plants across the Libyan Mediterranean coast. *Advances in Environmental Biology***,** 359-371.

LU, H., ZHANG, L., LIU, D., TANG, P. & SONG, F. 2014. Isolation and purification of psoralen and isopsoralen and their efficacy and safety in the treatment of osteosarcoma in nude rats. *African health sciences,* 14**,** 641-647.

LV, C., KONG, H., DONG, G., LIU, L., TONG, K., SUN, H., CHEN, B., ZHANG, C. & ZHOU, M. 2014. Antitumor efficacy of alpha-solanine against pancreatic cancer in vitro and in vivo. *PLoS One,* 9**,** e87868.

MALOMO, S., ADEBAYO, J., ARISE, R., OLORUNNIJI, F. & EGWIM, E. 2006. Effects of ethanolic extract of Bougainvillea spectabilis leaves on some liver and kidney function indices in rats. *Phytochemistry & Pharmacology-III,* 17**,** 261-272.

MCGUIRE, S. 2016. World cancer report 2014. Geneva, Switzerland: World Health Organization, international agency for research on cancer, WHO Press, 2015. Oxford University Press.

MISHRA, N., JOSHI, S., TANDON, V. & MUNJAL, A. 2009. Evaluation of antifertility potential of aqueous extract of Bougainvillea spectabilis leaves in swiss albino mice. *Int J Pharm Sci Drug Res,* 1**,** 19-23.

MORGAN, M., SABA, S. & GOWER, W. Fibronectin influences cellular proliferation and apoptosis similarly in LNCaP and PC-3 prostate cancer cell lines. Urologic Oncology: Seminars and Original Investigations, 2000. Elsevier, 155-159.

MUHAMMAD, G., HUSSAIN, M. A., ANWAR, F., ASHRAF, M. & GILANI, A. H. 2015. Alhagi: a plant genus rich in bioactives for pharmaceuticals. *Phytotherapy research,* 29**,** 1-13.

MUKASSABI, T., AHMIDAT, G., SHERIF, I., ELMOGASAPI, A. & THOMAS, P. 2012. Checklist and life forms of plant species in contrasting climatic zones of Libya. *Biological Diversity and Conservation,* 5**,** 1-12.

MÜLLER-PILLASCH, F., GRESS, T. & ADLER, G. 1997. Extracellular Matrix in Pancreatic Diseases. *Diagnostic Procedures in Pancreatic Disease.* Springer.

NAMKOONG, S., KIM, T.-J., JANG, I.-S., KANG, K.-W., OH, W.-K. & PARK, J. 2011. Alpinumisoflavone induces apoptosis and suppresses extracellular signal-regulated kinases/mitogen activated protein kinase and nuclear factor-κB pathways in lung tumor cells. *Biological and Pharmaceutical Bulletin,* 34**,** 203-208.

NAVONE, L., CASATI, P., LICONA-CASSANI, C., MARCELLIN, E., NIELSEN, L. K., RODRIGUEZ, E. & GRAMAJO, H. 2014. Allantoin catabolism influences the production of antibiotics in Streptomyces coelicolor. *Applied microbiology and biotechnology,* 98**,** 351-360.

NEWMAN, D. J. & CRAGG, G. M. 2016a. Drugs and drug candidates from marine sources: An assessment of the current "state of play". *Planta medica,* 82**,** 775-789.

NEWMAN, D. J. & CRAGG, G. M. 2016b. Natural Products as Sources of New Drugs from 1981 to 2014. *Journal of Natural Products,* 79**,** 629-661.

NKENGFACK, A. E., AZEBAZE, A. G., WAFFO, A. K., FOMUM, Z. T., MEYER, M. & VAN HEERDEN, F. R. 2001. Cytotoxic isoflavones from Erythrina indica. *Phytochemistry,* 58**,** 1113-1120.

ORGANIZATION, W. H. 2019. *WHO global report on traditional and complementary medicine 2019*, World Health Organization.

ORTHEN, B., POPP, M. & SMIRNOFF, N. 1994. Hydroxyl radical scavenging properties of cyclitols. *Proceedings of the Royal Society of Edinburgh, Section B: Biological Sciences,* 102**,** 269-272.

OSTLUND, R. E. & SHERMAN, W. R. 1996. Pinitol and derivatives thereof for the treatment of metabolic disorders. Google Patents.

PAN, S.-Y., ZHOU, S.-F., GAO, S.-H., YU, Z.-L., ZHANG, S.-F., TANG, M.-K., SUN, J.-N., MA, D.-L., HAN, Y.-F. & FONG, W.-F. 2013. New perspectives on how to discover drugs from herbal medicines: CAM's outstanding contribution to modern therapeutics. *Evidence-Based Complementary and Alternative Medicine,* 2013.

PARKIN, D. M., BRAY, F., FERLAY, J. & PISANI, P. 2005. Global cancer statistics, 2002. *CA: a cancer journal for clinicians,* 55**,** 74-108.

PATEL, J., CHOUBISA, B. & DHOLAKIYA, B. 2011. Plant derived compounds having activity against P388 and L1210 leukemia cells. *Chemical Sciences Journal.*

PELLETIER, S. W., CHOKSHI, H. P. & DESAI, H. K. 1986. Separation of diterpenoid alkaloid mixtures using vacuum liquid chromatography. *Journal of natural products,* 49**,** 892-900.

PIJUAN, J., BARCELÓ, C., MAIQUES, O., MORENO, D. F., SISÓ, P., MARTI, R. M., MACIÀ, A. & PANOSA, A. 2019. In vitro cell migration, invasion and adhesion assays: from cell imaging to data analysis. *Frontiers in cell and developmental biology,* 7**,** 107.

PINTATHONG, P., PINKET, P., PAPOODPLOOK, M., THITIPRAMOTE, N. & CHAIWUT, P. Phenolic antioxidants from Bougainvillea SPP. 1st Mae Fah Luang University International Conference, 2012. 29-30.

PISTELLI, L., BERTOLI, A., GIACHI, I. & MANUNTA, A. 1998. Flavonoids from Genista ephedroides. *Journal of natural products,* 61**,** 1404-1406.

PLOCHMANN, K., KORTE, G., KOUTSILIERI, E., RICHLING, E., RIEDERER, P., RETHWILM, A., SCHREIER, P. & SCHELLER, C. 2007. Structure–activity relationships of flavonoid-induced cytotoxicity on human leukemia cells. *Archives of biochemistry and biophysics,* 460**,** 1-9.

POONGOTHAI, G. & SRIPATHI, S. K. 2013. A review on insulinomimetic pinitol from plants. *International Journal of Pharma and Bio Sciences,* 4**,** 992-1009.

PRIYA, M. L., PRIYA, K. B., KOTAKADI, V. S. & JOSTHNA, P. 2015. Herbal and medicinal plants molecules towards treatment of cancer: A mini review. *Am J Ethnomed,* 2**,** 136-42.

RASHID, F., SHARIF, N., ALI, I., SHARIF, S., NISA, F. & NAZ, S. 2013. Phytochemical analysis and inhibitory activity of ornamental plant (Bougainvillea spectabilis). *Asian J Plant Sci Res,* 3**,** 1-5.

RASOOL, N., KHAN, A. Q., AHMAD, V. U. & MALIK, A. 1991. A benzoquinone and a coumestan from Psoralea plicata. *Phytochemistry,* 30**,** 2800-2803.

RASOOL, N., KHAN, A. Q. & MALIK, A. 1989. Psoracinol, a new lupane-type triterpene from Psoralea plicata. *Journal of Natural Products,* 52**,** 749-752.

RASOOL, N., KHAN, A. Q. & MALIK, A. 1990. Plicatin A and B, two phenolic cinnamates from Psoralea plicata. *Phytochemistry,* 29**,** 3979-3981.

RENGARAJAN, T., NANDAKUMAR, N., RAJENDRAN, P., HARIBABU, L., NISHIGAKI, I. & BALASUBRAMANIAN, M. P. 2014. D-pinitol promotes apoptosis in MCF-7 cells via induction of p53 and Bax and inhibition of Bcl-2 and NF-κB. *Asian Pac J Cancer Prev,* 15**,** 1757-1762.

SAAED, M. W., EL-BARASI, Y. M. & RAHIL, R. O. 2019. Our present knowledge about the history and composition of the vegetation and flora of Libya. *Webbia,* 74**,** 325-338.

SCHWARTSMANN, G., RATAIN, M., CRAGG, G., WONG, J., SAIJO, N., PARKINSON, D., FUJIWARA, Y., PAZDUR, R., NEWMAN, D. & DAGHER, R. 2002. Anticancer drug discovery and development throughout the world. *Journal of clinical Oncology,* 20**,** 47s-59s.

SCIMECA, J., FAST, D. & ZIMMERMAN, A. 2008. Use of allantoin as a pro-collagen synthesis agent in cosmetic compositions. Google Patents.

SHAIQ ALI, M., AMIR IBRAHIM, S., AHMED, F. & KASHIF PERVEZ, M. 2005. Color versus bioactivity in the flowers of Bougainvillea spectabilis (Nyctaginaceae). *Natural product research,* 19**,** 1-5.

SINGH, R., PANDEY, B., TRIPATHI, M. & PANDEY, V. 2001. Anti-inflammatory effect of (+)-pinitol. *Fitoterapia,* 72**,** 168-170.

SKEHAN, P., STORENG, R., SCUDIERO, D., MONKS, A., MCMAHON, J., VISTICA, D., WARREN, J. T., BOKESCH, H., KENNEY, S. & BOYD, M. R. 1990. New colorimetric cytotoxicity assay for anticancer-drug screening. *JNCI: Journal of the National Cancer Institute,* 82**,** 1107-1112.

SORDON, S., POPŁOŃSKI, J., TRONINA, T. & HUSZCZA, E. 2017. Microbial glycosylation of daidzein, genistein and biochanin A: Two new glucosides of biochanin A. *Molecules,* 22**,** 81.

SRIPATHI, S. K., GOPAL, P. & LALITHA, P. 2011. Allantoin from the leaves of Pisonia grandis R. Br. *International Journal of Pharmacy & Life Sciences,* 2.

SUDIPTA, K., LOKESH, P., RASHMI, W., VIJAY, R. & SSN, K. 2012. Phytochemical screening and in vitro antimicrobial activity of Bougainvillea spectabilis flower extracts. *International journal of phytomedicine,* 4**,** 375.

TJAHJANDARIE, T. S. & TANJUNG, M. 2015. Phenolic compounds from the stem bark of Erythrina orientalis and their cytotoxic and antioxidant activities. *Der Pharma Chem,* 7**,** 206-211.

UMAMAHESWARI, A., SHREEVIDYA, R. & NUNI, A. 2008. In vitro antibacterial activity of Bougainvillea spectabilis leaves extracts. *Adv Biol Res,* 2**,** 1-5.

VUKOVIC, N., KACANIOVA, M., HLEBA, L. & SUKDOLAK, S. 2013. Chemical Composition of the Essential oil of Bougainvillea spectabilis from Montenegro. *Journal of Essential Oil Bearing Plants,* 16**,** 212-215.

WAKSMUNDZKA-HAJNOS, M., KOWALSKA, T. & SHERMA, J. 2008. *Thin layer chromatography in phytochemistry*, CRC Press.

WANG, T., JIANG, Y., CHU, L., WU, T. & YOU, J. 2017. Alpinumisoflavone suppresses tumour growth and metastasis of clear-cell renal cell carcinoma. *American journal of cancer research,* 7**,** 999.

WANG, Y., HONG, C., ZHOU, C., XU, D. & QU, H.-B. 2011. Screening antitumor compounds psoralen and isopsoralen from Psoralea corylifolia L. seeds. *Evidence-Based Complementary and Alternative Medicine,* 2011.

WEISWALD, L.-B., BELLET, D. & DANGLES-MARIE, V. 2015. Spherical cancer models in tumor biology. *Neoplasia,* 17**,** 1-15.

WHELAN, L. & RYAN, M. 2003. Ethanolic extracts of Euphorbia and other ethnobotanical species as inhibitors of human tumour cell growth. *Phytomedicine,* 10**,** 53-58.

XU, W. H., AL-REHAILY, A. J., YOUSAF, M., AHMAD, M. S., KHAN, S. I. & KHAN, I. A. 2015. Two new flavonoids from Retama raetam. *Helvetica Chimica Acta,* 98**,** 561-568.

ZHANG, Q. W., LIN, L. G. & YE, W. C. 2018. Techniques for extraction and isolation of natural products: a comprehensive review. *Chin Med,* 13**,** 20.

ZHOU, J., CHAN, L. & ZHOU, S. 2012. Trigonelline: a plant alkaloid with therapeutic potential for diabetes and central nervous system disease. *Current medicinal chemistry,* 19**,** 3523-3531.